IJAIR

IMPACT FACTOR

7.36

International Journal of Advance and Innovative Research

* ISSN : 2394-7780 *

International Journal of

Advance and Innovative Research
(Conference Special)

President and Chairman's Message

I am immensely happy and proud to state that Department of Chemistry of JVM's Degree College, Airoli, has organized two days Virtual International Conference on Multifunctional Advanced Materials (VICMAM- 2021).

Multifunctional advanced materials are imperative to numerous technological innovations that offer clear benefits to society but the unique characteristics of it are not well understood. There is a lot of ongoing research happening in this field and bringing awareness of this new field to the new researchers is important. Organization of this International Conference is like another feather in the cap of our institution.

I am also proud to mention that JVM has been providing quality education and services in all the fields with excellent infrastructure, facilities and well qualified staff.

I extend my best wishes and congratulations to the Principal Dr. Leena Sarkar for taking the initiative in organizing this conference in collaboration with Association of Chemistry Teachers (ACT).

SHRI. M.S. BHOOMRADDI

PRESIDENT, JVM AND

CHAIRMAN, COLLEGE GOVERNING COUNCIL

Principal's Message

The path to excellence is through skill development and knowledge enhancement. Following this path, we, at JVM's Degree College, always strive to promote research culture and get scientific temper in our students and faculty and thereby connecting Science to society. To foster this spirit, Virtual International Conference on 'Multifunctional Advanced Materials' was organized by Chemistry Department of our college in collaboration with Association of Chemistry Teachers on 9th & 10th August 2021-22. We all know that the technologies are changing at a fast pace and the old ones become obsolete in a very short span of time. Material is the basis of all technological innovations. Keeping this in mind, this year's theme was decided as Multifunctional Advanced Materials which is revolutionizing around almost all the fields. The integration of different materials provides multi utility and functions which makes it much more desirable for the future, and can be applied to many areas leading to development of sustainable technologies. The future of this seems very wide due to its smart way of application. We expect many more breakthrough experiments and inventions in the future, so giving an impetus to this topic seemed right in today's scenario.

The College Trust upholds certain values and principles which cater to the development of the locality and nation's development at large. The encouragement we get from the management of the institution defines their dedication to the vision and motto, that is to make the institution a centre of excellence and a place of quality education. I express my deep gratitude towards our management members Shri. M.S. Bhoomraddi, President and Chairman, College Governing Council; Shri. V.N. Hegde, Vice President; Shri V. K. Hunnur, General Secretary; Shri K.H. Deshpande, Jt. General Secretary and other members.

We were honoured and are thankful to Dr. Ponnadurai Ramasami for accepting our invitation as Chief Guest. We are truly indebted to all the renowned speakers who joined us nationally and internationally in our endeavours to achieve our feet. Sincere thanks to all the eminent personalities who graced the occasion such as Prof. Dr. Rameshwar Adhikari, Former Executive Director, RECAST, Tribhuvan University, Kathmandu, Nepal; Prof. Dr. Thinakaran Narayanan, Higher National Youth Skill Institute of Sepang, Malaysia; Prof. Dr. A.H. Mijinyawa, Dr. G.M. Nazeruddin, Retd. Principal, Poona College of Arts, Science & Commerce and Professor Emeritus Abeda Inamdar Senior College, Pune; Prof. M. Swaminathan, Nanomaterials Laboratory, International Research Centre, Department of Chemistry, Kalasalingam Academy of Research and Education, Krishnankoil; Prof. Dr. W.B Gurnule, Kamala Nehru Mahavidyalaya, Nagpur. I heartly acknowledge the profound knowledge they shared with the participants and truly appreciate their high degree of commitment in imparting knowledge.

I express my sincere thanks to the Advisory Committee who have done the handholding for the fruition of such a wonderful conference. Prof. Brijesh Pare, President, ACT, Head of the Department of Chemistry, Madhav Science College, Ujjain, Madhya Pradesh; Prof. D.V.Prabhu, General Secretary, ACT, Wilson College, Mumbai; Dr. Hemant Pande, Vice President, ACT, West Zone, Mumbai; Prof. A.S.Aswar, Member, ACT, S.G.B, Amaravati University; Prof. Dr. W.B.Gurnule, Member, ACT, Kamala Nehru Mahavidyalaya, Nagpur.

A big salute to the organizers, teaching and non-teaching staff, participants, presenters and students whose wholehearted and untiring support made this International Conference a huge success. I

congratulate Mrs. Harshada Niju, Convenor, and Mrs. Sandhya Patil, Co-Convenor of this conference and each and every member of my Department and Organising team for the success of this conference.

I whole heartedly thank IARA publications for their efforts in publishing the papers of this conference.

Dr. Leena Sarkar

Principal &

(Chairperson, VICMAM-2021)

We are glad and obliged to have been given this opportunity to host two days Virtual International Conference (VICMAM - 2021) in collaboration with ACT.

This conference gave an opportunity to the participants to gain knowledge from the experience of eminent scientist working in the field of advanced materials. It helped the budding scientists and researchers to get exposed to the recent developments in advanced materials. They also got an opportunity to present their research work and interact with the eminent scientists.

We thank our honorable management members for their constant support and motivation for conducting this conference. We thank our Principal Dr. Leena Sarkar for her valuable inputs and guidance while conducting this international conference. We also thank all the members of organizing committee for extending their valuable help in organizing the conference. We thank the Eminent speakers, authors, reviewers of research papers/ Poster presenters for their active participation.

Asst. Prof. Harshada Niju   **Asst. Prof. Sandhya Patil**

(Convener VICMAM- 2021)   **(Co-Convener VICMAM- 2021)**

Chief Guest: - Ponnadurai Ramasami

Ph.D. in Physical Chemistry; University of Delhi, India

He is currently teaching at

(a) Merton College, Mauritius: Ordinary and Advance levels Chemistry

(b) University of Mauritius:

(i) Department of Chemistry

(ii) Department of Chemical Engineering

He has been awarded with Best Mauritian Scientist award in 2016.

He has done Supervision of 60 Undergraduate projects and 10 Postgraduate projects.

He has published 237 papers and has several books in his name.

Prof. Dr. Rameshwar Adhikari

(M. Sc., PhD. Chemistry)

He is Former Director, Research Centre for Applied Science and Technology (RECAST), Tribhuvan University, Kathmandu, Nepal and also Professor of Chemistry, Central Department of Chemistry, Tribhuvan University, Kathmandu.

He is an Associate member of CHEMRAWN Committee, National Representative for Chemical Education Committee and Polymer Division of the IUPAC Secretary of Humboldt Club Nepal . He is also a Founder President of Nepal Polymer Institute (NPI) and is re – elected as General Secretary, Nepal Chemical Society.

Shri. THINAKARAN NARAYANAN

Master of Science in Manufacturing Engineering, UTeM

He has an experience of teaching in Heavy Machinery Mechanics (Dec 2004-2011) and Architectural Design (Jul 2003-Nov 2004), panel beating & spray painting (Sept 2002-June 2003).

He had been invited as a Plenary Speaker for International Conference Polymer Processing & Characterization (ICPPC 2019) at Mahatma Gandhi University (MGU) Kerala and in a Symposium on Intelligent Manufacturing and Mechatronics (SIMM 2019). He was also invited in the proceeding of Mechanical Engineering Research Day 2019 (MERD 2019) and 9th National Conference in Education, Technical & Vocational Education & Training.

He has been awarded Gold Medals in innovation contest PERISA 19 organized by Community College of Selayang, Iinnovation contest index 19 organized by UiTM Shah Alam. Gold and Bronze Medal of IPITEX Innovation competition 2019, Bangkok Thailand

Prof. Dr. A. H. Mijinyawa

(M. Sc., Ph.D.)

He holds a First degree from Bayero University Kano, Nigeria. A Post graduation degree in Chemistry from Sharda University, Greater Noida, India. He was awarded a doctoral degree in Chemistry from Sharda University. His current research area is Development of materials for novel applications. He has published more than 12 research papers in National and International Journals.

Prof. Dr. W.B.Gurnule

(M. Sc., Ph.D.)

RTM Nagpur University, Nagpur

He has published more than 200 research papers in National and International reviewed journals and presented more than 110 research papers in National and International conferences. He is Reviewer of 38 International journals of repute having impact factor more than 2.0. He has received CRSI Best Teacher Award-2011 presented by Chemical Research Society of India, Bangalore at CRSI Symposium at Bhuwneshwar in 2011.

He has been awarded with Aufbau International Outstanding Researcher Award in 2016 by ACS publication Salem. He was also awarded with Best researcher award by Vishwashanti society at MDI Singapore in 2017.

He has successfully guided 22 students for Ph.D. degree and 21 M. Phil. Students.

He is an author of 32 Books/04 Chapters, 04 of which are of International level published by Apple Academic Press inc. Canada.

He is recently honored by Best Researcher Award by Rashtrasant Tukadoji Maharaj Nagpur University, Nagpur on 5th September 2018 and ISCAS prestigious Silver Medal Award on 11th ISCAS National Conference at Nagpur on 20th Dec. 2019.

Prof. Dr. M. Swaminathan

(M. Sc., Ph. D.)

He is a fellow member of Royal Society of Chemistry and a member of American Chemical Society.

He has been awarded with Tamil Nadu Scientist Award–2008 (TANSA, Government of Tamil Nadu), Silver Medal Award–2005 for research contribution by "Indian Association of Solid-State Chemists and Allied Scientists" and bronze medal award in 2012 for research contribution in Chemical Sciences by Chemical Research Society of India (CRSI). He has been also awarded with Life time achievement award for Material Science in 'International conference on Futuristic Materials' held at RTM University and ACT P.R. Singh award for outstanding contribution to chemical education in 2019 at NCCT-19 held at S.G.B. Amaravati University.

He has published two reviews on photocatalysis and is an Editor for three special issues of "International Journal of Photoenergy". He is the member of Editorial board of "International journal of Photoenergy".

He was a Council member of Chemical Research Society of India (2007-2014) and President of Indian Association of Solid-state chemists and Allied scientists. He was the Vice- President from 2014 to 2016 of Association of Chemistry Teachers, Mumbai and is EC member till now.

Dr. G. M. Nazeruddin

(M. Sc., B.Ed., M. Phil., & Ph.D..Chemistry)

He is working as Professor Emeritus in Department of Chemistry (PG and Research Centre) of Abeda Inamdar Sr. College, PUNE and has retired as the Principal & Head, Department of Chemistry Poona College of Art, Science and Commerce, Pune. He is a Recognized Research Guide in S.P. Pune University and Shree JJT University, Rajasthan. He has published 92 research papers in National and International Journals. He has given Invited talks at 3 State Level, 13 at National and 4 at International Level. He is a member of the Editorial Board of 4 National/ International Journals.

Guest Editors of Special Issue

Dr. Leena Sarkar

Principal

JVM's Degree College

Airoli, Navi Mumbai

Mrs. Harshada Niju

JVM's Degree College

Airoli, Navi Mumbai

Mrs Sandhya Patil

JVM's Degree College

Airoli, Navi Mumbai

International Journal of Advance and Innovative Research

SJIFactor

Scientific Journal Impact Factor

CERTIFICATE OF INDEXING (SJIF 2018)

This certificate is awarded to

International Journal of Advance & Innovative Research
(ISSN: 2394-7780)

The Journal has been positively evaluated in the SJIF Journals Master List evaluation process
SJIF 2018 = 7.363

SJIF (A division of InnoSpace)

SJIFactor Project Manager
International Advisory Services
INNOSPACE INTERNATIONAL

SJIFactor Project

International Journal of Advance and Innovative Research

CONTENTS

Research Papers

INVESTIGATION OF VOLATILE ORGANIC COMPOUNDS (VOCS) AT AN OUTSKIRTS AREA OF GORAKHPUR– A TERAI REGION OF NORTH INDIA

Amit Masih[1] and Shilpi Srivastava[*2]

[1]Environmental Research Lab, Department of Chemistry, St. Andrew's College, Gorakhpur, India
[*2]Department of Chemistry, Indira Ghandhi National Tribal University, Amarkantak, M.P. India

ABSTRACT

Volatile organic compounds (VOCs) are air pollutants of an important class and also at a low quantity; these have a huge potential risk to human well-being due to their carcinogenic nature. Thus, an investigation of ambient VOCs (benzene, toluene and xylene) was conducted at an outer edge area in Gorakhpur for a span of one year in order to ascertain the contamination levels. The levels of BTX were measured with the help of low volume sampler. Carbon disulphide was used for the extraction of samples by occasional agitation and then it was analyzed on GC-FID. The average concentration of total BTX in all samples was 12.7 µg/m³ and the total range was from 1.12 µg/m³ to 21.8 µg/m³ with the median of 8.2 µg/m³. The maximum concentration of total BTX was found to be 16.1 µg/m³ in winter season, followed by 12.3 µg/m³ in summer and 9.9 µg/m³ in monsoon season. Toluene contributed maximum (63%) followed by benzene (33%) and xylene (4%) and residential site (16%). The BTX concentration was in the order toluene > benzene > xylene. The hazard quotient was 3.8E-01, 4.3E-03 and 1.3E-02 of benzene, toluene and xylene respectively. Integrated lifetime cancer risk for benzene was 6.9E-06.

Keywords— VOCs, BTX, Carcinogenic/Non-carcinogenic risk, Terai region, Seasonal Variation.

INTRODUCTION

Volatile organic compounds (VOCs) are important tropospheric pollutants. During the recent decade's volatile organic compounds (VOCs) such as benzene, toluene and xylene (BTX) have gained interest in the field of indoor and outdoor air quality [1]. These mono-aromatic hydrocarbons are the sources of a variety of adverse health effects such as asthma, dizziness, fatigue, and eye, nose, and throat irritation. Moreover, nausea and similar nonspecific symptoms have been also associated with BTX [2]. Among BTX compounds, xylenes are highly reactive and contribute to ozone formation and hence to climate change [3].

Humans are exposed to benzene mainly through breathing polluted air [4]. Therefore, great efforts have been devoted to identifying the sources of benzene in both indoor and outdoor air [5]. Benzene is emitted by vegetation and petroleum reservoirs [6]. However, because it is present in crude oil, natural gas, and unleaded gasoline, anthropogenic sources are the main contributors [7]. Vehicular exhaust, incomplete fuel combustion and evaporative loss are considered as the chief reasons of benzene in ambient air. Xylene and toluene are much copious in gasoline than benzene and both are also used in solvents widely. Therefore, outdoor levels of these compounds were expected to be higher than that of benzene [8]. Due to adverse effects on human health, the analysis of benzene, toluene, and xylene (BTX) concentrations in air is necessary [9].

MATERIAL & METHODS

Site description, sampling and analysis

Air sampling was set up for a span of one year (Nov. 2014 to Oct. 2015) at an agrarian area '*bhathat*'. The monitoring was achieved once in a week for 24 hrs in a planned routine and a total of forty-eight (48) samples were collected. BTX were sampled and analysed using a methodology based on National Institute for Occupational Safety and Health (NIOSH) method 1501 [10] & [11]. BTX were sampled by drawing air through activated coconut shell charcoal tubes (CSC, 8 mm x 110 mm, 600mg) containing two sections of (main section 400 mg, second section 200 mg) separated by a 2 mm urethane foam (SKC Inc.), using a low-flow SKC Model 220 sampling pump (SKC, USA) at the flow rate of 250 ml/min for 20-24 hrs. Every week the rate of air suction was tested using rotameters which were calibrated with an accurateness of ±1%. Sampled air was then analysed with an HP 6890 gas chromatography/mass spectrometer and gas chromatography/ flame ionization detector [10] & [12].

RESULTS & DISCUSSION

The seasonal BTX levels determined at agrarian sites of Gorakhpur is shown in Figure 1. The concentration of benzene ranges from 3.5 µg/m³ to 34.1 µg/m³ with the mean value of 11.6 µg/m³. Toluene ranges from 9.4 µg/m³ to 47.1 µg/m³ having an average of 21.7 µg/m³. Xylene has a mean concentration of 1.3 µg/m³ with the range of 0.5 µg/m³ to 3.4 µg/m³. The total mean concentration of BTX was 12.7 µg/m³ at agricultural area of

Gorakhpur. Figure 2 depicts that toluene (63%) had the highest contribution followed by benzene (33%) and xylene (4%) of the total BTX at agricultural area.
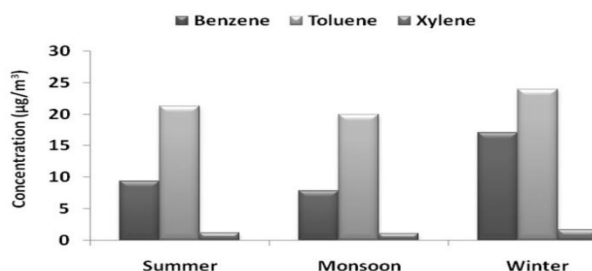
Figure 1: Seasonal BTX concentrations (µg m⁻³)

The interspecies ratios of VOCs with varying reaction rates against OH provide information about the characteristics of air at the sampling site. Average VOC relative ratios at Gorakhpur region with respect to benzene, toluene and xylene (BTX) were studied. Benzene and Toluene are chief constituents of gasoline emitted into the environment by vehicular exhausts.
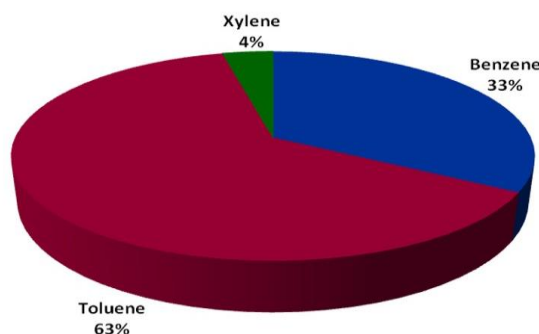
Figure 2: Individual Contribution (%) of BTX

Table 1 illustrates that the maximum B/T ratio was found during winter season (0.71) followed by summer (0.43) and monsoon seasons (0.39) indicating that increase in concentration from monsoon to winter season and from summer to winter season is higher for benzene as related to toluene and xylene.

Table 1: Average interspecies ratios (B/T and X/B)

	B/T Ratio	X/B Ratio
Summer	0.43	0.12
Monsoon	0.39	0.13
Winter	0.71	0.09

This fact is also supported by the X/B ratio which was found to be lowest in winter season (0.09) and increased during summer (0.12) and monsoon season (0.13). This may be explained on the account of prevalent usage of cow-dung cakes, charcoal, wood etc. for cooking throughout the year. Additionally, in winter season stubble, brushwood and straw are also used for heating purpose. The weather of Gorakhpur can be generally classified into three seasons, winter (November-February), summer (March-June) and monsoon (July-October).
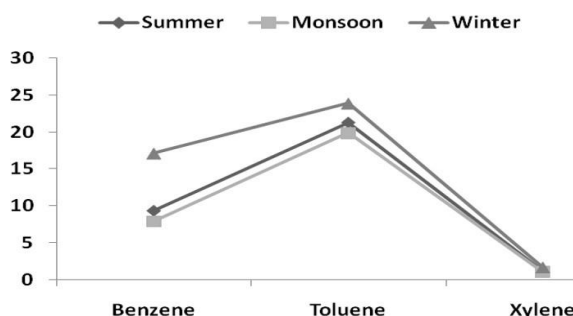
Figure 3: Seasonal BTX pattern at outskirts area

Figure 3 depicts the seasonal pattern of measured BTX in ambient air at agricultural area of Gorakhpur. The concentration of benzene in during winter, summer and monsoon seasons are in the order of 17.1, 9.3 and 7.9 $\mu g/m^3$ respectively, whereas toluene (23.9, 21.3 and 19.9 $\mu g/m^3$), and xylene (1.6, 1.1 and 1.0 $\mu g/m^3$). Although the trend of seasonal variation of BTX at agricultural area is similar with nature i.e. maximum concentration of BTX were found to be in winter (16.1 $\mu g/m^3$) followed by summer (12.3 $\mu g/m^3$) and monsoon (9.9 $\mu g/m^3$) seasons. The total BTX ratios for winter to summer (W/S) and winter to monsoon (W/M) were 1.3 and 1.5 at agricultural area indicating significant seasonal variations of BTX. Figure 4 shows the plot of toluene against benzene with R^2 value 0.91, which suggests a linear relationship between toluene and benzene. Additionally, it also identifies that benzene and toluene may have the same source *i.e.* the use of biomass fuel [03].
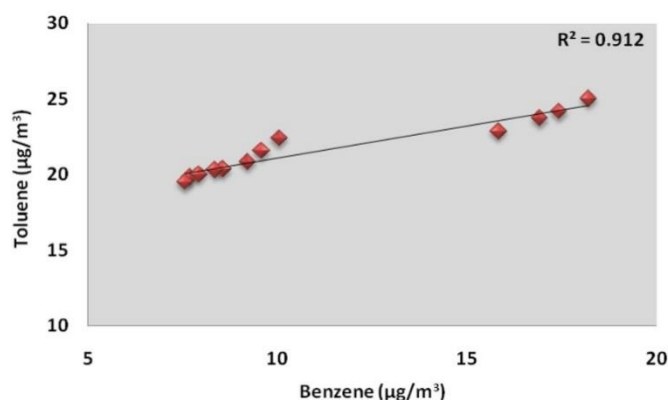
Figure 4: Correlation between Benzene and Toluene

In the present study, the non-cancer hazard quotient (HQ) and integrated lifetime cancer risk (ILTCR) due to the BTX exposure at their prevalent levels were assessed [13]. The (ILTCR) was determined from the given equation:

$$ILTCR = EL \ (mg \ kg^{-1}day^{-1}) \times CPF \ (mg \ kg^{-1}day^{-1})$$

Where, EL is the effective lifetime exposure and CPF is the carcinogenic potency factor or cancer slope factor. The inhalation cancer slope factor of carcinogenic compounds for benzene was obtained from Risk Assessment Information System (RAIS) as 2.73×10^{-2} mg $kg^{-1}day^{-1}$ [14]. A cancer risk of $> 10^{-6}$ was considered "carcinogenic effect of concern;" a value $\leq 10^{-6}$ was considered an "acceptable level" [15]. Non-malignant risk assessment was denoted by hazard quotient (HQ) and it was defined as the ratio of yearly average daily concentration received (EY) and the reference concentration (RfC), which was determined according to equation:

$$HQ = EY/RfC$$

Where RfC - the inhalation reference concentration of the non-carcinogenic compounds toluene and xylene was obtained from the Integrated Risk Information System (IRIS) as 5 and 0.1 mg/m^3, respectively [16] & [17]. The RfC of benzene for non-cancer risk is 0.03 [18]. The sum of HQs for specific pollutants gave Hazard Index (HI).

Table 2: Estimate of non-cancer and cancer risk

	HQ	ILTCR
Benzene	3.8E-01	6.9E-06
Toluene	4.3E-03	
Xylene	1.3E-02	

HQ: Hazard Quotient
ILTCR: Integrated Life Time Cancer Risk

Table 2 represents ILTCR and HQ risks (per individual residing time of 15 years). The risk of cancer estimated for benzene surpassed the permissible value of 1E-06 specifying further cancer risk from benzene because of its higher carcinogenicity. Toluene gives the highest non-cancer HQ followed by benzene and xylene. The individual HQs for BTX did not exceed unity anywhere indicating no serious threat of chronic non- cancer health effect in pollutant specific target organs for the city population [13].

REFERENCES

[1] Buczynska A.J., Krata A., Stranger M., Roekens E., Grieken R.V. 2009. Atmospheric BTEX-concentrations in an area with intensive street traffic. Atmospheric Environment 43; 311–318

[2] Masih A., Dviwedi S., Lal J.K. 2021. Source characterization and health risks of BTEX in indoor/outdoor air during winters at a terai precinct of North India. Environmental Geochemistry & Health 43:2985–3003

[3] Fan R, Li J, Chen L. 2014. Biomass fuels and coke plants are important sources of human exposure to polycyclic aromatic hydrocarbons, benzene and toluene. Environmental Research. 14;135: 1-8.

[4] Masih J, Masih A, Kulshrestha A, Singhvi R, Taneja A. 2010. Characterization of polycyclic aromatic hydrocarbons in indoor and outdoor atmosphere in the North central part of India. Journal of Hazardous Materials, 177: 190-198.

[5] Duarte-Davidson R, Courage C, Rushton L, Levy L, 2001. Benzene in the environment: an assessment of the potential risks to the health of the population. J Occ Env Med, 58: 2–13.

[6] CONCAWE (Conservation of Clean Air and Water in Europe), 1997. Exposure Profile: Gasoline. European Oil Companies' Organization for Environmental and Health Protection, Brussels

[7] Masih A., Lall AS., Taneja A., Singhvi R. 2017. Exposure profiles, seasonal variation and health risk assessment of BTEX in indoor air of homes at different microenvironments of a terai province of northern India. Chemosphere, 176: 8-17.

[8] Masih A, Lall AS, Taneja A, Singhvi R. 2018. Exposure profiles and health risk assessment of ambient BTX at urban and rural environments of a terai region of northern India. Environmental Pollution, 242, 1678-1683.

[9] Gallego E., F. X. Roca, X. Guardino, and M. G. Rosell. 2008. Indoor and outdoor BTX levels in Barcelona City metropolitan area and Catalan rural areas," Journal of Environmental Sciences 20(9); 1063–1069

[10] NIOSH. Pocket guide to chemical hazards NIOSH publications, Cincinnati, OH. 1994.

[11] Bureau of Indian Standard (BIS): 5182. 2006. Methods for Measurement of Air Pollution. New Delhi, India

[12] Masih A, Lall AS, Taneja A, Singhvi R. 2016. Inhalation exposure and related health risks of BTEX in ambient air at different microenvironments of a terai zone in north India. Atmospheric Environment, 147: 55-66.

[13] Majumdar D, Mukherje AK, Sen S. 2011. BTEX in an Ambient air of Metropolitan city. Journal of Environment Protection,2;11-20.

[14] RAIS. Toxicity profile. 2010. Available from: http://rais.ornl.gov/tools/tox_profiles.html

[15] Zhang Yujie , Mu Yujing , Liu Junfeng , Mellouki Abdelwahid. 2012. Levels, sources and health risks of carbonyls and BTEX in the ambient air of Beijing, China. Journal of Environmental Sciences; 24(1); 124–130

[16] USEPA. 2003. Toxicological review of xylene: In support of summary information on Integrated risk infor¬mation system (IRIS). www.epa.gov/iris

[17] USEPA. 2005. Toxicological review of toluene: In support of summary information on Integrated risk infor¬mation system (IRIS). www.epa.gov/iris

[18] ATSDR. 2010. Toxicological profile for ethylbenzene. Atlanta, GA, USA.

NANOTECHNOLOGY FOR HERBAL MEDICINES AND PLANT RESEARCH

D.T. Sakhare

U.G, P.G. & Research Centre, Department of Chemistry, Shivaji, Art's, Comm. & Science College Kannad. Dist. Aurangabad.431103, (M.S.) India

ABSTRACT

"Nanotechnology" depends on the acknowledgment of the particles not exactly the size of 100 nm. It is the designing and assembling of materials at the nuclear and atomic scale. The utilization of nanotechnology for "phytotherapy" or treatment of different infections by natural prescriptions/drugs, including home grown medication conveyance where current and arising nanotechnologies could empower altogether clever classes of therapeutics has been accounted for. The analysts have prevailed with regards to utilizing nanotechnology to embed and at the same time enact the qualities conveyed into plant cell dividers. The nanomaterial's can fundamentally improve the pharmacokinetics and restorative file of plant beginning medications. Strangely, drug sciences are utilizing nanoparticles to decrease poisonousness and symptoms of medications. The scientific experts are utilizing nanotechnology for plant exploration to be applied as "phytotherapy". The nanoparticles, alleged "mesoporous" present the quality and enact it in an exact and controlled way and without poisonous eventual outcomes. The organically combined nanoparticles with plant items have better chemotherapeutic impacts against microbial infections. With the execution of Nano mechanical creation methods, it is feasible to satisfy the significant need for artemisinin for intestinal sickness therapy and disease chemotherapy also. Utilizing nanotechnology, the analysts tracked down that another natural medication compound had the option to enter disease cells without harming the solid cells of the human body.

KEYWORDS: Cancer, diseases, herbal drugs, nanoparticles/nanotechnology, plants, research

1. INTRODUCTION:

The expression "nanotechnology" was inferred by Greek word "Nano", signifying "overshadow". The Nano gadget and Nano technique are one billionth of a meter or 10^{-9} m. The nanotechnology includes the clusters of iotas, atoms and sub-atomic sections into the minuscule particles somewhere in the range of 1 and 100 nm, and advances to the associations of sub-atomic level matters and designed materials naturally. Nanotechnology is the new arising innovation in the medication revelation and it has the property of self-focusing as in without the connection of a particular ligand, the nanoparticles can be utilized for focusing, due to their unmistakably little size, at the tainted obsessive regions. Medication conveyance framework brought a clever medication conveyance framework, an original way to deal with beat the disadvantages of the customary medication conveyance frameworks. Therapy of persistent illnesses like malignancy utilizing designated drug conveyance nanoparticles is the most recent accomplishment in the drug conveyance field [1].

The prefix "Nano" in the nanotechnology implies a billionth (1×10^{-9}). "Nanotechnology" depends on the acknowledgment of the particles not exactly the size of 100 nanometers (nm) bestow to nanostructures worked from them new properties and conduct. This happens in light of the fact that particles, which are more modest than the trademark lengths related with specific marvel frequently show new science and physical science, prompting new conduct which relies upon the size. Then again, "nanotechnology" is a cycle by which the capacity to control singular iotas and atoms can be created utilizing on set of exact instruments to assemble and work proportionately more modest set so on down to a required scale. As of late, nanotechnology has gotten perhaps the most significant and invigorating bleeding edge fields in science. It shows extraordinary guarantee for furnishing us soon with numerous leap forwards that will alter the course of mechanical advances in a wide scope of utilizations. Innovative work of this advanced field is coordinated towards making worked on material, gadgets and frameworks that abuse the new properties [2, 3]

To emphasize more clearly, "nanotechnology" is the engineering and manufacturing of materials at the atomic and molecular scale. In its strictest definition, "nanotechnology" alludes to structures generally in the 1-100 nm size systems in somewhere around one measurement. Despite this size restriction, "nanotechnology" commonly refers to structures that are up to several hundred nm in size, and that are developed by top-down or bottom-up engineering of individual components. The emergence of nanotechnology platforms can enable development and commercialization of entirely new classes of bioactive macromolecules that need precise intracellular delivery for bioactivity. While both organic and inorganic technologies are under development, controlled-release polymer technologies and liposomes will likely continue to have the greatest clinical impact for the foreseeable future [4]

Hence, in this paper, we focus on the use of nanotechnology for "phytotherapy" or treatment of various diseases by herbal medicines/drugs, including herbal drug delivery where current and emerging nanotechnologies could enable entirely novel classes of therapeutics. The herbal medicines are not a simple task since many factors influence the biological efficacy and reproducible therapeutic effect. Standardized herbal products of consistent quality and containing well-defined constituents are required for reliable clinical trials and to provide consistent beneficial therapeutic effects. Pharmacological properties of a herbal formulation depend on phytochemical constituents present therein. Improvement of legitimate logical strategies which can dependably profile the phytochemical piece, including quantitative examinations of market/bioactive mixtures and other significant constituents, is a significant test to researchers. The nanotechnology based herbal drugs possess improved solubility and enhanced bioavailability [5].

Ayurveda is the ancient Indian medical science based on herbal medicines/drugs and herbo-mineral preparations. Researchers from Lowa State University have succeeded in using nanotechnology to insert and simultaneously activate the genes delivered into plant cell walls, a discovery that has powerful implications for biotechnology. While the way toward conveying qualities into plant tissue isn't new, it has two phases. First, the gene is inserted into plant cell tissue and then afterwards chemicals are introduced into plant to trigger the genes function. The two-stage process has been imprecise as the presence of chemicals can be harmful to the plant. Researchers at Texas Agri Life Research are planning to use nanotechnology for detecting plant disease at an early stage so that tons of food is protected from the possible outbreak. Researchers of the US Department of Agriculture are working to find a solution for protecting the food and agriculture from bacteria, fungus and viral agents. As of now, the discovery method requires days to discover the plant illness and analysts are centering to track down a short and better recognition framework that can give results inside a few hours. Analysts are searching for a straightforward framework that is versatile and exact and doesn't need any convoluted strategy for activity, so that even a basic rancher can utilize the portable system and can address the disease. The major problems with plants is that unlike humans, they do not have immune system and if any new plant pathogen is present in the area, plants are not able to protect themselves [6].

Separation and extraction of normal items (or natural medications) is loaded with numerous specialized hitches. Inspite of this fact, the plant origin natural products have occupied lead positions as drugs in current pharmacopoeia and the improvement in this concern through Nano formulations using nanotechnology have been done. Known effects and no side effects have made natural products a powerful therapeutic solution to the organisms. But the delivery of plant origin therapeutic molecules as drugs is problematic due to poor solubility, poor permeability, low bioavailability, instability in biological milieu and extensive first pass metabolism. These limitations of plant origin drugs can be overcome by attaching or encapsulating them with suitable nanomaterial's. The nanomaterial's can significantly enhance the pharmacokinetics and therapeutic index of plant origin drugs. Designated conveyance and blend treatment can definitely work on the presentation of plant beginning medications [7].

2. NOVEL DRUG DELIVERY SYSTEM FOR HERBAL MEDICINE:

Ayurveda is one of the ancient medical sciences practiced in India [8]. Herbal medicines have been recognized by physicians and patients due to their potential therapeutic effect and also their fewer side effects as compared to other medicines, [9, 10] at the same time it also increases the bioavailability [11] of the medicine. For quite a while, home grown prescriptions were not considered for improvement of novel plans because of absence of logical avocation and preparing challenges. The cutting edge phyto-drug examination can tackle the logical necessities of natural meds in creating novel medication conveyance frameworks, for example, nanoparticles, miniature emulsion, grid framework, strong scattering, liposomes and solid lipid nanoparticles. The intricacy of dynamic constituents makes the advancement of novel medication conveyance framework for natural plans exceptionally testing. In the greater part of the regular measurements structures, just a restricted measure of controlled portion arrives at the designated site, while most of the medications get appropriated all through the body depending on physicochemical and biochemical properties[12,13]resulting in low therapeutic value.

Novel drug delivery system (NDDS) for herbal medicines includes targeted drug delivery, which reduces dosage frequency, increases the solubility and absorption whereas decreases elimination [14]. Among all the NDDS, Nanoparticles are considered to be an important one. Nanoparticle can be used to target the herbal medicines to individual organs which improve the targeted drug delivery, effectiveness and safety of the medicine. Fig.1. To stress more, Nanotechnology is the designing and assembling of materials at the nuclear and atomic level. In spite of the size limitation Nanotechnology ordinarily alludes to structures that are up to a few 100 nm in size. It is the utilization and control of issue at a little scope. At this size, iotas and atoms work in an unexpected way, and give an assortment of astounding and fascinating outcomes. Nanotechnology and Nano

science examines have arisen quickly during the previous years in a wide scope of item areas. It provides opportunities for the development of materials, including those for medical applications, where conventional techniques may reach their limits [15].
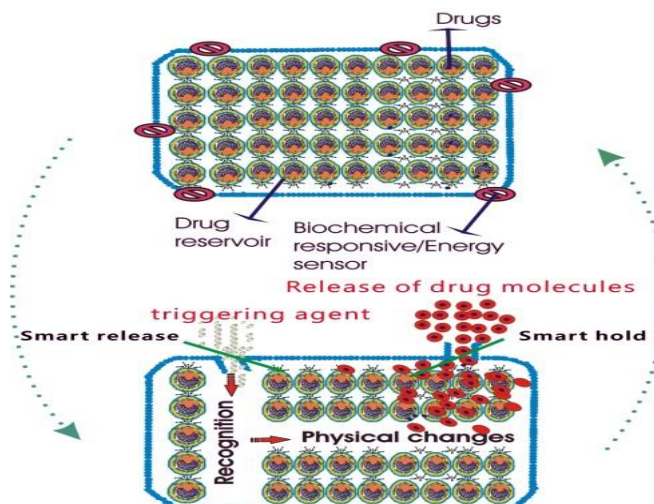
Fig 1: Release of medication atoms to the designated site.

3. NANOPARTICLE SYNTHESIS:

3.1 Polymer Nanoparticle:

Polymer Nanoparticles are defined as solid, colloidal particles in the range of 10-1000 nm. Polymer Nanoparticle is known as Nano sphere and Nano capsules. These can be arranged either from preformed polymers or by direct polymerization of monomers. Different methods like solvent evaporation, salting out, dialysis, supercritical fluid evaporation and rapid expansion of supercritical solution are being used [16]. The decision of planning technique is made based on various factors like the sort of polymeric framework, space of use, size prerequisite and so on. The polymeric nanoparticles which are synthesized by any of these techniques are proved for efficient therapeutic activity. A schematic diagram represents Fig. 2 how polymeric nanoparticles are synthesized.
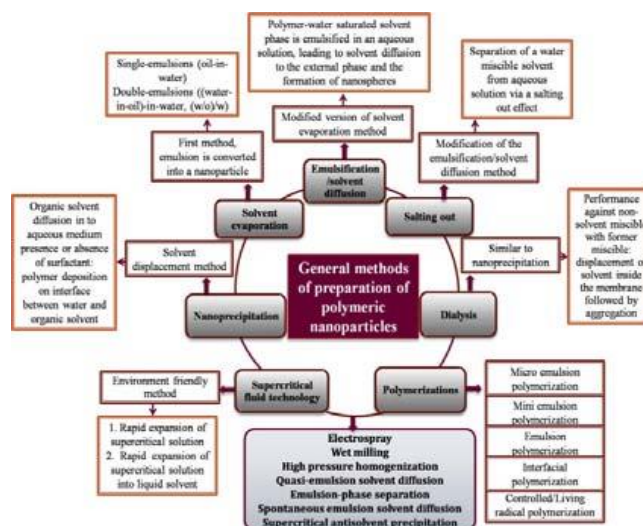
Fig 2: Schematic portrayal of different methods for planning of polymeric nanoparticles.

3.2 Metallic Nanoparticles

Metal nanoparticle is used to describe Nano sized metals with dimension (length, width and thickness) range between 1-100 nm. There are various liquid phase methods for preparing metallic nanoparticles, such as chemical reduction, sol gel, and reversed micelle. Nobel metal Nanoparticles with spherical shaped and size, were produced continuously by the chemical reduction methods [17, 18]. In this schematic diagram represents how the metallic Nanoparticles have been synthesized by different methods shown in Fig. 3. Metal nanoparticles are broadly utilized because of their trademark provisions, for example, huge surface advances, give explicit electronic design among sub-atomic and metallic states and cycle a huge number of low coordination sites. These are utilized in attractive partition of named cells and other natural substances,

restorative medication, quality and radionuclide conveyance, radio recurrence techniques for the catabolism of tumors by means of hyperthermia, and contrast enhancement agents for magnetic resonance imaging.
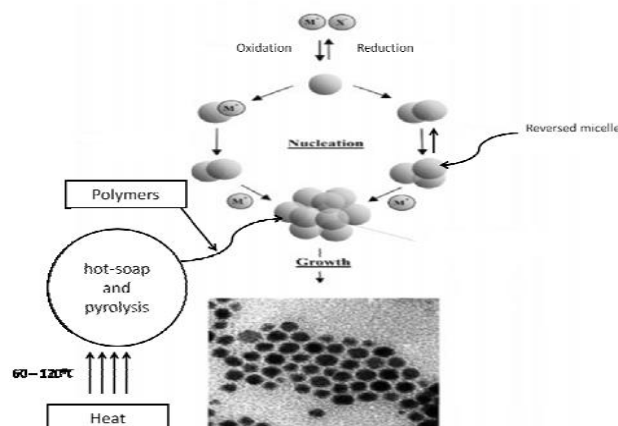
Fig 3: Schematic portrayal for readiness of metallic Nanoparticles.

3.3 Magnetic Nanoparticles

Magnetic Nanoparticles have been synthesized with number of different compositions and phases including pure metals like CO, Fe and Ni, metal alloys such as FePt, CoPt [19]. Utilizing attractive nanoparticles molecule size of around 3 nm can be acquired. The size of particles will be hundreds of atoms which enable us to make recording media of up to 1 Tb/in2 in recording density which can be achieved by correctly organizing the particles. Various methods are been reported few among them are coprecipitation, sonochemistry, colloidal method, solvothermal, combustion synthesis, hydrothermal method, micro emulsion and thermal decomposition methods [20].

The critical utilizations of MNPs are in Bio division where the formation of the objective biomolecules and MNPs which are functionalized with explicit receptors, structures edifices and can be without any problem drawn in by the applied attractive field and extricated from the immaculate combination, in this manner giving an advantageous and efficient methodology for bio partition when contrasted with customary technique like centrifugation and filtration. This technology is also used in bio sensing, drug delivery, magnetic resonance imaging and hyperthermia [21].

Fig. 4.
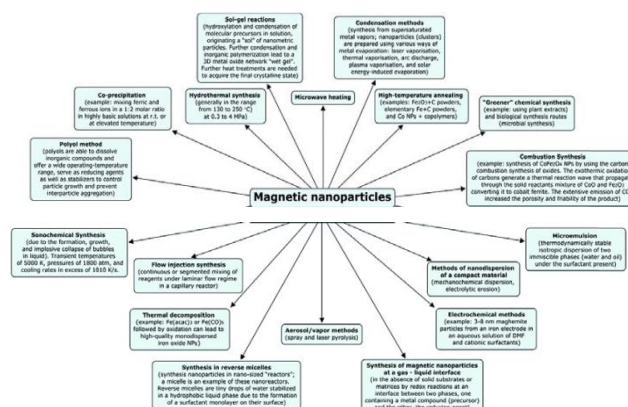
Fig 4: Schematic representation for preparation of Magnetic Nanoparticles.

4. NANOSIZED HERBAL MEDICINES TO CURE CANCER AND OTHER DISEASES:

Herbal drugs/medicines (or herbal remedies) and natural products are being used since ancient times to cure various diseases. In contrast to the current the allopathic framework, the natural medications have hundreds and thousands of constituents that all work together against sickness. The natural products produced by the organisms like fungi, bacteria, animals and plants act as biologically active agents. In contrast to the current the allopathic framework, the home grown medications have hundreds and thousands of constituents that all work together. Mostly, the traditional drugs or pharmacognostical items in the market are established from normal items and their subordinates with natural items are assuming critical part. TQDainst illnesses. Everywhere, the examination on such natural cures has been completed in various regions, e.g., drug store, pharmacology and medication.

Joining of these home grown concentrates into novel definition frameworks is to be done to enjoy benefits and to defeat their mass dosing and less assimilation which is the major problem being faced. A large number of the huge regular items and their determined dynamic parts present in the market are: paclitaxol, doxorubicin (both anticancer medications), lovastatin (anticholesterolemic), erythromycin, streptomycin, rafamycin (all anti-toxins), cyclosporine-A and tacrolimus (both immunosuppressive), and amphotericin-B (fungicidal). Actually, in the context of conventional pharmaceuticals, these drugs have their existence from herbal remedies. Many medications (e.g., asprin, salbutamol, digoxin, quinine, morphine, atropine, colchicine, bromelain, and so on) had been extricated from the plants as their dynamic segments for treating different sicknesses. Morphine was confined as a first medication by Serturner from the plant opium popy (Papaver somniferum) as a pain reliever. Quinine separated from the cinchona tree (Cinchona officinalis) is utilized to treat intestinal sickness, and anti-inflamatory medicine segregated from willow bark is utilized for the therapy of fever. The vast majority of the plants and details (e.g., Curcumin, Triphala, Pomegranate, Kalonji, Sariva, and so forth) have investigated the possibility to fix disease and aggravation [22].

The analysts have removed the fixings from Chinese plants to make another medication to battle against malignancy. By using nanotechnology, the research showed that the herbal drugs are able to enter cancer cells without damaging the healthy cells of the human body. The new medication was created by separating the malignancy battling elements of Chinese spices like milk vetch root, saltwort, cassia twigs and liquor ice root. The natural medication nanotechnology diminished these fixings to their littlest size, empowering them to enter dangerous cells without harming solid cells. It was likewise clarified that the medications first period of creature testing has effectively been effectively finished with the patent rights in 42 nations. This new medication enjoys four benefits: it just kills the dangerous cells; it has fast therapeutic impacts; it doesn't hurt different organs; and it tends to be ingested orally without a physician's oversight. When taken along with western medication, the medication is likewise ready to bring down the measurements and diminish protection from disease drugs, accordingly improving generally speaking effectiveness. During tests, the home grown medication was allegedly observed to be viable in lightening manifestations of the diseases of lung, bosom, bone, liver, tongue, cervix, ovary, mind and skin, and primary or metastatic lymphoma. The Nano herbal drug was also reported to work well, especially against the lymphoma, where the tumor was to have softened, grown smaller in size or disappeared altogether after 2 months of treatment [6].

The profoundly steady micelles with the size of 10 to 40 nm can be ready from poly (ethylene glycol)/phosphatidyl ethanolamine (PEG-PE) forms. These are easily soluble and can firmly retain substantial quantities of various poorly soluble anticancer drugs (m-porphyrin, tamoxifen, taxol). The stable drug-loaded polymeric micelles may represent a convenient drug delivery system into tumours utilizing the enhanced permeability and retention effect [23]. Late advances in drug conveyance frameworks of camptothecin have further developed this drug's proficiency in tumor because of improvement in Nano-sized dose types of camptothecin-determined medications. DNA topoisomerase is one of medication focuses in malignancy treatment. Camptothecin is a plant alkaloid got from the Chinese tree Camptotheca taper. The alkaloid camptothecin caused DNA damage by specifically targeting DNA topoisomerase, effectively devastating a broad spectrum of tumors [24].

Nanotechnology has drafted plant infections for drug conveyance in disease. The specialists have effectively altered a typical plant infection to convey sedates just to explicit cells inside the human body, without influencing encompassing tissue. These little "keen bombs" every one huge number of times less than the width of a human hair-could prompt more powerful chemotherapy medicines with extraordinarily decreased, or even eliminated, side effects. The researchers say that the virus is appealing in both its ability to survive outside of a plant host and its built-in "cargo space" of 17 nm, which can be utilized to convey chemotherapy sedates straightforwardly to tumor cells. The scientists convey the infection by joining little proteins, called "signal peptides", to its outside that influence the infection to "look for out" specific cells, like malignant growth cells. Those equivalent sign peptides fill in as "passwords" that permit the infection to enter the malignant growth cell, where it delivers its freight. Out of various nanoparticles as cell-focusing on vectors utilized, the plant infection is prevalent as far as security, simplicity of assembling, capacity to target cells and capacity to convey restorative payload. Calcium is the key to keeping the virus" cargo enclosed.

At the point when the infection is in the circulation system, calcium is additionally bountiful. Inside the individual cells, be that as it may, calcium levels are a lot of lower, which permits the infection to open, conveying the malignancy sedates just to the designated cells. Another factor that makes the infection exceptional is the sturdiness of its shell. At the point when the infection is in a shut state, nothing will spill out of the inside, and when it opens, it opens gradually, which implies that the infection has time to enter the cell

core prior to conveying its payload, which builds the drug's adequacy. The specialists accept that their technique will lighten the symptoms of normal chemotherapy medicines, while expanding the adequacy of the treatment.

The nanoparticles can be stabilized and targeted to specific cells (such as cancer cells) by attachment of specific proteins to the nanoparticles. Viruses that lack a lipid envelope (i.e., they consist of a genome surrounded by a protein capsid and other protein structures) provide a molecularly precise container of known structure and organization to which targeting molecules can be attached. Encapsidation of different nanoparticles up to 17 nm in width by the 36 nm breadth "Red Clover Necrotic Mosaic Virus" (RCNMV) has been accounted for. This plant virus has a genome consisting of two single strand RNA molecules.

The two genomic RNA atoms structure an intricate that ties the viral capsid protein and starts the gathering of the virion. A little RNA atom that imitates the site on the second genomic RNA needed to start virion assembly can be tethered to various nanoparticles and then serve to initiate virion gathering, shaping uniform infection like particles around 33 nm in distance across marginally more modest than the local infection particles-that encapsidate the nanoparticle inside the protein shell. The relatively small size of the virus-like particles is an advantage because particles in the 30 nm range can be delivered directly to the cell nucleus via the nuclear pore complex. The virus like particles are also sturdy enough to facilitate purification [25].

5. NANOTECHNOLOGY FOR PLANT RESEARCH:
The researchers from Iowa State University have succeeded in using nanotechnology to insert and simultaneously activate genes delivered into the plant cell walls, a discovery that has powerful implications for biotechnology. While the way toward conveying qualities into plant tissue isn't new, it has two phases. First, the gene is inserted into the plant cell tissue; and afterwards, the chemicals are introduced into the plant to trigger the genes function. The two-stage measure has been uncertain as the presence of synthetic substances can be hurtful to the plant. The new breakthrough solution uses what are called "mesoporous nanoparticles". These nanoparticles both present the quality and enact it simultaneously, in an exact and controlled way without harmful impacts.

The scientists could potentially use this as an aid in imaging analysis of plants, which have been activated with the appropriate materials. The nanoparticles are artificially covered and go about as compartments for the qualities that are conveyed to the plants. The coating induces the herbal plants to swallow the particles, effectively ingesting them inside the plant cell walls where the genes could be inserted. The scientists have prevailed with regards to utilizing this innovation to acquaint DNA with tobacco and corn plants, among others. With nanotechnology, the scientists can give a few substances to the plants, at the same time and delivery them in a period controlled way. Having the option to enter the cell mass of plant empowers scholars to see the universe of plant science in the entirety of its unpredictable and multifaceted detail, opening huge new frontiers of discoveries for agriculture and other industries that rely on the biotechnology [6].

A research center examination (at University of Delaware) has shown that the plants can attempt the nanoparticles and amass these nanoparticles in their tissues. It shows that the nanoparticles can enter into human food chain. The significant disservices with these nanoparticles are that the wellbeing hazard related with these particles has not yet been set up. There are many concerns with the use of these nanoparticles, and even they can enter through breathing and can damage our vital organs. The researchers used low frequency monotone for vibrating the dried pumpkin plant and unique magnetic signals were able to reveal the location of nanoparticles inside the plants. The agents further did the exploration on pumpkin filled in sand and soil, and found that there is pretty much nothing and no take-up of nanoparticles in contrast with the solid take-up in pumpkin plants filled in watery arrangement.

The investigators (at Texas Agri Life Research) are planning to use nanotechnology for detecting plant diseases at an early stage, so that tons of food is protected from the possible outbreak. Presently, the detection technique takes days to find plant diseases, but now the researchers are focusing to find a short detection system that can give results within a few hours. For accomplishing this objective, the plant pathologists are holding hands to the nanotechnology trained professionals, so the consolidated endeavors could prompt a superior recognition framework. The analysts are searching for a basic framework that is compact and exact, and doesn't need any confounded procedure for activity, so that even a straightforward rancher can use the portable system and can address the diseases [6].

6. FUTURE PROSPECT OF NANO SIZED HERBAL MEDICINES:
Nano sized herbal medicines can potentially enhance the biological activity and overcome the problems associated with pure herbal drugs. New challenges in the development of nanotechnology based drug delivery

system include the feasibility of scale up process that bring innovative therapeutic techniques to the market quickly, and the probability of getting multifunctional frameworks to satisfy a few organic and remedial prerequisites. Nanoparticles might apply toxicological impact; Nano toxicology has arisen as another part of toxicology for examining unwanted impact of Nanoparticle. In the past, health innovations were evaluated on their efficacy and improved patient quality of life. Currently, health care costs must also be considered. Nano therapeutic products, which are more complex in structure and more expensive than conventional alternatives, are designed to provide an overall reduction in health care costs [26].

7. CONCLUSION:

Nanotechnology has the property of self-targeting in the sense that without the attachment of a specific ligand, the nanoparticles can be used for targeting, due to their distinctively small size, at the infected pathological areas. Treatment of chronic diseases like cancer using targeted drug delivery nanoparticles is the latest achievement of nanotechnology. By analyzing the relationship between nanotechnology and biological medicine, the application of nanotechnological methods for bioavailability enhancement of herbal drugs can be brought about. With the application of nanotechnology of nanomization of herbal drugs, it will make the development of nanoherbal drugs possessing high bioavaibility, which consequently will open the new era of herbal drug discovery. At present, several nano drugs are under investigation for drug delivery and more specifically for cancer therapy.

REFERENCES:

[1]. Sakhare D.T. (2021). Nanotechnology for Herbal Drug and Its Uses, International Journal of Scientific Research in Science and Technology, Vol. 9(4), pp1-7.

[2]. Nalwa, H. S. (2000). Handbook of Nanostructured Materials and Nanotechnology, Vol. 1-5. Academic Press, Boston.

[3]. Poole, C. P. and F. J. Owens (2010). Introduction. In: Introduction to Nanotechnology. Wiley India (P.) Ltd., New Delhi. pp. 1-7.

[4]. Farokhzad, O. C. and R. Langer (2009). Impact of nanotechnology on drug delivery. ACS Nano, 3(1): 16-20.

[5]. Rasheed, A., B. Sravya Reddy and C. Roja (2012). A review on standardisation of herbal formulation. Inter. J. of Phytotherapy, 2(2) : 74-88.

[6]. Garg, G. P. (2010). Nanotechnology in herbal medicines. Herbal Tech Industry (English Monthly Newspaper), March, 2010.

[7]. Kumari, A., V. Kumar and S. K. Yadav (2012). Nanotechnology : A tool to enhance therapeutic values of natural plant products. Trends in Medical Res., 7: 34-42.

[8]. Kesarwani K, Gupta R. Bioavailability enhancers of herbal origin: An overview. Asian journal of tropical biomedicine. 2013; 3(4):253-266.

[9]. Goyal A, Kumar S, Nagpal M, Singh I, Arora S. Potential of novel drug delivery system for herbal system for herbal drugs. Indian journal of pharmaceutical education and research. 2011; 45:225-235.

[10]. Thakur L, Ghodasra U, Patel N, Dabhi M. Novel approaches for stability improvement in natural medicines. Pharmacognosy Reviews. 2011; 5:48-54.

11. Williamson EM. Synergy and other: Interactions in phytomedicines. Andreas Luch. 2001; 8(5):401-409.

[12]. Kumar K, Rai AK. Miraculous therapeutic effects of herbal drugs using novel drug delivery systems. International Research Journal of Pharmacy. 2012; 3:27-33.

[13]. Sharma AT, Mitkare SS, Moon RS. Multicomponent Pharmaceutical Science Review and Research. 2011; 6:185-187.

[14]. Yadev D, Suri S, Choudhary AA, Sikender M, Heman, Beg MN et al. Novel approach, herbal remedies and natural products in pharmaceutical science as nano drug delivery systems. International Journal of Pharm Tech Research. 2011; 3(3):3092-3116.

[15]. Ratnam DV, Ankola DD, Bhardwaj V, Sahana DK, Kumar MN. Role of antioxidants in prophylaxis and therapy: a pharmaceutical prospective. J Control Release. International Journal of Molecular Sciences. 2006; 113:189-207.

[16].Geckeler KE. J. Stirn Polyreaktionen Mechanismen, Systematik, Relevanz. Naturwissenschaften. 1993; 80:487-500.

[17].Wang W. Journal of Colloid and Interface Science, 2008, 323.

[18].Schwarz, James A. Dekker Encyclopedia of Nanoscience and Nanotechnology. Published by Marcel Dekker, New York, 2004.

[19].Iwaki T, Kakihara Y, Toda T, Abdullah M, Okuyama K. Preparation of High Coercivity Magnetic FePt Nanoparticles by Liquid Process. Journal of Applied Physics. 2003; 94:6807-6811.

[20].Sohn BH, Cohen RE, Chem Mater. Processible optically transparent block copolymerfilms containing super paramagnetic iron oxide nano preparation. 1991; 9(1):264-269.

[21].Boris I Kharisov, Rasika Dias HV, Oxana Kharissova V. Solubilization, dispersion and stabilization of magnetic Nanoparticles in water and non aqueous solvent: recent trands. 2014; 4:45354-45381.

[22] Yadav D, Suri S, Choudhary AA, Sikender M, Hemant, Beg NM, et al. Novel approach: Herbal remedies and natural products in pharmaceutical science as nano drug delivery systems. Int J Pharm Technol. 2011;3(3):3092-116.

[23].Gao Z, Lukyanov AN, Singhal A, Torchilin VP. Diacyllipid-polymer micelles as nanocarriers for poorly soluble anticancer drugs. Nano Lett. 2002;2(9): 979-82.

[24].Cuong NV, Hsieh MF, Huang CM. Recent development in Nano-sized dosage forms of plant alkaloid camptothecin-derived drugs. Publishing Technology [Internet]. 2013. Available from: http://www.google.com/ Publishing Technology website.

[25].Nanotechnology drafts plant viruses for drug delivery. Foresight Institute [Internet]. 2013. Available from: http://www.google.com/Foresight Institute website.

[26].Hoet PMH, Brnske HI, Salata OR. Nano particles known and unknown health risk. J Nanobiotecnol. 2004; 2:12.

THIN FILM ELECTROLUMINESCENT DEVICES AND MEDICAL IMAGING RADIATION APPLICATIONS

D. Srinivasa Rao and A. V. Narasimha Rao[*]
Department of Physics, APIIIT Ongole Campus, Ongole, Prakasam Dist, Andhrapradesh, India-523001

ABSTRACT

The phosphor Zn2SiO4:Eu was prepared in the air atmosphere by using solid state reaction method. Its characterization was systematically analyzed by SEM, X-ray diffraction (XRD) and photoluminescence spectra (PL). Photoluminescence emission spectra having excitations at around 254, 268nm revealed that Mn ions were present in trivalent oxidation states. The emission peaks are found at 525 nm(green) are observed. Surface morphology of the present phosphor was analysed by scanning electron microscopy method (SEM). The obtained results on Zn2SiO4:Mn(1.1%) is suitable for green light source using UV light as the primary excitation. So that this compound is used a t medical imaging radiation applications.

INTRODUCTION

Willemite possesses a wide Willemite (α- Zn2SiO4), with phenacite structure occurs naturally and belongs to the group of orthosilicates. According to willemite theory the glass ceramic materials behave different properties like electric insulator, pigments and glazes. Mn-activated willemite (Zn2SiO4 :Mn) is an efficient green phosphor, and it has attracted many researchers for its potential applications to various types of display panels such as plasma display panel ~PDP!, vacuum fluorescent display ~VFD!, and field emission display ~FED!. For enhancing the brightness and resolution of these displays, it is important to synthesize phosphors with high quantum efficiency, controlled morphology and small particle sizes either amorphous or crystalline in nature.Zinc silicate compounds haven been utilized as host materials of lamp phosphors for many years, thanks to their relatively low material cost, and reasonable stability in lamp application. The development of thefirst synthesized aluminates phosphor canbe traced back to 1970. In the 1980's rare-earth- activated aluminate phosphors were practically used in (BAM:Eu) fluorescent lamps. This was the first application of rare-earth-activated aluminates in tri band fluorescent lamps and represented a landmark in this history of fluorescent lamps developed.

Experimental: The starting materials were as follows: Zinc Oxide and Silicon dioxide and the molar ratio of rare earth Manganese oxide MnO (National Chemicals, Baroda, 99.999%) was used to prepare the phosphor .The mixture of reagents was ground together to obtain a homogeneous powder in acetone base. To ensure the best homogeneity we use the stoichiometric ratios by using an agate mortar , powder was transferred to alumina crucible, and then heated in a muffle furnace at 120 °C for 2 hr. The phosphor materials were cooled to room temperature naturally. All samples were found out to be white which are studied for photoluminescence. PL spectra were recorded at room temperature using spectrofluorophotometer.

S.No

Sample

λex

nm   Emission Intensities of different peaks(arb.u)

525 nm

1   Zn2SiO4:Mn(1.1%)   254   841

2   Zn2SiO4:Mn(1.1%)   268   886

S.No	Sample	λ_{ex} nm	Emission Intensities of different peaks(arb.u) 525 nm
1	Zn_2SiO_4:Mn(1.1%)	254	841
2	Zn_2SiO_4:Mn(1.1%)	268	886

Table-1: Intensities of different emission peaks for different excitations of   Zn2SiO4:Mn(1.1%) phosphor
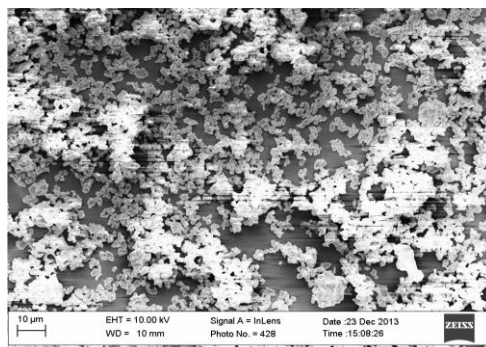
Fig.2: SEM of Zn2SiO4:Mn2+ (1.1%)

CONCLUSIONS:

Zinc silicate doped with Mn2+ phosphors were prepared via high temperature solid state reaction in air medium. Overall results show that the PL intensity monitored at 525nm with 254 nm excitations displays a good green emission from Zn2SiO4:Mn2+ phosphor system. The 4T1(4G)→6A1(6S) transition, is directly responsible for the green light emission at 525nm Zn2SiO4:Mn2+ is suitable for Green light source using UV light as the primary excitation. The morphological investigation of Mn doped Zn2SiO4 was carried out by scanning electron microscopy (SEM). The typical SEM image is shown in Fig. 2. SEM image reveals that the particles size and shape is irregular and size varies from 2-5µm.The phosphor was used at cathode ray tubes and luminescent lamp materials. because of its luminescent efficiency and chemical stability. It has also been tested in thin film electroluminescent ~EL! Devices, medical imaging radiation detectors, medical physics, health physics, radiology, or radiation oncology library. It is also used for scientists and engineers interested in learning about the current state of the art in radiation detectors and their applications in medical imaging.

REFERENCES:

[1] Phosphor Hand book, second edition edited by William M.Yen, Shigeo Shionoya, Hajime Yamamoto.Yen, W.M., and Weber, M.J.,Inorganic Phosphors (Compositions, Preparations and optical properties, CRC press, Boca Ration, 2004.

[2] Murthy, K.V.R. et al, MRB, Vol.41, 10, (2006), 1854-1860.

[3] Murthy, K.V.R., et al Philosophical Magazine Letters, Vol.90, No.9, Sept2010, 653–662.

[4] D.Srinivasa rao., et al Philosophical Magazine Letters, conference jain university, Karanataka,India.

[5] Ch.Kishore Babu, K.V.R.Murthy, B.Subba Rao,P.Sujitha, Synthesis and characterization of SrS: Eu,Ga Phosphor, International Journal on Science Innovations and Discoveries (IJSID)2012,2(3),ISSN: 2249-5347.

[6] Yen, W.M et.al,., Inorganic Phosphors, CRC Press.Boca Raton, FL (USA),(2004).

[7] Maniquiz M C, Jung K Y and Jeong S M 2010, J. Electrochem. Soc. 157 H1135.

[8] Hipolito M G, Ocampo A C, Fregoso O A, Martinez E, Mendoza J G and Falcony C 2004 Phys. Status Solidi a 201 72.

[9] Song H W and Wang J W 2006 J. Lumin. 118 220

[10] Ratinen H 1972 Phys. Solid State A 12 447

[11] Heyes A L, Seefeldt S and Feist J P 2006 Opt. Laser Technol.38 257

[12] Zhu Q, Li J-G, Li X D and Sun X D 2009 Acta Mater. 57 5975

[13] Di W, Wang X, Zhu P and Chen B 2007 J. Solid State Chem.180 467

[14] Wu X L, Li J-G, Li J K, Zhu Q, Li X D, Sun X D and Sakka Y 2013 Sci. Technol. Adv. Mater. 14 015006

[15] Azuel F 2004 Chem. Rev. 104 139

[16] Raukas M, Basun S A, van Schaik W, Yen W M and Happek U 1996 Appl. Phys. Lett. 69 3300 Sci. Technol. Adv. Mater. 16 (2015) 014902

[17] phosphor. D. Srinivasarao National Seminar on Novel Materials for Display Applications, 28 & 29 October, 2010, Sri Velagapudi Ramakrishna Memorial College, Nagaram, Guntur, AP.

[18] D.Srinivasa Rao, P Sai Raju, B.Subba Rao and K. V. R. Murthy International Journal of Luminescence and its applications (IJLA), Volume 4(II), 04/04/2014, ISSN 2277 – 6362 .

[19] SrLa2SiO6:Eu phosphor Synthesis and Characterization K.V.R.Murthy, P. Sai Raju, D. Srinivasarao, Sk. Erfan and B. Subba Rao International Journal of Advanced Research in Physical Science (IJARPS) Volume 2, Issue 1A, PP 119-121, January, 2015 ISSN: 2349-7874 (Print) .

[20] H.R. Taylor et al., Effect of ultraviolet radiation on cataract formation, New Engl. J. Med. 319 (1988), 1429–1133.

[21] B.L. Diffey, Solar ultraviolet radiation effects on biological systems, Phys. Med. Biol. 36 (1991), 299–328.

[22] R. Birkhahn, M. Garter and A.J. Steckl, Red light emission by photoluminescence and electroluminescence from Pr-doped

[23] GaN on Si substrate, Appl. Phys. Lett. 74(15) (1999), 2161–2163.

[24] V.K . Tikhomirov, K. Lakoubovskii, P.W. Hertogen and G.J. Adriaenssens, Visible luminescence from Pr-doped sulfideglasses, Appl. Phys. Lett. 71(19) (1997), 2740–2742.

[25] KVR Murthy, YS Patel, AS Sai Prasad, V Natarajan, AG Page, Radiation measurements 36 (1), 483-485

DEVELOPMENT OF ORGANIC ELECTROLUMINESCENT PHOSPHOR MATERIALS FOR DISPLAY DEVICES

Gajanan D. Zade

Jawaharlal Nehru Art's, Commerce & Science College Wadi, Nagpur, Maharashtra, India

ABSTRACT

An organic light emitting diode (OLED) also known as organic electroluminescent diode is a light emitting diode in which the emissive electroluminescent layer is a film of organic compound that emits light in response to an electric current. This organic layer is situated between two electrodes; typically at least one of these electrodes is transparent. The organic molecules have conductivity levels ranging from insulators to conductors, and are therefore considered as organic semiconductors. Organic semiconductors were synthesised by the method of Friedlander condensation reaction. Originally, the basic polymer synthesised organic material is Diphenylquinoline (DPQ) which consisted of a single organic layer for OLED. The family members of DPQ organic polymers were synthesised by attaching chlorine- methyl, bromine, methyl, methoxy, P- hydroxyl, P-Acetyl-biphenyl and P- Acetyl bi-chlorine to the structure of DPQ at various positions. All the synthesised polymers show crystalline in nature and emits blue colour under UV in various acidic as well as basic solvents like acidic acid, formic acid, chloroform, dichloromethane, tetrahydrofuran etc. The synthesised phosphors were characterised by different techniques, e.g. Fourier Transform infra-red (FTIR), UV- Visible absorption and photoluminescence spectra, X-Ray diffraction spectra (X-RD), Thermo gravimetric analysis (TGA) and Differential thermal analysis (DTA). All The blue emitting organic phosphors has generated considerable interest owing to their good photoluminescence efficiencies.

Keywords— OLED's, Solid state lighting, Friedlander condensation reaction, Organic Phosphors.

INTRODUCTION

Organic light emitting diodes (OLEDs) have gained considerable attention in the last two decades. The field of organic and polymeric light emitting diodes (PLEDs) has progressed rapidly since the initial reports by Tang and VanSlyke and Burroughes et al [1, 2]. Although researcher are trying to improve the quantum efficiency of both photoluminescence (PL) and electroluminescence (EL) OLEDs, the challenges still remain[3].Commonly, the blends of three primary (red, green and blue) or complementary colours (yellow and orange) entail white emission. Among all, the luminous efficiency of blue OLEDs still needs to be improved [4]. Hence it's an urgent task to design novel blue light emission materials which matches with their counterpart with respect to luminous efficiency, lifetime so as to design a stable white emission from them. In this regards, organic phosphors based on quinoline constitute an important class of heterocyclic group and thus generated considerable interest among the researchers globally. Poly (quinoline) s was first reported in the 1970s by Stille and co-workers [5] by employing Frielander condensation as a polymerization step, in order to increase the demands for thermally stable and mechanically strong polymers. The characteristic features make them interesting for electronic and/or electro-optical devices. Prior state of art revels that the researchers have extensively investigated the optical and electronic properties of poly (quinoline) s including photo-conductivity [6], optical nonlinearity [7-10], photoluminescence [11-13], electroluminescence [14-17], Charge transfer [18] and electron transporting properties [19] for their potential applications in OLEDs, organic photovoltaic devices [20].

SYNTHESIS PROCESS

Organic semiconductors were synthesised by the method of Friedlander condensation reaction [21]. The DPQ polymer and their family members were synthesised by taking proper chemical compositions in a three neck flask placed in a oil bath maintained at 90 ^{0}C for one hour and then at 140^{0} C for four hours as shown in figure- 1.
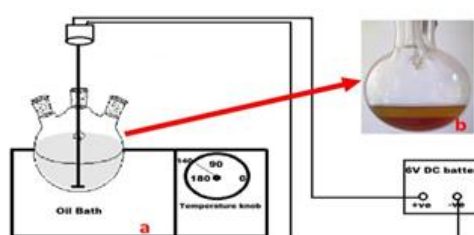
Fig.1 Synthesis process

After completing the heating and stirring process, the flask was taken out of the oil bath for cooling up to eight hours. Organic samples were purified by proper method to get yellowish organic powder. All the derivatives of DPQ couldn't emit light but they are tested for the emission of light in various solvents and they emit blue light under UV source. The structure of synthesised organic material Diphenylquinoline (DPQ) is shown in figure-2.
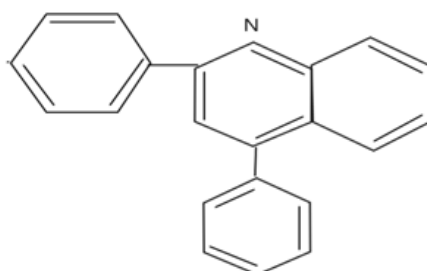
Fig: 2- Chemical structure of DPQ

The synthesised derivatives of DPQ obtained by above mentioned method are chlorine – methyl-Diphenylquinoline, bromine-Diphenylquinoline, methyl-Diphenylquinoline, methoxy- Diphenylquinoline, P-hydroxyl- Diphenylquinoline, P-Acetyl-biphenyl-Diphenylquinoline and P- Acetyl bi-chlorine-Diphenylquinoline.

CHARACTERIZATION

Physical, chemical and optical properties of the synthesized organic phosphor were studied using X-ray diffraction (XRD), Thermo gravimetric and differential thermal analysis (TGA/DTA), Fourier Transform Infrared (FTIR) and photoluminescence (PL) spectra. Well resolved distinct peaks in the XRD pattern of the sample confirm its crystalline nature. The TGA curve infers that the complex maintains its properties with greater stability. DTA curve displays sharp melting point of the samples. FTIR spectra of all the organic derivatives shows proper peaks showing the element attached to the original structure of DPQ with type of bonding. The PL spectrum illustrates strong excitation and emission in the visible range showing blue colour wavelength in the range 365 -460 nm, which lie in the blue region of the electromagnetic spectrum. Figure -3 shows some of the characterization of the organic samples.
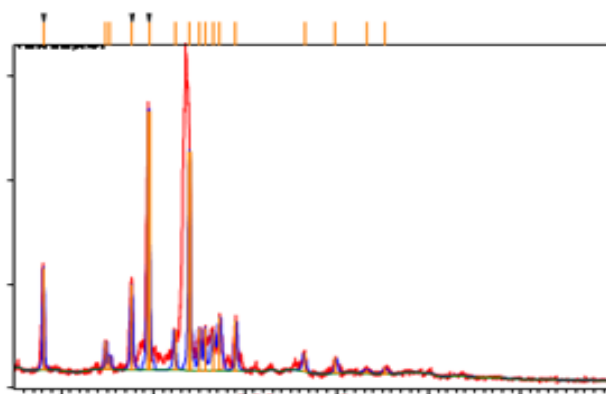
Fig: 3- X Ray diffraction spectra.
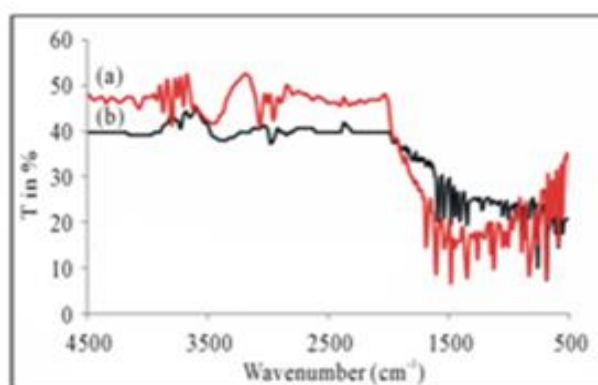
Fig: 4- FTIR Spectra.
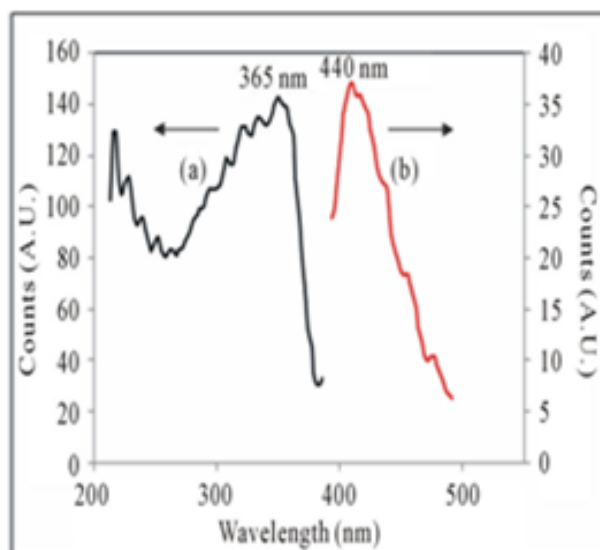
Fig: 5- Emission & Excitation Spectra.
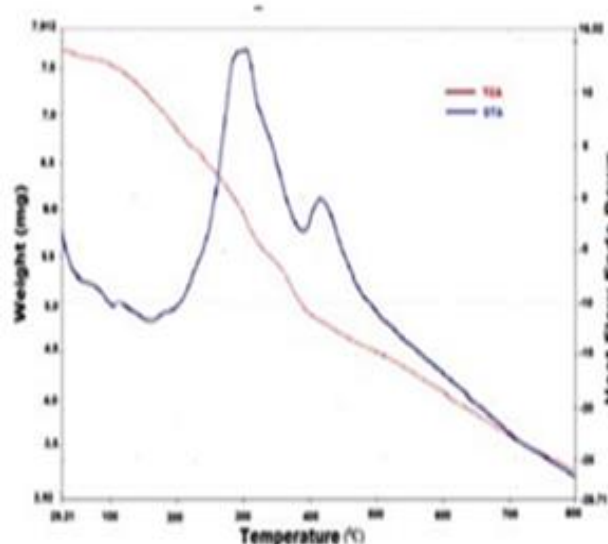
Fig: 6- TGA & SDTA Curve.

RESULT

We have synthesised organic phosphor material DPQ and its derivative by attaching various compounds at different positions to the original structure of DPQ. All the organic compounds shows good thermal stability, sharp melting point in the curve, crystalline in nature. The elements present in the sample was also confirmed from FTIR spectra and shows peaks as per the bonding of the elements. All the samples emits blue colour under UV in various solvents.

CONCLUSION

These results reflect that the synthesised organic phosphor materials can be used as tenable emissive materials in the visible range of blue colour emission in the fabrication of solid state devices and flat panel display.

REFERENCES

1. C. W. Tang and S. A. VanSlyke, Appl. Phys. Lett., 51 **(1987)** 913.

2. J. H. Burroughes, Nature, 347 **(1990)** 539.

3. Yan Zhu, Maksudul M. Alam, and Samson A. Jenekhe, Macromolecules, 36 **(2003)** 8958-8968.

4. G. W. Kang, C. H. Lee, C. Seoul, Inha University, Incheon, Korea, proc.-EL 231 **(2000)** 44.

5. J. K. Stille, Macromolecules, 14 **(1981)** 870-880.

6. K. A. Kim, S. Y. Park, Y. J. Kim, J. Appl. Polym. Sci., 46 **(1992)** 1-7.

7. S. H. Lee, B. K. Rhee, Opt. Quant. Electron 27 **(1995)** 371-377.

8. T. A. Chen, A. K. Y. Jen, Y.M. Cai, Chem. Mater., 8 **(1996)** 607-609.

9. A. K. Y. JAEN, x. m. Wu, H. Ma, Chem. Mater., 10 **(1998)** 471-473.

10. A. K. Agrawal and S. A. Jenekhe, Macromolecules, 26 **(1993)** 895-905.

11. W. Y. Huang, H. Yun, H. S. Lin, T. K. Kwei, Y. Okamoto, Macromolecules, 32 **(1999)** 8089-8093.

12. J. L. Kim, J. K. Kim, H. N. Cho, Macromolecules, 33 **(2000)** 5880-5885.

13. J. L. Kim, H. N. Cho, J. K. Kim, S. I. Hong, Macromolecules, 32 **(1999)** 2065-2067.

14. X. Zhang, A. S. Shetty, S. A. Jenekhe, Acta. Polym., 49 **(1998)** 52-55.

15. T. W. Kwon, M. M. Alam, S. A. Jenekhe, Chem. Mater., 16 **(2004)** 4657-4666.

16. X. J. Zhang, S. A. Jenekhe, Macromolecules, 33 **(2000)** 2069-2082.

17. X. J. Zhang, A. S. Shetty, S. A. Jenekhe, Macromolecules, 32 **(1999)** 7422-7429.

18. S. A. Jenekhe, L. D. Lu, M. M. Alam, Macromolecules, 34 **(2001)** 7315-7324.

19. C. J. Tonzola, M. M. Alam, B. A. Bean, S. A. Jenekhe, Macromolecules, 37 **(2004)** 3554-3563.

20. M. M. Alam, S. A. Jenekhe, J. Phys. Chem. B., 105 **(2001)** 2479-2482.

21. G. D. Zade, S. J. Dhoble, S. B. Raut, R. B. Pode, J. Mod. Phy. 2 **(2011)** 1523-1529).

22. S. Y. Mullemwar. G. D. Zade, N. Thejo Kalyani, S. J. Dhoble, International Journal of Luminescence and Its applications 6 (2016) 68.

23. N. Thejo Kalyani, S. J. Dhoble, R. B. Pode, J. Korean Physical Society, 57 (4) 92010) 746.

24. H. K. Dahule, N. Thejo Kalyani, S. J. Dhoble, Luminescence, 30 (2015) 405-410.

25. S. Y. Mullemwar, G. D. Zade, N. Thejo Kalyani, S. J. Dhoble, Optik, Volume 127, Issue 22, 2016, 10546-10553.

THE IMPACT OF TRANSITION METAL, CU2+ SUBSTITUTION ON THE STRUCTURAL, OPTICAL AND ELASTIC PROPERTIES OF FERRIMAGNETIC NICKEL FERRITES

H.S. Ahamad[1], N.S. Meshram[2], K.G. Rewatkar[3] and S.J. Dhoble[4]
[1]St. Francis De Sales College, Seminary Hills Nagpur -440006, India
[2,3]Dr. Ambedkar College, Deekshabhoomi, Nagpur-440010, India
[4]P.G.T.D. Physics, RTM Nagpur University, Nagpur-440033, India

ABSTRACT

Spinel nano-ferrites with the general chemical formula Ni(1–x)CuxFe2O4 (x = 0.0, 0.2, 0.4, 0.6, 0.8, and 1.0) were synthesized by sol-gel microwave-assisted auto-combustion method. Samples were calcined at 800 oC for 4 hours in the air. X-ray diffraction (XRD) study was carried out to establish phase and structural analysis. A phase transformation from cubic to tetragonal was observed for x = 0.8 and x = 1.0 of Cu2+ ion substitution. The particle size of the ferrites samples was calculated using Scherrer's formula and Williamson-Hall's (W-H) Method. For the concentration of Cu2+ ion on lattice parameter, X-ray density bulk density, and dislocation density, lattice strain, and hopping radius was calculated for the samples. Nelson-Riley (N-R) Functions were plotted for the accurate estimation of lattice parameters. The optical nature of the samples was studied from ultraviolet-visible (UV-vis) spectroscopy. Tauc's plots were employed to estimate the optical band gap for the samples. FTIR study was used to confirm the presence of tetrahedral and octahedral sites and to determine force constants and investigate the elastic properties. The study shows the structural, optical, and elastic properties of Nickel ferrites are highly influenced by Cu2+ substitution.

Keywords— Copper-Nickel ferrite, Sol-gel synthesis, X-ray diffraction, Jahn-Teller effect, Elastic properties, Debye Temperature

INTRODUCTION

Copper ferrites have been of special interest in the recent past. Cu2+ (3d9) is John–Teller active ion and results unexpected properties [1,2]. It is different than other spinel ferrites in two ways (i) it has distorted tetragonal structures at low temperatures and (ii) its inability to have a cation to oxygen ratio higher than 0.75 [3,4]. Properties of copper ferrites are highly dependant on synthesis methods and heat treatment given to them [5,6]. It has a stable tetragonal structure with space group I41/amd (141) at room temperature and changes into cubic phase around 400 oC temperature due to cooperative John-Teller distortion [7]. Study of crystalline field symmetry indicates that if John-Teller active cation is present at the tetragonal site then the tetragonal ratio, c/a < 1 and if John-Teller active cation is present in the octahedral site then, c/a > 1 [6]. The tetragonal phase in copper ferrite evolves due to distortion along one of the axes of the octahedron, originated due to the occurrence of Cu2+ ions (3d9), inducing the cooperative Jahn-Teller (J-T) deformation as an elimination of the eg orbital degeneracy [8,9]. As Cu2+ and Fe3+ cations occupy the B-sites (i.e. same sites) in the distorted tetragonal CuFe2O4, the unit cell is often represented having, Fe3+ ions same distortion, even though the crystal-field stabilization energy (CFSE) is related with the distortion at the Fe3+ (3d5) sub-lattice is zero [10–12]. The conventional high-temperature synthesis with maintained stoichiometry and slow cooling favours a tetragonal structure like hausmannite with space group I41/amd (141) containing four formula units of CuFe2O4 (Z = 4) with unit cell parameters $a = b = 0.581\,nm$ and $c = 0.868\,nm$ so that tetragonal ratio, c/a ~1.50. If the value of the tetragonal ratio, c/a > 1 then, the majority cation distribution of Cu2+ ions resides in octahedral sites [11,13]. For convenience, often this unit cell is represented by tetragonally distorted, non-standard face-centered spinel unit cell with space group F41/ddm with lattice constant, $a' = a(2)^{0.5} = 0.822\,nm$ and $c' = c = 0.868$ nm so that, c/a ~1.056 [1,13–15]. The tetragonal c/a ratio is strongly influenced by Cu2+ distribution, sintering temperatures, and rate of cooling. Quenching of Cu ferrites compels to freeze some of the Cu2+ ions in tetragonal sites resulting in less tetragonal distortions promoting a more cubic phase [1,16]. Copper ferrite has an almost entirely inverse spinel structure. In the cubic phase, there are more cupric ions at the tetrahedral site than in the tetragonal phase and hence cubic phase possess a greater magnetic moment than the tetragonal [17,18]. Nickel ferrite is inverse spinel ferrites with nickel ions (Ni2+) are located in the B-sites and ferric ions (Fe3+) occupying both A-sites and B-sites. Ni-ferrites possess high electrical resistivity and low eddy current, large magnetic permeability at high frequencies, low dielectric loss, and good chemical stability at relatively low cost [19–22]. Cu2+ being J-T active as well as its possible to occupy either of the two available sites, tetrahedral or octahedral, replacement of Ni2+ and Fe3+ with Cu2+ in Ni ferrite may favorably cause structural phase transition, influencing structural, physical, magnetic, electrical, and optical properties useful in fundamental science and technological applications [23–28]. One important

observation is seen that copper ferrite CuFe2O4, which has a tetragonal structure, acquires a cubic structure with the substitution of Ni2+ due to the cooperative J-T effect i.e. more structural symmetry is achieved with the addition of nickel [29]. Copper-doped nickel ferrites exhibit an important role amongst magnetic materials owing to their high electrical resistance, high saturation magnetization, and high magnetic permeability. Although Cu substituted Ni ferrites have been investigated extensively by many researchers employing different synthesis methods, according to the author, the elastic and optical properties of Cu-Ni ferrites by sol-gel with microwave-induced auto-combustion synthesis method with CO(NH2)2 as fuel is not reported in detail. Nickel ferrite doped with different copper content is expected to have properties of mixed, copper-nickel ferrites. Some interesting new properties with the advantages of both the ferrites may be useful in many scientific and technological applications [30–32]. And, therefore the present paper focuses on the synthesis of nanostructured nickel ferrites with different compositions of copper (x = 0.0, 0.2, 0.4, 0.6, 0.8, 1.0) by microwave-assisted sol-gel auto-combustion method with urea as fuel. Here we discuss the substitution of Cu2+ in Ni ferrite matrix and its effect on structural, optical, and elastic properties.

EXPERIMENTAL

The samples of spinel ferrite with formula CuxNi1-xFe2O4 (x = 0.0, 0.2, 0.4, 0.6, 0.8, 1.0) were synthesized by microwave-assisted sol-gel auto-combustion technique[33,34]. The preparation of the nano-ferrites method involved the auto-combustion reaction of redox mixture, in which metal nitrates worked as an oxidizing and urea as a reducing reactant [35,36]. The composition of precursor nitrates and fuel, CO(NH2)2 was based on the total oxidizing and reducing valency of the oxidizers using the chemistry of propellants [36,37]. The stoichiometric amounts of AR grade Ni(NO3)2.6H2O, Cu(NO3)2.3H2O, Fe(NO3)3·9H2O, and CO(NH2)2 dissolved in a minimum quantity of de-ionized water at room temperature in a beaker. The solution was continuously stirred for 15 minutes and then heated on a magnetic stirrer with a hot plate at 70 oC for about 4 hours to get a viscous gel. The gel was then exposed to microwaves in an oven operating at 2.45 GHz. Spontaneous self-combustion of the gel starts within 1-2 minutes and starts to burn spontaneously at a temperature above 10000C releasing a high amount of heat and a large number of gases (N2, NH3, and CO) and converts into floppy ash [36]. The complete combustion process, which produces nanostructured nickel-copper ferrite powders in a microwave oven, requires about 4 min [36,38–40]. This burnt ferrite was then crushed and milled for 4 hours in an agate mortar into a fine powder. Milling also promotes the homogeneous mixing of any un-reacted oxides and reduces the particle size [41]. The ferrite powders were then sintered at 8000C for 4 hours in a muffle furnace. Sintered powder samples were then mixed with polyvinyl alcohol (PVA) as a binder and palletized to the size of 13mm diameter with a Hydraulic Press Machine at 30-ton pressure. The pallets were then heated at 400 oC for 2 hours to remove the binder.

CHARACTERIZATION

The X-ray diffraction measurement of the nano ferrite samples was carried out on Bruker AXS D8 advanced X-ray diffractometer operating at 35KV, 15mA with a monochromatic X-ray source at CuK_α-radiation $\left(\lambda = 1.54056\,\text{Å}\right)$. The measurement was done in the range of the Bragg angles $10°$ to $80°$ with step size $0.020o$. The 2θ vs. intensity data is as shown in XRD figures. All Bragg reflections have been indexed using MDI JADE 5.0 and X- powder software. The optical nature of the sample was studied by UV-Vis analysis study. FTIR analysis was carried out to confirm the presence of tetrahedral and octahedral sites and to study the elastic properties of the samples.

RESULT AND DISCUSSION

Structural Analysis

The Bragg reflections of all the samples, obtained in X-ray diffraction (XRD) patterns have been indexed which included (111), (220), (311), (400), (511) or (333) and (440) planes, which confirm the formation of spinel structure with space group Fd$\overline{3}$m (227) for samples x = 0.0, 0.2, 0.4, and 0.6 were matched to ICDD card # 00-010-0325. The strongest Bragg reflection comes from the (311) plane of all the cubic samples and (211) plane in tetragonal structures (for samples x = 0.8, 1.0). The sample with composition x = 0.8 i.e. Cu0.8Ni0.2Fe2O4 showed mixed-phase i.e. tetragonal and cubic phase, with space groups, I41/amd (141), which matched to ICDD card # 00-034-0425 of tetragonal CuFe2O4 and cubic Nickel ferrite (Trevorite), ICDD card # 00-010-0325 with space group $Fd\overline{3}m$ (227). Also, a small third phase of CuO has been observed for sample x = 0.8. In sample (x = 1.0) i.e. CuFe2O4 has a single-phase distorted tetragonal structure with body-centered space groups, I41/amd (141), which matched to ICDD card # 00-034-0425 of tetragonal CuFe2O4. The strongest reflection in samples x = 0.8 and x = 1.0 were observed to originate from (211) planes. The distorted tetragonal structures for samples x = 0.8 and x = 1.0, are considered due to cooperative John-Teller

distortion which is believed to be an order-disorder phenomenon whose exact nature is still to be completely explored [1,42].

Fig. 1(a)
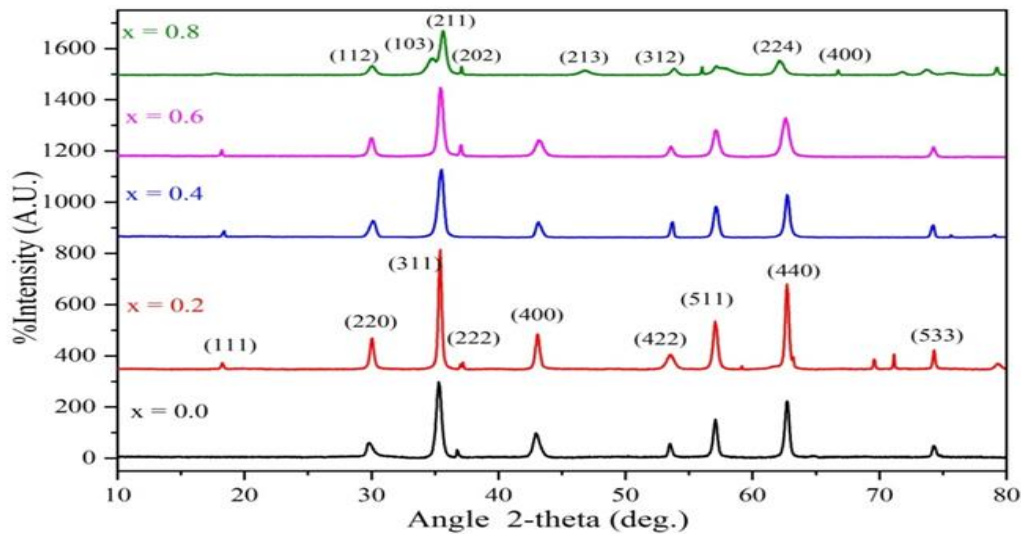
Fig 1(b)
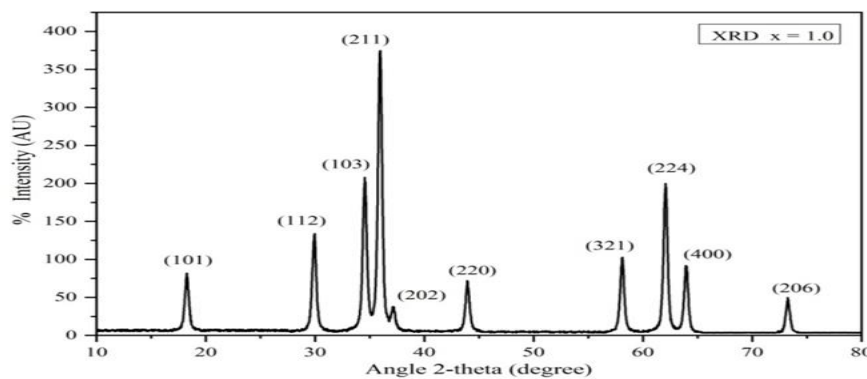
Fig. 1: X-ray diffraction patterns of CuxNi(1-x)Fe2O4 for (a) x = 0.0, (b) x = 1.0

The X-ray diffraction patterns of CuxNi(1-x)Fe2O4 are shown in figures (a) for x = 0.0, 0.2, 0.4, 0.6, 0.8 and in figure 1(b)   for x = 1.0 .The average crystallite size of the samples was calculated from the most intense peaks (311) for cubic samples x = 0.0, 0.2, 0.4, 0.6) using Scherer's formula[43],

$$D = \frac{0.9\lambda}{\beta\cos\theta}$$

(1)

while taking into account the instrumental broadening [44,45]. Here $\lambda = 1.54056\,\overset{o}{A}$ is the wavelength of monochromatic X-ray of CuK_α radiation, 2θ is Bragg's diffraction angle and β is full width at half maxima (FWHM) in radian of most intense Bragg's diffraction peak.

To take into account the lattice strain of the sample, Williamson–Hall (W-H) method was employed. In the W-H method, the integral breadth of the diffraction peak is used for the estimation of crystallite size. The integral breadth of a peak is the integrated intensity divided by maximum intensity [46]. The observed peak broadening, Bo, maybe written as,

$$B_o = B_i + B_{CS}$$

Here Bi is the instrumental broadening, already explained above, and B_{CS} is the broadening due to the small size of crystallites and lattice strain. This equation is only true for a diffraction peak with a purely Cauchy profile. If we consider the diffraction peak consists of partly Cauchy profile and partly Gaussian profile, the following equation provides a better estimate [47],

$$\beta_{CS}^2 = \left[\left(\beta_o - \beta_i \right) \left(\beta_o^2 - \beta_i^2 \right)^{1/2} \right]^{1/2}$$

The peak broadening due to the fine size of crystals, β_C according to Scherrer's formula is,

$$\beta_C = \frac{K\lambda}{D\cos\theta}$$

Where K is the shape factor also known as Scherrer's constant, K = 0.94 for spherical shape with cubic symmetry nanoparticles.

The broadening of the peak due to lattice strain (β_S), according to Wilson [48] may be expressed as

$$\beta_S = \varepsilon \tan\theta$$

Here ε is the lattice strain in the material. The net peak broadening β_{CS} is, therefore,

$$\beta_{CS} = \beta_C + \beta_S$$

$$\beta_{CS} = \frac{K\lambda}{D\cos\theta} + \varepsilon \tan\theta$$

$$\beta_{CS} \cos\theta = \frac{K\lambda}{D} + \varepsilon \sin\theta \qquad (2)$$

A graph of $\beta_{CS} \cos\theta$ against $\sin\theta$ for all the diffraction peaks of the samples plotted gives an equation of the straight line of the form, y = mx + c with a slope equal to micro-structural strain, m $= \varepsilon$ and intercept, $C = \frac{K\lambda}{D}$, from which average crystallite size D, can be estimated [49,50]. The W-H plots are shown in figure 2. The crystallite size for different samples is summarized in table 1. The samples x = 0.2 and x = 0.4 show negative slopes or negative microstrain in W-H plots indicating the elastic contraction of crystal lattice [51]. The crystallite sizes obtained by the W-H method and Scherer formula for the (311) plane are listed in table 1. It is seen that the crystallite size obtained from the W-H method is larger than Scherrer's formula.

LATTICE PARAMETER
Lattice parameters were estimated from inter-planer spacing d for all samples. For the synthesized materials, x=0.0, 0.2, 0.4, 0.6 having cubic symmetry and inter-planer spacing, d and lattice constant, a are related by the relation,

$$\frac{1}{d^2} = \frac{h^2 + k^2 + l^2}{a^2} \qquad (3)$$

For most intense (311) plane above expression of lattice constant reduces to $a = d\sqrt{3^2 + 1^2 + 1^2} = d\sqrt{11}$. Volume of unit cells for these cubic sample, x = 0.0, 0.2, 0.4, 0.6 is calculated by using relation $V = a^3$. The samples, x = 0.8 and x = 1.0 exhibit tetragonal structures, inter-planer distance d and lattice parameter a are related by relation

$$\frac{1}{d^2} = \frac{h^2 + k^2}{a^2} + \frac{l^2}{c^2} \qquad (4)$$

The volume of the unit cell with tetragonal symmetry was estimated by using relation, $V = c \times a^2$ in the case of tetragonal samples. The volume of the unit cell decreases as lattice constants decrease with the increment of copper. The indexed d–values and lattice parameters and volume of unit cell V of samples are summarized in table format (Table 1). In general, in a solid solution of spinel ferrites within miscible limits, a linear variation in lattice parameters with the concentration of the Cu components is seen [52]. The lattice parameter a was observed to increases as the concentration of copper increases except for x = 0.6 and follow Vegards' law as reported by others [53]. The linear increase in lattice constant is due to the replacement of the Ni2+ cations having a smaller ionic radius (0.069 nm) by Cu2+ cations which has relatively larger ionic radius (0.073 nm)

and due to the replacement of some Fe3+ ions from tetrahedral A site to octahedral B site [54–56]. To estimate the precise lattice parameters of the unit cell for samples, the Nelson-Riley extrapolation technique was employed. The values of lattice parameter, calculated, from each crystal plane are plotted against Nelson-Riley (N-R) function,

$$F(\theta) = \frac{1}{2}\left[\frac{\cos^2\theta}{\sin\theta} + \frac{\cos^2\theta}{\theta}\right] \qquad (5)$$

The corrected value of lattice parameter is obtained with extrapolation for $F(\theta)=0$ or $\theta=0$ [57,58]. The N-R functions for the samples x = 0.0, x = 0.2, and x = 0.6 are shown in the figure 4 and the extrapolated values of the lattice parameter are listed in the table 1.

X-ray diffraction study and lattice parameter analysis of the

Fig 2(a)

samples x = 0.8 and 1.0 indicates a tetragonal unit cell with space group I41/amd (141). For convenience, the Jahn-Teller distorted tetragonal unit cell of the samples x = 0.8 and x = 1.0 can be represented by tetragonally distorted, non-standard face-centered spinel unit cell with space group F41/ddm with $a' = \sqrt{2} \times a = 1.414213 \times a$ and $c' = c$ which yields a' = 8.2652 $\overset{o}{A}$ and c = 8.6304 $\overset{o}{A}$ for the sample x = 0.8 and a' = 8.2753 $\overset{o}{A}$ and c' = 8.6854 $\overset{o}{A}$ for x = 1.0 sample. The corresponding unit cell volumes for x = 0.8 and x = 1.0 are 589.57 ($\overset{o}{A}$)3 and 594.78 ($\overset{o}{A}$)3 respectively. The tetragonal ratio for the unit cell, c/a for the sample x = 0.8 and 1.0 are 1.0442 and 1.0496 respectively. The ratio c/a >1 indicates John-Teller distortion in these samples x = 0.8 and 1.0 are accompanied by an expansion in the structure at octahedral positions and most of the Cu2+ ions are present in the octahedral sites [13]. Due to the structural phase transition of the John-Teller effect in the lattice, the Oxygen framework at the octahedral sites gets distorted and the orbital degeneration of electron states is removed by the system to attain the minimum total energy state [59].

Specific surface area (SSA) of nano-materials belongs to a property of solids defined as the total surface area per unit of mass. Assuming the particles to be spherical, the specific surface area in m2/g of the ferrite powdered sample was evaluated by using the Sauters' relation,

$$SSA = \frac{6000}{\rho_x D} \qquad (6)$$

Where, ρ_x is the X-ray density in g/cm3, D is the crystallite size in nm. The variation of specific surface area and dislocation density with Cu content is shown in figure 4.5.

The length of dislocation lines per unit volume gives the number of dislocation density or defect in the crystal lattice is estimated using relation [60].

$$\delta = \frac{1}{D^2} = \left(\frac{\beta\cos\theta}{0.9\lambda}\right)^2 \qquad (7)$$

Dislocation density is maximum for sample with x = 0.8 and least for the x = 0.2

Fig 1(b)

Fig 2(e)

Fig 2(c)

W-H plot for x = 0.4
D = 20.6 nm
$\varepsilon = -5.4 \times 10^{-3}$

Fig 2(d)

W-H Graph for x = 1.0
D = 22.4 nm
$\varepsilon = -6.01 \times 10^{-3}$
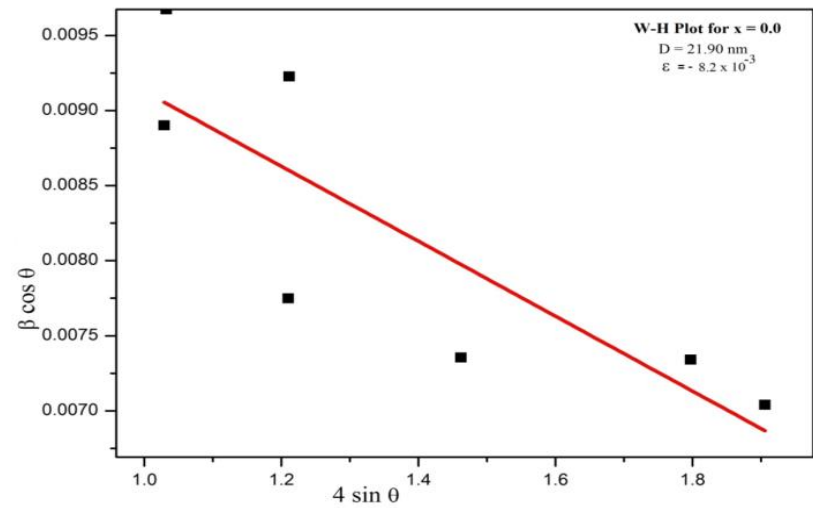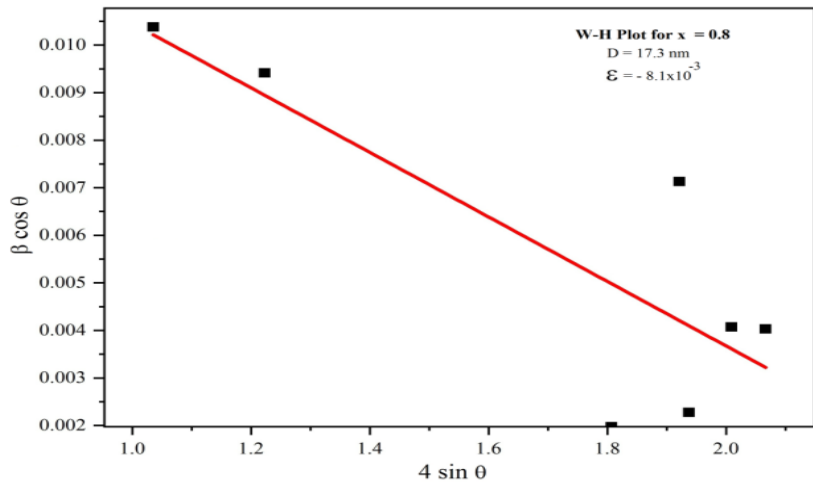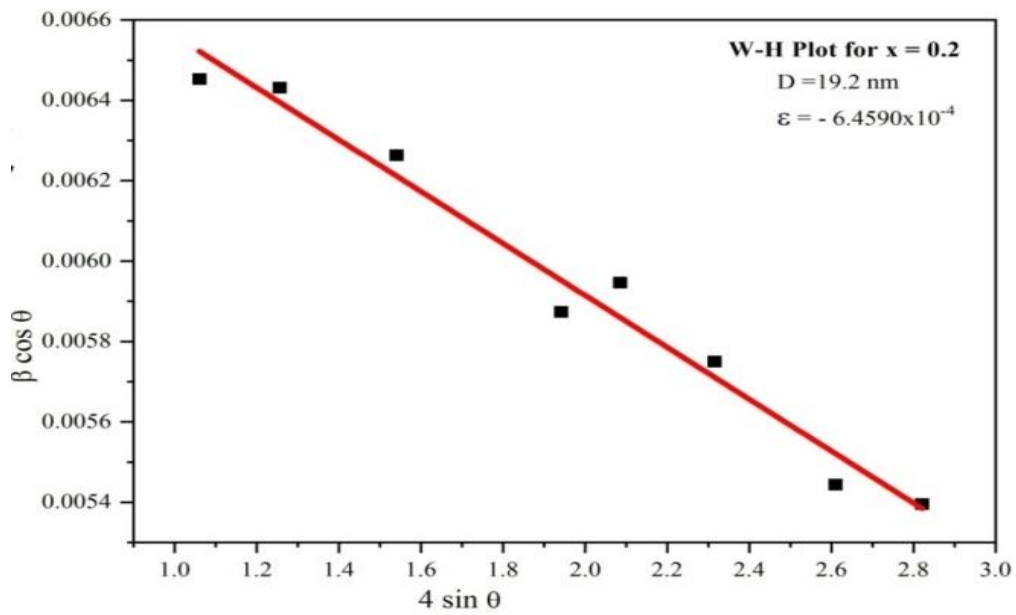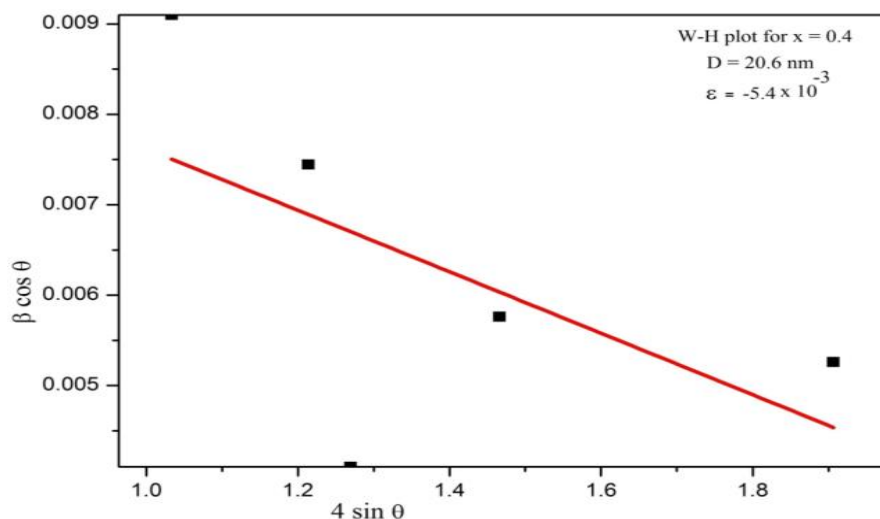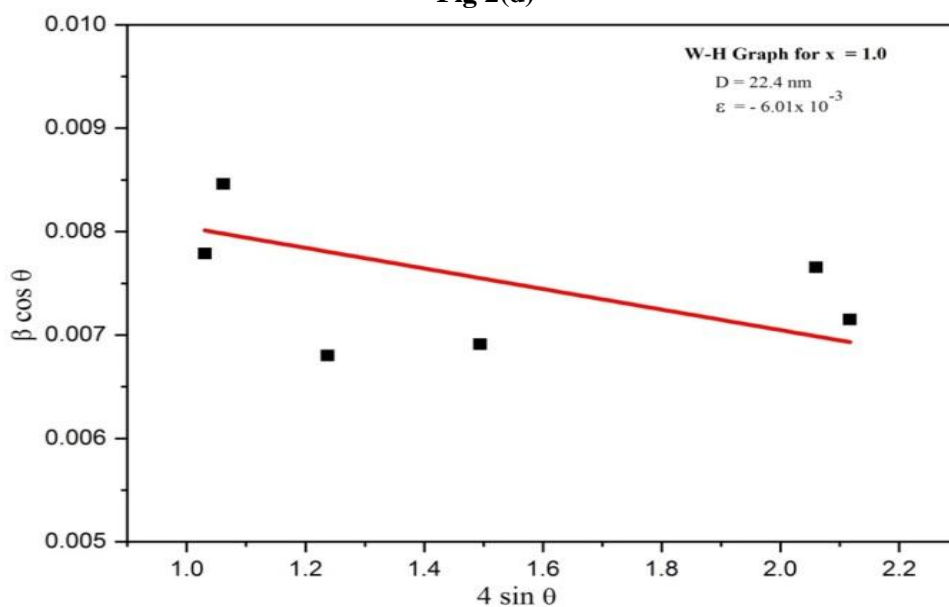
Fig 2(f)

Fig 2 Plot of crystallite size of synthesized nanoparticles vs Cu content

W-H Plot for x = 0.6
D = 18.2 nm
$\varepsilon = -7.2 \times 10^{-3}$
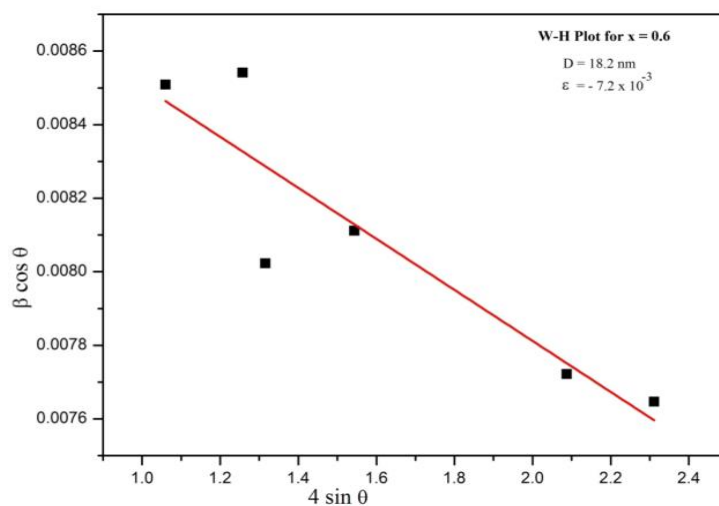
Fig 2: Williamson-Halls' plots for CuxNi(1-x)Fe2O4 for 2(a) x=0.0, 2(b) 0.2, 2(c) 0.4, 2(d) 0.6, 2(e) 0.8 and 2(f) x = 1.0

Fig 3(a)
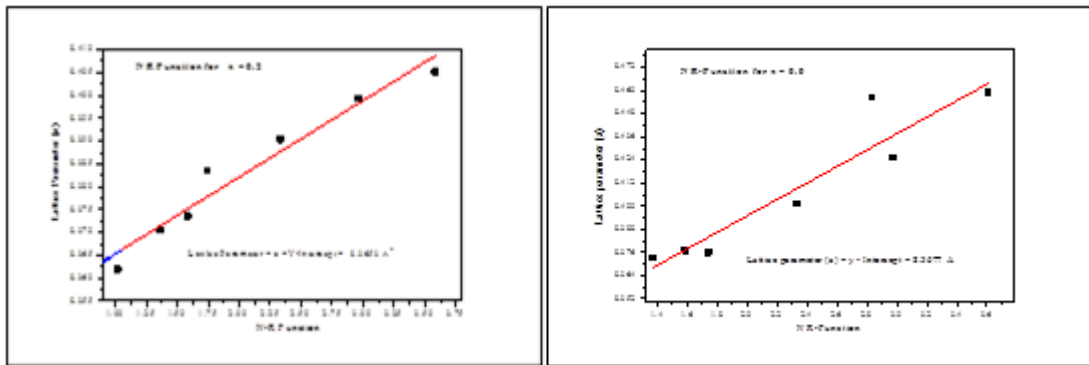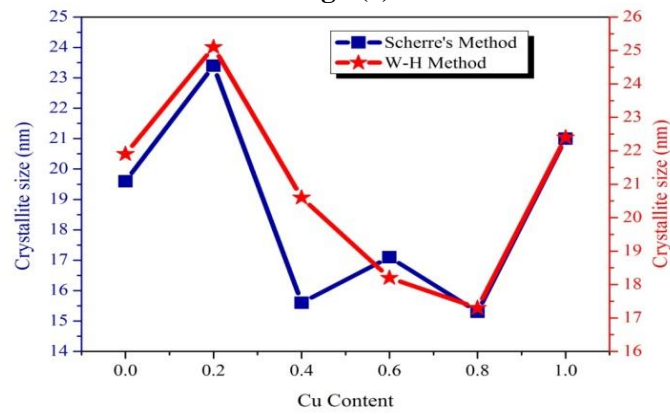
Fig 4(b)   **Fig 4(c)**
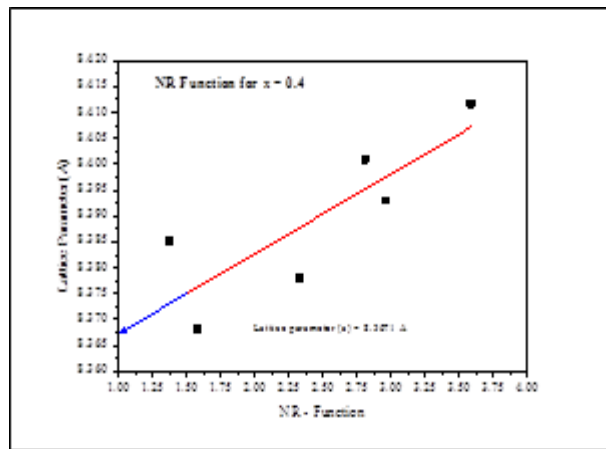
Fig 4(d)

Figure 4: N-R Function for (a)x = 0.0, (b) x= 0.2, (c) x = 0.4 and (c) x= 0.6
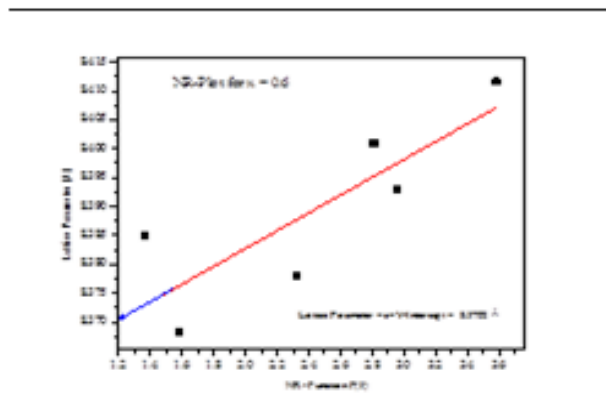
Figure 4: N-R Function for (a)x = 0.0, (b) x= 0.2, (c) x = 0.4 and (c) x= 0.6

TABLE 1 STRUCTURAL AND PHASE PARAMETERS OF THE SAMPLES CuxNi(1-x)Fe2O4

Parameter / Sample		x = 0.0	x = 0.2	x = 0.4	x = 0.6	x = 0.8	x = 1.0
2- theta		35.307	35.415	35.435	35.443	35.620	35.984
Interplaner spacing d (Ao) (311) plane		2.5400	2.5325	2.5311	2.5306	2.5184	2.4937
FWHM (degree) (311) plane		0.450	0.387	0.448	0.510	0.567	0.410
Space group		Fd$\bar{3}$m (227)	Fd$\bar{3}$m (227)	Fd$\bar{3}$m (227)	Fd$\bar{3}$m (227)	I41/amd (141)	I41/amd (141)
Lattice Constants (Ao)	By usual Method	8.3390	8.3867	8.4150	8.3950	a=b=5.8444 c = 8.6304 c/a = 1.477	a=b= 5.8515 c = 8.6854 c/a = 1.484
	By NR-Function	8.3677	8.3653	8.4157	8.3704	---	----
Volume of unit cell (A3)		579.89	589.89	595.89	589.77	294.79	294.27
Crystallite size D (nm)	Scherrer's Method	19.6	23.4	19.8	17.1	15.3	21.0
	W-H Technique	21.90	25.1	20.6	18.2	17.3	22.4

Density and Porosity

Density and porosity play a significant role in deciding the properties of the spinel ferrites the two quantities are related inversely [61]. The porosity of the magnetic material is an important micro-structural aspect that affects the movement of the domain wall and the pores which form pin the domain wall resulting in their motion. Actual density (X-ray density) ρ_X of the synthesized samples was estimated using relation given by Smit and Wijn [62],

$$\rho_x = \frac{Z\,M}{N_A\,V} \qquad\qquad (8)$$

Where M is the molecular weight of the sample, NA is the Avogadro's number (6.023 x 10-23), Z is the number of chemical formula units in the unit cell of spinel ferrites, Z = 8 for cubic samples (x = 0.0, 0.2, 0.4, 0.6) and for tetragonal samples i.e. for (x = 0.8 and x = 1.0), Z = 4 formula units. X-ray density of the samples initially decreases up to x = 0.4 and is then found to increases with increment in Cu content. An increase in X-ray density with Cu content can be attributed to the higher density of Cu (8.95 g/cc) than Ni (8.09 g/cc). The bulk density (ρ_B) of the samples were calculated by relation,

$$\rho_B = \frac{m}{\pi\,r^2\,h} \qquad\qquad (9)$$

Measuring mass (m) using precision electronic balance and volume by measuring height (h) and radius (r) using electronic screw gauge of the samples in the form of cylindrical pallets. It was found that bulk density increases with the increase of Cu up to x = 0.8 beyond which, the Cu bulk density is observed to decrease which is expected due to structural phase transition from cubic to tetragonal due to cooperative Jahn-Teller effect. The variation of X-ray density and bulk density with Cu content is shown in figure 7.

The porosity of nanomaterials is quantified by the void fraction in a material. Percentage porosity of the nano ferrites samples was determined using relation,

$$P = \left(1 - \frac{\rho_x}{\rho_B}\right) \times 100 \qquad\qquad (10)$$

The variation of % porosity and strain with the Cu content is shown in figure 8.

The bulk density (ρ_B) of the samples were calculated by relation, $\rho_B = \frac{m}{\pi r^2 h}$, measuring, mass (m) using precision electronic balance and volume by measuring height (h) and radius (r) using electronic screw gauge of the samples in the form of cylindrical pallets. It was found that bulk density increases with the increase of Cu

up to x = 0.8 beyond which, the Cu bulk density is observed to decrease which is expected due to structural phase transition from cubic to tetragonal due to cooperative John-Teller effect. The variation of X-ray density and bulk density with Cu content is shown in figure 6. The porosity of nanomaterials is quantified by the void fraction in a material. Percentage porosity of the nano ferrite samples was determined using relation,

$$P = \left(1 - \frac{\rho_B}{\rho_x}\right) \times 100 \qquad (11)$$

The variation of % porosity with the Cu content is shown in the graph 5.

Average lattice strain was calculated by Stoke-Wilson's equation [63,64],

$$\varepsilon = \frac{1}{2} \times \frac{FWHM}{\tan\theta} \qquad (12)$$

The estimated values of strain with Cu2+ substitution is listed in table 2. The strain is minimum -0.646×10^{-4} for the sample x = 0.2. Negative strains for all the samples indicate the contraction in the lattice. The hopping length is the distance among the centers of adjacent magnetic ions. The hoping lengths for tetrahedral A- site (LA-A), and octahedral B-site (LB-B) was determined using relations, $L_{AA} = \frac{\sqrt{3}}{4}\,a$, $L_{BB} = \frac{\sqrt{2}}{4}\,a$ and $L_{AB} = \frac{\sqrt{11}}{8}\,a$. The variation of hoping length with Cu composition is shown in figure 9.

Fig 4 Variation of lattice constant a with composition for cubic samples
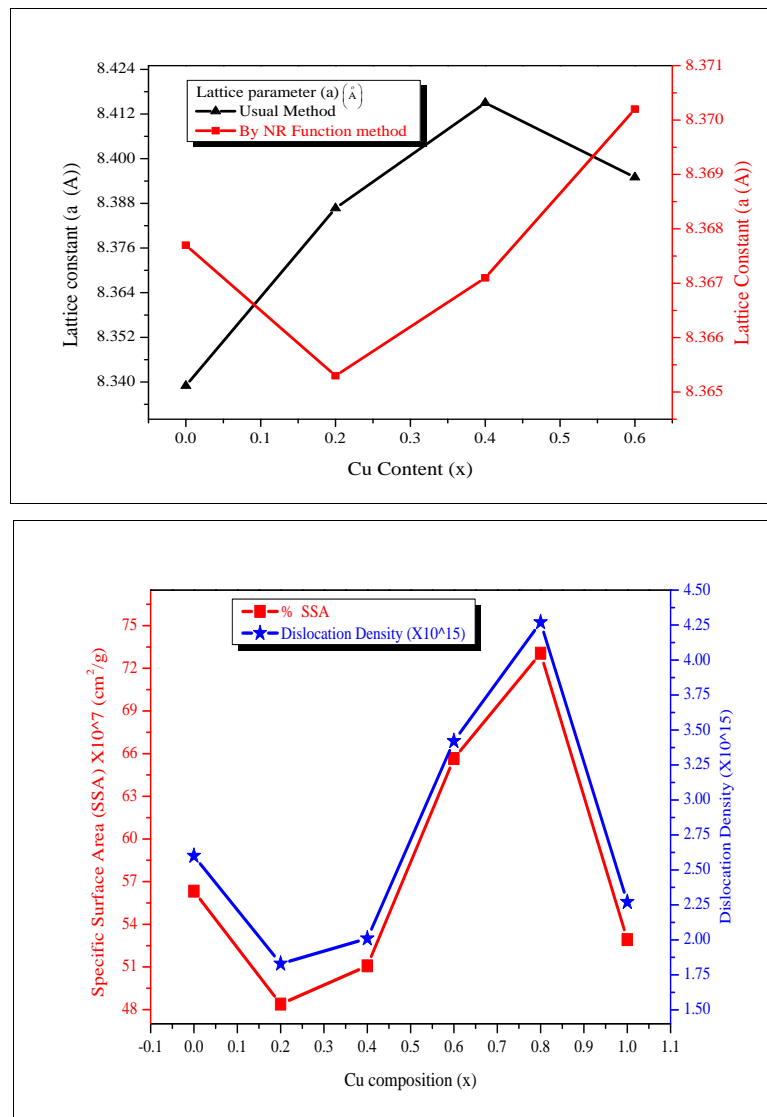
Fig 5 Specific surface area and dislocation density vs. Cu composition
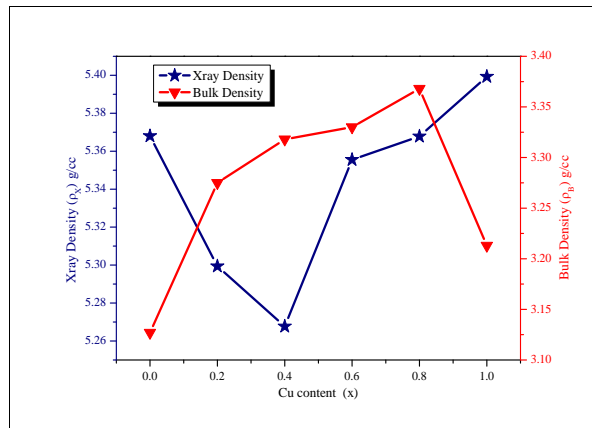
Fig 6 X-ray density and Bulk density vs. composition
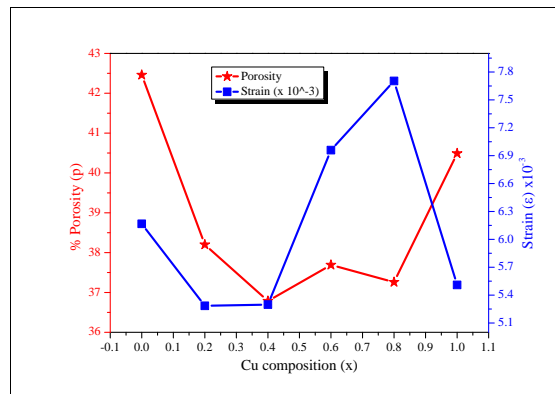
Fig 7 Porosity and strain vs. composition for CuxNi(1-x)Fe2O4
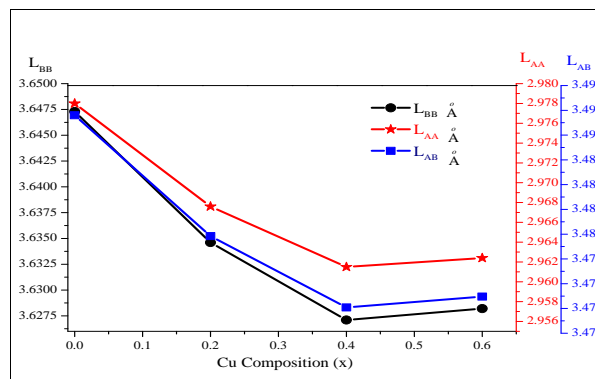
Figure 8 Variation of hopping lengths LAA , LBB and LAB with Cu composition for cubic Ni(1−x)CuxFe2O4 samples

TABLE 2 MICRO-STRUCTURAL PARAMETERS OF THE SAMPLES CuxNi(1-x)Fe2O4

Parameter / Sample		x = 0.0	x = 0.2	x = 0.4	x = 0.6	x = 0.8	x = 1.0
Strain ε	Scherrer's Method (x 10-3)	6.167	5.29	5.30	6.96	7.70	5.51
	W-H Method (x10-3)	-8.21	-0.646	-5.43	-7.22	-8.17	-6.01
Dislocation Density $(\frac{1}{D^2})$ x1015		2.603	1.83	2.55	3.42	4.27	2.268
Density	X-Ray Density, ρ_X g/cc	5.368	5.30	5.27	5.36	5.37	5.40
	Bulk Density ρ_B g/cc	3.127	3.28	3.318	3.33	3.368	3.21
% Porosity P		42.46	38.20	36.79	37.69	37.26	40.5
Hoping Length LAA (Ao)		2.9780	2.9676	2.9615	2.9624	--	--
Hoping Length LBB (Ao)		3.6473	3.6346	3.6271	3.6282	--	--
Hoping Length LAB (Ao)		3.4920	3.4798	3.4726	3.4737		
SSA m2/g		93.9273	58.9734	90.5367	74.211	89.3473	52.9199

Optical Analysis (UV-Visible Study)

UV-Visible spectra of all the samples show strong absorption in the wavelength range 700nm-230nm which decreases with the wavelength as can be seen in figure 10. The absorption in the visible region by the ferrite is attributed to electron excitation from the O-2p level into the Fe-3d level which is observed for the spinel-type compound [34,65,66]. A broad range of optical absorption indicates a quantum confinement effect due to the wide variation in the size of nanoparticles [67]. From the spectra, it is observed that the edge shifted towards the

higher frequency side indicating a blue shift with the substitution of Cu2+. The optical band gap energy, E_g of the nano-ferrites were obtained by Tauc's model by extrapolation of the absorption edge given by the equation,

$$(\alpha h\nu)^n = C(h\nu - E_g) \qquad (13)$$

Here $h\nu$ is the photon energy, α is the absorption coefficient, C is a constant, and n is another constant which depends on the nature of the transition of the electron. As Cu-Ni ferrite posseses direct band gap, n = 2 [68,69].

The Tauc's plot for the sample x = 0.2 is shown in figure 11. The extrapolated E_g and its variation with the Cu content is listed in table 3 and is shown in figure 12. E_g is maximum for the sample with x = 0.0 which can be attributed to the absence of metal cation Cu2+ and is minimum for the sample with x = 0.4. According to Al-Hazmi, Al-Ghamdi et al. [70] study of $Cu_xNi_{1-x}Fe_2O_4$ synthesized via mechano-chemical root the optical bandgap of the samples decreases sharply from 2.62eV to 1.95 eV for $0 \leq x \leq 0.5$ with Cu2+ substitution and it decreases slowly from 1.95 to 1.57eV for $0.5 \leq x \leq 0.9$. In our study, there are sharp decreases in E_g from 2.14eV to 1.77eV with Cu2+ substitution can be attributed to the cation migration from octahedral to tetrahedral sites which causes single-phase cubic structure of Ni(1–x)C uxFe2O4 whereas, there is a slite increase in E_g from 1.77eV to 1.87 as the Cu2+ is increased from x = 0. to x = 0.8 which is expected due to phase transition from cubic to tetragonal structure. The estimated values of the optical bandgap for different samples are listed in table 3.

FTIR Study

A Fourier Transform Infrared spectrum of the samples was recorded in the range 400 to 4000 cm-1 and is shown in the figure16. Absorption bands in the range 400 to 700 cm-1 are the characteristic bands of the spinel ferrites. There are two main bands of frequencies, stretching vibrational frequencies, ν_1 around 600 cm-1 corresponding to tetrahedral site and relatively lower stretching vibrational frequencies, ν_2 around 400 cm-1 corresponding to octahedral site. The shorter stretching vibrational frequencies of the octahedral site than the tetrahedral site is attributed to the smaller bond length of the tetrahedral site than octahedral sites. The variation in bond lengths of the ions occupying the sites has resulted in the change in vibrational frequencies [81,82,87]. The frequencies 1628.6 cm-1 and 1521.17 cm-1 indicates the small presence of stretching vibrations due to moisture (H–O–H) in the sample x = 0.8 and the frequency 3445.31 cm-1 indicates bending vibrations due to small O-H molecules [83,84].

The absence of other peaks confirmed the organic sources were removed from the calcined samples [86]. To determine the strength of bonding at higher and lower stretching vibrational frequencies the force constant at

tetrahedral and octahedral lattice sites were calculated using the relation $F = 4\pi c^2 \nu^2 \mu$, where c is the speed of light $c = 2.99 \times 10^{10}$ cm/s, ν is the vibrational frequency of stretching vibrations corresponding to tetrahedral or octahedral sites, and μ is reduced mass of Fe3+ and O2- ions ($\mu = 2.601 \times 10^{-23}$ g) [85]. The tetrahedral and octahedral vibrational frequencies ν_1, ν_2 and the corresponding calculated values of the force constants of these samples are listed in table 3.
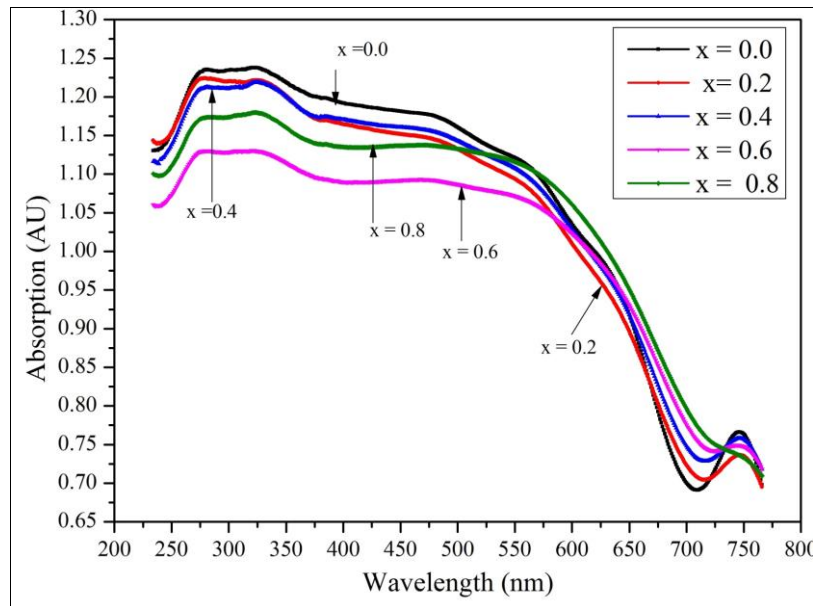
Fig 9 UV-Visible absorption of Ni(1–x)CuxFe2O4 samples, x = 0.0, 0.2, 0.4, 0.6 , 0.8

Elastic Properties

Infrared (IR) spectroscopic analysis of the solid samples can be extended to obtain the elastic and thermal properties of the spinel ferrites. The conventional method to study the elastic properties of solids is the ultrasonic (US) technique which requires the large quantity of samples (about 10 mm thickness) through which ultrasonic waves are passed to measure the velocity of the wave. In most cases, the synthesized sample quantity is very little. IR method provides reliable elastic properties with advantages over ultrasonic (US) technique [71]. The Debye temperature is an essential property of a solid material that co-relates its elastic properties to thermal characteristics such as specific heat [17,18]. It is the temperature at which lattice vibrations occur with the highest amplitude and sets the limit below which the quantum effects are effective. According to Waldron, the Debye temperature of the samples can be calculated from the relation [19]

$$\theta_D = \frac{h c v_{tO}}{2 \pi k_B} = 1.438 \, v_{tO}$$

(14)

where v_{tO} is the average wave number corresponding to the stretching vibration of the tetrahedral and octahedral sites, $v_{tO} = \dfrac{v_1 + v_2}{2}$, c is the speed of light in free space ($c = 3 \times 10^8$ m/s, k_B is the Boltzmann constant $k_B = 1.38 \times 10^{-23} \, J/K$, h is Planck's constant $h = 6.624 \times 10^{-34} \, J-s$.
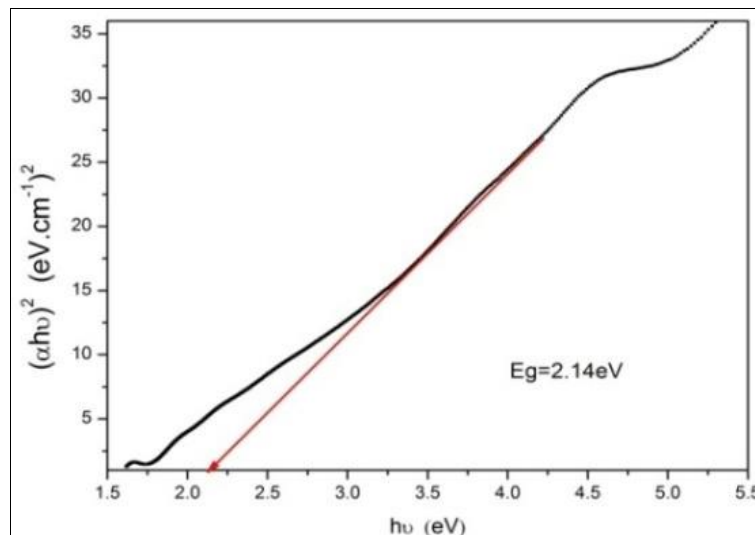
Fig 10(a)
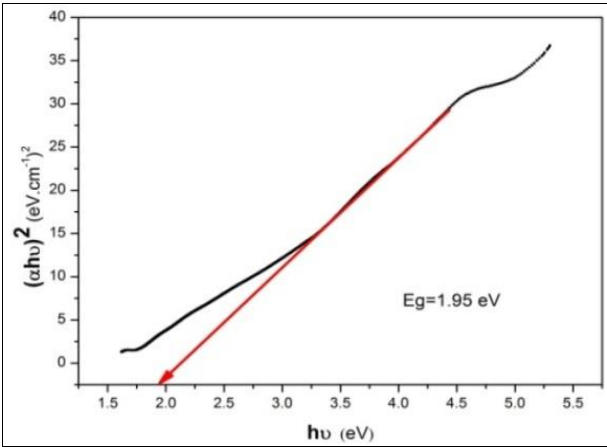
Fig 11(b)
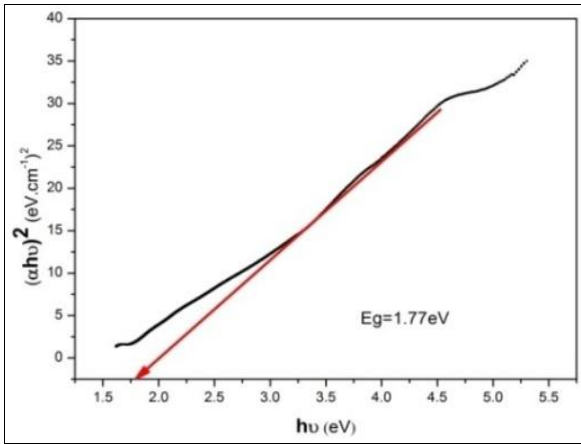
Fig 11(c)
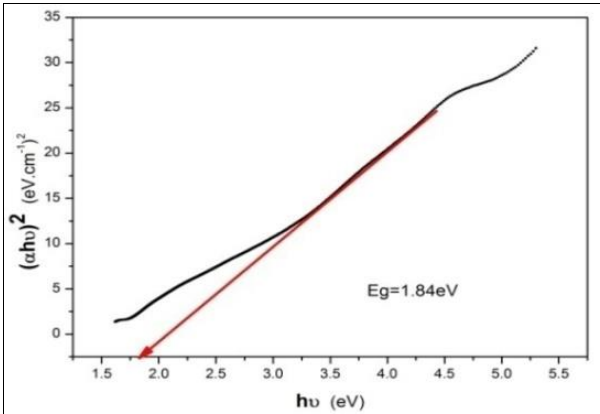
Fig 11(d)
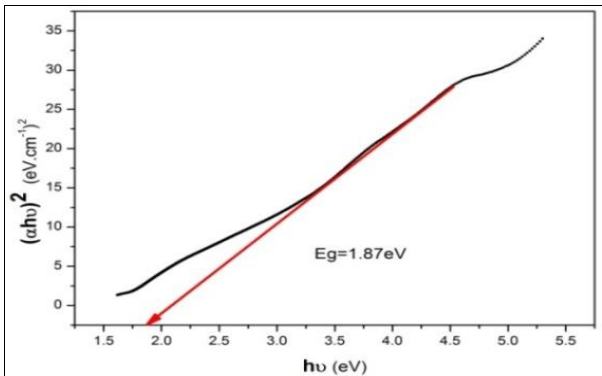
Fig 11(e)

Figu 11: Tauc's plot for Ni(1–x)CuxFe2O4 sample x = 0.0, 0.2, 0.4, 0.6 and 0.8
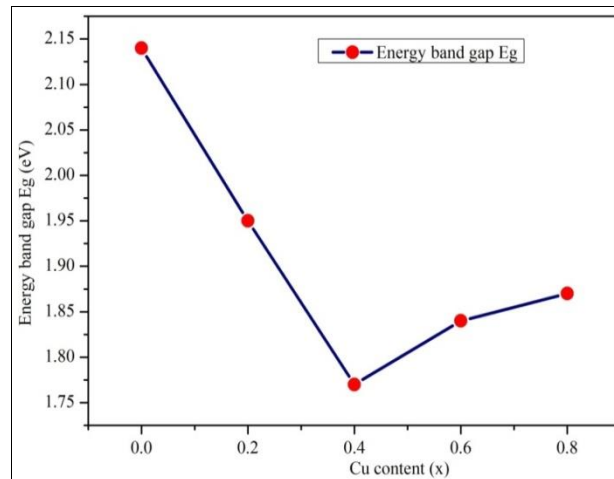
Figure 11 Variation of Energy band gap Eg for Ni(1–x)CuxFe2O4

Composition x	Eg Eg (eV)	Tetrahedral wave number ν_1	Octahedral wave number ν_2	Force constant for tetrahedral site Ft ($\times 10^5$) dyne/cm	Force constant for octahedral site Fo($\times 10^5$) dyne/cm	Debye temperature θ_D (K)
0.0	2.14	599.78	410.78	3.307	1.551	726.59
0.2	1.95	595.92	406.9	3.264	1.522	721.03
0.4	1.77	601.71	399.21	3.328	1.465	719.66
0.6	1.84	595.9	401.14	3.264	1.479	719.75
0.8	1.87	524.57	424.28	2.530	1.655	682.22

The Debye temperature of the samples was observed to decrease with the Cu2+ substitution. The estimated values of the Debye temperatures are listed in table 4. The decreased θ_D indicates the there is a decrease in rigidity of the synthesized nano ferrites and lattice vibrations. The decrease in θ_D implies an increase in the conduction electron (increase in n-type charge carriers). These conduction electrons are responsible for the absorption of heat causing a decrease in Debye temperature. The decreased Debye temperature indicates the increased electrical conductivity due to the enhanced number of electrons in these samples [72].

Relation (2) given above assumes Uniform Deformation Model (UDM) which considers uniform strain in all directions in a crystal. From well known Hooks law of elasticity within the elastic limit, the average force constant $F_{av} = \dfrac{F_t + F_o}{2}$ is the product of stiffness constant (C11) and lattice parameter (a) estimated from XRD data and therefore,

$$C_{11} = \frac{F_{av}}{a}$$

(15)

The Poisson's ratio (σ) is related to pore fraction or porosity (P) and is given by $\sigma = 0.324(1 - 1.043P)$. σ lies within range -1 to 0.5. Another stiffness constant C12 is given by,

$$C_{12} = \frac{\sigma C_{11}}{1 - \sigma}$$

(16)

The different elastic moduli of cubic structures, Young's Modulus (E), Bulk modulus (B), and rigidity modulus (G) is given by

$$E = \frac{(C_{11} - C_{12})(C_{11} + 2C_{12})}{C_{11} + C_{12}}$$

(17)

$$B = \frac{(C_{11} + 2C_{12})}{3}$$

$$(18)$$
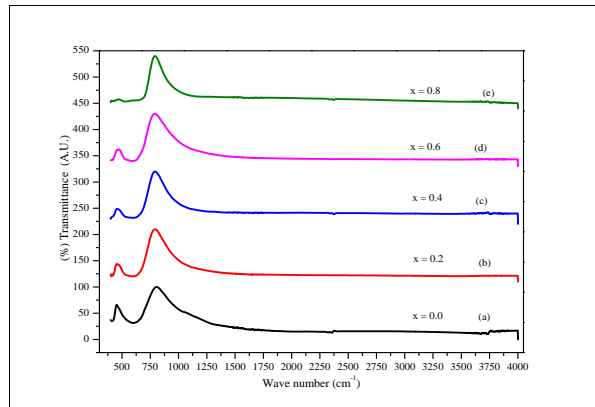
Figure 12 FTIR transmittance spectrum vs. wave number

TABLE 3 STRETCHED VIBRATIONAL FREQUENCIES, FORCE CONSTANT OF TETRAHEDRAL AND OCTAHEDRAL SITES, OPTICAL BAND GAP (EG) OF SAMPLES AND DEBYE TEMPERATURE.

TABLE 4 STIFFNESS CONSTANTS C11, C12 , POISSON RATIO (σ), YOUNG'S MODULUS (E), BULK MODULY (B) AND SHEAR MODULUS (G), RIGIDITY MODULUS WITH ZERO POROSITY (GO)

x	C11	C12	σ	Elastic Modulii (in GPa)			
				E	B	G	Go
0.0	291.28	64.34	0.181	268.0	139.99	113.47	787.13
0.2	285.33	69.24	0.195	258.29	141.27	108.05	460.74
0.4	284.79	71.21	0.200	256.30	142.40	106.79	404.18
0.6	282.49	69.30	0.197	255.18	140.37	106.59	434.61
0.8	252.86	62.60	0.199	228.01	126.02	95.13	374.05

TABLE 5 LONGITUDINAL WAVE VELOCITY (VL) , TRANSVERSE OR SHEAR WAVE VELOCITY (VS) AND MEAN ELASTIC VELOCITY (VM) AND LAME'S CONSTANT (λ_L)

	Elastic wave velocities (in m/s)			$\lambda_L (\times 10^9)$
x	Vl	VS	Vm	kg/m-s2
0.0	7366.32	4252.95	5502.89	97.09
0.2	7337.33	4236.21	5481.23	95.11
0.4	7351.17	4244.20	5491.57	94.93
0.6	7259.70	4191.39	5423.24	94.16
0.8	6862.05	3961.81	5126.18	84.29
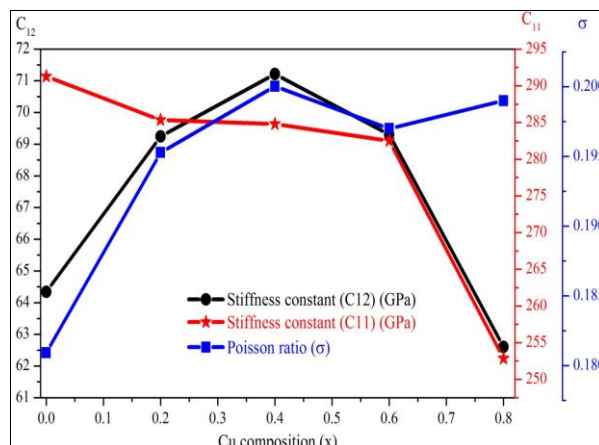
Figure 13 Variation of elastic parameters C11, C12 and Poisson ratio σ with Cu composition
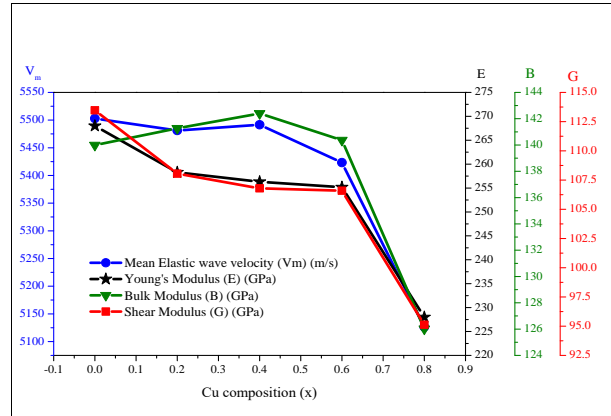
Figure 14 Variation of elastic parameters E , B, G and Vm with Cu composition
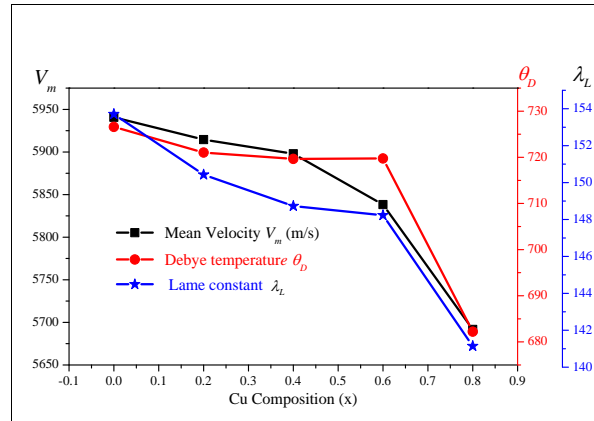
Figure 15 Variation of elastic parameters Vm , θ_D and λ_L with Cu composition

For isotropic materials with cubic symmetry like spinel ferrites, $C11 \approx C12$ so that bulk modulus is approximately equal to the stiffness constant (i.e. $B \approx C11$).

And

$$G = \frac{(2\sigma - 1)C_{11}}{2(\sigma - 1)} \qquad (19)$$

Rigidity modulus with zero porosity (Go) is given by

$$\frac{1}{G_o} = \frac{1}{G}\left[1 - \frac{15P(1-\sigma)}{7-5\sigma}\right] \qquad (20)$$

The longitudinal elastic wave velocity (Vl), transverse or shear wave velocity (VS), and the mean elastic wave velocity (Vm) are given by

$$V_l = \left(\frac{C_{11}}{\rho_x}\right)^{1/2} \qquad (21)$$

$$V_s = \left(\frac{G_o}{\rho_x}\right)^{1/2} \qquad (22)$$

$$V_m = \left[\frac{1}{3}\left(\frac{2}{V_s^3} + \frac{1}{V_l^3}\right)\right]^{-1/3} \qquad (23)$$

And Lame's constant was calculated λ_L [73] from the relation

$$\lambda_L = \left(V_l^{\ 2} - 2\ V_S^{\ 2} \right) \rho_x \qquad (24)$$

The estimated values of the stiffness constants C11, σ, E, B, G, and Go are presented in table (5) and Vl, VS, Vm and are presented in table λ_L 6. It can be seen that the Poisson ratio (σ) has values between 0.181-0.200 which are in a well-consistent range of -1 to 0.5 indicating the validity of the theory of elasticity for isotropic solids. The variation of C11, C12, and Poisson ratios is shown in figure 17. The stiffness constants C11 decreases whereas C12 increases with the Cu increment. In general stiffness, constants indicate the tightness of atomic boding in a solid. A decrease in C11 with an increment of Cu indicated a weakening of atomic bonding. The variation of Vm, E, B, and G with the Cu composition is shown in figure 18. Young's module (E) and shear or rigidity modulus (G) decrease with the Cu substitution. The decrease in E and G is with Cu is small till x = 0.6 and is rapid for the sample x = 0.8 which can be attributed to the J-T structural phase transition from cubic to the tetragonal structure.

For estimating the elastic parameter for an isotropic solid like spinels and garnets with cubic symmetry Ravinder et al. [74,75] and Mazen et al. [76] have used the assumption C11$\approx$C12 which leads to a relatively larger error. Anupama et al. [77] suggested an improvement to the calculations by considering C11$\approx$3C44 and C12$\approx$C13$\approx$C44. The average force constant was then, $F_{av} = \dfrac{F_t + 2F_o}{3}$. The average stiffness constant in terms of the average force constant is given by $C_{av} = \dfrac{F_{av}}{a}$. The stiffness constants C11 and C12 are obtained using relations $C_{11} = (9/5)C_{av}$ and $C_{12} = (3/5)C_{av}$. The bulk modulus B is obtained using approximation, $B \approx C_{av}$. The longitudinal and shear wave velocities are obtained using relations $V_l = \sqrt{\dfrac{C_{11}}{\rho_x}}$ and $V_S = \sqrt{\dfrac{C_{12}}{\rho_x}}$ respectively [78]. The mean elastic wave velocity (Vm) is estimated using equation (23).

TABLE 6 AVERAGE FORCE CONSTANT (FAV'), AVERAGE STIFFNESS CONSTANTS (CAV'), STIFFNESS CONSTANTS (C11', C12'), POISSON RATIO (σ'), YOUNG'S MODULUS (E'), BULK MODULY (B') AND SHEAR MODULUS (G'), RIGIDITY MODULUS WITH ZERO POROSITY (GO'), LONGITUDINAL WAVE VELOCITY (VL') , TRANSVERSE OR SHEAR WAVE VELOCITY (VS') , MEAN ELASTIC VELOCITY (VM) AND LAME'S CONSTANT (λ_L) BY ANUPAMA ET. AL METHOD.

Parameter	Sample				
	x = 0.0	x = 0.2	x = 0.4	x = 0.6	x = 0.8
Fav ($\times 10^5$) (dyne/cm)	2.14	2.10	2.09	2.07	1.95
Cav (GPa)	256.19	250.71	247.89	247.05	235.24
C11 (GPa)	461.13	451.29	446.20	444.69	423.43
C12 (GPa)	153.71	150.43	148.73	148.23	141.14
Vl (m/s)	9268.46	9227.58	9201.55	9108.52	8879.80
VS (m/s)	5351.15	5327.55	5312.52	5258.81	5126.75
Vm (m/s)	5940.79	5914.59	5897.90	5838.27	5691.67
B (GPa)	256.19	250.71	247.89	247.05	235.24
G (GPa)	153.71	150.43	148.73	148.23	141.14
E (GPa)	363.04	359.61	356.97	354.87	338.31
σ	0.25	0.25	0.25	0.25	0.25
λ_L (GPa)	153.71	150.43	148.73	148.23	141.14

The Young's modulus (E) and shear modulus (G) are estimated using equations

$$G = V_s^{\ 2} \times \rho_x \qquad (25)$$

$$E = 2G(1+\sigma) \qquad (26)$$

With Poisson's rati

$$\sigma = \frac{3B - 2G}{6B + 2G} \qquad (27)$$

The estimated values of the Fav', Cav', C11', C12', Vl', VS', Vm', B', G', E', σ' and λ_L' are presented in table 6. The values obtained are much higher than the Ravinder et. al. method. The variation of elastic parameters however is more systematic in this method. In case of Modi et. al method the bulk modulus increase slightly initially with Cu2+ till x = 0.4 and then decrease for the samples x = 0.6 and x = 0.8. However, in the present method, the values of B decrease systematically. The trend of variation in other elastic parameters is also more systematic. The values σ remain constant at 0.25 for all the samples, indicating better results.

CONCLUSIONS

Copper substituted Nickel nano-ferrites with the general chemical formula Ni(1–x)CuxFe2O4 (x = 0.0, 0.2, 0.4, 0.6, 0.8, and 1.0) were synthesized successfully by sol-gel microwave auto-combustion method, using urea as a chelating agent. X-ray diffraction study of the synthesized nano ferrites had shown that mean crystallite size between 15-25 nm. The samples x = 0.0, 0.2, 0.4, 0.6 exhibited cubic phase with space group (space group $Fd\bar{3}m$ (227). The lattice parameter increases with the substitution of Cu2+. The samples x = 0.8 and x = 1.0 exhibited mixed tetragonal and cubic phases with space group I41/and (141) due to John-Teller distortion. The ratio c/a >1 confirmed that majority of the Cu2+ ions occupy octahedral sites in tetragonal phase of the sample x = 0.8 and x = 1.0. An optical study by UV-Visible spectroscopy suggested the semiconducting behavior of the Ni(1–x)CuxFe2O4 with optical band gap 1.77-2.14 eV. FTIR analysis confirmed the existence of tetrahedral and octahedral sites in the samples. The infra-red study enabled estimation of the elastic properties which were interpreted in terms of tightness of atomic boding in samples.

Conflict of Interest

The authors declare no conflict of interest.

REFERENCES
[1] J. Darul, Thermal instability of the tetragonally distorted structure of copper-iron materials, Z. Krist. Suppl. 30 (2009) 335–340. doi:10.1524/zksu.2009.0049.

[2] S.J. Stewart, M.J. Tueros, G. Cernicchiaro, R.B. Scorzelli, Magnetic size growth in nanocrystalline copper ferrite, Solid State Commun. 129 (2004) 347–351. doi:10.1016/j.ssc.2003.11.010.

[3] P. Tailhades, C. Villette, A. Rousset, G.U. Kulkarni, K.R. Kannan, C.N.R. Rao, M. Lenglet, Cation Migration and Coercivity in Mixed Copper–Cobalt Spinel Ferrite Powders, J. Solid State Chem. 141 (1998) 56–63. doi:10.1006/jssc.1998.7914.

[4] X. Zuo, A. Yang, C. Vittoria, V.G. Harris, A. Yang, C. Vittoria, V.G. Harris, Computational study of copper ferrite (CuFe2O4), 909 (2006) 99–102. doi:10.1063/1.2170048.

[5] Á. Yebra-rodríguez, E. Bailón-garcía, Effect of calcination temperature of a copper ferrite synthesized by a sol-gel method on its structural characteristics and performance as Fenton catalyst to remove gallic acid from water, J. Colloid Interface Sci. (2017). doi:10.1016/j.jcis.2017.09.117.

[6] V.A. Zhuravlev, R. V. Minin, V.I. Itin, I.Y. Lilenko, Structural parameters and magnetic properties of copper ferrite nanopowders obtained by the sol-gel combustion, J. Alloys Compd. 692 (2017) 705–712. doi:10.1016/j.jallcom.2016.09.069.

[7] M.H. Abdellatif, C. Innocenti, I. Liakos, A. Scarpellini, S. Marras, M. Salerno, Effect of Jahn-Teller distortion on the short range magnetic order in copper ferrite, J. Magn. Magn. Mater. 424 (2017) 402–409. doi:10.1016/j.jmmm.2016.10.110.

[8] P.F. Bangers, Crystal chemistry and magnetism of oxide materials, Philips Tech. Rev. 28 (1967) 13–28.

[9] L. E. Orgel, J. D. Dunitz, Stereochemistry of Cupric Compounds, Nature. 179 (1957) 462–465.

[10] F. Caddeo, D. Loche, M.F. Casula, A. Corrias, Evidence of a cubic iron sub-lattice in t-CuFe2O4 demonstrated by X-ray Absorption Fine Structure, Sci. Rep. 8 (2018) 797. doi:10.1038/s41598-017-19045-8.

[11] A.M. Balagurov, I.A. Bobrikov, V.Y. Pomjakushin, D. V Sheptyakov, V.Y. Yushankhai, Interplay between structural and magnetic phase transitions in copper ferrite studied with high-resolution neutron diffraction, J. Magn. Magn. Mater. 374 (2015) 591–599. doi:10.1016/j.jmmm.2014.08.092.

[12] A. Goldman, Modern Ferrite Technology, 2nd ed., Springer, 2006. doi:10.1007/978-0-387-29413-1.

[13] A.M. Balagurov, I.A. Bobrikov, M.S. Maschenko, D. Sangaa, V.G. Simkin, Structural Phase Transition in CuFe2O4 Spinel, Crystallogr. Reports. 58 (2013) 710–717. doi:10.1134/S1063774513040044.

[14] T. Florin, I. Chicinas, Structural and magnetic properties of the copper ferrite obtained by reactive milling and heat treatment, Ceram. Int. 39 (2013) 4179–4186. doi:10.1016/j.ceramint.2012.10.274.

[15] R. Koferstein, T. Walther, D. Hesse, S.G. Ebbinghaus, Crystallite-growth, phase transition, magnetic properties, and sintering behaviour of nano-CuFe2O4 powders prepared by a combustion-like process, J. Solid State Chem. 213 (2014) 57–64. doi:10.1016/j.jssc.2014.02.010.

[16] A. Hajalilou, S.A. Mazlan, K. Shameli, A comparative study of different concentrations of pure Zn powder effects on synthesis, structure, magnetic and microwave-absorbing properties in mechanically-alloyed Ni-Zn ferrite, J. Phys. Chem. Solids. 96–97 (2016) 49–59. doi:10.1016/j.jpcs.2016.05.001.

[17] R.J. Hill, J.R. Craig, G. V. Gibbs, Systematics of the spinel structure type, Phys. Chem. Miner. 4 (1979) 317–339. doi:10.1007/BF00307535.

[18] M.A. Ali, M.N.I. Khan, D.K. Saha, S.M. Hoque, S.I. Liba, S. Akhter, M.M. Uddin, Effect of Sintering Temperature on Structural and Magnetic Properties of, J. Phys. Conf. Ser. (2015) 2–11.

[19] A.D. Deshpande, V.M. Nanoti, K.G. Rewatkar, An Approach to Study Applications of Doped Calcium Hexaferrites, IOSR J. Appl. Phys. 2014 (2014) 75–78.

[20] S.N. Sable, K.G. Rewatkar, V.M. Nanoti, Structural and Magnetic Behavioral Improvisation of Nanocalcium Hexaferrites, Mater. Sci. Eng. B. 168 (2010) 156–160. doi:10.1016/j.mseb.2009.10.034.

[21] H. Ghayour, M. Abdellahi, N. Ozada, S. Jabbrzare, A. Khandan, Hyperthermia application of zinc doped nickel ferrite nanoparticles, J. Phys. Chem. Solids. 111 (2017) 464–472. doi:10.1016/j.jpcs.2017.08.018.

[22] Z.K. Heiba, A.M. Wahba, M.B. Mohamed, Structural analysis and magnetic properties of biphasic chromium-substituted copper ferrites, J. Mol. Struct. 1147 (2017) 668–675. doi:10.1016/j.molstruc.2017.07.003.

[23] H. Bhargava, V.D. Sudheesh, J. Nehra, V. Sebastian, N. Lakshmi, Size-Dependent Magnetic Properties in Cu0.25Co0.25Zn0.5Fe2O4, Bull. Mater. Sci. 37 (2014) 953–961. doi:https://doi.org/10.1007/s12034-014-0031-4.

[24] K.H.C. Mojtaba Amini, Maryam Hosseinpour Kafshdouzsani, Ali Akbari, Sanjeev Gautam, Cheol Hwee Shim, Spinel copper ferrite nanoparticles : Preparation, characterization and catalytic activity, Appl Organometal Chem. 32 (2018) 1–8. doi:10.1002/aoc.4470.

[25] B.I. Kharisov, H.V.R. Dias, O. V. Kharissova, Mini-review: Ferrite nanoparticles in the catalysis, Arab. J. Chem. (2014). doi:10.1016/j.arabjc.2014.10.049.

[26] L. Zhou, Y. Wei, Core-shell structural iron oxide hybrid nanoparticles : from controlled synthesis to biomedical applications, J. Mater. Chem. 21 (2011) 2823–2840. doi:10.1039/c0jm02172e.

[27] S.R. Momin Nooris, Deshmukh Aparna, Synthesis and characterization of MFe2O4 (M = Co, Ni, Mn) magnetic nanoparticles for modulation of angiogenesis in chick chorioallantoic membrane (CAM), Eur Biophys J. 45 (2015) 139–148. doi:10.1007/s00249-015-1083-0.

[28] N. Momin, A. Deshmukh, S. Radha, nanoparticles for various biomedical applications : cell viability and cell death evaluations, J. Nano Res. 34 (2015) 1–8. doi:10.4028/www.scientific.net/JNanoR.34.1.

[29] F. Kenfack, H. Langbein, Spinel ferrites of the quaternary system Cu-Ni-Fe-O: Synthesis and characterization, J. Mater. Sci. 41 (2006) 3683–3693. doi:10.1007/s10853-006-6263-y.

[30] M. Ramesh, G.S.N. Rao, K. Samatha, B.P. Rao, Cation distribution of Ni – Cu substituted Li-ferrites, Ceram. Int. 41 (2015) 1765–1770. doi:10.1016/j.ceramint.2014.09.122.

[31] K.V. Babu, G.V.S. Kumar, G. Satyanarayana, B. Sailaja, C.C.S. Lakshmi, Microstructural and Magnetic properties of Ni1-xCuxFe2O4 (x=0.05, 0.1, 0.15 and 0.2) nano-crystalline ferrites, J. Sci. Adv. Mater. Devices. 4 (2018) 1–21. doi:10.1016/j.jsamd.2018.04.003.

[32] K.G. Rewatkar, Magnetic Nanoparticles: Synthesis and Properties, Solid State Phenom. 241 (2016) 177–201. doi:10.4028/www.scientific.net/SSP.241.177.

[33] A. Hajalilou, S.A. Mazlan, A review on preparation techniques for synthesis of nanocrystalline soft magnetic ferrites and investigation on the effects of microstructure features on magnetic properties, Appl. Phys. A. 122 (2016) 680. doi:10.1007/s00339-016-0217-2.

[34] H.S. Ahamad, N.S. Meshram, S.B. Bankar, S.J. Dhoble, K.G. Rewatkar, Structural properties of CuxNi1-xFe2O4nano ferrites prepared by urea-gel microwave auto combustion method, Ferroelectrics. 516 (2017) 67–73. doi:10.1080/00150193.2017.1362285.

[35] R.C. Pullar, Hexagonal ferrites: A review of the synthesis, properties, and applications of hexaferrite ceramics, Prog. Mater. Sci. 57 (2012) 1191–1334. doi:10.1016/j.pmatsci.2012.04.001.

[36] S.R. Gawali, K.G. Rewatkar, V.M. Nanoti, Structural and Electrical Properties of M-type Nanocrystalline Aluminium substituted Calcium Hexaferrites, Adv. Appl. Sci. Res. 3 (2012) 2672–2678.

[37] K.C. Patil, Advanced ceramics: Combustion synthesis and properties, Bull. Mater. Sci. 16 (1993) 533–541. doi:10.1007/BF02757654.

[38] M.R. de Freitas, G.L. de Gouveia, L.J. Dalla Costa, A.J.A. de Oliveira, R.H.G.A. Kiminami, Microwave Assisted Combustion Synthesis and Characterization of Nanocrystalline Nickel-doped Cobalt Ferrites, Mater. Res. 19 (2016) 27–32. doi:10.1590/1980-5373-mr-2016-0077.

[39] A. Sutka, G. Mezinskis, Sol-Gel Auto-Combustion Synthesis of Spinel-Type Ferrite Nanomaterials Sol-gel auto-combustion synthesis of spinel-type ferrite nanomaterials, Front. Mater. Sci. 6 (2012) 128–141. doi:10.1007/s11706-012-0167-3.

[40] P. Innocenzi, The Sol to Gel Transition, Springer International Publishing AG Switzerland, 2016. doi:10.1007/978-3-319-39718-4.

[41] A.S. Fawzi, A.D. Sheikh, V.L. Mathe, Structural, dielectric properties and AC conductivity of Ni(1-x)ZnxFe2O4spinel ferrites, J. Alloys Compd. 502 (2010) 231–237. doi:10.1016/j.jallcom.2010.04.152.

[42] H. V. Kiran, A. L. Shashimohan, D. K. Chakrabarty, A. B. Biswas, Structural and Magnetic Properties of Copper-Nickel Ferrites, Phys. Stat. Sol. 66 (1981) 743–747. doi:https://doi.org/10.1002/pssa.2210660240.

[43] L. He, J. Liu, H. Xie, C. Zhang, Greatly enhanced magneto-dielectric performance of the annealed ferrite powders for antenna applications, J. Mater. Res. 31 (2016) 3675–3681. doi:10.1557/jmr.2016.417.

[44] L. Alexander, H.P. Klug, L. Alexander, H.P. Klug, Determination of Crystallite Size with the XRay Spectrometer Determination of Crystallite Size with the X-Ray Spectrometer, J. Appl. Phys. 21 (1950) 137–142. doi:10.1063/1.1699612.

[45] B.D. Cullity, Elements of Diffraction, 2nd ed., Addison-Wesley Publishing Company Inc., 1978.

[46] B. Singh, A. Kaushal, I. Bdikin, K.V. Saravanan, J.M.F. Ferreira, Effect of Ni doping on structural and optical properties of Zn1- x NixO nanopowder synthesized via low-cost sonochemical method, Mater. Res. Bull. 70 (2015) 430–435. doi:10.1016/j.materresbull.2015.05.009.

[47] B.R. Rehani, P.B. Joshi, K.N. Lad, A. Pratap, Crystallite size estimation of elemental and composite silver nano-powders using XRD principles, Indian J. Pure Appl. Phys. 44 (2006) 157–161.

[48] A.J.C. Wilson, X-ray Optics, Methuen & Co. Ltd. London, 1949.

[49] G. K. Williamson, W. H. Hall, X-Ray Line Broadening From Filed Aluminium and Wolfram, Acta Metall. 1 (1953) 22–31. doi:https://doi.org/10.1016/0001-6160(53)90006-6.

[50] R.E. Dinnebier, S.J.L. Billinge, Powder diffraction: Theory and practice, The Royal Society of Chemistry, 2008. doi:10.1039/9781847558237.

[51] W.S. Galvão, R.M. Freire, T.S. Ribeiro, I.F. Vasconcelos, L.S. Costa, V.N. Freire, F.A.M. Sales, J.C. Denardin, P.B.A. Fechine, Cubic superparamagnetic nanoparticles of NiFe2O4 via fast microwave heating, J. Nanoparticle Res. 16 (2014) 2803. doi:10.1007/s11051-014-2803-6.

[52] V.K. Lakhani, Studies on pre-and post effect of rapid thermal quenching on magnetic and transport properties of copper-ferri-aluminates, Saurashtra University, 2011. http://etheses.saurashtrauniversity.edu/877/1/lakhani_vk_thesis_physics.pdf.

[53] Y. Lo Vegard, Die Konstitution der Mischkristalle und die Raumfüllung der Atome, Zeitschrift Für Phys. 5 (1921) 17–26. doi:https://doi.org/10.1007/BF01349680.

[54] K.A. Mohammed, A.D. Al-rawas, A.M. Gismelseed, A. Sellai, H.M. Widatallah, A. Yousif, M.E. Elzain, M. Shongwe, Infrared and structural studies of Mg1–xZnxFe2O4 ferrites, Phys. B J. 407 (2012) 795–804. doi:10.1016/j.physb.2011.12.097.

[55] L. Sun, J. Guo, R. Zhang, E. Cao, Y. Zhang, W. Hao, L. Ju, Influence of Cu2+ doping on the structure, dielectric and magnetic properties of NiFe2O4 prepared by the sol-gel method, J. Magn. Magn. Mater. 449 (2018) 545–551. doi:10.1016/j.jmmm.2017.10.104.

[56] C. Rath, S. Anand, R.P. Das, K.K. Sahu, S.D. Kulkarni, C. Rath, S. Anand, R.P. Das, Dependence on cation distribution of particle size, lattice parameter, and magnetic properties in nanosize Mn – Zn ferrite Dependence on cation distribution of particle size, lattice parameter, J. Appl. Phys. 2211 (2002) 1–6. doi:10.1063/1.1432474.

[57] M.A.M. Quraishi, M.H.R. Khan, Synthesis and Characterization of Lithium-Substituted Cu-Mn Ferrite Nanoparticles, Indian J. of materials Sci. 2013 (2013). doi:http://dx.doi.org/10.1155/2013/910762.

[58] J.B. Nelson, D.P. Riley, An experimental investigation of extrapolation methods in the derivation of accurate unit-cell dimensions of crystals, Proc. Phys. Soc. 57 (1945) 160–177. doi:10.1088/0959-5309/57/3/302.

[59] A. Evdou, V. Zaspalis, L. Nalbandian, Ferrites as redox catalysts for chemical looping processes, Fuel. 165 (2016) 367–378. doi:10.1016/j.fuel.2015.10.049.

[60] M.A. Amer, A. Matsuda, G. Kawamura, R. El-Shater, T. Meaz, F. Fakhry, Structural, magnetic, vibrational and optical studies of structure transformed spinel Fe2+-Cr nano-ferrites by sintering process, J. Alloys Compd. 735 (2018) 975–985. doi:10.1016/j.jallcom.2017.11.198.

[61] A. Hajalilou, S.A. Mazlan, A review on preparation techniques for synthesis of nanocrystalline soft magnetic ferrites and investigation on the effects of microstructure features on magnetic properties, Appl. Phys. A Mater. Sci. Process. 122 (2016) 680. doi:10.1007/s00339-016-0217-2.

[62] J. Smit, H.P.J. Wijn, Ferrites, Philips Technical Library, 1959.

[63] A. R. Stokes, A. J. C. Wilson, The diffraction of X rays by distorted crystal aggregates - I, PHYS. SOC. LVI, 3. 56 (1944) 174–181.

[64] S. Vives, E. Gaffet, C. Meunier, X-ray diffraction line profile analysis of iron ball milled powders, Mater. Sci. Eng. A. 366 (2004) 229–238. doi:10.1016/S0921-5093(03)00572-0.

[65] A.I. Ahmed, M.A. Siddig, A.A. Mirghni, M.I. Omer, A.A. Elbadawi, Structural and Optical Properties of Mg1-xZnxFe2O4 Nano-Ferrites Synthesized Using Co-Precipitation Method, Adv. Nanoparticles. 4 (2015) 45–52. doi:10.4236/anp.2015.42006.

[66] P.S. Tamboli, C.V. Jagtap, V.S. Kadam, R.V. Ingle, R.S. Vhatkar, S.S. Mahajan, H.M. Pathan, Spray pyrolytic deposition of α-MoO3 film and its use in dye-sensitized solar cell, Appl. Phys. A Mater. Sci. Process. 124 (2018). doi:10.1007/s00339-018-1763-6.

[67] N.G. Surendra Singh, Anshuman Sahai, S.C. Katyal, Structural, optical and vibrational study of zinc copper ferrite nanocomposite prepared by exploding wire technique, Mater. Sci. 36 (2018) 722–732. doi:10.2478/msp-2018-0084.

[68] S. Joshi, M. Kumar, S. Chhoker, G. Srivastava, M. Jewariya, V.N. Singh, Structural, magnetic, dielectric and optical properties of nickel ferrite nanoparticles synthesized by co-precipitation method, J. Mol. Struct. 1076 (2014) 55–62. doi:10.1016/j.molstruc.2014.07.048.

[69] Y. Hong, A. Ren, Y. Jiang, J. He, L. Xiao, W. Shi, Sol-gel synthesis of visible-light-driven Ni(1-x)CuxFe2O4 photocatalysts for degradation of tetracycline, Ceram. Int. 41 (2015) 1477–1486. doi:10.1016/j.ceramint.2014.09.082.

[70] A.A. Al-Ghamdi, F.S. Al-Hazmi, L.S. Memesh, F.S. Shokr, L.M. Bronstein, Evolution of the structure, magnetic and optical properties of Ni(1−x)CuxFe2O4 spinel ferrites prepared by soft mechanochemical method, J. Alloys Compd. 712 (2017) 82–89. doi:10.1016/j.jallcom.2017.04.052.

[71] S.S. Bhatu, V.K. Lakhani, A.R. Tanna, N.H. Vasoya, J.U. Buch, P.U. Sharma, U.N. Trivedi, H.H. Joshi, K.B. Modi, Effect of nickel substitution on structural, infrared and elastic properties of lithium ferrite, Indian J. Pure Appl. Phys. 45 (2007) 596–608.

[72] E.H. El-Ghazzawy, M.A. Amer, Structural, elastic and magnetic studies of the as-synthesized Co(1-x)SrxFe2O4 nanoparticles, J. Alloys Compd. 690 (2017) 293–303. doi:10.1016/j.jallcom.2016.08.135.

[73] V.K. Lakhani, K.B. Modi, Al3+modified elastic properties of copper ferrite, Solid State Sci. 12 (2010) 2134–2143. doi:10.1016/j.solidstatesciences.2010.09.012.

[74] D. Ravinder, T.A. Manga, Elastic behaviour of Ni-Cd ferrites, Mater. Lett. 41 (1999) 254–260.

[75] D. Ravinder, Elastic behaviour of Cu – Zn ferrites, Mater. Lett. 38 (1999) 22–27. doi:10.1016/S0167-577X(98)00126-8.

[76] S.A. Mazen, N.I. Abu-Elsaad, IR Spectra, Elastic and Dielectric Properties of Li–Mn Ferrite, ISRN Condens. Matter Phys. 2012 (2012) 1–9. doi:10.5402/2012/907257.

[77] A. V. Anupama, V. Rathod, V.M. Jali, B. Sahoo, Composition dependent elastic and thermal properties of Li–Zn ferrites, J. Alloys Compd. 728 (2017) 1091–1100. doi:10.1016/j.jallcom.2017.09.099.

[78] R.D. Waldron, Infrared Spectra of Ferrites, Phys. Rev. 99 (1955) 1727–1735. doi:10.1103/PhysRev.99.1727.

[79] S. Joshi, M. Kumar, S. Chhoker, G. Srivastava, M. Jewariya, V.N. Singh, Structural, magnetic, dielectric and optical properties of nickel ferrite nanoparticles synthesized by co-precipitation method, J. Mol. Struct. 1076 (2014) 55–62. doi:10.1016/j.molstruc.2014.07.048.

[80] Y. Hong, A. Ren, Y. Jiang, J. He, L. Xiao, W. Shi, Sol-gel synthesis of visible-light-driven Ni(1-x)Cu(x)Fe2O4photocatalysts for degradation of tetracycline, Ceram. Int. 41 (2015) 1477–1486. doi:10.1016/j.ceramint.2014.09.082.

[81] P. Laokul, V. Amornkitbamrung, S. Seraphin, S. Maensiri, Characterization and magnetic properties of nanocrystalline CuFe2O4, NiFe2O4, ZnFe2O4 powders prepared by the Aloe vera extract solution, Curr. Appl. Phys. 11 (2011) 101–108. doi:10.1016/j.cap.2010.06.027.

[82] A. V. Humbe, P.B. Kharat, A.C. Nawle, K.M. Jadhav, Nanocrystalline Ni0.70−xCuxZn0.30Fe2O4with 0 ≤ x ≤ 0.25 prepared by nitrate-citrate route: structure, morphology and electrical investigations, J. Mater. Sci. Mater. Electron. 29 (2018) 3467–3481. doi:10.1007/s10854-017-8281-8.

[83] C. Venkata Reddy, C. Byon, B. Narendra, D. Baskar, G. Srinivas, J. Shim, S. V. Prabhakar Vattikuti, Investigation of structural, thermal and magnetic properties of cadmium substituted cobalt ferrite nanoparticles, Superlattices Microstruct. 82 (2015) 165–173. doi:10.1016/j.spmi.2015.02.014.

[84] C. Sujatha, K.V. Reddy, K.S. Babu, A.R. Reddy, K.H. Rao, Effect of sintering temperature on electromagnetic properties of NiCuZn ferrite, Ceram. Int. (2012) 1–10. doi:10.1016/j.ceramint.2012.09.087.

[85] K.S. Rao, P.A. Rao, M.C. Varma, K.H. Rao, Development of least sized magnetic nanoparticles with high saturation magnetization, J. Alloys Compd. 750 (2018) 838–847. doi:10.1016/j.jallcom.2018.04.002.

[86] Md Atiqur Rahman, Mohammad Tariqul Islam, Mandeep Singh Jit Singh, Md Samsuzzaman & Muhammad E. H. Chowdhury, Synthesis and characterization of Mg–Zn ferrite based flexible microwave composites and its application as SNG metamaterial, Scientific reports 11.1 (2021) 1-14. doi:10.1038/s41598-021-87100-6

[87] Wahba, A. M., & Mohamed, M. B. (2014). Structural, magnetic, and dielectric properties of nanocrystalline Cr-substituted Co0. 8Ni0. 2Fe2O4 ferrite. Ceramics International, 40(4), 6127-6135. doi: 10.1016/j.ceramint.2013.11.064

SYNTHESIS AND CHARACTERIZATION OF NOVEL TRANSITION METAL ION COMPLEXES WITH (E)-2-((7H-PURIN-6-YLIMINO) METHYL)-4-BROMOPHENOL AND THEIR STUDY ON ANTIBACTERIAL SCREENING AND MAGNETIC SUSCEPTIBILITY

Mangesh S. Tihile*[1] and Gajanan N. Chaudhari[2]

[1]Department of Chemistry, Smt. Narsamma Atrs, Comm. & Science College, Kiran Nagar, Amravati, Maharashtra, India

[2]Department of Chemistry, Shri Shivaji Science College, Amravati, Maharashtra, India

ABSTRACT

The novel transition metal ion complexes were synthesized by refluxing the ethanolic solutions of Metal Acetates with Schiff base in 1:2 ratios. The Structure & Characterization of synthesized complexes of Mn (II), Co (II), Ni (II),Cu (II) & Zn (II) with Schiff Base (E)-2-((7H-purin-6-ylimino) methyl)-4-bromophenol were elucidated by using ^1H NMR, FT-IR, UV-Vis, & X-Ray spectroscopic techniques. The synthesized Schiff Base & complexes were screened against the bacteria. The novel compounds were further carried out for the study of magnetic susceptibility.

Keywords - Schiff Base; transition Metal ion complexes; Antibacterial Screening; Magnetic Susceptibility.

I.   INTRODUCTION

Schiff-Base macro ligands synthesized from reaction of dialdehydes and amino compounds [1-3] form stable complexes, perhaps selective to specific metallic ions with applications in electrochemistry, bioinorganic, antimicrobial activity, fluorescence properties, catalysis, metallic deactivators, separation processes, and environmental chemistry among others [3]. In asymmetric catalyst systems, small changes in donating ability of the ligand or the size of its substituents can have a dramatic effect on catalyst efficiency and enantioselectivities [3-4]. In continuation of our research on preparation of Schiff bases [4-5] and their complexes [6–9], we decided to prepare new Schiff bases containing electronwithdrawing and donating substituents. This article describes the synthesis and spectroscopic characterization of several Schiff bases and their complexes with transition metal ions. The corresponding materials were characterized by spectroscopic (IR, UV-Vis, ^{1}H- NMR) and physical (melting point, Magnetic Susceptibility) data.

II.   MATERIALS AND METHODS

Preparation of Schiff Base (L$_1$) Derived From Adenine and 4-Nitrosalicylaldehyde:

Synthesis of (E)-2-((7H-purin-6-ylimino) methyl)-4-bromophenol. (ABS-3) (L$_3$)

The Schiff base (ligand ABS-3) was synthesized by taking adenine (0.01 M) and 4-Bromosalicylaldehyde (0.01 M) in ethanolic medium followed by the addition of 2-3 drops of conc. sulphuric acid in a catalytic amount and poured it in a round bottom flask connected with a reflux condenser. The above given reaction mixture was reflux for 7-8 hrs. Water formed during the reaction was collected through Deane Stark funnel. The solvent was removed under sunlight irradiation. The chemical reaction mentioned below in figure 2.1. The resulting pale yellowish solid was recrystallized from ethanol. Color - (Pale yellow), M.P.–124.0 ^{0}C, Yield- 60%.
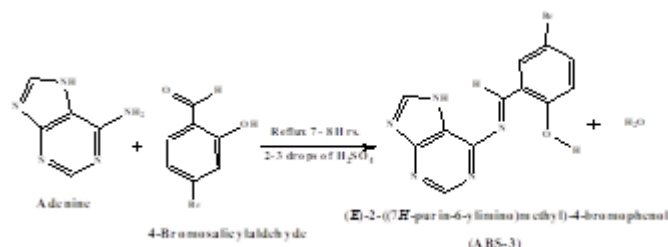
Figure 2.1: Preparation of (E)-2-((7H-purin-6-ylimino) methyl)-4-bromophenol .(ABS-3) from Adenine and 4-bromosalicylaldehyde.

Synthesis of Transition Metal-Ligand Complexes of Schiff Base (L$_3$) Derived From Adenine and 4-Bromosalicylaldehyde.

The Metal-Ligand mole ratio was taken in 1:2 proportions. Metal Acetate salt (0.01M) and (E)-2-((7H-purin-6-ylimino) methyl)-4-bromophenol (ABS-3) (0.02 M) was dissolved in 50 ml ethanolic solutions with vigorous stirring and warm it until the solution will not become clear. Then the solution was poured in round bottom flask equipped with refluxed condenser and refluxed it for 4 to 5 Hrs. The Solid complex with characteristic

colored was formed within few minute after cooling at room temperature. The resultants filtered off by using whatman-41 filter paper and wash it with ethanol. The product was dried by irradiation with sunlight. The synthetic route of formation of complex is mentioned below in Figure.

Reaction:
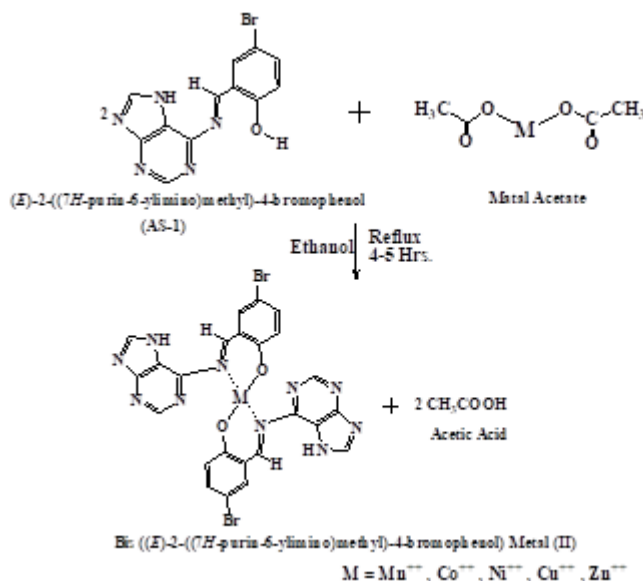
Figure 2.2: Preparation of Bis ((E)-2-((7H-purin-6-ylimino) methyl)-4-bromophenol) Metal (II) complex.

III. RESULTS AND DISCUSSION

Instrumentation: FTIR spectra in the range, 4000-400 cm^{-1}, were recorded on Agilent Technology Spectrophotometer; Uv-visible spectra were measured by using Shimadzu 160 spectrophotometer in the range 200-800 nm. The magnetic susceptibility values of the prepared complexes were obtained at room temperature using Magnetic Susceptibility on Bruker Magnet B.M.6, The ^{1}H nuclear magnetic resonance spectra were recorded on a Bruker Advanced-II 400 MHz spectrometer the DMSO solvent was used, Tetramethylsilane (TMS) was used as an internal standard. Melting points were recorded on a Tanco Laboratory melting point apparatus.

(E)-2-((7H-purin-6-ylimino) methyl)-4-bromophenol. (ABS-3) (L$_3$)**:**

Solid, M.P.-124.0^{o}C, **UV (λ max) in ethanol:** 290 nm, **(IR) υ max (KBr/cm^{-1}):** 3630.05 (Ar-OH), 3290.30 (Ar-N-H), 3088.15 (Ar-C-H), 1670.55 (Ar-C=C), 1590.63 (Ar-C=N), 1315.10 (C-C), 1244.26 (C-N), 1110.21 (C-O), 932.22 (Trans disubstituted C=N), 760.56 (Ortho disubstituted aromatic), 670.48 (C-Br). **^{1}H-NMR (δ-ppm):** 5.00 (s, 1H, Ar-O-H), 6.70 (d, 1H Ar-H), 7.25(d, 1H Ar-H), 8.40 (s, 1H Ar-H), 8.50 (s, 1H, Ar-N=C-H), 8.30 (d, 1 H Ar-N=C-H), 9.30 (s, 1H, Ar-N=C-H), 10.35 (d, 1H, Ar-N-H).

Bis((E)-2-((7H-purin-6-ylimino)methyl)-4-bromophenol)Manganese(II)complex. (ABSM-1):

Solid, M.P.-150.2^{0}C, **UV (λ max)** in ethanol: 288 nm, **(IR) υ max (KBr/cm^{-1}):** 3295.36 (Ar-N-H), 3095.14 (Ar-C-H), 1665.58 (Ar-C=C), 1555.10 (Ar-C=N), 1335.47 (C-C), 1252.66(C-N), 1095.53(C-O), 935.89 (Trans disubstituted C=N), 795.12 (Ortho disubstituted aromatic), 717.45 (Mn-O (Stretching)) 675.22 (C-Br). **^{1}H-NMR (δ-ppm):** 6.30 (d, 1H Ar-H), 7.00 (d, 1H Ar-H), 8.20 (s, 1H Ar-H), 8.40 (s, 1H, Ar-N=C-H), 8.10 (d, 1 H Ar-N=C-H), 9.10 (s, 1H, Ar-N=C-H), 10.15 (d, 1H, Ar-N-H).

Bis((E)-2-((7H-purin-6-ylimino)methyl)-4-bromophenol)Cobalt(II)complex.

(ABSC-2):

Solid, M.P.-161.4^{0}C, **UV (λ max)** in ethanol: 285 nm, **(IR) υ max (KBr/cm^{-1}):** 3293.22 (Ar-N-H), 3115.78 (Ar-C-H), 1655.15 (Ar-C=C), 1560.56 (Ar-C=N), 1335.22 (C-C), 1248.89 (C-N), 1090.18 (C-O), 940.14 (Trans disubstituted C=N), 790.23 (Ortho disubstituted aromatic), 722.86 (Co-O (Stretching)) 672.98 (C-Br). **^{1}H-NMR (δ-ppm):** 6.35 (d, 1H Ar-H), 7.00 (d, 1H Ar-H), 8.25 (s, 1H Ar-H), 8.35 (s, 1H, Ar-N=C-H), 8.15 (d, 1 H Ar-N=C-H), 9.20 (s, 1H, Ar-N=C-H), 10.20 (d, 1H, Ar-N-H).

Bis((E)-2-((7H-purin-6-ylimino)methyl)-4-bromophenol)Nickel(II)complex.

(ABSN-3):

Solid, M.P.-140.5^{0}C, **UV (λ max)** in ethanol: 280 nm, **(IR) υ max (KBr/cm^{-1}):** 3296.54 (Ar-N-H), 3118.96 (Ar-C-H), 1645.47 (Ar-C=C), 1555.89 (Ar-C=N), 1325.78 (C-C), 1242.45 (C-N), 1088.53 (C-O), 930.78 (Trans disubstituted C=N), 790.64 (Ortho disubstituted aromatic), 725.78 (Ni-O (Stretching)), 668.89 (C-Br). **^{1}H-NMR (δ-ppm):** 6.92 (d, 1H, Ar-H), 6.24 (d, 1H, Ar-H), 8.32 (s, 1H, Ar-N=C-H), 8.10 (s, 1H, Ar-H), 8.00 (d, 1 H, Ar-N=C-H), 10.10 (d, 1H, Ar-N-H), 9.10 (s, 1H, Ar-N=C-H).

Bis((E)-2-((7H-purin-6-ylimino)methyl)-4-bromophenol)Copper(II)complex.

(ABSC-4):

Solid, M.P.-153.9^{0}C, **UV (λ max)** in ethanol: 295 nm, **(IR) υ max (KBr/cm^{-1}):** 3289.41 (Ar-N-H), 3125.16 (Ar-C-H), 1659.55 (Ar-C=C), 1573.33 (Ar-C=N), 1341.28 (C-C), 1300.48 (C-N), 1080.56 (C-O), 936.32 (Trans disubstituted C=N), 791.26 (Ortho disubstituted aromatic), 732.59 (Cu-O (Stretching)), 671.70 (C-Br). **^{1}H-NMR (δ-ppm):** 6.35 (d, 1H Ar-H), 7.10 (d, 1H Ar-H), 8.25 (s, 1H Ar-H), 8.40 (s, 1H, Ar-N=C-H), 8.15 (d, 1 H Ar-N=C-H), 9.15 (s, 1H, Ar-N=C-H), 10.25 (d, 1H, Ar-N-H).

Bis((E)-2-((7H-purin-6-ylimino)methyl)-4-bromophenol)Zinc(II)complex. (ABSZ-5):

Solid, M.P.-162.3^{0}C, **UV (λ max)** in ethanol: 282 nm, **(IR) υ max (KBr/cm^{-1}):** 3290.44 (Ar-N-H), 3117.16 (Ar-C-H), 1660.19 (Ar-C=C), 1600.33 (Ar-C=N), 1322.55 (C-C), 1244.59 (C-N), 1070.22 (C-O), 937.29 (Trans disubstituted C=N), 789.63 (Ortho disubstituted aromatic), 729.58 (Zn-O (Stretching)), 672.16 (C-Br). **^{1}H-NMR (δ-ppm):** 6.25 (d, 1H Ar-H), 7.50 (d, 1H Ar-H), 8.10 (s, 1H Ar-H), 8.25 (s, 1H, Ar-N=C-H), 8.00 (d, 1 H Ar-N=C-H), 9.25 (s, 1H, Ar-N=C-H), 10.10 (d, 1H, Ar-N-H).

Table: Magnetic Moment, Conductivity measurements in DMF solvent

Symbol	Conductivity ohm^{-1}cm^2 mol^{-1}	Magnetic moment (B.M)	Suggested structure
(ABS-3) (L$_3$)	-	-	-
(ABSM-1)	16	4.25	Tetrahedral
(ABSC-2)	12	4.20	Tetrahedral
(ABSN-3)	15	4.30	Tetrahedral
(ABSC-4)	30	1.88	Square planner
(ABSZ-5)	14	3.90	Tetrahedral

IV. PHARMACOLOGY
Antibacterial activity

The titled compounds were screened for their antibacterial activity using disc diffusion method. The bacterial organisms used included both gram positive and gram negative strains like Staphylococcus aureus, Escherichia coli, Salmonella enteric Ser para typhi, Klebsiella Pneumonia and Pseudomons aeruginosa.

For antibacterial susceptibility testing of title compounds, the sterile disc of 6 mm diameter (SD067, Hi-Media, Mumbai) was loaded with 20µl of title compound solution (1000 µg/ml) in DMF. The discs were then placed at centre on the Mueller-Hinton agar seeded with bacterial inoculums approximately 106 CFU/ ml, incubated at 37° C for 24 hrs and growth inhibition zone formed around disc was measured. Test was done in triplicate and mean value was considered as inhibition zone. Solvents do not showed inhibitions in initial studies. Copper & Nickel complexes showed best activities against the respective bacteria and rest of the complexes showed moderate activity [7].

Table: Antimicrobial Activity

Compound	Gram positive bacteria	Gram negative bacteria			
	S. aureus	S. enterica S. Typhi	E. Coli	K. Pneumonia	P. aeruginosa
AS-1(L$_1$)	++	+	++	-	+
ASM-1	-	++	-	++	+
ASC-2	+	-	++	+	+

ASN-3	++	+	+	+	-
ASC-4	+++	++	++	++	++
ASZ-5	++	+++	+++	++	++

+++ = Zone size 16-22 mm; ++ = Zone size 9-15 mm; + = Zone size 6-8 mm; ▬ = No inhibition.

Infra-red spectroscopy: The above given data of FT-IR spectrum of the ligand ABS-3, shows the characteristic bands at 3630.05 cm^{-1}, 3290.30 cm^{-1} & 1590.63 cm^{-1} which are assigned to Ar-O-H, Ar-N-H & C=N stretching respectively. These bands reveal the formation of Schiff Base. The formation of complexes of Schiff Base with Mn (II), Co (II), Ni (II), Cu (II) and Zn (II) acetates was confirmed by the disappearance of –O-H band in the region of 3200-3600 cm^{-1} and occurrence of Metal-Oxide bands at 717.45 cm^{-1}, 722.86 cm^{-1}, 725.78 cm^{-1}, 732.59 cm^{-1} and 729.58 cm^{-1} for Mn-O, Co-O, Ni-O, Cu-O, Zn-O stretching respectively. In the free ligand, the band at 1590.63 cm^{-1} was assigned to the stretching of C=N bond. On complexation this band was shifted to a lower frequency region. This shift is due to the metal-ligand electron sharing effect. The IR data of the compounds are shown in the table lists the stretching frequency (υ) for some of the characteristics groups exhibited by the ligand and complexes.

Ultraviolet-visible spectroscopy: The ultraviolet visible electronic spectrums of the compounds were recorded in DMSO solvent. The bands at wavelengths (290, 288, 285, 280, 295 and 282 nm) these transitions are attributed to π→π* electronic transition [11]. The electronic spectra of complexes showed, as expected, different absorptions from that of the free ligand. In the complexes these bands were shifted to different wavelength than the corresponding bands in the ligand as shown above, which appears in the wavelength range between 280-300 nm. The ligand field electronic transitions between the metal d orbital's appear in Ni (II) and Cu (II) bands located in the visible region at 460 nm for Ni (L)$_2$ assigned to the transition 3A2→3T1 (p) and 610 nm for Cu (L)$_2$ assigned to the transitions 2B1g→2A1g. The other complexes were diamagnetic as expected for d10 ions so that no (d-d) transition can be expected in the visible region.

NMR spectroscopy: The data of proton NMR of the ligand (ABS-3) and its complexes displayed good solubility in DMSO. The proton nuclear magnetic resonance spectral data gave additional support for the composition of the complexes. The observed changes are the evidences of complexation had happened because the chemical shift of a compound is heavily depended on its electronic environment. The ^{1}HNMR spectrum of the complexes confirmed the disappearance of O-H signal at 5.00 ppm in the free ligand. The δ 6.25-8.50 ppm resonance signal protons of the aromatic ring shifted to the higher field upon complexation. It is most likely that shift is due to the decrease of electron density at ^{1}H protons when oxygen is bonded to metal ion.

Magnetic susceptibility and conductivity measurements: The experimental magnetic moments for metal complexes are listed in Table. Magnetic measurements are widely used in studying transition metal complexes. The magnetic properties are due to the presence of unpaired electrons in the partially filled d-orbital in the outer shell of these elements. This magnetic measurement gives an idea about the electronic state of the metal ion in the complexes. The magnetic moment for Ni (II) in any complex is approximately 4.30 B.M., this value refers to a high spin tetrahedral structure, while the value of Cu (II) is approximately 1.88 led to suggest the square planar structure which can become in a good agreement with the data of electronic transitions. Other complexes have no magnetic moment because it's diamagnetic. Molar conductivity measurement in DMF solvent at 25ºC showed that the complexes were non-electrolyte [11].

V. CONCLUSION

The ligand (E)-2-((7H-purin-6-ylimino) methyl)-4-bromophenol (ABS-3) was successfully synthesized by condensation method. The ligand (ABS-3) was treated with Mn(II),Co(II),Ni(II),Cu(II),Zn(II) metal acetate salts to afford the corresponding complexes. The Characterization data of ^{1}H NMR, IR & UV-Vis reveals the successful formation of ligand and their complexes. The Magnetic susceptibility data was attributed to the Square planar geometry of Cu (II) complex and Tetrahedral geometry of other complexes. The Antibacterial Study reveals that Cu(II) & Zn(II) metal ion complex showed best inhibition activity towards all the strains of bacteria where as other complexes showed good activity against the gram positive and gram negative bacteria.

VI. REFERENCES:

1] W. Rehman, M.K. Baloch, A.Badshah (2004), *European Journal of Medicinal Chemistry*, 43 , 2380-2385.

2] K. Sundavel, E. Suresh, M. Palaniandavar (2009), *Inorganica Chimica Acta*, 362, 199-207.

3] M.S. Masoud, A. El-Merghany, M.Y. Abd El-Kaway (2009), *Synthesis and Reactivity in Inorganic, Metal-Organic, and Nano-Metal Chemistry*, 39:537–553.

4] Hossein N. and Mohsen M. (2010); *Journal of Coordination Chemistry*, 63(1), 156–162.

5] Zdeněk T., Roman B. and Ivan N. (2014), *Molecules*, 19, 13509-13525.

6] M. Sankarganesh , J. Rajesh , G.G. Vinoth Kumar , M. Vadivel , L. Mitu , R. Senthil Kumar , J. Dhaveethu Raja (2018), *Jouranal of Saudi chemical society* 22,416-426.

7] J. Senthil Kumarana, J. Muthukumaranb , N. Jayachandramanic and S. Mahalakshmic (2015); *Journal of Chemical and Pharmaceutical Research*, 7(4):1397-1409.

8] Gamze K., Hale K. , Demet A. , Đhsan Y. , Stephen T. A. (2011); *GU J Sci* 24(3):407-413.

9] P. Jayaseelan, E. Akila, M. Usha Rani, R. Rajavel (2016); *Jouranal of Saudi chemical society,* 20,625-634.

10] Said Amer, Nadia El-Wakiel , Hoda El- Ghamry (2013); *Journal of Molecular Structure* 1049, 326–335.

11] A. Palanimurugan , A. Dhanalakshmi , P. Selvapandian , A. Kulandaisamy (2019); *Heliyon*

SEMICONDUCTING PROPERTIES OF ORGANIC COPOLYMER SYNTHESIZED FROM 2-HYDROXY, 4-METHOXY BENZO-PHENONE, AND 1, 5-DIAMINONAPHTHALENE

Narayan C. Das[1] and Wasudeo B. Gurnule[2*]
[1]Department of Chemistry, Dr. Ambedkar College, Chandrapur-442401 (M. S.), India
[2]Department of Chemistry, Kamla Nehru Mahavidyalaya, Nagpur-440024 (M. S.), India

ABSTRACT-

Copolymer 2-H, 4-MBP-1,5-DANF-I has been synthesized from 2-hydroxy, 4-methoxybenzophenone, and 1,5-diaminonaphthalene with formaldehyde by polycondensation method in acidic medium with 1:1:2 molar ratios of reacting monomers. The copolymer has been characterized by elemental analysis, UV-visible, FT-IR and ^{1}H-NMR spectra. Electrical conductivity measurement has been carried out to ascertain the semiconducting nature of the copolymer resin. The electrical conductivity of the copolymer has been found to be 1.212×10^{-11} to 1.701×10^{-7} ohm^{-1}cm^{-1} in the temperature range 313-428 K. The activation energy of electrical conduction has been found to be 16.37×10^{-20} J/K. The plots of log σ Vs 10^3/T are found to be linear over a wide range of temperature, which obeyed the Wilson's exponential law σ = σ$_0$ exp(−ΔE/KT) and the copolymer can be ranked as semiconductor.

Keywords - Resin, condensation, synthesis, electrical conductivity semiconductors,

INTRODUCTION

Polymer offers versatility and novelty hence they inhabit the main roll in semiconductor. The polymer scientists are trying to improve the properties of polymeric resins such as thermal stability, high chemical resistivity, durability, conductivity in the domain of desired applicability. Semiconducting polymers have been the subject of study for many decades for day to day application in modern electronics including antistatic coating, corrosion protection, in biosensors for coupling of electron transfer, fabrication of electrochemical windows, gas sensors, radio, computers, telephones, and many other electronic devices. Such devices include transistors, solar cells, the light-emitting diode, the silicon controlled rectifier, and digital and analog integrated circuits [1-4].

Chinchamalatpure and coworker have reported the electrical conductivity of some copolymers and its polychelates [5]. Gabal et al. have reported the synthesis, characterization and electrical conductivity of polyaniline-Mn$_{0.8}$Zn$_{0.2}$Fe$_2$O$_4$ nano-composites [6]. Gupta has studied the electrical conductance behaviour of terpolymer resin-II derived from p-hydroxybenzaldehyde, urea and ethylene glycol [7]. Electrical conductivity study of thermally stable newly synthesized terpolymer has reported by Niley and coworker [8]. Khedkar et al. [9] have studied the electrical conducting behaviour of newly synthesized m-cresol-hexamine-formaldehyde terpolymeric resin and its polychelates. Thakre [10] has synthesized the resins of 4-hydroxybenzoic acid, adipamide and formaldehyde and also studied the electrical conductance properties. Electrical conductivity measurement of salicylic acid hexamethylene-diamine- formaldehyde resin has studied by Masram et al. [11]. Electrical conductivity of salicylidene - anthranilic acid - schiff base formaldehyde resin (R-AASA) was reported by Abbas and coworker [12]. The present study deals with synthesis, characterization of a new 2-hydroxy, 4-methoxybenzophenone and 1,5-diaminonaphthalene with formaldehyde copolymer resin and its electrical conductivity measurement.

II. EXPERIMENTAL

The chemicals, like 2-hydroxyl, 4-methoxy benzo-phenone (Sigma Aldrich, India), 1,5-diaminonaphthalene (Himedia, India) and formaldehyde (S. D. Fine Chemicals, India) were procured from market and were of chemically pure grade.

A) Synthesis of 2-H, 4-MBP-1, 5-DAF-I copolymer

The copolymer 2-H, 4-MBP-1, 5-DANF-II was synthesized by condensing 2-hydroxy, 4-methoxy benzo-phenone and 1, 5-diaminonaphthalene with formaldehyde in 1:1:2 molar ratio of reacting monomers in the presence of 2M, 200 ml HCl as a catalyst at 126 $\pm$ 2 ^{0}C for about 5 hrs. in an oil bath with occasional shaking. The separated brown color copolymer was washed with hot water and methanol to remove unreacted starting materials and acid monomers. Properly washed resin was dried powdered and then extracted with diethyl ether to remove 2-hydroxy, 4-methoxy benzophenone formaldehyde copolymer along with 2-H, 4-MBP-1, 5-DANF-I copolymer. It was further purified by dissolving in 8% NaOH and then filtered. The purified copolymer resin was finely ground to pass through 300-mesh size sieve and kept in a vacuum over silica gel. The yield of the

copolymer resin was found to be 82% .The reaction and suggested structure of 2-H, 4-MBP-1, 5-DANF-I has been presented in Figure 1.
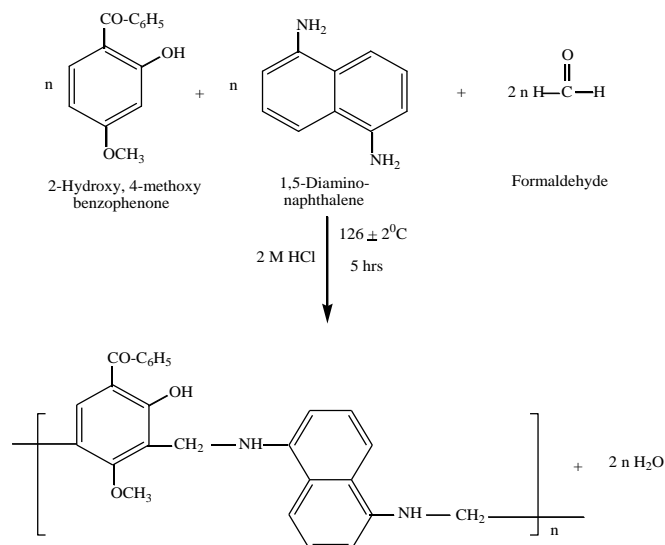
Fig. 1 Synthesis of 2-H, 4-MBP-1, 5-DANF-I copolymer resin

B) Analytical and Physico-Chemical Studies

The elemental analysis was carried out on Elemental Vario EL III Carlo Erba1108 elemental analyzer instrument. The electronic absorption spectra of the copolymer in DMSO was recorded on double beam spectrophotometer in the range of 200-800 nm. Infrared spectra of copolymer was carried out in najol mull on Perkin-Elmer-Spectrum RX-I, FT-IR spectrophotometer in KBr pellets in the range of 4000-500 cm^{-1}. Proton NMR spectrum was recorded on Bruker Advance –II 400 MHz NMR spectrophotometer using DMSO-d$_6$ as a solvent. SEM has been scanned by a JEOL JSM-6380, an analytical scanning electronic microscope. All the analytical and spectral studies were carried out at Sophisticated Analytical Instruments Facility SAIF, Cochin University, Cochin, India.

C) Electrical Conductivity

To prepare the pellet, the copolymer resin was thoroughly ground in agate pestle and mortar. The well powered copolymer was isostatically in a steel die at 10 tones /inch with the help of hydraulic press. On both sides of pellet, a thin layer of colloidal graphite in acetone was applied to ensure a good contact with the electrode. A typical sample holder was designed for the purpose of resistivity measurement and pellet is mounted on it. For measurement of resistivity at different temperature, a suitable electrical furnace was used. Auto LCR-Q meter 4910 was used to measure the electrical conductivity of copolymer resin. The temperature variations of resin were studied by placing the sample holder along with the pallet in the electric furnace that was then heated slowly. The resistances of the sample pallets were measured by two probes (terminals) method.

Resistivity (ρ) was then calculated using the relation:

$\rho = R. \times A/l$

The DC resistivity were measured from 313 to 428 K. The electrical conductivity (σ) varies exponentially with the absolute temperature. According to the well-known relationship:

$\sigma = \sigma_0 \exp(-Ea/kT)$

The relationship has been modified as:

$\log \sigma = \log\sigma_0 + (-Ea/2.303kT)$

According to this relation, a plot of log σ Vs 1/T would be linear with negative slope. From the

Slope of the plots, the activation energy was calculated [13, 14].

III. RESULTS AND DISCUSSION

The synthesized copolymer was found to be brown color and soluble in solvents such as dimethyl formamide (DMF), Dimethyl sulphoxide (DMSO), Tetrahydrofuran (THF) and conc. H$_2$SO$_4$ but insoluble in almost all organic and inorganic solvents.

A) Elemental Analysis

The 2-H, 4-MBP-1, 5-DANF-II copolymer was analyzed for the carbon, hydrogen and nitrogen content. The composition of copolymer obtained on the basis of elemental analysis data was found to be in good correlation which is presented in Table I.

Table I. Elemental analysis and empirical formula of copolymer resin

Copolymer resin	% C Obse-rved (cal.)	% H Obse-rved (cal.)	% N Obse-rved (cal.)	% O Obse-rved (cal.)
2-H,4-MBP-1,5-DAF	75.03 76.09	5.11 5.36	6.42 6.82	12.04 11.70

B) UV-Visible Spectra

The electronic spectra of 2-H, 4MBP-1, 5-DANF copolymer sample has been recorded in pure DMSO in the region 190-800 nm and shown in Figure 2. The spectra displayed two characteristics broad band at 280 nm and 330 nm. These observed position for absorption bands indicate the presence of a carbonyl (>C=O) group having a carbon oxygen double bond which is in conjugation with the aromatic nucleus. . The appearance of former band can be accounted for $\pi \rightarrow \pi^*$ transition while the letter band may be due to $n \rightarrow \pi^*$ electronic transition. The shift from basic value may be due to conjugation effect and presence of phenolic hydroxyl group is responsible for hyperchromic effect [15, 16].
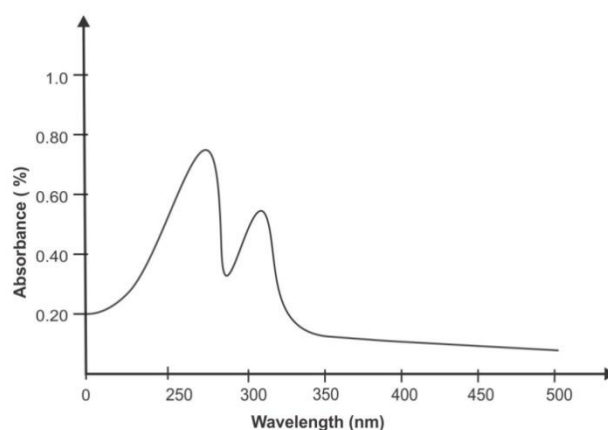
Fig. 2 UV-visible spectra of 2-H, 4-MBP-1, 5-DANF copolymer resin

C) FT-IR Spectra
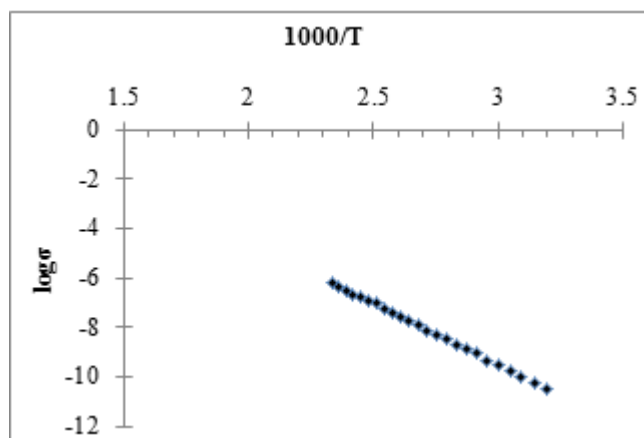
Infrared spectra of 2-H, 4-MBP-1, 5-DANF copolymer resin is shown in Figure 3. A broad and strong band appeared at 3325 cm^{-1} may be due to the stretching vibration of the phenolic hydroxyl group exhibiting intramolecular hydrogen bonding with –NH group. A sharp and strong band at 1619 cm^{-1} may be assigned to the stretching vibration of >C=O group. The strong band observed at 2936 cm^{-1} may be due to the stretching

vibrations of –NH (imide) group. The strong band obtained at 1107 cm⁻¹ region may be due to the Ph-O-CH$_3$ ether linkage. The weak band at 1343 cm⁻¹ is attributed to –CH$_2$ methylene bridge. [17-19].
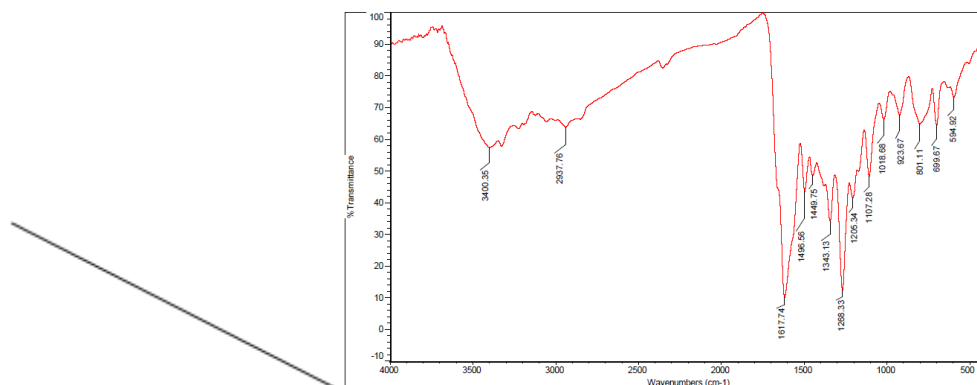
Fig. 3 FT-IR spectra of 2-H, 4-MBP-1,5-DANF copolymer resin

D) ¹H-NMR Spectra

The ¹H-NMR spectra of 2-H, 4-MBP-1,5-DANF copolymer is presented in Figure 4. The weak multiplet signal (unsymmetrical pattern) in the region at δ 7.6 ppm, which may due to proton of aromatic ring (Ar-H). The weak signal in the region δ 7.2 ppm is attributed to phenolic –OH proton in intramolecular hydrogen bonding (Ar-OH). The presence of singlet at δ 3.4 ppm reveals the presence of Ar-O-CH$_3$ proton. The methylenic proton of Ar-CH$_2$-N linkage may be recognized from signal which appears in the region of δ 3.8 ppm. The triplet signal in the region δ 6.7 ppm may be due to proton of –NH bridge [20-22].
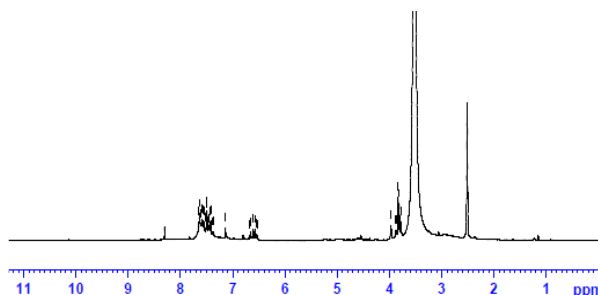
Fig. 4 ¹H-NMR spectra of 2-H, 4-MBP-1,5-DANF-I copolymer resin

E) Electrical Conductivity of 2-H, 4-MBP-1, 5-DANF Resin

The temperature dependence of the electrical conductivity of the copolymer is shown in Figure 5.The electrical conduction of polymeric material depends upon incalculable parameters such as pressure, method of preparation, porosity, atmosphere etc; energy of activation (Ea) is not affected by these parameters and, therefore, it is fairly reproducible. The magnitude of activation energy depends on the number of electrons present in semiconductor materials. The more the number of π– electrons lowers the magnitude of activation energy and vice versa. Generally polymers containing aromatic nuclei in the backbone exhibit lower activation energy than those with aliphatic system.

Fig. 5 Electrical Conductivity Plot of 2-H, 4-MBP-1,5-DANF Resin

The 2-H, 4-MBP-1,5-DANF copolymer shows the electrical conductivity in the range of 1.212×10^{-11} - 1.701×10^{-7} ohm^{-1}cm^{-1} and the plots of log σ versus 1/T is found to be linear in the temperature range under study, which indicate that the Wilson's exponential law $\sigma = \sigma_o \exp(-\Delta E/kT)$ is obeyed. The activation energy (Ea) of electrical conduction calculated from the slopes of the plots is found to be in the range of 16.37×10^{-20}J/K. Thus, the low magnitude of activation energy may be due to the presence of large number of π-electrons in the polymer chain. This is in good agreement with the most probable structure proposed for the newly synthesized resin under investigation [22-25].

IV. CONCLUSION

The data of elemental analysis, UV-Visible, FT-IR spectra,¹H - NMR spectra, supports to the above tentative structure of 2-H, 4-MBP-1,5-DANF resin. Electrical conductivity of the copolymer resin increases with increase in temperature (1.212×10^{-11} - 1.701×10^{-7} ohm^{-1}cm^{-1}). The low activation energy of conduction (16.37×10^{-20} J/K) of resin may be due to presence of large number of delocalized π-electrons in the polymer chain. The plot of log σ versus1/T is found to be linear in the temperature range 313-428 K, which indicates that the Wilson's

exponential law is obeyed. Hence this copolymer may be ranked as semiconductor for temperature range under study.

REFERENCES

1. S. S. Pande and W. B. Gurnule, Synthesis, characterization and semiconducting studies of salicylaldehyde-formaldehyde-melamine copolymers, *International Journal on Recent and Innovation Trends in Computing and Communication,* 3(2), 49-52, 2015.

2. A. N. Gupta, N. T. Khati, V. V. Hiwase, and A. B. Kamble, Semiconducting properties of terpolymer derived from p-hydroxybenzaldehyde, adipic acid and ethylene glycol., *ICRTEST*, 5(22), 318-320, 2017.

3. W. B. Gurnule and S. K. Mandavgade, Electrical conductance properties of a copolymer resin: synthesis, characterization and its applications, *RJPBCS,* 5(4), 737-747, 2014.

4. M. Nagmote, J. Dontulwar and R. Singru, Electrical conductivity study of resin synthesized from 1-naphthol-4-sulphonic acid and hexamethylene diamine and formaldehyde, *Der Pharma Chemica*, 6(6), 427-434, 2014.

5. V. R. Chinchamalatpure and P. P. Kalbende, Synthesis, characterization and electrical conductivity of some copolymers and its polychlates, *International of Scientific Research and Review,* 7(3), 562-576, 2018.

6. M. A. Gabal, M. A. Hussein, A. A. Hermas, Synthesis, characterization and electrical conductivity of polyaniline $Mn_{0.8}Zn_{0.2}Fe_2O_4$ nano-composites, *Int. J. Electrochem. Sci.,* doi: 10.20964/2016.06.20, 4526-4538, 11, 2016.

7. A. N. Gupta, Electrical conductance behaviour of terpolymer resin-II derived from p-hydroxybenzaldehyde, urea and ethylene glycol, *Perspectives in Science*, 8, 207-209, 2016.

8. S. N. Niley, K. P. Kariya, B. N. Berad, Electrical conductivity study of thermally stable newly synthesized terpolymer, *Technical Research Organization India*, 5(1), 242-249, 2018.

9. K. M. Khedkar, V. V. Hiwase, A. B. Kalambe and S. D. Deosarkar , Electrical conducting behaviour of newly synthesized m-cresol-hexamine-formaldehyde terpolymeric resin and its polychelates, *J. Chem. Pharm. Res.,* 4(5), 2468-2474, 2012.

10. M. B. Thakre, Electrical conductance properties of terpolymer resin: synthesis, characterization and its applications, *International Journal for Environmental Rehabilitation and Conservation,* IV(1), 89 – 96, 2013.

11. D. T. Masram, K. P. Kariya and N. S. Bhave, Thermal degradation and electrical conductivity measurement study of resin derived from salicylic acid, hexamethylenediamine and formaldehyde, *Elixir Appl. Chem.,* 48, 9557-9562, 2012.

12. Hayat H. A. and Roza A. Salih, Synthesis, characterization, thermal degradation and electrical conductivity of salicylidene - anthranilic acid - schiff base formaldehyde resin (R-AASA), *International Journal of Advanced Research,* 2(1), 1037-1040, 2014.

13. D.T. Masram, K. Kariya and N. S. Bhave, Kinetic and electrical conductivity study of resin resulting from salicylic acid and phenylenediamine with formaldehyde, *British Journal of Research*, 1(2), 43-52, 2014.

14. W. B. Gurnule, C. S. Makde, M. Ahamed, Synthesis, characterization, morphology, thermal, electrical and chelation ion exchange properties of copolymer resin, *J. Environ. Res. Develop.,* 7(3), 1183-1192, 2013.

15. M. M. Yeole, S. Shrivastava, W. B. Gurnule, Synthesis and characterization of copolymer resin derived from 4-methyl acetophenone, phenyl hydrazine and formaldehyde, *Der Pharma Chemica*, 7(5), 124-129, 2015.

16. W. B. Gurnule and N. C. Das, Kinetic study of Non-isothermal decomposition of copolymer resin derived from 2,4-dihydroxypropiophenone, 1,5-diaminonaphthalein and formaldehyde, *Materials Today Procedings*, 15, 611-619, 2019.

17. W. B. Gurnule and N. C. Das, Thermal degradation study of copolymer derived from 2-hydroxy, 4-methoxybenzophenone, 1,5-diaminonaphthalene and formaldehyde, *Int. J. Of current engineering and scientific research*, 6(1), 1414-1425, 2019.

18. W. B. Gurnule, C. S. Makde, M. Ahamed, Synthesis, characterization, morphology, thermal, electrical and chelation ion exchange properties of copolymer resin, *J. Environ. Res. Develop.,* 7(3), 1183-1192, 2013.

19. R. N. Singru, V. A. Khati, W. B. Gurnule, A. B. Zade, J. R. Dontulwar, Studies on semiconducting, chelating and thermal properties of p-Cresol–oxamide-formaldehyde terpolymer resin, *Anal. Bioanal. Electrochem.,* 3(1), 67-86, 2011.

20. M. M. Patel, M. A. Kapadia, G. P. Patel, J. D. Joshi, Lanthaides (III) polychelates with benzophenone based resin derivatives and study of their antimicrobial activities, *Iranian Polymer Journal,* 16(62), 113-122, 2007.

21. R. N Singru, Semiconducting and chelating applications of synthesized terpolymer, *Advances in Applied Science Research,* 2(6), 206-214, 2011.

22. D. T. Masram, K. P. Kariya and N. S. Bhave, Electrical conductivity study of resin synthesized from salicylic acid, butylenediamine and formaldehyde, *Archives of Applied Science Research,* 2 (2), 153-161, 2010.

23. K. M. Khedkar, V. V. Hiwase, A. B. Kalambe and S. D. Deosarkar , Electrical conducting behaviour of newly synthesized m-cresol-hexamine-formaldehyde terpolymeric resin and its polychelates, *J. Chem. Pharm. Res.,* 4(5), 2468-2474, 2012.

24. S. S. Rahangdale and W. B. Gurnule, Synthesis and electrical condunctance studies of p-cresol-adipamide-formaldehyde, *Archives of Applied Science Research,* 2(6), 53-58, 2010.

25. W. B. Gurnule and N. C. Das, Electrical conducting behavior of copolymer resin-III synthesized from 2,4-dihydroxy propiophenone, 1,5-diaminonaphthalein and formaldehyde, Ajanta, 8(1), 16- 25, 2019.

COMPARATIVE ACCOUNT OF ANTIMICROBIAL ACTIVITY OF SYNTHESIZED MALTOSYL NANOPARTICLES

Nikita V. Awajare and Poonam T. Agrawal*

Department of Chemistry, Shri. R.L.T. College of Science, Akola

ABSTRACT

In the present work, antimicrobial activity of nanoparticles of maltosyl thicarbamates and maltosyl thiocarbamides is compaired with bulk one. Which completely states that maltosyl nanoparticles shows effective zone of inhibition against all the bacterial strains listed in observation table. Because of such properties of n-linked sugar derivatives provided a very facile and easy way to increase its potency and enhanced the route for biomedical analysis. On the basis of experiences gained recently from work being carried out in the laboratory , it appeared quite interesting to carry out the synthesis of nanoparticles of new N-linked Maltose Thiocarbamates and their derivatives by the reaction between Maltosyl isothiocyanate and various alcohols. The characterization of new compounds and biologically made nanoparticles has been carried out by Melting point, antimicrobial activity, usual chemical transformation, NMR, IR and Mass spectral studies.

Keywords— Maltose, Thiocarbamates, Thiocarbamides, Nanoparticles.

I. INTRODUCTION

Nanotechnology has been the most explored and extensively studied area in recent times. Nanoparticles play very important role in the development of novel diagnosis methods and in the advanced design of drug delivery system[1,2]. Silver nanoparticles and Gold nanoparticles particularly, shows an excellent anti-microbial properties and hence are rapidly being used in to medicines etc. to increase the lifestyle of human being and beneficial for mankind and environment[3,4]. Glyco-nanoparticles shows several advantages such as their synthesis can be performed under biomimetic conditions result in nanoparticles without traces of chemicals responsible for adverse cellular responses and carbohydrates which are on the surface can act as targeting molecules and trigger cellular uptake via specific receptors or mediate specific cellular responses[5]. Derivatives of Carbohydrate have been reported as inflammatory, analgesic, fungicidal, herbicidal & pesticide agents[6-8]. Because of the tremendous biological importance, carbohydrates are very essential to our daily lives. They have more importance in synthesis and medicinal chemistry[9,10]. Maltose is the second member of an important biochemical series of glucose chains. Maltose, or malt sugar, is a disaccharide formed from two units of glucose joined with an α (1→4) linkage. Maltose is not common in food, but can be formed from the digestion of starch and is heavy in the sugar in malt, the juice of barley and other grains.

Isothiocyanates and isocyanates are a group of very reactive chemical compounds. Once they have reacted, the resulting product is usually less harmful than the chemical itself. This chemical is used in the manufacture of carbamates and thiocarbamates. Due to high reactivity towards compounds containing active hydrogen atom isocyanates and isothiocyanates are one of the most versatile classes of functional groups. They are important intermediates; the chemistry of these molecules is dominated by the nucleophilic addition reaction. Reactions with carbon nucleophiles provide a useful synthetic access to substituted amides and other derivatives.

II. EXPERIMENTAL

The prepared Compounds and their nanoparticles have been screened for antimicrobial activity using Cup plate agar diffusion method. By measuring zone of inhibition in mm antimicrobial activity has been studied. By using DMSO as a solvent the concentration of compound were 1 mg/ ml. Amikacin (100 μg/ml) was used as a standard. Compounds were screened for antimicrobial activity against microbes (listed in table 2) in nutrient agar medium. Determining the difference between melting point of compounds and their nanoparticles is one way to test if the nanoparticle is prepared or not. So the M.P. of compounds and their nanoparticles has been taken using melting point apparatus. H[1] NMR data of the compounds were measured using CDCl$_3$ solvent on 300 MHz frequency. And their chemical shift values are in (ppm) units using TMS as a reference. IR spectral data of the compounds were recorded on FTIR-RXI spectrophotometer. Confirmation of products and reaction progress carried out by TLC using Hexane : Ethyl acetate solvent system and identification of spots carried out by using iodine chamber and KMnO$_4$ spray.

III. METHOD OF PREPERATION

Step 1 : preparation of Maltose Octabenzoate: 55 ml dry Pyridine and 55 ml dry Chloroform were taken in a 1 lit. tight cork glass bottle and cooled in an ice-salt bath. To this solution previously prepared cooled solution of

55 ml Benzoyl Chloride in 55 ml dry Chloroform was added with constant stirring. To this mixture 20 gm. of dry powder of Maltose was added in small instalments with constant stirring by maintaining the temperature below 5 °C. After 24 hrs. mixture was washed several times with dil. Aq. Sulphuric acid, followed by aq. Sodium Bicarbonate and lastly with water. By using separating funnel Chloroform layer was separated which contains desired product. Product was triturated several times with petroleum ether until white powder obtained with M.P. 112 ° C.

Step 2 : Synthesis of hepta-O-benzoyl-α-D Maltosyl Bromide:

10g fine powdered of maltose octabenzoate was added to the brominating agent (mixture of Red Phosphorus, Glacial Acetic acid & molecular Bromine). After that flask was kept for 2 hrs at room temperature, finally 70 ml Chloroform was added to the reaction mixture with vigorous shaking. The resultant mixture was poured in an ice cold water to separate Chloroform layer. It was washed several times with aq. Sodium bicarbonate to remove excess of acetic acid followed by aq. Sodium metabisulphite to remove excess of bromine and finally 2-3 times with water. By using separating funnel the solution was removed and addition of petroleum ether results a solid mass.

Step 3: Synthesis of hepta-O-benzoyl-β-D-maltosyl isothiocyanate: Lead thiocyanate was prepared by mixing aq. Solution of lead nitrate and ammonium thiocyanate. To a suspension of hepta-O-benzoyl-α-D-maltosyl bromide (15gm) in sodium, dried xylene (60 ml) & lead thiocyanate (5 gm) was added. The reaction mixture was refluxed for 3 hrs, gentle shaking. After cooling liberated lead bromide was removed by filtration. The xylene filtrate was treated with petroleum ether with stirring, finally a white solid mass obtained.

Step 4: Synthesis of N-maltosylated Thiocarbamates: Reaction of hepta-O-benzoyl-β-D-maltosyl isothiocyanate and various alcohols has been refluxed for 5 hrs. On cooling and mixing with water most of the alcohols gave a white granular solid was purified by Chloroform-Petroleum ether. Melting point ranges from 140-170 ° C for all alcohol derivatives.

Step 5: Synthesis of N-maltosylated Thiocarbamides: Reaction of hepta-O-benzoyl-β-D-maltosyl isothiocyanate and various aryl amines has been carried out in boiling benzene for 3 hrs. The solvent benzene was distilled off and sticky mass was isolated as residue. Then triturated several times with petroleum ether was converted to granular solid. Crystallized from chloroform-ether.

Step 6 : Preparation of Nanoparticles (Biologically) : Small pieces of potato was boiled in little amount of water in a beaker for about 10 min. Filtered the semi hot solution through filter paper, remaining filtrate obtained called potato extract. 1 gm. of compound was dissolved in 2 ml of DMSO, clear solution was obtained. Then 2,3 drops of potato extract was added to the clear solution, suddenly white precipitate of nanoparticles was obtained.

IV. SCHEME

R1= a) ethyl b) methyl c) n-propyl d) isopropyl e) n-butyl f) t-butyl

R2= a) Phenyl b) o-tolyl c) m-tolyl d) p-tolyl e) o-Cl-phenyl f) m-Cl-phenyl g) p-Cl-phenyl

V. RESULT AND DISCUSSION

Antimicrobial activity (Thiocarbamates) (Table 1)

Antimicrobials	Bulk	Nanoparticles
E. coli	10 mm	13 mm
S. aureus	11 mm	13 mm
S. typhi	11mm	14 mm
P. vulgaris	09 mm	12 mm
Amikacin	10 mm	17 mm
Clandamycine	12 mm	14 mm
DMSO	26 mm	20 mm

Antimicrobial activity (Thiocarbamides)   (**Table 2**)

Antimicrobials	Bulk	Nanoparticles
E. coli	09 mm	12 mm
S. aureus	11 mm	14 mm
S. typhi	12mm	15 mm
P. vulgaris	10 mm	13 mm
Amikacin	09 mm	18 mm
Clandamycine	11 mm	14 mm
DMSO	28 mm	21 mm

*Including the well diameter of 8 mm. **Zone of inhibition in mm (15 or less) resistance, (16-20 mm) moderate and (> 20 mm) sensitive.*

The prepared Compounds and their nanoparticles have been screened for antimicrobial activity using Cup plate agar diffusion method. By measuring zone of inhibition in mm antimicrobial activity has been studied. By using DMSO as a solvent the concentration of compound were 1 mg/ ml. Amikacin (100 µg/ml) was used as a standard. Compounds were screened for antimicrobial activity against microbes (listed in table 1) in nutrient agar medium. Zone of inhibition of nanoparticles were more than bulk, which confirms better antimicrobial activity of nanoparticles in comparison to bulk one.

(Table 3)

Sr. No.	Aryl amines	1-hepta-O-benzoyl-β-D-maltosyl-3-aryl thiocarbamates	Yield %	Melting point of Bulk ᵒC	Melting point of Nanoparticles ᵒC
1.	Ethyl	O-ethyl thiocarbamate	71	121-123	90
2.	Methyl	O-methyl thiocarbamate	82	124	109
3.	n-propyl	O-n-propyl thiocarbamate	85	146	124-126
4.	Isopropyl	O-isopropyl thiocarbamate	81	146-149	123-129
5.	n-butyl	O-n-butyl thiocarbamate	69	141	121
6.	t-butyl	O-t-butyl thiocarbamate	76	149-155	119-123

(Table 4)

Sr. No.	Aryl amines	1-hepta-O-benzoyl-β-D-maltosyl-3-aryl thiocarbamides	Yield %	Melting point of Bulk ᵒC	Melting point of Nanoparticles ᵒC
1.	Aniline	-3-phenyl thiocarbamide	70	120-125	87
2.	o-Cl-Aniline	-3-o-Cl-phenyl thiocarbamide	85	125	112
3.	m-Cl-Aniline	-3-m-Cl-phenyl thiocarbamide	80	143	123-128
4.	p-Cl-Aniline	-3-p-Cl-phenyl thiocarbamide	82	145-150	125-130
5.	o-toluidine	-3-o-tolyl thiocarbamide	71	138	115
6.	m-toluidine	-3-m-tolyl thiocarbamide	80	150-155	120-125
7.	p-toluidine	-3-p-tolyl thiocarbamide	72	128-130	110

The characterization of compounds have been confirmed by IR spectroscopy which shows C=S, N-H, C-N, C=O, C-O stretching frequencies at different absorption bands. H1 NMR shows signal due to N-H proton at 8.07 ppm and maltosyl protons at 5.58 – 3.79 ppm. and benzoyl protons at 6.78 – 3.90 ppm. The Characterization of nanoparticles have been carried out by UV visible spectroscopy. The band gap difference increases as the size of nanoparticles decreases. The decrease in melting point confirms the nanoparticles were prepared.

VI. CONCLUSION

The synthesised nanoparticles were characterized by antimicrobial activity, UV spectroscopy, X-Ray diffraction and melting point determination. Antimicrobial activity of Maltosyl nanoparticles shows better result as compared to the bulk one. That means , maltosyl nanoparticles shows effective zone of inhibition against all the bacterial strains listed in observation table. Because of such properties of n-linked sugar derivatives provided a very facile and easy way to increase its potency and enhanced the route for biomedical analysis. N-linked nanoparticles have found interesting applications in a wide spectrum of biomedical utilities like imaging, sensing, drug delivery and gene targeting. On the basis of which nanoparticles obtained was confirmed.

REFERENCES:

1. Gao, J., Gu, H., Xu, B. (2009). *Acc Chem Res*, 42 (8), 1097-1107.

2. Lai, C. H., Chang, T. C., Chuang, Y. J., Tzou, D. L, Lin, C. C. (2013). *Bioconjug Chem*, 24 (10), 1698-1709.

3. Reidy, B., Haase, A., Luch, A., Dawson, K., Lynch, I. (2013) *Materials,* 6 (6): 2295-2350.

4. Sun, T. Y., Gottschalk, F., Hungerbühler, K., Nowack, B. (2014). *Environ Pollut*, (185), 69-76

5. Farr, T.D., Lai, C. H., Grünstein, D., Orts-Gil, G., Wang C. C., Boehm-Sturm, P., Seeberger, P. H., Harms, C., (2014) *Nano Lett*, 14 (4), 2130-2134.

6. Lans, V. D., R. G. J. M. (1967*). Proceedings of the 4th British Insecticide and Fungicide Conference*, (2), 562- 569.

7. Achgill, R. K., Call, L. W. (1989). *Erdelen, C*., EP 339964.

8. Heuer, L., Kugler, M., Paulus, W., Lorentzen, J and Dehne, H. W. (1993). *Erdelen, C*., EP 571857.

9. Yarema, K. J., & Berrtozzi, C. R. (1998). Curr. Opin, Chem. Boil., *2*, 49.

10. Witezak, Z. J., & Neiforth, K. A. (1997). Carbohydrates In Drug Design.

11. Mi, Y. D., Yao, X. S., Yi, T. C., Lin, C., Ming, L. X. (2007). Chinese Science Bulletin., (52), 2913-2918.

12. El-Boubbou, K., Zhu , D. C., Vasileiou, C., Borhan , B., Prosperi, D., Li, W., Huang, X. (2010). J. Am. Chem. Soc., (132), 4490-4499.

13. Lai, C. H., Lin, C. Y., Wu, H. T., Chan, H. S., Chuang, Y. J., Chen, C. T., Lin, C. C. (2010). Adv. Funct. Mater., (20), 3948-3958.

14. Parry, A. L., Clemson, N.A., Ellis, J., Bernhard, S.S.R., Davis, B. G., Cameron, N. R. (2013). J. Am. Chem. Soc., (135), 9362-9365.

15. Fischer, E. (1914). Ber., (37), 1377-1381.

16. Johnson, T. B., Bergmenn, W. (1932). J. Am. Chem. Soc., (54), 3360.

17. Ichikawa, Y., Nishiyama, T., Isobe, M. (2004). Tetrahedron, (60), 2621-2627.

STUDY OF SEED GERMINATION ACTIVITY OF 4-(N-OCTYLOXY) BENZOIC ACID AND ITS Cr (III) AND CU (III) COMPLEXES ON BRASSICA NIGRA L. (BLACK MUSTARD)

Noor Mohammad[1] and Nitin G. Asole[2]

[1,2]Department of Chemistry, B.S. Patel college of Arts, Commerce and Science, Pimpalgaon Kale, Jalgaon Jamod, Buldhan

ABSTRACT

The seed germination activity of 4-(n-octyloxy) benzoic acid and its Cr (III) and Cu (III) complexes on Brassica nigra L. (black mustard) have been studied at pH 6.5 and 9.5 in order to clarified whether this ligand and its ternary complexes of can be used as seed germination activity by measurement of parameters like percentage of germination, survival, seedling height, soot length, root length, root/soot ratio and width of young leaf. The average values of these parameters have been used to make a justification about seed germination activity of ligand and its ternary complexes.

KEYWORDS Plant regulator, seed germination, ligand, metal, shoot length, root length, root/shoot ratio.

INTRODUCTION

Plants though they come into view common place and reactive, proved to be complex and attractive functions of systems and accepting them is difficult task, for both the students and scientists. Of course, the job is beyond anyone creature and scientists have busy on it. The study becomes mainly passionate in current years. Plants are autotrophic in nature, they produce their acquire food. But we are

completely and extremely dependent on plants for the requirements of life. So that it is essential to do agricultural research is the making of novel and better character and variety of harvest plants, the enhancement of plant growth ,defense against insects, diseases and weeds, the manage of soil fertility. The biological action of metal chelate presented.1-3 Deosarkar et al4have been study of plant growth regulating activity of (2-chlorophenyl) (5-(2-hydroxyphenyl)-3-(pyridin-3-yl)-1h-pyrazol-4-yl) methanone and its Fe(iii) and cu (ii) complexes on trigonella foenum-graecum. Ligands and its metal ions complexes have been studied to be useful in agriculture as plant growth regulating.5-15

To study the germination and growth pattern cost-effective plants Brassica nigra L. (black mustard) is preferred economical significance of this plant by its broad use for the species purposes. Benzoic acid derivative have been found to play an important role in a number of biological processes. They operate in plants as antioxidants, antimicrobials, photoreceptors, visual attractors, feeding repellants, and for light screening. Therefore, the present work is carried out to study the plant growth regulating activity of like 4-(n-octyloxy) benzoic acidand its Cr(III) and Cu (III) complexes on Brassica nigra L. (black mustard)have been studied at pH 6.5 and 9.5.

EXPERIMENTAL METHODS

The entire chemicals are analytical reagent (AR) grade with were obtained from Sd Fine chemicals, India which is worn as such without further purification. Water which was used in the experiment, distilled and degassed prior to manufacture solutions. The solution of 4-(n-octyloxy) benzoic acid ligand of 0.01 mol/dm3 concentration was prepared in distilled water. The selective biological applications were deliberate at pH 6.5 and 9.5 and at 0.1mol/dm3 ionic strength of KNO3 solution. Fertilized soil was composed from agricultural land. Stones and other unwanted materials were kept out. Two parts of this finely powdered soil was uniformly mix with one part of filtered pink-stone-sand. This soil was full in wooden trays having compartments of identical size. The soil in the tray was moistened with distilled water. After one hour passed the sowing of seeds was done in this soil. The well seeds of black mustard haing equal size were selected. 250 seeds were soaked in distilled water and kept back in refrigerator for 3 hours. The healthy seeds of equal size were preferred out of which 50 seeds each were soaked in distilled water, ligand solution, and ternary complex solution with Cr (III) and Cu (III) of pH 6.5and 9.5for 6 hours. The pH was maintained using ELICO-pH meter-L1-10 (accuracy ±0.05 units). The seeds soaked were free out of each solution and washed with distilled water. The seeds were sowed in the wooden trays. Effect of Cr (III) and Cu (III) complexes deliberate at different pH (6.5 and 9.5), the seeds being immersed in experimental solution for 6 hours. Germination and survival were distinguished after 7 days and 10 days respectively. By noting survival of the plants after 10 days, they were taken out of the soil. The properties such as seedling height, shoot length, root length, root/shoot ratio, and thickness (width length) of young leaf of survived plant were calculated.

RESULTS AND DISCUSSION

Parameters such as percentage of germination, survival, seedling height, shoot length, root length, root/shoot ratio, and thickness of young leaf was monitored on the basis of seed germination or plant growth regulator .The mean values of these parameters are shown in following table. The plant regulator like root/shoot ratio is one of the method of overall health of the plants and it was found by using equation (1).

root/shoot ratio = dry weight for roots/dry weight for top of plant……………(1)

The dry weight was evaluated by keeping 50 fresh plantlets in oven first at 70°C and later at 100°C to find a constant weight. It can be shown from table that there is change in the root: shoot ratio over control (water) which indicates the change in overall growth of the plant. In this work the root: shoot ratio has greater than before for both Cr(III) and Cu (III) complex at pH 6.5 and 9.5 as compared to control action, this remarkable growth is a indication of a in good health plant compared to other treatments. Boost in this ratio came from bigger root size and not from a reduce in shoot weight.

Vigor index was determined using equation (2).

Vigour index = % germination X (root length in mm + shoot length in mm)……..(2)

The higher rate of vigor index at pH 6.5 and 9.5 are revealed for the treatment of Cu (III) complex solutions. The vigor index rates for various treatments are increased as compared to control.

The order of plant growth regulators found at various pH is shown below:

At pH 6.5 and 9.5, Cu (III)-Ligand complex solution > Cr (III)-Ligand complex solution > Ligand > Control (water).

The Cu (III) - 4-(n-octyloxy) benzoic acid complex solution is proposed as a plant growth regulator at pH 9.5 for *Brassica nigra L. (black mustard)*plant.

Table : Effect of ligand and its complexes with Cr (III) and Cu (III) on growth parameters of *Brassica nigra L. (black mustard)* plant (I=0.1 mol/dm^3 KNO$_3$)

Parameters	Effect of following solutions on different growth parameters			
	Control	Ligand	Ni (III)-Ligand complex	Cu (III)-Ligand complex
pH 6.5				
Germination seed number	50	50	50	50
% Germination after 10days	63	68	83	76
% Survival after 12 days	75	79	86	99
Seedling height (cm)	6.8	7.3	7.8	8.5
Root length (cm)	2.6	2.9	3.6	3.6
Shoot length (cm)	4.9	5.5	5.9	6.5
Root/shoot	0.39	0.48	0.59	0.68
Vigor index	4027	4747	6789	6468
Width of young leaf (cm)	0.5	0.6	0.7	0.7
pH 9.5				
Germination seed number	50	50	50	50
% Germination after 10days	64	65	72	79
% Survival after 12 days	77	81	87	95
Seedling height (cm)	7.9	8.5	8.5	8.7
Root length (cm)	2.7	3.4	3.9	4.0
Shoot length (cm)	4.7	5.1	5.8	6.2
Root/shoot	0.49	0.56	0.65	0.73
Vigor index	4335	4746	6034	7282
Width of young leaf (cm)	0.5	0.3	0.6	0.7

REFERENCES

[1] H Gershon; R Parmegiani; WJ Nicerson. *Appl. Microbiol*., **1962**, 10(6),556-   560.

[2] H Gershon; R Parmegiani. *Appl. Microbiol*., **1963**, 11(1), 62-65.

[3] Noor Mohammad , *Ph.D. Thesis, Chemistry*, **2014**, S.G,B,Amravati University, Amravati (MS) India.

[4] S. D. Deosarkar, S. A. Chavan and Avinash L. Puyad, *J. Chem. Pharm. Res., 2011, 3(4):703-706*

[5]   ML Narwade. *Ph.D. Thesis, Chemistry*, **1974**, B. A. M. University, Aurangabad (MS) India.

[6]   M Dixon; EC Webb. *Enzymes*, Longmans, Green and Co., London, **1964**.

[7]   RC Sharma; SP Tripathi; S Khanna; RS Sharma. *Curr. Sci*., 1981, 50, 748-750.

[8]   AB Patil. *Orient. J. Chem.*, **2009**, 25(2), 459-460.

[9]   V. J. Thakare. *Ph.D. Thesis*, *Chemistry*, 2007, S. G. B. Amravati University, (MS) India.

[10] CM Adams; EA Bernays. *Entomol. Exp. Appl*., **1978**, 23, 101-109.

[11] UP Meshram; BG Khobragade; ML Narwade; VB Khobragade. *Der Pharma Chemica*, **2011**,3(2), 376-382.

[12] VP Singh; Yashovardhan; SK Bhati. *Int. J. ChemTech Res.,* **2011**, 3 (2), 892-900.

[13] AV Mane; RR Sankpal; LA Mane; MS Ambawade. *J. Chem. Pharm. Res.,* **2010**, 2(5), 206-215.

[14] Ghani, S. B. A.; Mugisha, P. J.; Wilcox, J. C.; Gado, E. A. M.;Medu, E. O.; Lamb, A. J.; Brown, R. C. D. Synth. Commun. 2013, 43,1549–1556.

[15] Maicheen, C.; Jittikoon, J.; Vajragupta, O.; Ungwitayatorn, J.Med. Chem. 2013, 9, 329–339.

THERMAL DEGRADATION STUDIES OF COPOLYMER OBTAINED FROM 2, 4-DIHYDROXYACETOPHENONE-GUANIDINE-FORMALDEHYDE.

Preeti A. Mishra and W. B. Gurnule

Department of Chemistry, Kamla Nehru Mahavidyalaya, Sakkardara, Nagpur, (Maharashtra) INDIA

ABSTRACT

Copolymer (DAPGF) has been synthesized utilizing the monomers 2,4-Dihydroxyacetophenone, guanidine and formaldehyde by the condensation polymerization reaction in the presence of 2M HCl as a catalyst using 1:1:2 molar ratios of reacting monomers. The structure of DAPGF copolymer has been elucidated on the basis of elemental analysis, and various physicochemical techniques, i.e., UV-Visible, FT-IR and 'H-NMR spectroscopy. Detailed thermal degradation study of the new copolymer has been carried out to determine its thermal stability. Thermal degradation curve is discussed which shows various decomposition steps. The activation energy (Ea.) and thermal stability calculated by using the Sharp-Wentworth and Freeman-Carroll methods. Thermodynamic parameters such as entropy change (ΔS), apparent entropy change (S*) and frequency factor (z) have also been evaluated on the basis of the data of Freeman-Carroll method. The order of reaction (n) is found out to be 0.8.

Keywords - Synthesis; Polycondensation; Thermal; Kinetic parameter; Spectral methods.

INTRODUCTION

For the progression in the field of material science, copolymers found by numerous scientists have amazingly extraordinary applications. A large number of copolymers have been synthesized by various chemists in large amounts and discover huge applications like cement, bundling, covering in electrically stable materials, impetus, thermally stable materials [1,2], ion-exchangers [3,4], high dielectric constant for energy storage capacitors [5] and semiconductors which have many applications.[6]. A remarkable effort has been made to work on the nature of copolymer either by monomers or by changing different strategies. The thermal properties of various copolymers have been studied by utilizing the method of thermogravimetric analysis (TGA) by a wide range of scientists. S. Ullah et al had *studied the* Synthesis and thermal degradation studies of melamine-formaldehyde resin [7]. The thermal properties and behavior of newly synthesized copolymer derived from salicylic acid and thiosemicarbazone have been investigated by Kamlakar *et al* [8]. The thermal degradation and kinetics of terpolymer resin derived from p-hydroxybenzaldehyde, succinic acid with ethylene glycol were examined by A. Gupta and co-workers [9]. Thermogravimetric analysis of terpolymer resin derived from salicylic acid, hexamethylenediamine with formaldehyde was studied by D.T. Masram [10] and thermal analysis of 8-hydroxyquinoline and formaldehyde was done by P. E.P. Michael *et al* [11]. The thermal decomposition reaction of salicylic acid, diaminonaphthalene with formaldehyde was investigated by D.T. Masram [12]. S. Butoliya *et al* have taken interest in the study of non-isothermal decomposition and kinetic analysis of 2,4-dihydroxybenzoic acid, the melamine-formaldehyde copolymer [13]. A thorough study of literature survey reveals that copolymer derived from substituted hydroxyl or acetyl group, propionyl group, and methoxy group with formaldehyde shows improved thermal resistance, electrical property, antimicrobial property, light-emitting property, and morphology.

The current study deals with the preparation of 2,4-dihydroxyacetophenone-Guanidine hydrochloride-formaldehyde copolymer in 1:1:2 molar extents. The structure of 2,4-DAPGF copolymer has been drawn based on elemental analysis and various physicochemical techniques, such as ultraviolet-visible spectroscopy, Fourier transforms infrared spectroscopy,₁H-NMR spectroscopy. To study the thermal stability of DAPGF copolymer, detailed thermal degradation analysis has been carried out. The thermal degradation curve is discussed, which shows four decomposition steps. By using Freeman–Carroll method and Sharp–Wentworth methods, the activation energy (*Ea*) and thermal stability are calculated.

Materials*:*

Entire synthetic substances such as 2,4-Dihydroxyacetophenone and guanidine hydrochloride were purchased from Central Scientific Company, Dharampeth, Nagpur, was of A.R. grade. The chemicals like Hydrochloride, formaldehyde, and dimethyl sulphoxide were used from the Post Graduate Department of chemistry, Kamla Nehru Mahavidyalaya, Nagpur, India.

Synthesis of DAPGF Copolymer Resin

2,4-Dihydroxyacetophenone[0.1mol], and Guanidine hydrochloride [0.1mol], were weighed properly using the electric weighing machine. The mixture of these two was taken in round bottom flask and 37%formaldehyde

[0.2 mol] in the presence of 2M hydrochloric acid (200 ml) was added to flask and heated in an oil bath at 124°C ± 20°C for 5 h with occasional shaking [10-12]. The separated resinous product (DAPGF) was washed with hot water to remove untreated monomers. The resin was purified. The purified copolymer resin was finally ground well to pass through a 300-mesh size sieve and kept in a vacuum over silica gel for 24 hours. The yield of DAPGF copolymer resin was found to be 80-82%. The reaction taking place is as shown in Fig. 1
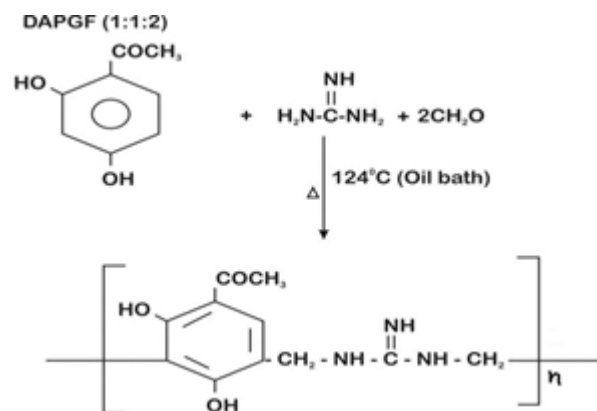
Fig. 1: Synthesis of 2,4-DAPGF Copolymer resin

Characterization of Copolymer

The elemental analysis of DAPGF copolymer resin was recorded on the Elemental Vario EL III Carlo Erba 1108 elemental analyzer instrument. The UV-Visible spectra of the copolymer were carried out at room temperature in DMSO on a double beam spectrophotometer fitted with an automatic pen chart recorder in the range of 200nm – 800nm. Infrared spectra of copolymer have been scanned indanol mull on Perkin-Elmer-Spectrum RXI, FT-IR Spectrophotometer in KBr pellets in the range of 4000-500 cm-1. The surface analysis of the sample was examined by scanning electron microscope (SEM)using JEOL-JSM-6380 at different magnifications. The proton NMR spectrum of the copolymer was carried out using DMSO-d6 as a solvent on Bruker Advance -II400 MHz NMR spectrophotometer. The TGA has been scanned by using a Perkin Elmer diamond TGA/DTA analyzer. All the spectral and detailed analytical studies for the newly synthesized copolymer were carried out at Sophisticated Analytical Instruments Facility (SAIF), STIC, Cochin University, Cochin, India.

Thermal Studies

The thermal analysis method is based on the change in weight of the sample per degree change of temperature. Heating is performed under highly systematic and controlled conditions and degradation of various functional groups was studied. The non-isothermal thermogravimetric analysis was performed in an air atmosphere with a heating rate of $10°C$ min^{-1}using 5-6 mg of samples from the temperature range 40°C to 750°C and a thermogram was recorded.

Theoretical Consideration

The thermogram of the DAPGF copolymer was examined and interpreted to obtain information regarding the percentage weight loss of copolymer samples at different temperatures which gives information about sample composition, the product formed after heating, and kinetic parameters. Thermodynamic and kinetic parameters have been calculated and analyzed using Sharp-Wentworth and Freeman-Carroll methods as follows.

A] Freeman-Carroll Method (FC): In this the kinetic parameters are determined by the formula,

$\Delta \log(dw/dt)/\Delta \log Wr = [-Ea/2.303R] \times \Delta(1/T)/\Delta \log Wr + n$.

Where,

dw/dt =Rate of change of weight with time,

Wr =Difference between weight loss at the completion of the reaction and at time t,

Ea=activation energy, n=order of reaction.

B] Sharp-Wentworth method (SW): Following expression is used to evaluate the kinetic parameters,

$Log (d\alpha/dt)/(1-\alpha)^n = \log A/\beta - Ea/2.303 RT$

Where $d\alpha/dt$ is the fraction of weight loss with time, n is the order of reaction, A is frequency factor,

B is linear heating rate and α is the fraction of amount of reactant.

RESULTS AND DISCUSSION
Elemental and Physico-chemical Analysis
Elemental analysis is a technique that determines the molecular structure of all substances. DAPGF copolymer has been analyzed for carbon, hydrogen, and nitrogen content present in it. The empirical formula and empirical formula weight have been calculated which is presented in table 1. The % of carbon, nitrogen, and hydrogen element of the copolymer DAPGF determined by elemental analysis is found to be in accord with the calculated values.

Table 1: Elemental analysis and empirical formula of the copolymer resin

Copolymer	Empirical formula of repeated unit	Empirical formula weight	%C (found/cal.)	%H (found/cal.)	%N (found/cal.)
DAPGF (1:1:2)	$C_{11}H_{13}N_3O_3$	235	57.94(55.93)	4.16(5.9)	15.55(16.61)

The non-aqueous conductometric titration in DMF against KOH in 50% (v/v) DMF/ alcohol mixture using 100 mg of resin sample was carried out to determine the molecular weight of the copolymer resin. A plot of specific conductance against the milliequivalents of potassium hydroxide required for neutralization of 100 g of copolymers was done. The study of such a plot affirms that there are many breaks in this plot. From this plot, the first break and the last break were noted to calculate the degree of polymerization Dp (Fig.2). The calculation of molecular weight by this method is based on the following consideration. From the graph the first and the last break was observed. The first break corresponds to the neutralization of the more acidic phenolic hydroxy group of all the repeating units and it is the break in the graph beyond which a continuous increase in conductance is observed which represents the stage at which the phenolic hydroxy group of all repeating units are neutralized [14].

On the basis of the above observation, the average degree of polymerization ($\overline{Dp}$)and ($\overline{Mn}$) is calculated by using the following formulae:

$$\overline{Mn} = \overline{Dp} \text{ x repeat unit weight}$$

Total Meq. of base required for complete neutralization i.e., last break

$$\overline{Dp} = \frac{\text{Total Meq. of base required for complete neutralization i.e., last break}}{\text{Meq. of base required for smallest interval i.e., first break}}$$

Meq. of base required for smallest interval i.e., first break
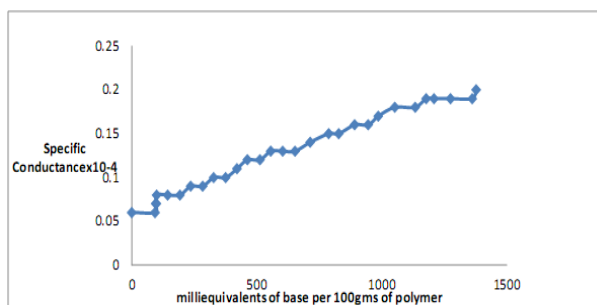
Fig.2: Non-aqueous Conductometric titration of DAPGF copolymer.

Table 2: Determination of number average molecular weight

Polymer	1st phase of neutralization	Final phase of neutralization	Degree of polymerisation	Emperical weight	Number average molecular weight
DAPGF (1:1:2)	93	1361	14	235	3453

UV-Visible Spectra
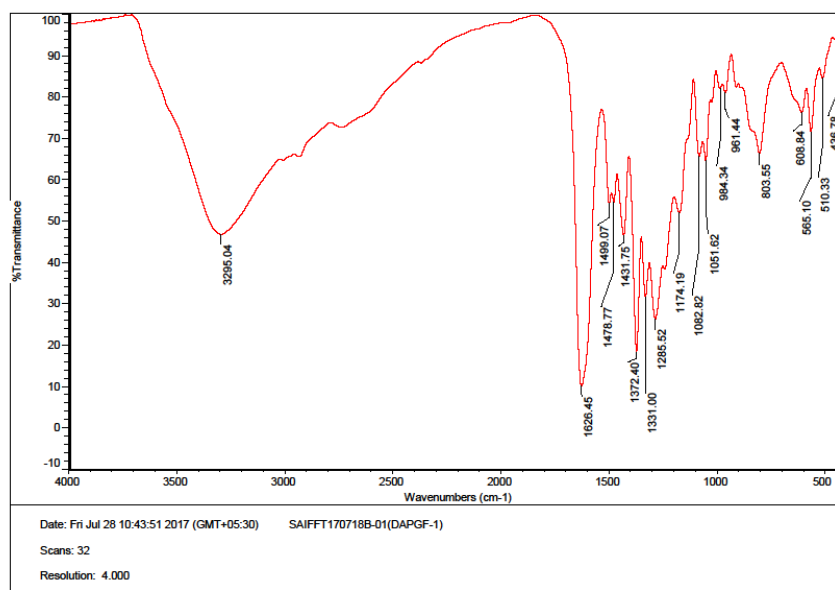
Fig.3 UV-visible spectra of DAPGF copolymer

The UV-visible spectra of DAPGF copolymer resin are presented in figure 3. UV-visible spectra of copolymer samples have been recorded in pure DMSO in the region of 200 to 800 nm. The spectrum exhibits two absorption maxima i.e., two peaks which are observed in the region 270 nm and 330 nm. This position of the absorption band which is observed for copolymer DAPGF indicates the presence of the ketonic group (carbonyl) having a carbon-oxygen double bond which is in conjugation with the aromatic nucleus. The appearance of the first band which is more intense can be accounted for $\pi \rightarrow \pi^*$ transition while the second band which is less intense may be due to $n \rightarrow \pi^*$ electronic transition. The shift from the basic value (viz. 240 nm and 310 nm respectively) may be due to the conjugation effect and the presence of phenolic hydroxyl group (auxochrome) is responsible for hyperchromic effect i.e., the higher value of $\in$ max is indicated.

FT-IR Spectra

The FT-IR spectra of the DAPGF copolymer are presented in figure 4 and spectral data are specified. A broad and strong band has appeared in the region 3295cm^{-1} which may be due to the stretching vibration of the phenolic hydroxyl group. The strong band at 1626 cm^{-1} may be assigned due to the stretching vibration of the Ar-CO- group. A sharp band appearing at 1478 cm^{-1} describes the presence of>C=C< (aromatic) group. The sharp and strong band observed at 1372.4cm^{-1} suggests the presence of -CH$_2$- methylene bridge in the copolymer chain. Weak bands appearing in the region 905-860 cm^{-1}may be due to the presence of 1,2,3,4and 5-pentasubstituted aromatic rings [15].
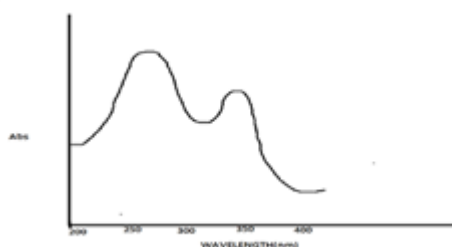
Fig.4 FT-IR spectra of DAPGF copolymer

Table 3: FT-IR spectra of DAPGF copolymer

Observed band frequencies(cm^{-1})	Assignment of groups	Expected band frequencies(cm^{-1})
3295	-OH phenolic	3500-2800
1626	Ar-CO- group	1670-1630
1478	Aromatic ring	1445-1485
1372.4	-CH$_2$- bridge	1380-1350

| 803.55 | -NH group | 900-650 |
| 1051.62 | Substituted benzene ring | 1058 |

₁H-NMR Spectra

The 1H-NMR spectra of DAPGF copolymer are depicted in figure 5 and spectral data are assigned below. The spectrum reveals a different pattern of peaks since each of them possesses a set of protons having a different proton environment. The weak multiplicity signals (unsymmetrical pattern) in the region δ 7.1 ppm are due to the aromatic protons (Ar-H). A significant signal appearing at δ 6.4ppm is attributed to the phenolic -OH proton in intramolecular hydrogen bonding. The medium triplet signal observed at δ7.6 ppm may be due to the amido proton Ar-CH2-NH- of copolymer chain. The proton of methylene bridge Ar-CH₂- NH- may be recognized from the doublets signal which appears in the region δ 2.6 ppm. A peak appeared in the region δ 1.2 ppm may be due to methyl proton of the Ar-COCH3 group [16].
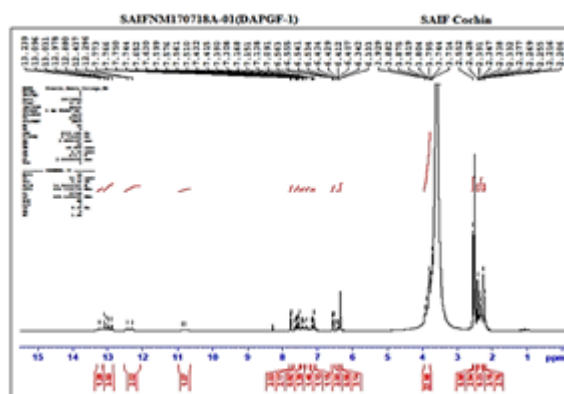
Fig.5. Proton NMR spectra of DAPGF copolymer

Table 4:1H-NMR spectra of DAPGF copolymer resin.

Observed chemical shift δ(ppm)	Nature of proton assigned	Expected chemical shift δ(ppm)
6.4	Phenolic -OH (S)	4-7
7.1	Ar-H	6.5-9
2.3	α H next to C=C	2-3
2.6	Ar-CH2-N moiety	2.0 -3
7.8	Methyl proton of-COCH3	6.5-8.5

Scanning Electron Microscopy

scanning electron micrograph DAPGF copolymer resin was analyzed at different magnification to study the surface morphology which is presented in figure 6. It gives information about surface topography and defects in the structure. At lower magnification, it shows spherules in which the crystals are arranged more closely in smaller surface areas. At higher magnification, it shows a more amorphous character with a less close-packed surface having deep pits. Thus, the resin is crystalline as well as
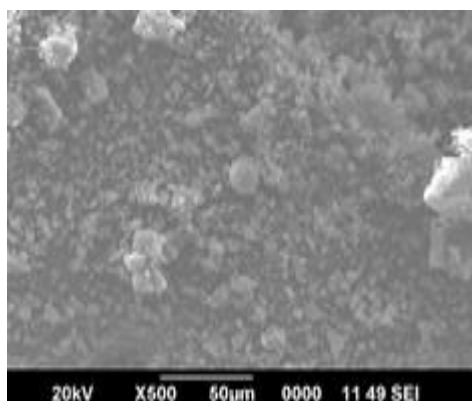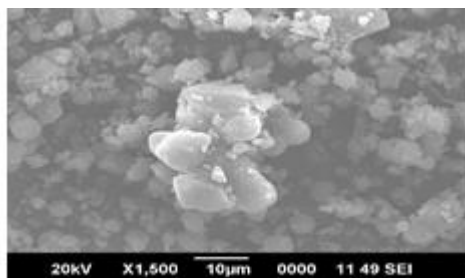
Fig 6 scanning electron micrograph DAPGF copolymer amorphous or transitions between crystalline and amorphous in structure and character [17].

Thermogravimetry Analysis of the Copolymer

The copolymer DAPGF has been subjected to thermogravimetric analysis and data used to access the degradation pattern. The thermal decomposition behavior curve for the resin is depicted in figure 7 which exhibits four-stage decomposition and its ranges are incorporated in the table4. The first stage decomposition was slow and ranged between 40- 260°C, corresponds to mass loss of 6.55% found and 7.11% calculated which may be due to entrapped water molecules. The second stage decomposition starts from 260 °C to 370 °C, corresponding to the gradual mass loss of 39.92% found and 40.11 % calculated which represents the degradation of two hydroxyl groups and –$COCH_3$ group attached to an aromatic benzene ring. The third stage decomposition at370-570 °C, corresponding to 70.35% rapid mass loss of aromatic nucleus against calculated 70.55%. The fourth stage starts from 570 °C to 620 °C corresponding to the removal of the entire acetophenone moiety with an observed mass loss of 99.88% against calculated 100%. The half decomposition temperature for DAPGF copolymer is found to be480°C.
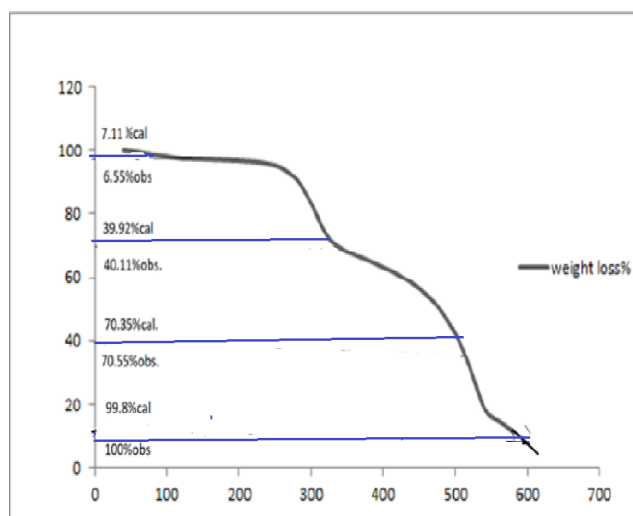
Fig.7: Thermogravimetric analysis of DAPGF copolymer

Table 4: Degradation of copolymer at different temperature range

Copolymer resin	Temperature range	Group degraded	%Weight loss Obs.	Cal.
First stage	40-260°C	Water -NH and -CH_2	6.55	7.11
Second stage	260-370°C	-OH and -$COCH_3$	39.92	40.11
Third stage	370-570°C	Aromatic nucleus	70.35	70.55
Fourth stage	570-620°C	acetophenone moiety	99.8	100

Thermoanalytical Data

For the copolymer DAPGF, a plot of percentage mass loss versus temperature is presented in Figure 6. To obtain the relative thermal stability of the copolymer, the method described by Sharp-Wentworth and Freeman-Carroll was adopted. The thermal stability of copolymer, based on the initial decomposition temperature, has also been used here to their relative thermal stability, neglecting the degree of decomposition. By applying the above methods, the activation energy (Ea) is calculated which is not perfectly in agreement with each other. But

the 'average Ea' calculated by Freeman-Carroll and Sharp-Wentworth methods is nearly the same. A representative thermal activation energy plot of Sharp-Wentworth (Figure 8) and Freeman-Carroll (Figure 9, 10) method for the copolymer has been shown. Thermodynamic parameters such as entropy change (ΔS), free energy change(ΔF), frequency factor (Z), apparent entropy change (S*), calculated based on thermal activation energy (Ea) using equations (3), (4), (6) and (7). These values are incorporated in Table 5.

Entropy change

Intercept=log KR/hϕEa +ΔS/2.303R $\qquad$ (3)

Where,

K=1.3806x10^{-16} erg/deg/mole $\qquad$ R=1.987 cal/deg/mole,

h=6.625 x10^{-27} erg sec, ϕ=0.166, ΔS=change in entropy,

Ea=activation energy from graph

$\Delta F = \Delta H - T\Delta S$ $\qquad$ (4)

Where,

ΔF=free energy change ΔH=activation energy, T=temperature in Kelvin

ΔS=entropy change from equation (3)

Frequency factor

B$_{2/3}$=log ZEa/Rϕ ………… (5)

B$_{2/3}$= log (3) +log [1-3$\sqrt{1-\alpha}] - logp(x)$ … … (6)

Where,

Z = Frequency factor, B=Calculated from……… (6)

B = Calculated from ……….. (6),

Log p(x) = Calculated from Doyle table corresponding to activation energy

Apparent entropy change

S* = 2.303 Rlog Zh/RT*……….. (7)

Where,

T* = Temperature at which half of the compound decomposed from its total loss

Fairly good straight-line plots are obtained using the two methods. This indicates the decomposition of copolymer does not obey the first-order kinetics perfectly. Due to the abnormally low value of the frequency factor, it may be concluded that the decomposition reaction of DAPGF copolymer can be classed as a 'slow 'reaction. The slow reaction is also predicted by negative values of entropy change. The negative values mean the disorder is less and the reaction is carried out in a more orderly manner, making it slower.[30].
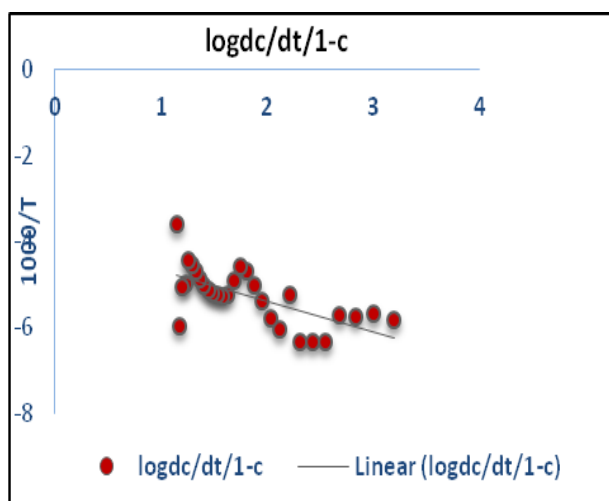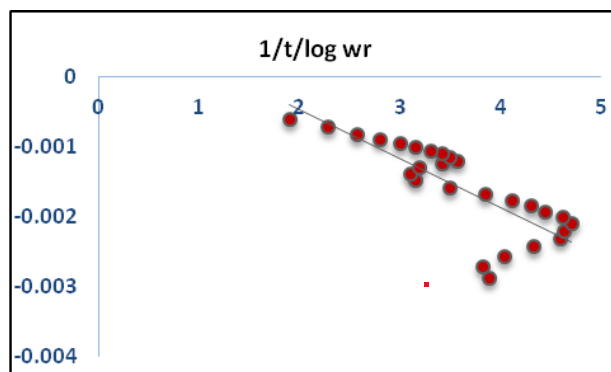
Fig.8 Sharp-Wentworth Plot of DAPGF copolymer   Fig.9 Freeman-Carroll Plots of DAPGF copolymer

Table 5 Results of thermogravimetric analysis of DAPGF (1:1:2) copolymer resin

Ternoly mer	Half decomp osition temp.(K)	Activation energy Ea FC SW	Entropy change ΔS	Free energy ΔF	Frequency factor (Z)	Apparent entropy (s*)	Order of reaction
DAPGF (1:1:2)	480°C	11.715 10.95	-370.92	116.106	461.35	-54.49 J	0.78

CONCLUSIONS

DAPGF copolymer resin was prepared from 2,4-dihydroxyacetophenone, guanidine hydrochloride with formaldehyde in the presence of acid catalyst by condensation polymerization technique. The proposed structure of the synthesized copolymer has been confirmed from the elemental analysis, FTIR and1H-NMR spectral studies. The Thermogram of the copolymer shows four stages of decomposition. The values of activation energy evaluated by both Sharp-Wentworth and Freeman-Carroll methods are in good agreement with each other. Positive values of activation energy corresponding to the energy of activation due to the oxidation-reduction process of the copolymer in the higher temperature range. The negative values for entropy indicate that the activated polymer has a more ordered structure than the reactants. A low value of frequency factor may be concluded that the decomposition reaction of the copolymer can be classified as a slow reaction. Thermogravimetric study reveals that DAPGF copolymer resin isothermally stable even at high elevation temperature.

REFERENCES

1. S. Pashaei, S. Siddaramaiah, M.M. Avval, and A.A. Syed."*Thermal degradation kinetics of nylon-6/gf/crysnanonanoclay nanocomposites by TGA*," Chemical Industry and Chemical Engineering Quaterly.; 17(20): p.141-151 2011.

2. G.E. Zaikov," *Degradation and Stabilization of Polymers, Theory and Practice*," Nova Science Publishers,New Delhi, India,1995.

3. W.B. Gurnule, P.K. Rahangdale, L.J. Paliwal, R.B. Kharat," *Chelation ion-exchange properties of copolymer resin derived from 4-hydroxyacetophenone, oxamide and formaldehyde,*" J. Appl. Polym.Sci. vol.89(3), pp 787-790, 2003.

4. A.D. Kushwaha, A.B. Kalambe, V.V.Hiwase, D.N. Urade," *Structural and antibacterial study of resin-II derived from p-nitrophenol, resorcinol and formaldehyde,* J.Chem. Pharma, Res, vol. 4 (2), pp111-116,2012.

5. S.K. Kapse, V.V. Hiwase, A.B. Kalambe," *Synthesis and semi conducting behaviour of the terpoly ligand derived from p-hydroxy acetophenone, quinhydrone and melamine,*" J. Chem. Pharma.Res, vol.4(3), pp 1734–1739,2012.

6. W. Hackenberger, R. Alberta, W. Paul, D. Jeong, and Q. Zhang," *High dielectric constant terpolymers for energy storage capacitors,*" in Proceedings of the 25th Symposium for Passive Components, Palm Springs, pp 239–243. 2005

7. S. Ullah, M.A. Bustam, M. Nadeem, M.Y. Naz, W.L.Tan, A.M. Shariff," *Synthesis and thermal degradation studiesof melamine formaldehyde resins*," The Scientific World J.,Article ID 940502,pp 1-6,2014.

8. K.A.Nandekar, J.R.Dontulwar, W.B.Gurnule, *"Thermal behavior of newly synthesized copolymer derived from salicylic acid and thiosemicarbazide,"*Der Pharma Chemica. Vol.4(4) , pp 1644-1652,2012.

9. A.N.Gupta, V.V.Hiwase and A.B.Kalambe*," Thermal degradation and kinetic study of terpolymer resin-I derived from p-hydroxybenzaldehyde, succinic acid and ethylene glycol*," Der Pharmacia Lettre,vol.5 (2) ,pp.105-112, 2013.

10. N.C. Das, W.B.Gurnule, *"Kinetic Study of Non-Isothermal Decomposition of Copolymer Resin Derived from 2,4-Dihydroxy-propiophenone,1,5-Diaminonaphthalene and Formaldehyde*. Material Today Proceeding. 2019.

11. P.E.P. Michael, J.M. Barbe, H.D.Juneja, L.J. Paliwal," *Synthesis, characterization and thermal degradation of 8-hydroxyquinoline-guanidine-formalde-hydeterpolymer,"* Europ.Polym. J., vol.43(12) pp.4995–5000,2007.

12. D.T. Masram," *Thermal Degradation study of salicylic acid, diaminonaphthalene and formaldehyde terpolymer*,"E-J. Chem., vol.6(3) pp.830-834,2009.

13. S.S. Butoliya, W.B. Gurnule, A.B. Zade," *Study of non-isothermal decomposition and kinetic analysis of 2,4-dihydroxybenzoic acid-melamine-formaldehyde copolymer,"* E-Journal of Chemistry,vol. 7(3) pp.1101-1107,2010.

14. M.M. Yeole, S.Shrivastava, W.B. Gurnule, "*Synthesis and characterization of copolymer resin derived from 4-methyl acetophenone*, *phenyl hydrazine and formaldehyde*," Der Pharma Chemica,vol. 7(5) pp.124-129,2015.

15. D.B. Patle, W.B. Gurnule," *An eco-friendly synthesis, characterization, morphology and ion exchange properties of terpolymer resin derived from p-hydroxy benzaldehyde,"* Arab. J. Chem, pp.1-11,2011.

16. W.B. Gurnule, C.S. Makde, M. Ahmed," *Synthesis, characterization, morphology, thermal electrical and Ion exchange properties of a copolymer resin,*" J. Environ. Res. Develop,vol. 7(3) pp.1183-1192,2013.

17. W.B. Gurnule, S.P. Dhote*," Synthesis, characterization and thermal degradation studies of copolymer resin derived from 4-hydroxybezophenone, melamine and formaldehyde,*" J. Chem. Pharm.Res., vol.5(12), pp.942-949,2013.

18. R.N.Singru, A.B.Zade, W.B. Gurnule*," Thermoanalytical study and kinetics of new 8-hydroxyquinoline-5-sulphonic acid-oxamide-formaldehyde copolymer resin,"* E-Journal of Chemistry,vol. 6(S1), pp.171-182,2009.

SORPTION CAPACITY OF BENTONITE CLAY FOR REMOVAL OF HEAVY METAL Se (IV) IONS FROM AQUEOUS SOLUTION

Priyanka Rathore[1] and Rashmi Verma[2]
[2]Department of Chemistry, Dr. C.V. Raman University Kargi Road Kota Bilaspur (C.G.) India
[1]Research Scholar, Department of Chemistry, Dr. C.V.R.U. Kargi Road Kota Bilaspur (C.G.) India

ABSTRACT

The present study removal of Se (IV) ion on Bentonite clay from aqueous solution under different experimental conditions. Lagergren's first-order, pseudo-second-order kinetic equation and Langmuir's and Freundlich adsorption isotherm has been used to discuss the adsorption capacity of bentonite clay to removal of Se (IV) Ion. Thermodynamic parameter such as free energy change, enthalpy change and change entropy have been evaluated and discussed and an idea process are spontaneity and feasibility of the adsorption process and also study adsorption capacities are effected different pH, different concentration, different temperature and contact time of shaking. This study was focused on the use of bentonite clay as an alternative adsorbent for the removal of Se (IV) from wastewater. The maximum adsorption 86.00% was found at pH 2 with initial metal ion concentration 100 mg/L. Adsorption of Se (IV) ions depend upon the pH of metal ions. The value of R2 ≈ 0.997 and R2 ≈ 0.994 for Freundlich and Langmuir plots respectively suggested that adsorption of Se (IV) by bentonite clay obey Freundlich model more appropriately than Langmuir model. Kinetic models plotted for the obtained results showed that the adsorption of Se (IV) by bentonite clay is of second order reaction. Kinetic studies showed that experimental data was best described by pseudo second order model.

Keywords: Effect of pH, Adsorption Capacity of Bentonite Clay, Removal of Toxic Heavy Metal Ion, Kinetic, Equilibrium and Thermodynamic Study, Removal of Se (IV) Ion.

1. INTRODUCTION

In nature, selenium is an essential element for humans and animals so as that it is used as a nutritional additive element. It should be controlled with regard to both toxicity and decencies in humans and livestock. Therefore, adverse effects on human health occur from both too much and from too little exposure to selenium. Selenium is also known to be mutagenic and teratogenic. Selenium is introduced in the environment from different sources, both natural and anthropogenic. Selenium mobility in the environment, availability for biota and toxicity depends on its oxidation state and so its speciation is necessary. In the environment, selenium can exist in different oxidation states, elemental selenium (Se), selenite (SeO32−), selenide (Se2−), selenate (SeO42−) and organic selenium. Selenite and selenate are found to be thermodynamically stable under the pH and Redox conditions that are found in most aqueous media and are the predominant chemical forms. Selenite is present in mildly oxidizing, neutral pH environments and typical humid regions. Selenate is the predominant form under ordinary alkaline and oxidized conditions. The presence of selenium in waste and surface waters is becoming a severe environmental and public health problem. A variety of treatment technologies have been reported for selenium removal from contaminated waters. Aqueous environment is a source media for selenium. Because of the toxicity of selenium and its inorganic compounds generally ought to necessary remediation from the different media. The most widely used methods for removing selenium from wastewaters include ion-exchange, chemical precipitation, reverse osmosis, evaporation, membrane filtration, adsorption, and biosorption. Among these technologies, adsorption onto bentonite is one of the most effective and reliable technologies for wastewater treatment. In general, bentonite is broadly applied effective adsorbents for wastewater treatment. In this study, organic pillared bentonite was prepared and adsorption of selenium from aqueous solution was studied as a function of the initial selenium concentration, pH and shaking time. The speciation of Se (IV) includes H_2SeO_3, $HSeO_3^-$ and SeO_3^{2-} , but under the typical pH conditions of clay pore water the oxyanion $HSeO_3^-$ is predominant (Torres et al., 2011). It is the most important species for the safety assessment of a repository because of its low retention in clays and the resulting high mobility in the geo sphere. Many researchers have reported that anions diffuse through the free pore space and cations diffuse through the interlayer space of bentonite. In this study, the effect of the concentration and other parameter on the adsorption of Se (IV) on bentonite was investigated using a kinetic, equilibrium and thermodynamic method.

1. REGARDED REAGENT & METHODS

All chemical used our investigation of analytical reagent (A.R.) or laboratory reagent (L.R.) greed. Selenium oxide (98.20%), Sodium hydroxide and sulphuric acid (99%w/w) supplied by molly chem. Limited Mumbai by help of Javed Trading raigarh (C.G.) Product code 17120, distilled water used in preparation of bentonite clay supplied by Titan biotech ltd. Bhiwandi. 1.0 g of bentonite clay was in 25 ml aqueous solution of Se (IV) ion of

given Different concentration in eight different glass bottles was shaken in shaking machine at Different time interval (20 to 160 min.) after shaken solution centrifuged, filter and analysed for liquid part by AAS. Initial Conc. Se (IV) metal ion (50, 100, 150, 200, 250 mgL^{-1}), pH (2.0, 4.0, 6.5, 8.0, 10.0) and temperature (303K, 313K, 323K) initial Conc. Se (IV) ion used were 25, 50, 75, 100, 125, 150, 175, 200, 225, 250 mgL^{-1} for the equilibrium study.

The following mass balance equation was used to calculate the amount of Se (IV) ion adsorbed:-

$$qe = \frac{(Ci - Ce)V}{m},$$

$$\% \text{ removal} = \frac{(Ci - Ce)}{ci} 100$$

where Ci are before adsorption Se (IV) ion concentration, Ce are after adsorption Se (IV) ion concentration, V is volume of adsorbate in litre and m is weight of the adsorbent in grams. The % of removal of Se (IV) ion was calculated from the equation.

2. RESULT AND DISCUSSION

3.1 Effect of Initial Se (IV) ion Concentration

Fig.-1 Represents % removal of Se (IV) ion versus initial metal ion concentration. Graph study Initial metal ion concentration increase from 50mgL^{-1} to 250mgL^{-1}. The % removal Se (IV) ion decrease from 68.48 % to 56.24 %. Because adsorption possesses a limited number of active sites and theses active sites become saturated at certain concentration.

Fig-2 Represents increase metal ion concentration the amount of adsorbent at equilibrium qe mgg^{-1} increase as initial metal ion concentration increase from 50 mg/L to 250 mg/L the amount of adsorbent increase from 0.856 mgg^{-1} to 3.515 mgg^{-1}. Because due to the fact that mass transfers resistance of Se (IV) ion between aqueous phase and solid phase is possibly overcome by the initial metal ion concentration.
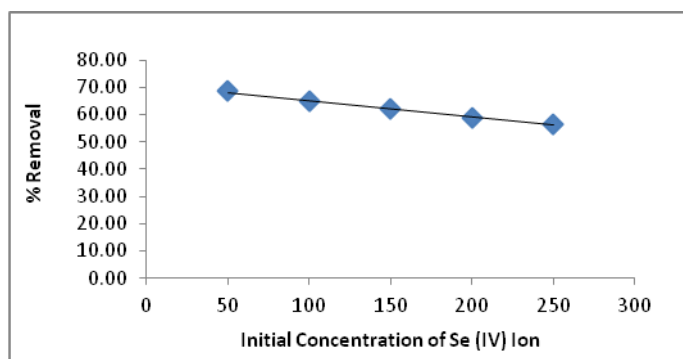
Fig-1:- Effect of initial concentration of Se (IV) ion adsorption
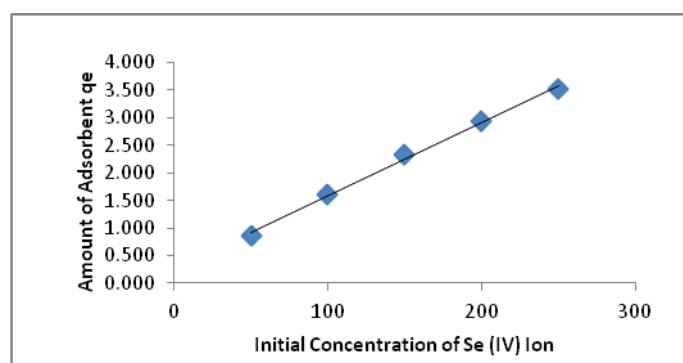
Fig-2:- Effect of initial concentration of Se (IV) ion adsorption

1. Effect of Contact Time

Fig-3 Represents the effect of contact time on the adsorption of Se (IV) ion on Bentonite clay the Fig-3 evidence that amount adsorption increase with increase Time in minute. Initial the rate of adsorption if fast which gradually slows down till equilibrium is reached.

2. Effect of pH

Fig-4 Represents effect of pH on adsorption increasing pH from 2.0 to 10.0 the amount of adsorption decrease from 2.15 mg g^{-1} to 1.186 mg g^{-1} because decrease pH negative Se (IV) ion absorption is easily.
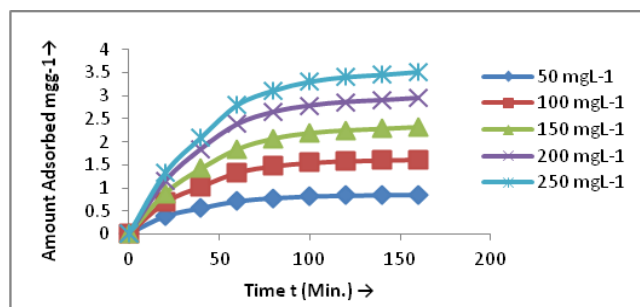
Fig-3:- Effect of contact time on Se (IV) adsorption
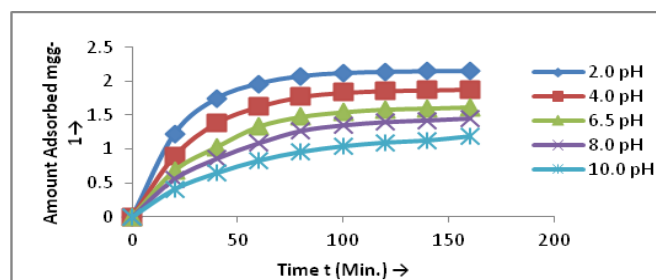
Fig-4:- Effect of pH on Se (IV) adsorption

3. Effect of Temperature

Fig-5 The temperature effected adsorption of Se (IV) from west water temperature increasing from 303K to 313K processor to endothermic amount of adsorption is also increases from 1.618 mgg^{-1} to 1.910 mgg^{-1} at 303K, 313K and 323K are increase temperature with respect indicate the amount of adsorption increase.
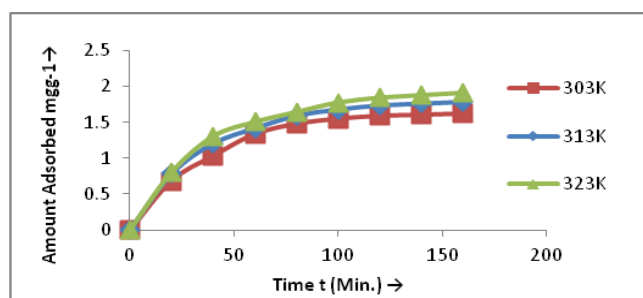
Fig-5:- Effect of temperature on Se (IV) adsorption

4. Effect of Particle Size

The effect of particle size of bentonite clay on adsorption of Se (IV) ion has been shown in figure-6. The particle size of bentonite clay increase from 45μ to 150 μ by amount of adsorption of Se (IV) decreasing from1.618 mgg^{-1} to 1.011mgg^{-1} this decreases in amount of Se (IV) ion on bentonite is due to decreases surface area of bentonite clay particle with increasing particle size.
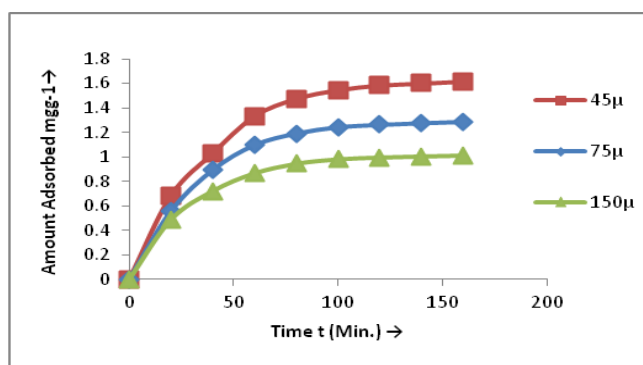
Fig-6:- Effect of particle size on Se (IV) adsorption

3. KINETIC STUDIES

In order to clarify the adsorption kinetics, Lagergren's pseudo-first-order and pseudo-second-order kinetic equation will be applied to the experimental data the linearized form of the well known Lagergren equation for adsorption kinetic at different concentration is as below:-

$$\text{Log } (q_e\text{-}q_t) = \log q_e - \frac{t.k_1}{2.303}$$

Where q_e and q_t are the amounts of the metals sorbent at equilibrium and time "t" respectively and k_1 is the rate constant of sorption can be determined experimentally by plotting of $\log (q_e\text{-}q_t)$ versus t.
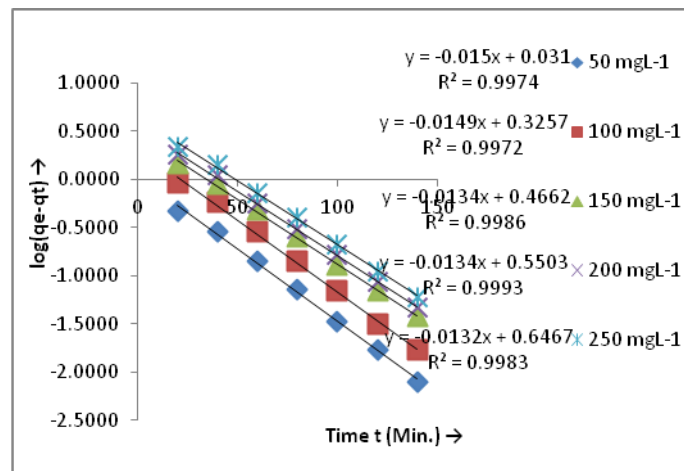
Fig:-7 Lagergren's pseudo-first-order kinetic adsorption of Se (IV) ion on bentonite clay The pseudo-second-order kinetic equation is given as

$$\frac{t}{q_t} = \frac{1}{k_2 q_e^2} + \frac{t}{q_e}$$

Where k_2 is the rate constant of the second order equation, q_t the amount of adsorption after time t and q_e is the amount of adsorption at equilibrium k_2 can be determined experimentally by plotting of t/q_t versus t.
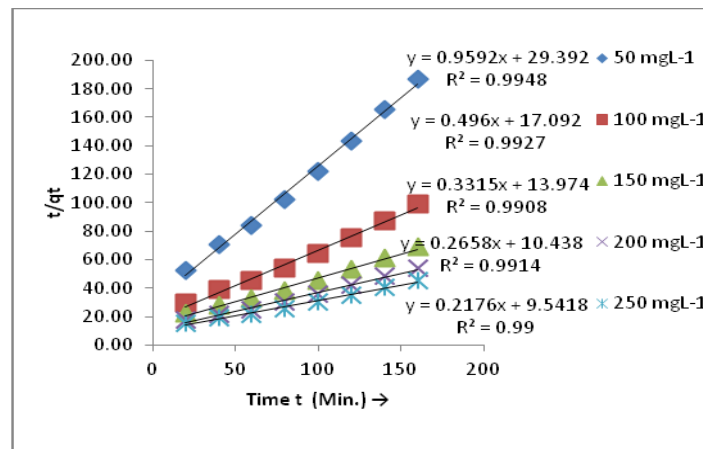
Fig:-8 Pseudo-second-order kinetic adsorption of Se (IV) ion on bentonite clay

Table-1 (a) Kinetic Parameter for Adsorption of Se (IV) ion on bentonite clay

Con. mgL^{-1}	Lagergren-first-order			
	K_1 (min^{-1})	q_{cal} (mgg^{-1})	q_{exp} (mgg^{-1})	R^2
50	3.45 X 10^{-2}	1.074	0.856	0.997
100	3.22 X 10^{-2}	2.113	1.618	0.997
150	2.99 X 10^{-2}	2.924	2.327	0.998
200	2.99 X 10^{-2}	3.548	2.949	0.999
250	2.99 X 10^{-2}	4.426	3.515	0.998

Table-1 (b) Kinetic Parameter for Adsorption of Se (IV) ion on bentonite clay

Con. mgL^{-1}	Pseudo-second-order			
	K_2 (gmg^{-1}min^{-1})	q_{cal} (mgg^{-1})	q_{exp} (mgg^{-1})	R^2
50	3.129 X 10^{-2}	1.043	0.856	0.994

100	1.440×10^{-2}	2.016	1.618	0.992
150	0.078×10^{-2}	3.021	2.327	0.990
200	0.067×10^{-2}	3.774	2.949	0.991
250	0.049×10^{-2}	4.608	3.515	0.990

4. EQUILIBRIUM STUDIES

The Langmuir adsorption isotherm model

Experimental equilibrium data obtained will be discussed using Langmuir adsorption isotherm modal assumes adsorption on a homogeneous surface by monolayer adsorption without interaction between adsorbed molecule the linear form of Langmuir isotherm which is as below-

$$\frac{C_e}{q_e} = \frac{1}{Q.b} + \frac{C_e}{Q}$$

Where q_e is the amount of Se (IV) ion adsorbed per gram of the adsorbent at equilibrium, C_e (mgL^{-1}) is equilibrium concentration of Se (IV) ion in the solution, Q and b are Langmuir constant representing the adsorption capacity and adsorption energy respectively. The value of Q and b slope and intercept of the straight line graph plotting between C_e/q_e Vs C_e.

The Freundlich adsorption isotherm model

For sorption on heterogeneous surface this model is used. It's linearized from is represent as

$$\text{Log } q_e = \log k_f + \frac{logC_e}{n}$$

"Where k_f and n is freundlich constant related to sorption capacity and intensity of the sorbent"[14] the value of k_f and n calculate slope and intercept of the straight line graph plotting between log q_e verses log C_e is linear. It indicates the applicable of the above model.
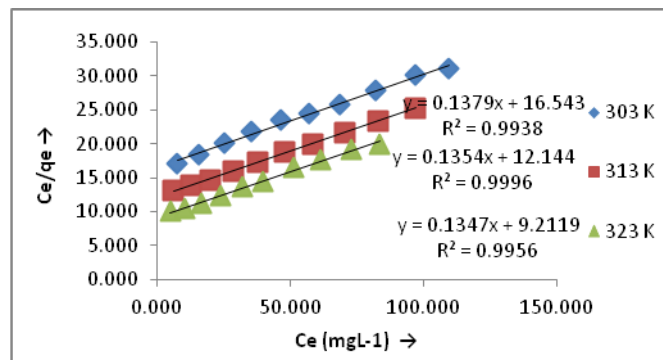
Fig 9:- Langmuir isotherm for the adsorption of Se (IV) ion on bentonite clay
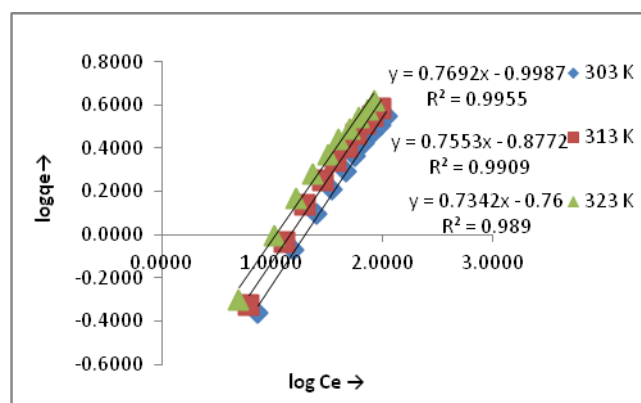
Fig 10:- Freundlich isotherm for the adsorption of Se (IV) ion on bentonite clay

Table-2 Isotherm constant for adsorption of Se (IV) ion on bentonite clay

Temp. (K)	Langmuir Isotherm Parameter			Freundlich Isotherm Parameter		
	Q	B	R^2	n	k_f	R^2
303	7.30	0.083×10^{-2}	0.993	1.30	10.05×10^{-2}	0.995

313	7.41	0.111×10^{-2}	0.999	1.32	13.27×10^{-2}	0.990
323	7.46	1.455×10^{-2}	0.993	1.36	17.38×10^{-2}	0.989

5. THERMODYNAMIC PROCESS

The Gibb's free energy (ΔG^0), the entropy (ΔS^0) and the enthalpy (ΔH^0) will be calculated for study different temperature from 303K to 313K using following equation

$$\text{Log } K_c = \frac{\Delta S^0}{2.303R} - \frac{\Delta H^0}{2.303RT}$$

Were Cs is the equilibrium concentration of adsorbent in mgL^{-1}, Ce is equilibrium concentration of adsorbate in solution in mgL^{-1} and Kc is the equilibrium constant. ΔG^0 has been calculated from the above equation. Plot graph between logKc verses $\frac{1}{T}$ gives strait line. Slope and intercept of this line give the value of ΔH^0 and ΔS^0.

Figure 11 give various graphs between logKc verses $\frac{1}{T}$ and show in fig-11. The value of ΔH^o and ΔS^o all value listed table -3

Table-3 Thermodynamic study for adsorption of Se (IV) ion bentonite clay

Tem. K	ΔG^0 k Jmol^{-1}	ΔH^0 k Jmol^{-1}	ΔS^0 J mol^{-1}	E_a kJ mol^{-1}	S* JKmol^{-1}
303	-1.53				
313	-2.38	23.11	81.39	16.36	5.35×10^{-5}
323	-3.15				

Figure 11 give various graphs between LogKc verses $\frac{1}{T}$
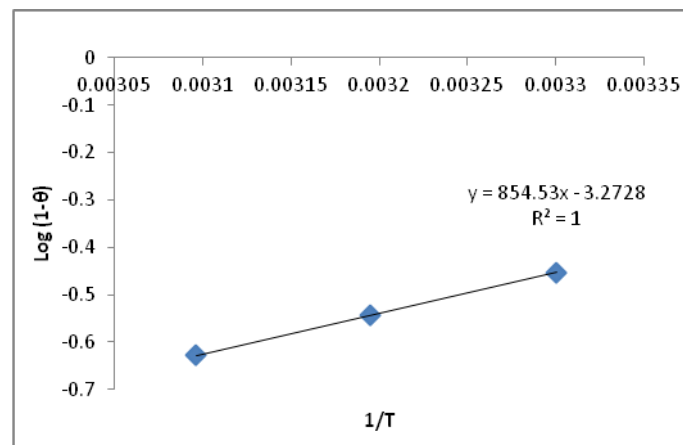
Fig.12 gives various graphs between Log (1-θ) verses $\frac{1}{T}$

6. CONCLUSION

In the different parameter best evidence the initial concentration of Se (IV) ion effect of adsorption on Bentonite clay are best adsorbent under specific condition. Experimental equilibrium data Se (IV) ion effect of pH, initial

concentration, temperature and contact Time are best evidence by Langmuir and Freundlich adsorption isotherm, Lagergren first and pseudo second order equation thermodynamic parameter also favour the adsorption and kinetic studies showed that experimental data was best described by pseudo second order model.

ACKNOWLEDGEMENT

REFERENCES

1. Ahmad A. et al. (2009), Removal of Cu(II) and Pb(II) ion from aqueous solution by adsorption onto Sawdust of migrant wood, Desalination 247(3), 636-646.

2. Ali. A. Singh. D and Rathore. P. (2019), Adsorption Potential on the removal of Cr (VI) ion on Kaolinite clay by equilibrium studies from wastewater, Our Heritage Journal, 67(2), 1244-1252.

3. Cho H., Oh D. and Kim K. (2005), a study on removal characteristics of heavy metals from aqueous solution by fly ash. J. Haz. Mat., B127, 187-195.

4. Dehirham, C., Mustafa, T.S. 2010. Speciation of Mn(II) and Mn(VII) samples by co-precipitation-atomic absorption spectrometry combination. J. Hazardous Matter, 173: 773-777.

5. Ho Y.S. and Mckay G. (2000), the kinetics of sorption of divalent metal ions onto sphagnum moss peat. Water Res. 34(3) 735-742.

6. Kotash J. and Stasicka Z. (2000), Chromium occurrence in the environment and methods of its speciation. Environ. Pollution, 107: 263-283.

7. Kumar Sujata, Singh D., Upadhyay M., Mishra A.K. and Kumar S. (2014), Red mud as Adsorption to removal Lead (II) from aqueous solution, Res. J. Recent Sci. 3(7), 18-27.

8. Lagergren S. (1898), about the theory of so-called adsorption of soluble substances, der Sogenanntenadsorption geloster stoffe Kungliga Svenska psalka de Miens Handlingar., 24, 1-39.

9. Langmuir I. (1918), the sorption of gases on plane surfaces of glass, mica and platinum. J. American Chem. Soc., 40: 1361-1403.

10. Mohammad Al-amber (2012), Removal of Fe(III) from model solution using Jordanian natural zeolites, Asian J. of chemistry, 19(5), 3493-3501.

11. Mungasavali, DeepaPrabhu, Viraghavan, Thiruvenkatachari, Yee-Chung, J. (2007). Biosorption of Chromium from aqueous solutions by pretreated Aspergillus Niger: Batch and column studies. Colloids and surfaces A: Physiological Engineering Aspects, 301(1-3), 214-223.

12. Shrivastava, N.K., Majumbar, C.B. (2008). Novel Bio-filtration methods for the treatment of heavy metals from industrial waste water. J. Hazardous Mater, 151(1): 1-8.

13. Tachi, Y., Yotsuji, K., (2011). Diffusion and sorption of Cs^+, I^- and HTO in samples of the argillaceous Wakkanai Formation from the Horonobe URL, Japan: Clay-based modeling approach. Geochim. Cosmochim. Acta 75, 6742-6759.

14. Tachi, Y., Yotsuji, K., (2014). Diffusion and sorption of Cs^+, Na^+, I^- and HTO in compacted sodium montmorillonite as a function of porewater salinity: Integrated sorption and diffusion model. 21 Geochim. Cosmochim. Acta 132, 75-93.

15. Tian, W., Li, C. and Liu, X., (2013). The effect of ionic strength on the diffusion of 125I in Gaomiaozi Bentonite, J Radioanal Nucl. 295, 1423-1430.

16. Tores, J., Pintos, V., and Kremer, E., (2011). Selenium chemical speciation in natural waters: Protonation and complexation behavior of selenite and selenate in the presence of environmentally relevant cations. Chem. Geol. 288, 32-38.

17. Van Loon, Glaus, M.A., Muller, W., (2007). Anion exclusion effects in compacted Bentonite: Towards a better understanding of anion diffusion. Appl. Geochem. 22, 2536-2552.

SYNTHESIS, CHARACTERIZATION, AND THERMAL PROPERTIES OF 2-AMINO 6-NITROBENZOTHIAZOLE AND MELAMINE WITH FORMALDEHYDE COPOLYMER

Punam G. Gupta[1], R. H. Gupta[2] and W. B. Gurnule[1]*

[*1]Department of Chemistry, Kamla Nehru Mahavidyalaya, Sakkardara, Nagpur – 440024 (M.S) India

[2]Department of Chemistry, KZS Science College, Kalmeshwar, Dist. Nagpur

ABSTRACT

2-amino 6-nitrobenzothiazole melamine-formaldehyde (BMF-I) copolymer has been synthesized by condensation polymerization method utilizing monomers 2-amino 6-nitrobenzothiozol (B), and melamine (M) with formaldehyde (F) in presence of 2M HCl as an acid catalyst in 1:1:3 molar ratios. The structure of the incorporated BMF-I copolymer has been interpreted and confirmed based on elemental analysis and various spectral techniques like UV-visible, FTIR, and 1H-NMR methods. The surface morphology of copolymer was studied by scanning electron microscopy (SEM). The molecular weight of the BMF-I copolymer was dictated by the non-aqueous conductometric titration method. The TGA analysis of synthesized copolymer has been done by non-isothermal thermogravimetric technique in which sample is subjected to the condition of continuous increase in temperature at a heating rate of 100C/min in a nitrogen atmosphere, and which is used to study decomposition rate and thermal stability of newly synthesized copolymer. The activation energy (Ea) and the thermal stability have been calculated by using Sharp-Wentworth and Freeman-Carroll methods. The thermodynamic parameters such as entropy change (ΔS), free energy change (ΔF), apparent entropy (S), frequency factor (Z) were calculated by using data obtained by Freeman-Carroll and TGA curves. The thermal activation energy determined with the assistance of those methods was in good agreement with one other. The order of the decomposition reaction was found to be 1.21.*

Keywords- Copolymer, melamine, polycondensation, thermogravimetric, kinetic parameter, activation energy.

INTRODUCTION

The copolymer is a type of polymer formed when two or more different types of monomers are combined, they are known for their adaptable uses and are discovered to be amorphous, crystalline, or resinous. Presently days, the utilization of copolymer has been expanded due to high thermal stability and electrical conductivity properties. Copolymers are utilized in a wide scope of uses, for example, high energy materials [1], ion exchangers [2], semiconductors [3], fireproofing agents [4], antioxidants [5], etc. Ion exchange properties of a copolymer were studied by W.B.Gurnule et al. resulting from o-aminophenol, urea, and formaldehyde. [6] and shows that o-APUF copolymer acts as an astounding and promising cation exchanger to eliminate the poisonous and unsafe metal ions from the wastewater bodies and mechanical effluents. Chelation ion-exchange application of copolymer resin was revealed by M.M.Yeole et al [7] which was synthesized by condensation polymerization of p-hydroxybenzaldhyde and oxamide with formaldehyde and suggested that synthesized copolymer showed higher selectivity for Fe+3, Cd+2, and Co+2 than for Cu+2 and Pb+2 ions.

Benzothiazole-based aromatic polymers contain nitrogen, oxygen, and sulfur donor atoms [8] [9] which are utilized to synthesized thermally stable [10], biologically active polymers [11], and pharmacological applications [12] [13]. M.A.R. Ahamed et al. have reported antimicrobial application of transition metal complexes of benzothiazole-based copolymer [14]. Thiazole-based novel copolymer ligand and its transition metal complexes have been accounted for by M.A.R. Ahamed and co-workers [15]. Cation exchange properties have been reported by A.R. Burkandeen et al. derived from 2-amino 6-nitrobenzothiazole and thiosemicarbazide with formaldehyde [16].

Because of the high thermal stability of copolymer, a unique consideration has been engaged to investigate the synthesis of the copolymer. Thermogravimetric investigation gives the data about the degradation and thermal stability of materials and in this way, numerous analysts combined copolymer to improve the thermal stability [17] [18] [19]. The kinetic parameter i.e. activation energy (Ea) and thermodynamic parameter such as entropy change (ΔS), free energy change (ΔF), apparent entropy (S*), frequency factor (Z) can be determined by analyzing the thermoanalytical information [20] [21] [22] from Sharp-Wentworth [23], Freeman-Carroll [24] and Phadnis-Deshpande techniques [25]. Pratik et al. considered the thermal degradation of the copolymer from salicylic acid, guanidine, and formaldehyde [26], Velmurugan and co-worker [27] examined the thermal behavior of terpolymer and its composites. Thermodynamic parameters of copolymer blended from salicylic acid and thiosemicarbazide with formaldehyde were accounted for by Nandekar et al. [28]. Thermokinetic parameters of resin got from m-cresol and hexamine with formaldehyde have been announced by Hiwase et al. [29]. Subsequently, the current examination was focused on the synthesis of 2-amino 6-nitrobenzothiazole-

melamine-formaldehyde copolymer and characterized by elemental, physico-chemical method, and spectral studies.

MATERIALS AND METHODS
Materials

The chemically pure and analytical grade the chemicals and solvents are used for the synthesis.

Synthesis of BMF-I copolymer

2-Amino 6-nitrobenzothiazole (1.95gm, 0.1mole) and melamine (1.26gm, 0.1mole) with formaldehyde (11.25ml, 0.3mole) was taken as a monomer in a clean round bottom flask and refluxed water condenser using 2M HCl (200ml) in 1:1:3 ratio. The homogeneous mixture was refluxed in an oil bath at $122^{0}C \pm 2^{0}C$ with constant stirring for 5Hrs. The reaction mixture was equilibrated overnight. A pale yellow colored precipitate was thus obtained which was separated by filtration method and washed with cold water to remove unreacted monomer, then it was air-dried and powdered. The dried copolymer was further purified by dissolving in 8%NaOH and regenerated in1:1 (v/v) HCl/H2O. The procedure was repeated several times to urge the pure copolymer. The resulting copolymer was washed with boiling water, air-dried, powdered, and kept in a vacuum desiccator with silica gel. Scheme 1 shows a schematic representation of the synthesis of BMF-I copolymer.

CHARACTERIZATIONS
Elemental Analysis

The elemental analysis has been disbursed from STIC Cochin by using Vario EL III (Elementar, Germany) to seek out the proportion of elements, like carbon (C), hydrogen (H), nitrogen (N), and sulfur (S) present within the BMF-I copolymers.

Molecular Weight Determination by Non-aqueous Medium

The non-aqueous conductometric titration method is used to determine the number average molecular weight of the BMF-I copolymer in DMSO medium by using 50mg of BMF-I copolymer sample and ethanolic KOH as the titrant, then a graph of the specific conductance against the milliequivalents of KOH has to neutralize 100gm of the copolymer was plotted and it shows that numbers of breaks within the plot and from it, the primary and last break within the plot were determined. The number average molecular weight should be determined by the subsequent equation which the based on the average degree of polymerization.

DP = Total meq. of base required for complete neutralization

Meq. of base required for smallest interval

Mn = Dp X Repeat unit weight

UV-visible spectroscopy

UV-visible spectra of BMF-I copolymer were studied by using Shimadzu spectrophotometer UV-1800 in DMSO solvent in the range 200-800 nm at Shivaji Science College, Nagpur.

1H-NMR Spectroscopy

The 1H-NMR spectra were recorded from SAIF Chandigarh, on a Bruker Avance-II 400 MHz NMR spectrometer (USA) using DMSO-d6 as a solvent.

SEM analysis

The surface morphology of the BMF-I copolymer was examined at different magnifications by using Jeol 6390 LV which is carried at STIC, Cochin.

Thermogravimetric Analysis

The non-isothermal thermogravimetric analysis of BMF-I copolymer was performed in an air atmosphere with a heating rate of $20^{0}C.min^{-1}$ from a temperature range of 40 to $800^{0}C$ using DTG-60, Shimadzu under nitrogen purging using platinum crucible. The thermograms were scanned at RUSA Centre for Bio-Actives and Natural Products, Rashtrasant Tukadoji Maharaj Nagpur University, Nagpur.

RESULTS AND DISCUSSION
Solubility Test

The newly blended BMF-I copolymer was found to be yellow. The copolymer is soluble in solvents such as DMF, DMSO, THF, and conc. H2SO4 while insoluble in almost all inorganic and organic solvents. The yield of the copolymer was found to be 82 %.

Elemental analysis

The results of the elemental analysis which are accustomed analyze the percentage of carbon, nitrogen, sulfur, and hydrogen in the sample are shown in Table: 1. The composition of the copolymer obtained based on elemental analysis data was found to be in good correlation with the calculated values which shows that, empirical formula and empirical weight of a repeated unit of BMF-I copolymer were found to be C13H12N9O2S and 359 respectively.

Molecular weight by non-aqueous conductometric titration

The non-aqueous conductometric titration method in DMSO medium using standard potassium hydroxide (0.05M) in absolute ethanol as a titrant has been used to evaluate the number average molecular weight (Mn) of this copolymer. Each copolymer's specific conductance was plotted against the milliequivalents of ethanolic KOH requisite to neutralize 100g of each copolymer. A plot revealed the number of breaks within the plot. The first break at 112 milliequivalents of base and the last break at 1008 milliequivalents of the base were noted and which has been depicted in Fig 1. Multiplying the average degree of polymerization (DP) by the formula weight of the repeating unit yields the number average molecular weight (Mn) of the copolymer. The number average molecular weight determination by non-aqueous
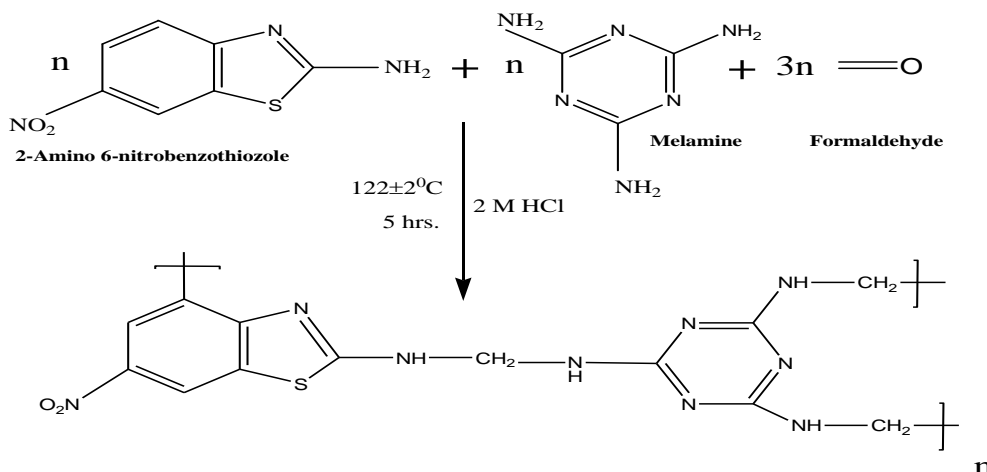
Scheme 1: Schematic representation of the synthesis of BMF-I copolymer

conductometric titration method is a simple and effective method that has been demonstrated by previous workers [30] [31]. Conductometric titration curve results are presented in Table 2.
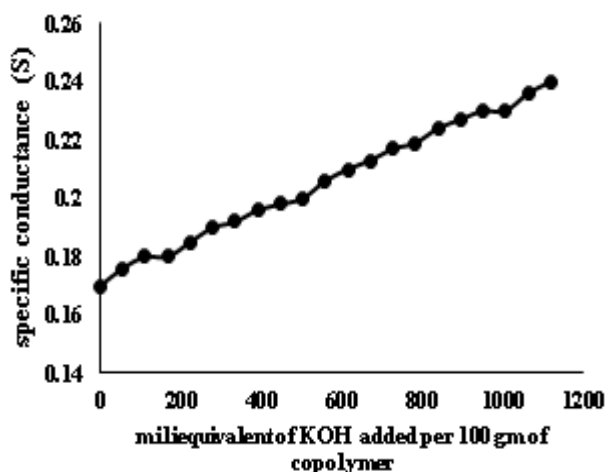
Fig 1: Conductometric titration curve of BMF-I copolymer

UV-visible Spectroscopy

Copolymer	The empirical formula of repeating unit	Empirical formula weight	%C Found (Cal.)	% H Found (Cal.)	% N Found (Cal.)	% S Found (Cal.)
BMF-I	$C_{13}H_{12}N_9O_2S$	359	43.15(43.57)	3.12(3.37)	35.04(35.57)	8.34(8.94)

The UV-visible spectrum of the BMF-I copolymer is depicted in Fig 2 which is recorded in DMSO in the 200-800nm range. The newly synthesized BMF-I copolymer exhibits two characteristic bands at 286nm and 363nm. The absorption band shown by copolymer have two different intensities, these observed positions of two absorption bands indicate the presence of chromophore group like NO2, >C=N, C=C which are in conjugation with the aromatic nucleus i.e. benzothiazole ring and –NH groups respectively. The absorption band at 286nm is less intense due to $\pi \rightarrow \pi^*$ allowed transition and the band at 363nm are because of $n \rightarrow \pi^*$ transition which is more intense. Hence, the presence of aromatic nucleus is confirmed by $\pi \rightarrow \pi^*$ transition and –NH groups by $n \rightarrow \pi^*$ transition [32].

TABLE 1: THE PHYSICOCHEMICAL AND ANALYTICAL DATA OF THE BMF-I COPOLYMER
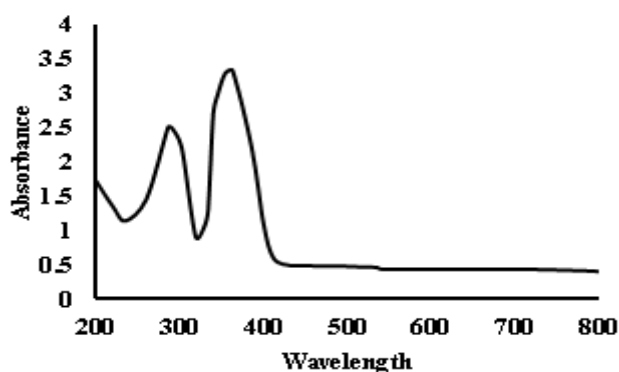
Fig 2: UV-visible spectra of BMF-I copolymer

1H-NMR Spectroscopy

The 1H-NMR spectrum of BMF-I copolymer was scanned in DMSO-d6 solvent which is shown in Fig 3. The signals observed in the 1H-NMR spectra of BMF-I copolymer were interpreted based on the literature [15] [32]. The singlet signal appearing in the region of 8.72 ppm is due to the -NH proton of the benzothiazole ring. The singlet signal at 4.49ppm is assigned to the –NH proton of the melamine ring. The signal that appeared at 2.50 ppm is attributed to methylene protons of the copolymer. The weak multiple signals that appeared in the region of 7.18-8.29 ppm are due to all the protons of the aromatic ring.

Polymer	1st phase of neutralization	The final phase of neutralization (Meq/100g sample)	Degree of polymerization ($\overline{Dp}$)	Empirical weight (gm)	Number average molecular weight ($\overline{Mn}$)
BMF	112	1008	9	359	3231

TABLE 2: MOLECULAR WEIGHT DETERMINATION OF BMF-I COPOLYMER
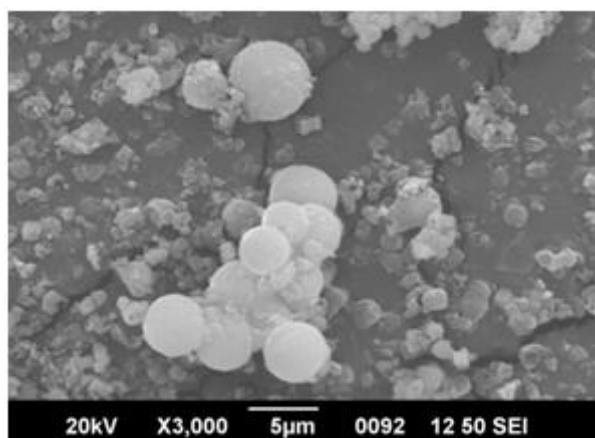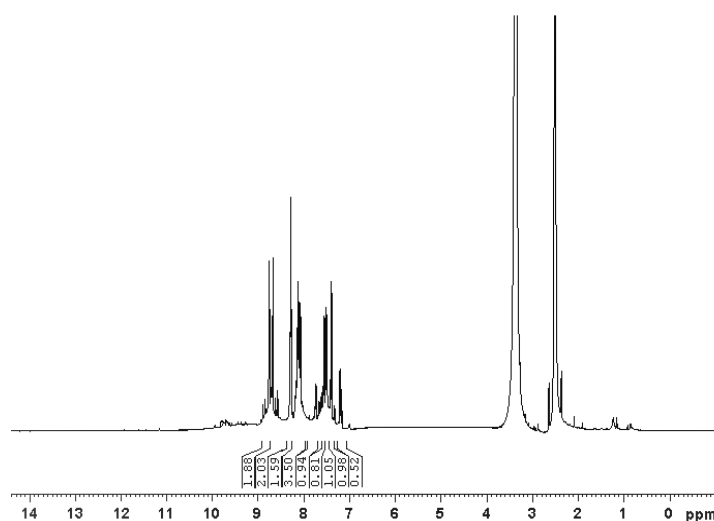
Fig 3: 1H-NMR spectra of BMF-I copolymer

Scanning Electron Microscopy

The SEM micrograph of the BMF-I copolymer obtained in x3000 and x3500 magnification is used to understand the surface morphology of the copolymer which is shown in Fig 4. The BMF-I copolymer shows the irregular granular particles-like appearance and it exhibits a closed packed arrangement with deep pits and more active sites. From the SEM photograph, it is quite clear that the copolymer is porous and the surface morphology of the BMF-I copolymer depicted a fringed model of the semicrystalline structure. The fringes in the micrograph show that copolymer exhibit transition state between amorphous and crystalline state. During the polymerization crystalline structure of the monomer is converted into the amorphous phase of the copolymer. There are some holes and cracks are seen which may be because of air voids.
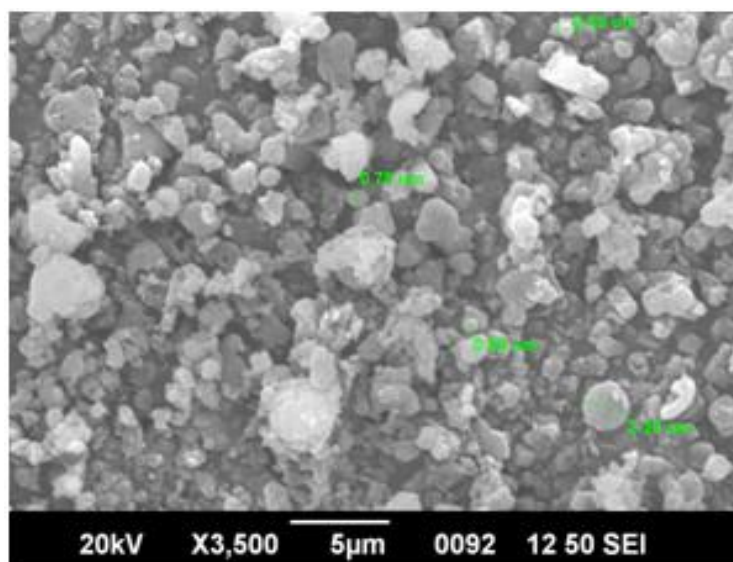
Fig 4: SEM images of BMF-I copolymer

Thermogravimetric analysis

The thermogram of BMF-I copolymer Fig 5, portrays three stages in decay response (120-3200C, 320-5400C, and 540-8000C), after the loss of water molecule in the temperature range 40-8000C. The first disintegration happens between 40-1200C compares to 4.35% calculated which might be credited to loss of water molecule against determined 4.77% present per repeat unit of the polymer. The principal stage decay from 120-3200C may be because of loss of benzothiazole ring (noticed 51.11% and determined 51.98%). The second step of disintegration begins from 320-5400C comparing to 78.98% loss of the disposal of basic molecules like –NH and –CH2 group present in the copolymer against determined 79.31%. The third step begins from 540–8000C affirming the degradation of the melamine from the copolymer (98.79% noticed and 100% determined). The half decomposition temperature for copolymer is discovered to be 3100C.
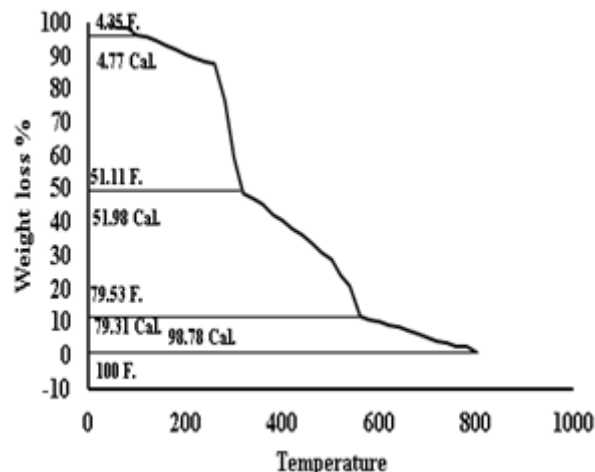
Fig 5: Decomposition pattern of BMF-I copolymer

With the assistance of thermogravimetric information the kinetic parameters like activation energies (Ea) and order of reaction (n) and thermodynamic parameters such as entropy change (ΔS) apparent entropy change (S*), and frequency factor (Z) are resolved and detailed in Table 3 which was determined by examining the strategies depict by Sharp-Wentworth and Freeman-Carroll.

Sharp-Wentworthmethod:

By using the Sharp and Wentworth equation,

$$\log[(dc/dT)/(1-c)]=\log(A/\beta)–[Ea/2.303R].1/T…………..(1)$$

Where,

dc/dT is a rate of change of weight with change in temperature

β=linear heating rate dT/dt.

By plotting the graph between (logdc/dt)/(1-c) vs1/T obtained the straight line which gives activation energy (Ea) calculated from its slope (Fig 6)

Where,

β is the conversion at time t,

R = Gas constant (8.314 J mol-1 K-1),

T is the absolute temperature.
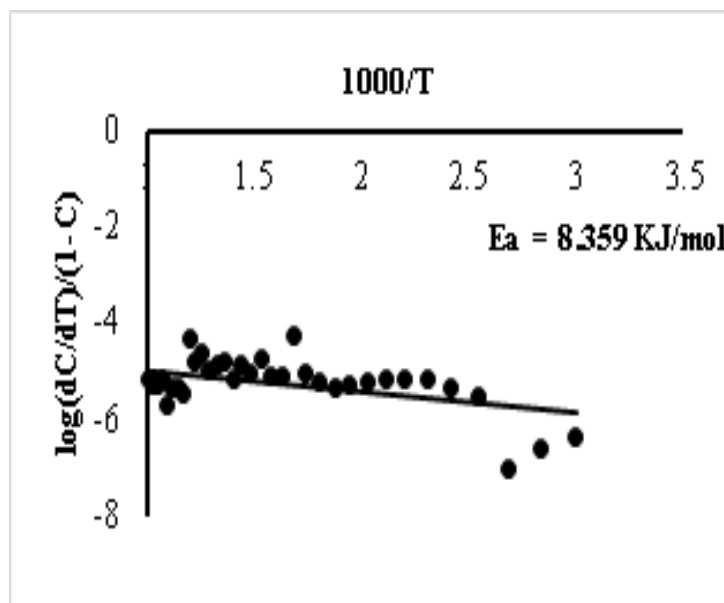
Fig 6: Sharp-Wentworth plot of BMF-I copolymer
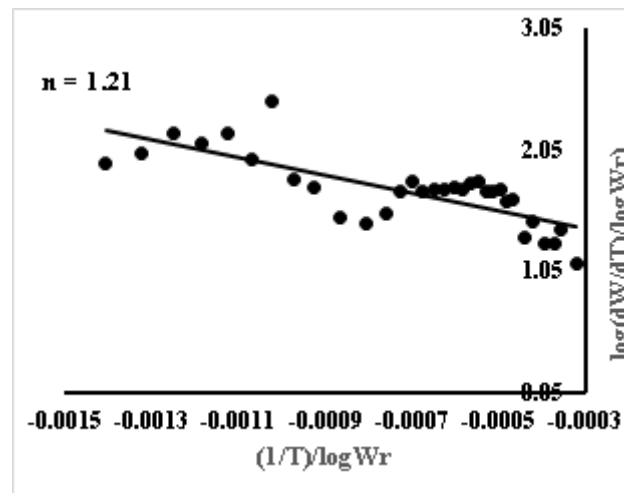
Fig 7: Freeman –Carroll plot of BMF-I copolymer
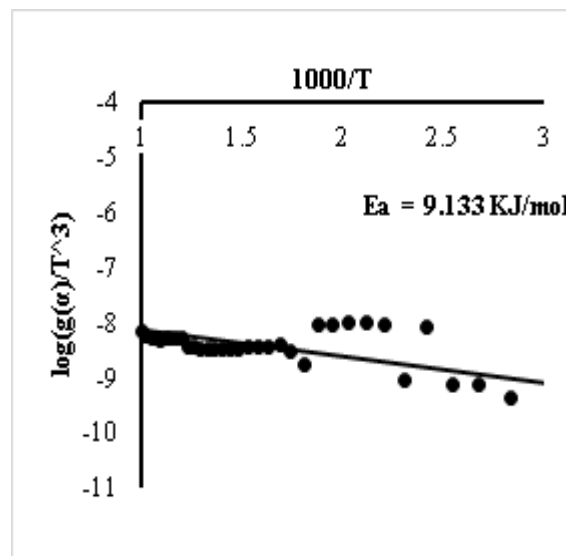
Fig 8: Thermal activation energy plot of BMF-I copolymer

Freeman-Carroll method:

The equation derived by Freeman and Carroll is:

$[\Delta\log(dw/dt)]/\Delta\log Wr=(-E/2.303R).\Delta(1/T)/\Delta\log Wr+n$----(2)

Where, dw/dt=rate of change of mass with time.

Wr=Wc-W

Wc=weight loss after the reaction.

W=fraction of weight loss at time t.

Ea=energyof activation

n=order of reaction.

The plot of [log (dw/dt)] / log WrVs (1/T) / log Wr yields a straight line, and we calculated the energy of activation (Ea) and the intercept on the Y-axis as the order of reaction (n) from the value of the slope (Fig 7 and 8). The change in entropy(S), frequency factor (Z), apparent entropy(S*) also can be calculated by further calculations [23][24].

Change of Entropy:

Intercept = [log KR/hφE] + S / 2.303 R ----------------- (3)

Where, K = 1.3806 x 10-16 erg/deg/mole,

R = 1.987 Cal/deg/mole

h = 6.625 x 10-27 erg sec,

ϕ = 0.166

S = Change in entropy,

E = Activation energy from graph.

Free Energy Change:

ΔF=ΔH–TΔS-------------------------------------(4)   Where,

ΔH = Enthalpy Change = activation energy

T = Temperature in K

S = Entropy change from (i) used.

Frequency Factor:

Bn= Log ZEa / ϕR ------------------------------- (5)

B1=log [ln1/1-α]-log P(x) --------------------------- (6)

Where, Z = frequency factor,

B = calculated from equation (6)

Log P(x) = calculated from Doyle's table corresponding to the activation energy.

Apparent Entropy Change:

S* = 2.303logZh/KT*-------------------------- (7)

Z = from relation (5)

T* = half disintegration temperature

The Ea values calculated by SW and FC methods are in good agreement with each other which are presented in Table 3. Based on the initial deterioration temperature, the thermal stabilities of the copolymer have additionally been utilized here to characterize thermal stability, ignoring the degree of disintegration. The decomposition reaction of BMF-I copolymer takes place in a slow phase because of the abnormally low value of frequency factor (Z), and the negative value of the entropy change simply adds to the evidence. Straight-line plots are obtained using the two methods shown in Fig 7 and from the plot, the order of reaction (n) of BMF-I copolymer was found to be 1.21. From the above data, it is quite clear that the decomposition reaction approximately follows first-order kinetics.

CONCLUSION
The BMF-I copolymer was synthesized by polycondensation polymerization with good yield. The proposed structure of copolymer resin has been elucidated by elemental analysis, FTIR, 1H-NMR, and UV–visible spectral studies. The surface morphology confirmed the semicrystalline nature of copolymer. The non-isothermal thermogravimetric analysis shows that the synthesized copolymers were thermally stable and from the values of activation energy calculated by using SW and FC methods, are in close agreement with each other. Degradation of the copolymer is slow reaction is explained based on the low value of frequency factor and from the value of the order of reaction, copolymers approximately follow first-order kinetics.

ACKNOWLEDGMENTS

REFERENCES
[1] Y. Wang, X. Haung, T. Li, Z. Wang, L. Li, X. Guo, and P. Jiang, "Novel cross-linkable high-k copolymer dielectrics for high-energy-density capacitors and organic field-effect transistor applications," Journal of Materials Chemistry A, vol. 5, pp. 20737-20746, 2017.

[2] W. B. Gurnule, K. Vajpai, and A. D. Belsare, "Selective removal of toxic metal ions from waste water using polymeric resin and its composite," Materialstoday Proceeding, vol. 36, no. 3, pp. 642-648, 2021.

[3] E. Lee, W. Shin, O. Bae, F. S. Kim, and Y. J. Hwang, "Synthesis and Characterization of a highly crystalline benzotriazole-selenophene copolymer semiconductor," Polymer, vol. 184, p. 121856, 2019.

[4] L. Wan, C. Deng, Z. Y. Zhao, H. Chen, and Y. Z. Wang, "Flame Retardation of Natural Rubber: Strategy and Recent Progress," Polymers, vol. 12, no. 2, p. 429, 2020.

[5] V. Taresco, F. Crisante, I. Francolini, A. Martinelli, L. D`llario, L. Ricci-Vitiani, M. Buccarelli, L. Pietrelli, and A. Piozzi, "Antimicrobial and antioxidant amphiphilic random copolymers to address medical device-centered infections.," ActaBiomaterialia, vol. 22, pp. 131-140, 2015.

[6] W. B. Gurnule, and D. B. Patle, "Preparation, characterization and chelating ion-exchange properties of terpolymer resins derived from o-aminophenol, urea, and formaldehyde," Elixir Appl. Chem., vol. 50, pp. 10338-10345, 2012.

[7] M. M. Yeole, S. Shrivastava, and W. B. Gurnule, "Synthesis, characterization and mathematical modelling of chelation ion-exchange applications of copolymer resin," IJCESR, vol. 6, no. 1, pp. 2394-0697, 2019.

[8] M. A. R. Ahamed, and A. R. Burkanudeen, "Metal complexes of a novel terpolymer ligand: synthesis, spectral, morphology, thermal degradation kinetics, and antimicrobial screening," Journal of Inorganic and Organometallic Polymers and Materials, vol. 22, no. 5, p. 1046, 2012.

[9] J. Joseph, G. BoomadeviJanaki and J. Dharmaraja, "Metal complexes of 2–aminobenzothiazole derivatives as a versatile system tuning up their structural and biological properties," Journal of Chemical and Pharmaceutical Research, vol. 8, no. 1(S), pp. 133-152, 2016.

[10] H. Q. Xie, Z. H. Liu, H. Liu, and J. S. Guo., "Non-linear optical cross-linked polymers and interpenetrating polymer networks containing azo-benzothiozole chromophore groups," J. S. Polymer, vol. 39, no. 12, p. 2393–2398., 1998.

[11] F. Delmas, A. Avellaneda, C. D. Giorgio, M. Robin, E. D. Clercq, P. Timon-David, and J. P. Galy, J. P., "Synthesis and antileshmanial activity of (1,3- benzothiazole-2-yl)amino-9-(10H)-acridinone derivatives," Eur. J. Med. Chem. , vol. 39, p. 685–690., 2004.

[12] N. Mathur, N. Jain, and A. K. Sharma, "Biocidal Activities of Substituted Benzothiazole of Copper Surfactants over Candida albicans&Trichodermaharziamunon on Muller Hinton Agar," Open Pharmaceutical Sciences Journal, vol. 5, pp. 24-35, 2018.

[13] R. K. P. Tripathi, and S. R. Ayyannan, "Design, Synthesis, and Evaluation of 2-Amino-6-nitrobenzothiazole-Derived Hydrazones as MAO Inhibitors: Role of the Methylene Spacer Group," ChemMedChem, vol. 11, no. 14, pp. 1551-67, 2016.

[14] M. A. R. Ahamed, R. S. Azarudeen, and N. M. Kani, " Antimicrobial applications of transition metal complexes of benzothiazole based terpolymer: Synthesis, characterization, and effect on bacterial and fungal strains," Bioinorganic Chemistry and Applications, vol. Article ID 764085, pp. 1-16, 2014.

[15] M. A. R. Ahamed, and A. R. Burkanudeen, "Thiazole-based novel terpolymer ligand and its transition metal complexes: Thermal and biological Studies," Advances in Polymer Technology, vol. 32, no. 4, pp. 21376-21392, 2013.

[16] M. A. Ahamed, D. Jeyakumar, and A. R. Burkanudeen, "Removal of cations using ion-binding terpolymer involving 2-amino-6-nitro-benzothiazole and thiosemicarbazide with formaldehyde by batch equilibrium technique," Journal of Hazardous Materials, vol. 59, no. 68, pp. 248-249, 2013.

[17] H. Patel, M. Patel, K. Patel, and R. Patel, " Novel acrylic copolymers: synthesis, characterization and antimicrobial studies," E-polymers, vol. 125, pp. 1-11, 2007.

[18] A. R. Burkanudeen, M. A. R. Ahamed, R. S. Azarudeen, M. S. Begum, and W. B. Gurnule, "Thermal degradation kinetics and antimicrobial studies of terpolymer resins," Arabian Journal of Chemistry, vol. 9, p. S296–S305, 2016.

[19] S. P. Chakole, K. A. Nandekar, and W. B. Gurnule, Photoluminescent studies of 2, 2'-dihydroxybiphenyl, ethylenediamine - formaldehyde copolymer, Journal of Physics: Conference Series, 1913, 1-8, 2021

[20] A.W. Coats, and J. P. Redfern, "Kinetic parameters from thermogravimetric data," Nature, vol. 201, no. 4914, pp. 68-69, 1964.

[21] D. R. Dowdy, "Meaningful activation energies from complex systems," Journal of Thermal Analysis. , vol. 31, no. 1, pp. 137-147, 1987.

[22] C. Popescu, "Integral method to analyze the kinetics of heterogeneous reactions under non-isothermal conditions a variant on the Ozawa-Flynn-Wall method," ThermochimicaActa. , vol. 285, no. 2, pp. 309-323, 1996.

[23] J. B. Sharp, and S. A. Wentworth, "Kinetic analysis of thermogravimetric data," Analytical Chemistry, vol. 41, no. 14, pp. 2060-2062, 1969.

[24] E. S. Freeman, and B. Caroll, "The application of thermoanalytical techniques to reaction kinetics: The thermogravimetric evaluation of the kinetics of the decomposition of calcium oxalate monohydrate," The Journal of Physical Chemistry, vol. 62, no. 4, pp. 394-397, 1958.

[25] A. B. Phadnis, and V. V. Deshpande, "Determination of the Kinetics and Mechanism of a Solid-State Reaction. A simple approach," Thermochim. Acta, vol. 62, no. 2-3, pp. 361-367, 1983.

[26] P. E. P. Michael, P. S. Lingala, H. D. Juneja, and L. J. Paliwal, "Synthetic, structural and thermal degradation of terpolymer derived from salicylic acid, guanidine, and formaldehyde," Journal of Applied Polymer Science, vol. 92, no. 4, pp. 2278-2283, 2004.

[27] R. G. Velmurugan, K. R. Ahamed, and R. S. Azarudeen, "A novel comparative study: Synthesis, characterization and thermal degradation kinetics of a terpolymer and its composite for the removal of heavy metals," Iranian Polymer Journal, vol. 24, pp. 229-242, 2015.

[28] K. A. Nandekar, J. R. Dontulwar, and W. B. Gurnule, "Thermal behaviour of newly synthesized copolymer derived from salicylic acid, and thiosemicarbazide," Der PharmaChemica, vol. 4, no. 6, pp. 1644-1652, 2012.

[29] W. B. Gurnule, R. N. Singru. Thermogravimetric Study of 8-Hydroxyquinoline 5-Sulphonic acid-Melamine-Formaldehyde Terpolymer Resin –II, Journal of Thermal Analysis and Colorimetry, 100, 1027-1036, 2010.   [30] C. G. Kohad, and W. B. Gurnule, "Synthesis and thermal degradation studies of p-toludine, ethylenediamine, and formaldehyde copolymer resin," IJCESR, vol. 6, no. 1, pp. 503-512, 2019.

[31] Y. U. Rathod, and W. B. Gurnule, "Synthesis, characterization and thermal behaviour studies of terpolymer resin derived from 8-hydroxyquinoline-5-sulphonic acid and anthranilic acid," Current Applied Polymer Science, vol. 4, pp. 47-54, 2021.

[32] M. A. R. Ahamed, R. S. Azarudeen, N. Prabu, and A. R. Burkanudeen, "Studies of Retention and Reusable Capacities of Melamine Formaldehyde Based TerpolymerAgainst Some Toxic Metal Ions by Batch Equilibrium Method," Separation Science and Technology, vol. 50, p. 1925–1939, 2015.

MOLECULAR INTERACTION AND ULTRASONIC VELOCITY STUDIES OF ALKANOLS WITH O-NITRO TOLUENE AT GIVEN TEMPERATURES

Rajendra Pawar[1], Sandip Patil[2] and G. P. Waghulde[3]

[1]Arts, Commerce and Science College, Yawal India, K.B.C.N.M.U. University
[2]Arts, Commerce and Science College, Chopda, K.B.C.N.M.U. University
[3]D. D. N. Bhole College, Bhusawal, K.B.C.N.M.U. University

ABSTRACT

*Ultrasonic Velocity (U), Density (ρ) and Viscosity (η) values for the binary mixture system of 1-butanol and 3-methyl, 1-butanol with O-Nitro toluene including those of pure liquids were measured over entire mole fraction range at 298.15 K and 308.15 K .The related parameters of molecular interaction and sound velocity were studied in present work. From experimentally determined values excess molar volume (V E), Viscosity deviation (Δη) and deviation isotropic compressibility (ΔKs), excess free length (LfE), available volume (VaE) and Gibb's free energy (G*E) have been calculated. These results have been explained on the basis of intermolecular interaction between the components in the liquid mixture and correlations among the parameters are discussed.*

Keywords— Ultrasonic Velocity, Density, Viscosity, Excess molar volume, Excess free length, Gibb's free energy.

INTRODUCTION

Ultrasonic velocity investigations along with viscometric and volumetric studies of liquid and liquid mixture are considerable of importance. They play an impotent role in understanding intermolecular interaction among the different component molecules. It also findings extensive application in industrial and technological process [1,2]. Several researchers [3-8] have measured viscosity, Density and Ultrasonic velocity for different binary mixture, containing alcohols as one of the components and these properties were discussed in term of specific and non-specific interaction. Generally alcohols are strongly associated in solution because of its dipole-dipole interaction and hydrogen bonding. They play important role in Chemistry, Biology and Studies in hydrogen bonding in liquid mixture. Alcohols are widely used are solvents. Alcohols play an important role in understanding the behavior of hydrogen bonding with other functional groups.

Aromatic group is highly non-polar and can associate with any other group having same degree of polar attractions. In present work has been reported on alcohols as one of the component in binary mixture of 1-butanol and 3- methyl, 1-btanol with O-Nitro toluene at 298.15 K and 308.15 K. The investigations of thermodynamic properties of multi component liquid mixture and data in term of various models are important for pharmaceutical and industrial application [9]. The excess thermodynamic functions [10, 11] are dependent on difference in intermolecular force and difference in size of the molecules. The magnitude and signs of these excess values can throw light on the strength of intermolecular interactions. So from the experimentally determined values of speed of sound, density and viscosity and other parameters like excess isotropic compressibility, excess molar volume (VE), excess free length (LfE) have been calculated. In present work, is to determine thermodynamics and transport properties of binary mixtures (12-15).

In present investigation we report the result and discuss excess parameter using data at two different temperatures.

MATERIALS AND METHOD

The chemicals 1-butanol, 3- methyl, 1-btanol and O-Nitro toluene used were of analytical grade (A.R) minimum assay of 99.9% obtained from s. d. fine chemicals India. Which are used as such chemical without further purification. The densities of pure components and binary mixtures were measured by using a Bi-capillary pycnometer. The purities of the above chemicals were checked density determination. The binary liquid mixtures of different known concentration were prepared in stopper measuring flask. The weight of the sample was measured using electronic digital balance with an accuracy of ± 0.1mg. The viscosity was measured using Ubbelohde viscometer (20ml) and the efflux time was determined using a digital clock to within ± 0.015. The ultrasonic velocities (U) in liquid mixtures have been measured using an ultrasonic interferometer (Mittal type, model F-81) working at 2 MHz frequency The accuracy of sound velocity was ±0.1 ms-1.

Theory and calculation

Following equations been used to calculate different parameters in binary solutions

1) The excess molar volume (V^E)

$$V^E = \frac{M_1X_1 + M_2X_2}{\rho_{12}} - \frac{M_1X_1}{\rho_1} - \frac{M_2X_2}{\rho_2} \quad (1)$$

(2) The viscosity deviation ($\Delta\eta_m$)

$$\ln\eta_m = X_1\ln\eta_1 + X_2\ln\eta_2 \quad (2) \qquad \Delta\eta_m = \eta_{12} - X_1\eta_1 - X_1\,\eta2 \quad (3)$$

3) Deviation in isentropic compressibility (Δk_S)

$$\Delta k_S = k_S - \Phi_1 k_{S1} - \Phi_2 k_{S2} \quad (4)$$

Where kS1, kS2 and kS are isentropic compressibility of liquid mixtures and Φ is volume fraction of pure ith component in the mixture and is defined as

$$\phi = \frac{(Xi\ Vi)}{(\Sigma\ Xi\ Vi)} \quad (5)$$

Where x1 and Vi are mole fraction and molar volume of ith component in the mixture.

4) The excess free length (LfE)

LfE=Lfmix-x1Lf1–x2Lf2   (6)

AE=Aexp–Aid   (7)

Where Aid = $\sum$ Ai Xi, Ai is any acoustical parameters and Xi the mole fraction of the liquid component.

5) Available volume (Va)

Va = (Vm-V0) = Vm (1-U/Um)   (8)

Where Vm = M/ρ, is the molar volume, U=Velocity, V0=M/ρ0 = molar volume at absolute zero temperature and Um = Schaaf's limiting value taken as 1600m/s for liquids.

6) The excess Gibbs free energy of flow (G*E)

G*E=RT[In(ηV) - x1In (η1V1)- x2In(η2V2)   (9)

Where Vi is the molar volume of ith component.

7) Internal pressure (πi)

πi = bRT (K □ / U)1/2 (□□ 2/3 / M7/6)   (10)

Where b is packing factor, K is a constant independent of temperature having value of 4.28 x 109,

R is gas constant and M is molecular weight the other symbols have their usual meaning.

RESULT AND DISCUSSION

In pure state , the self association of alcohols   decreases with increasing chain length , when alcohols mixed with O-Nitro toluene then there is interaction between their individual functional groups (-OH and –NO2) . The presence of electron withdrawing group on benzene ring decreases electron densities. The polarity of alcohols is less hence there is a degree of self association is less than compare to O-Nitro toluene.

The measured volumes of ultrasonic velocity, density, viscosity, excess molar volume (VE), viscosity deviation (Δn) and deviation in isentropic compressibility (ΔKs) parameters for the binary liquid mixtures 1-butanol and 3- methyl, 1-btanol with O-Nitro toluene including those of pure liquids were measured over entire mole fraction range at 298.15 K and 308.15 K are reported in table 1 and table 2 respectively while Excess free length(LfE), Internal pressure (πE) ,available volume (VaE) and Gibbs free energy(G*E) are given in Table-3 and Table-4 respectively. Figure :- 1, A,and B shows Excess molar volume (VE), Viscosity deviation (Δ) against mole fraction for binary system of 1-butanol and 3- methyl, 1-butanol at 298.15 K respectively. All these parameters shows negative deviations with minima at about X2= 0.4 for excess molar volume and X2 = 0.6-0.8 for deviation in viscosity. And Figure:-2, A and B shows available volume (VaE) and Gibbs free energy(G*E) against mole fraction for binary system of 1-butanol and 3- methyl, 1-butanol at 298.15 K respectively The parameters Gibb's free energy are negative but available volume was positive this may be due to presence of stronger solute solvent interactions in between highly polar functional groups Nitro and -OH.

Ultrasonic velocity and viscosity measurement of alcohols with O-Nitro toluene gives reliable information about molecular interaction between the components of mixtures. Alcohols in pure state get associated. The association of alcohols decreases with increase in chain length and substituent.

The excess parameters of alcohols become less negative with increased of temperature. The negative values of excess parameters shows that the existence of dispersion and dipole-dipole interaction between unlike molecules.

V. RESULT AND DISCUSSION

The experimental data of ultrasonic velocity, density and viscosity are reported for binary system of 1-butanol and 3- methyl, 1-butanol with O-Nitro toluene including those of pure liquids were measured over entire mole fraction range at 298.15 K and 308.15 K. Calculated excess molar volume deviation in viscosity and deviation in isentropic compressibility shows large negative deviation for most of binary mixtures these concluded that the existence of molecular interaction exist in above binary mixture which may be due to presence of more chain length and methyl substituent. It is well notified that most of values are negative due presence of polar functional group on aromatic ring alcoholic –OH group which increases salvation effect in solution so it shows that structure making interaction between solvent and solute.

TABLE-I: Values of densities viscosities, ultrasonic velocity, excess molar volumes and deviation in viscosity and deviation in isentropic compressibility for binary system of 1-butanol and O-Nitro toluene at 298.15 and 308.15 K.

Temp K	X1	ρ (gm /cm3)	η103 (Nsm-2)	U(MS-1)	VEx106 (m3/mole)	Δ ηx103 (Kg m-1s-1)	Δksx1011 (m2N-1)
298.15	0.0000	0.80540	2.52940	1499.6	0.0000	0.000	0.000
	0.1156	0.83310	2.35250	1515.8	-0.8195	-14.302	-6.34
	0.2019	0.85980	2.11890	1548.9	-1.4049	-33.919	-19.52
	0.3188	0.89320	2.00670	1531.8	-2.5991	-41.017	-25.48
	0.4265	0.92540	1.93240	1566.9	-3.4923	-43.822	-31.19
	0.5251	0.95760	1.87980	1599.5	-4.2497	-43.923	-44.38
	0.6048	1.05690	1.82200	1662.4	-6.4269	-43.890	-49.80
	0.7257	1.07230	1.73500	1682.9	-6.3425	-46.003	-30.72
	0.8283	1.11090	1.78750	1682.7	-7.2998	-33.194	-27.89
	0.9129	1.14890	1.83100	1715.1	-3.0733	-20.098	-16.53
	1.0000	1.06920	1.92950	1932.0	0.0000	0.000	0.000
308.15	0.0000	0.79800	1.99670	1401.4	0.0000	0.000	0.000
	0.1156	0.82500	1.84770	1441.1	-0.7698	-12.706	-31.44
	0.2019	0.85150	1.70580	1467.2	-1.3594	-24.468	-45.34
	0.3188	0.88360	1.60400	1516.5	-2.4488	-31.975	-50.40
	0.4265	0.91660	1.55200	1517.4	-3.4626	-34.175	-64.69
	0.5251	0.94880	1.53910	1532.5	-4.2493	-32.119	-65.27
	0.6048	1.04710	1.49980	1566.6	-5.4740	-32.278	-80.87
	0.7257	1.06250	1.40870	1598.2	-6.3805	-29.116	-69.71
	0.8283	1.10080	1.47670	1603.4	-8.3379	-25.413	-60.98
	0.9129	1.13800	1.51100	1633.3	-8.0581	-16.310	-48.90
	1.0000	1.06030	1.60760	1665.8	0.0000	0.000	0.000

Table2. Values Of Densities Viscosities, Ultrasonic Velocity, Excess Molar Volumes And Deviation In Viscosity And Deviation In Isentropic Compressibility For Binary System Of 3-Methyl,1-Butanol And O-Nitro Toluene At 298.15 And 308.15 K.

Temp K	X1	ρ (gm /cm3)	η103 (Nsm-2)	U(MS-1)	VEx106 (m3/mole)	Δ ηx103 (Kg m-1s-1)	Δksx1011 (m2N-1)
298.15	0.0000	0.80660	3.74590	1488.6	0.0000	0.000	0.000
	0.1066	0.83550	3.36850	1499.7	-1.1321	-25.644	-13.44
	0.2138	0.86450	2.82450	1525.5	-2.1086	-67.057	-23.52
	0.3212	0.88920	2.60070	1545.6	-2.3422	-75.269	-33.18
	0.4301	0.95330	1.95640	1601.2	-3.0904	-104.459	-46.97

Temp K	X1	ρ (gm /cm3)	η103 (Nsm-2)	U(MS-1)	VEx106 (m3/mole)	Δ ηx103 (Kg m-1s-1)	Δksx1011 (m2N-1)
	0.5091	0.96100	2.32250	1610.0	-5.0368	-91.284	-35.24
	0.6149	0.99590	2.13420	1630.7	-5.9413	-72.022	-27.94
	0.7159	1.08460	2.08160	1642.0	-6.3053	-57.520	-24.64
	0.8203	1.10090	1.96870	1687.8	-5.8342	-46.922	-20.59
	0.9128	1.11900	1.92200	1694.5	-4.3612	-27.525	-11.98
	1.0000	1.06920	1.92950	1832.0	0.0000	0.000	0.000
308.15	0.0000	0.79940	2.79410	1449.2	0.0000	0.000	0.000
	0.1066	0.82790	2.59620	1450.2	-1.1181	-11.892	-10.08
	0.2138	0.85640	2.16230	1516.7	-2.0672	-46.799	-14.29
	0.3212	0.88090	2.03580	1538.3	-2.3002	-85.194	-28.36
	0.4301	0.94430	1.49470	1597.0	-4.0742	-94.349	-37.92
	0.5091	0.95230	1.79070	1600.2	-5.0371	-73.928	-46.73
	0.6149	0.98660	1.64660	1619.2	-5.9090	-56.521	-52.31
	0.7159	1.07570	1.70020	1633.0	-12.4484	-38.252	-40.82
	0.8203	1.09120	1.67040	1667.9	-10.8883	-26.934	-38.54
	0.9128	1.10940	1.61370	1678.3	-9.4195	-16.883	-24.62
	1.0000	1.06030	1.60760	1719.2	0.0000	0.000	0.000

Table.3. Values Of Excess Free Length (Lfe), Internal Pressure (Πe) ,Available Volume (Vae) And Gibbs Free Energy(G*E) For Binary System Of 1-Butanol And O-Nitro Toluene At 298.15 And 308.15 K.

Temp. K	X1	LfE x 10-10 m	VaEx10-6 m3mol-1	πE x 106 Nm-1	G*E Jmol-1
298.15	0.0000	0.000	0.000	0.000	0.000
	0.1156	-0.004	0.977	-3036.9	-156.3
	0.2019	-0.011	1.118	-7074.8	-380.9
	0.3188	-0.014	4.416	-7717.9	-492.6
	0.4265	-0.016	4.840	-8921.1	-549.4
	0.5251	-0.021	5.627	-9789.3	-572.0
	0.6048	-0.022	11.955	-8895.1	-756.3
	0.7257	-0.021	10.008	-7003.6	-767.9
	0.8283	-0.018	8.915	-3755.8	-626.9
	0.9129	-0.010	5.176	-2429.4	-485.7
	1.0000	0.000	0.000	0.000	0.000
303.15	0.0000	0.000	0.000	0.000	0.000
	0.1156	-0.014	0.222	-3746.6	-180.7
	0.2019	-0.022	0.566	-6786.0	-358.3
	0.3188	-0.026	1.290	-9023.3	-498.6
	0.4265	-0.034	1.953	-9226.4	-558.8
	0.5251	-0.044	2.337	-8805.3	-645.3
	0.6048	-0.050	4.946	-6729.4	-735.0
	0.7257	-0.045	3.021	-7609.6	-797.5
	0.8283	-0.036	2.239	-4549.2	-624.6
	0.9129	-0.029	1.133	-1789.2	-500.2
	1.0000	0.000	0.000	0.000	0.000

14) M. Gowrisankar, P. Venkateswarlu, K. Siva Kumar and S. Sivarambabu, J. Mol. Liq., 173, 172 (2012).

15) M. Gowrisankar, P. Venkateswarlu, K. Siva Kumar and S. Sivarambabu, J. Soln. Chem., In press (2012

(A)
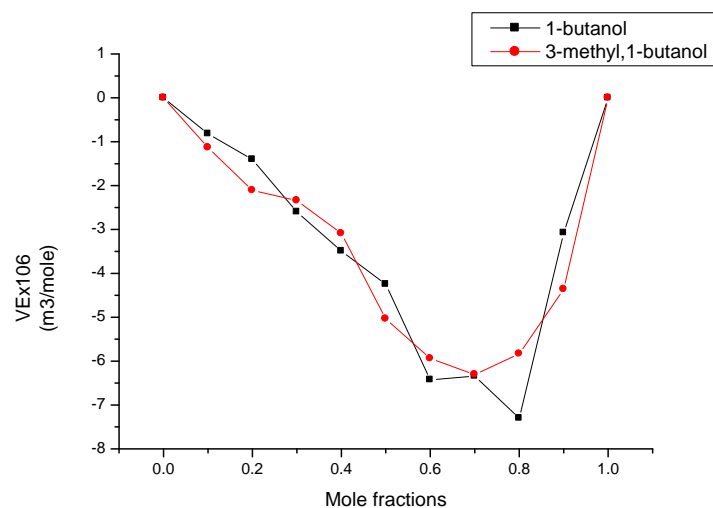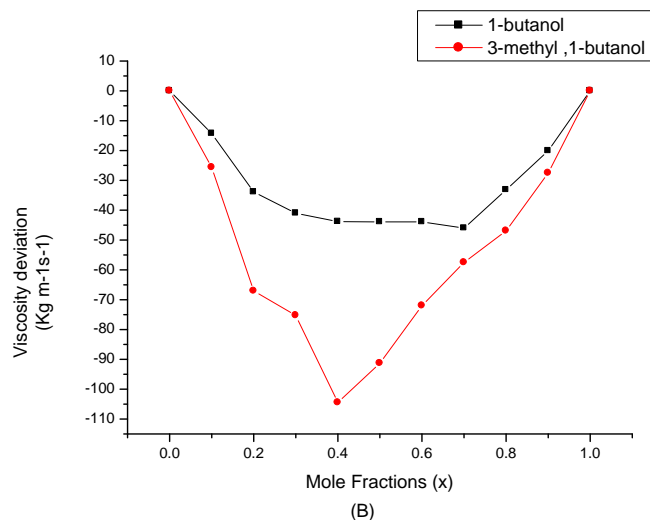
Figure1.

(A) Excess molar volume (VE) against mole fraction for 1-butanol and 3-methyl, 1-butanol at 298.15 K

(B) Deviation in viscosity (Δn) against mole fraction for 1-butanol and 3-methyl, 1-butanol at 298.15 K

(A)

(B)
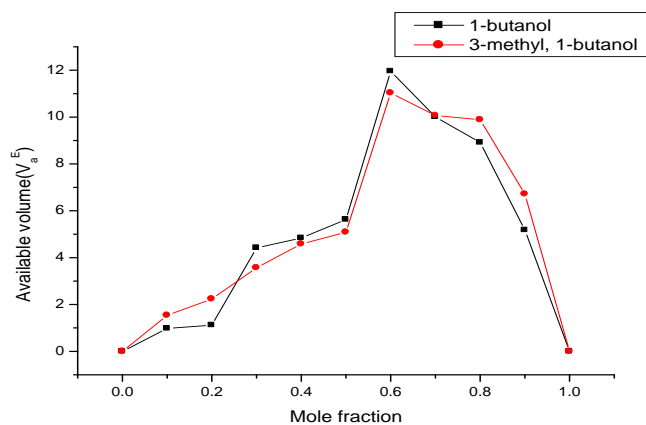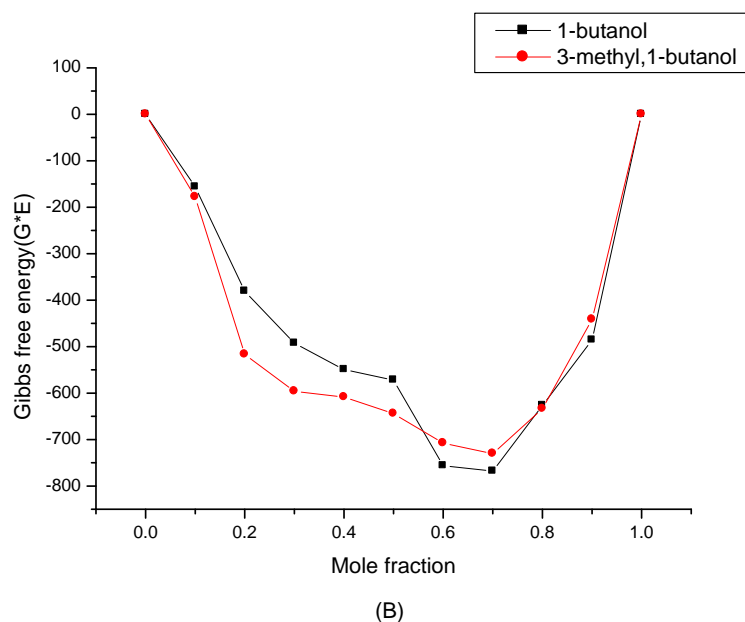
Figure :-2

(A) Available volume (VaE) against mole fraction for 1-butanol and 3-methyl, 1-butanol at 298.15 K

(B) Gibbs free energy (G*E) against mole fraction for 1-butanol and 3-methyl, 1-butanol at 298.15 K

TABLE.4. VALUES OF   EXCESS FREE LENGTH (LFE), INTERNAL PRESSURE (IIE) ,AVAILABLE VOLUME (VAE) AND GIBBS FREE ENERGY(G*E) FOR BINARY SYSTEM OF 3-METHYL, 1-BUTANOL AND O-NITRO TOLUENE AT 298.15 AND 308.15 K.

Temp. K	X1	LfE x 10-10 m	VaEx10-6 m3mol-1	πE x 106 Nm-1	G*E Jmol-1
298.15	0.0000	0.000	0.000	0.000	0.000
	0.0668	-0.001	1.536	-2751.6	-178.1
	0.1383	-0.011	2.236	-7530.4	-516.9
	0.2163	-0.022	3.567	-8801.9	-596.3
	0.3002	-0.021	4.582	-13887.0	-608.7
	0.3914	-0.025	5.085	-13935.0	-644.3
	0.4910	-0.018	11.030	-12903.9	-707.8
	0.5998	-0.015	10.070	-9072.6	-730.4
	0.7203	-0.014	9.885	-7082.3	-633.8
	0.8528	-0.010	6.714	-4249.0	-441.4
	1.0000	0.000	0.000	0.000	0.000
303.15	0.0000	0.000	0.000	0.000	0.000
	0.0668	-0.004	1.283	-1454.8	-118.5
	0.1383	-0.020	1.853	-7098.5	-505.4
	0.2163	-0.022	2.739	-7952.1	-552.5
	0.3002	-0.042	3.178	-13479.8	-633.1
	0.3914	-0.032	4.570	-8392.9	-691.0
	0.4910	-0.031	7.926	-8011.6	-782.3
	0.5998	-0.026	5.635	-4112.7	-693.3
	0.7203	-0.023	4.769	-2869.1	-528.3
	0.8528	-0.019	3.954	-2121.1	-394.3
	1.0000	0.000	0.000	0.000	0.000

REFERENCES:-

1) S. L. Oswal, P. Oswal, R. P. Shalak. "Speed of sound, is ntropic compressibility and excess molar volumes of binary mixtures containing p-dioxane." J Sol Chem. 27(1998) p. 507-20

2) H. Kumar, M. Kaur, R Gaba, K. Kaur. " Thermodyanamics of binary liquid mixtures of cyclopentane with 2-propanol, 1-butanol and 2-butanol at different temperature." J Therm. Anal. Calorim. 105(2011) p.1071-1080.

3) E. Zorebski, E. Waligora. " Densities, Excess molar volumes and Isobaric Thrmal Expansibilities for 1,22Ethanediol + 1-Butanol, or 1-Hexanol, or 1-Octanol in the Temperature range from (293.15 – 313.15) K". J. Chem. Eng. Data. 53 (2008) p. 591-595.

4) A. Borun, M. Zurada, A Bald, "Densities and Excess molar volumes for mixtures of methanol with other alcohols at temperature (288.15-313.15 K)" J Therm. Anal. Calorim. 100(2010) p. 707-715.

5) S. S. Sastry, Babu S, T. Vishwam, K. Parvateesam, H. S Tiong. "Excess parameters for binary mixtures of ethyl benzonate with 1-propanol, 1-butanol and 1-pentanol at T=303, 308, 313, 318, and 323 K". Phys B. 420 (2013) p. 40-48.

6) R. F. Checoni. "Excess molar enthalpy for methanol, ethanol, 1-propanol, 1-butanol + n-butylamine mixtures at 288.15 and 308.15 K at mospheric pressure". J Therm. Analo. Calorim. 101 (2010) p. 349-57.

7) S. Sreehari Sastry, Shaik. Babu, T. Vishwam, Ha.Sie Tiong. Study of molecular interaction in the mixture of some primary alcohols with equimolar mixtures of 1-propanol and alkylbenzoates at T=303.15 K. J. Chem. Thermodynamics, 68 (2014) p. 183-192.

8) S. Sreehari Sastry, S. M. Ibrahim, L. Tanuj Kumar, Shaik. Babu, Ha. Sie Tiong. Excess thermodynamics and coustic properties for equimolar mixture of ethyl benzoate and 1-alkanols with benzene at 303.15 K. International Journal Of Engineering Reserch and Technologies, 4(2015) p. 315—324.

9) J. M Resa, C. Gonzalez, JM Goenaga, M. Iglesias, "Influence of Ethanol+water+1-propanol mixtures". J Therm Anal Calorim. 87. (2007) p. 237-45.

10) S. Sharma, B Jasmin, J. Ramani, R Patel. "Density, excess molar volumes and refractive indices of β-pinene with o, m, p- xylene and toluene at 303.15, 308.15 and 313.15 K". Phys. Chem. Liq. 49 (2011) p. 765-76.

11) A. I Vogel. "Text book of organic chemistry". 5th ed. New York: John Wiley; 1989.

12) M. Gowrisankar, K. Rambabu, P. Venkateshwarlu and G. K. Raman, Phys. Chem. Liq., 28,29 (1994).

13) M. Goweisankar, S. Sivarambabu, P. Venkateswarlu and K. Siva Kumar, Bull. Korean Chem. Soc., 33, 1686 (2012).

14) M. Gowrisankar, P. Venkateswarlu, K. Siva Kumar and S. Sivarambabu, J. Mol. Liq., 173, 172 (2012).

15) M. Gowrisankar, P. Venkateswarlu, K. Siva Kumar and S. Sivarambabu, J. Soln. Chem., In press (2012).

SYNTHESIS, CHARACTERIZATION AND SEMICONDUCTING STUDIES OF2,4-DIHYDROXYBENZALDEHYDE-FORMALDEHYDE - ETHYLENE DIAMINE COPOLYMERS

S. P. Dhote[1.] and W.B. Gurnule[2*]

[1]Department of Chemistry, The Royal Gondwana Public School, Nagpur – 441108. M.S. India
[2*]Department of Chemistry, Kamla Nehru Mahavidyalaya, Nagpur -440024. M.S. India

ABSTRACT

Copolymer(2,4-DHBEDF) was synthesized by the condensation of 2,4-Dihydroxybenzaldehyde [2,4-DHB] and ethylene diamine [ED] with formaldehyde [F] in presence of acid catalyst using varied molar ratios of reacting monomers. A copolymer composition has been determined on the basis of their elemental analysis and the number average molecular weight of this copolymer was determined by conductometric titration in non-aqueous medium. Viscosity measurement in Dimethyl sulphoxide have been carried outin order too ascertain the characteristic functions and constantsof 2, 4 DHBEDF copolymer resin. The newly synthesized copolymer resin was characterized by IR spectra and HNMR spectra. The electrical properties of (2, 4-DHBEDF copolymers were measured over a wide range of temperature (303-423 K). From electrical conductivity of these copolymers, the activation energies of electrical conduction have been evaluated and values lies in the range of13.24× 10-23 – 10.80× 10-23 J. The plots ofof log σ vs. 1/T has been found to be linear temperature range under study which indicates that the Wilsons exponential lawσ = σ0 exp(-Ea/ K)1/T is obeyed. On the basis of above studies, these copolymers can be ranked as semiconductors. When a voltage is applied to a thin film of this copolymer resin then it emitted light. This property of 2,4-DHBEDF copolymer resin may be used to make a semiconducting and electronic devices such as transistors, light emitting diodes, solar cells.

Keywords: Resin, Synthesis, Electrical conductivity.

I. INTRODUCTION

The copolymer resins showssemiconducting property. This type of discovery has led to emergency of not only new types of materials capable of replacing metals but also new concept to explain their high conductivity. In fact, the electrical conductivity and other properties such as thermo-conduction, photoconduction, luminescence etc. are in close connection with their physical and chemical structure. Semiconducting polymers have been the subject of study for many decades for day to day application product for example, uses in electrical sensors and electronic devices.[1]

Bakr et al studied the optical and electrical conductivity investigation of Fe3+-(acrylonitrile-butadiene-styrene) terpolymer complex system[2]. Gupta et al have measured the electrical conductivity of p-hydroxybenzaldehyde- adipic acid- ethylene glycol[3].Pancholi et al studied the electrical resistivity of 2-hydroxyacetophenone-thiourea-trioxane and these polymers ranked as semiconductors.Urade et al have studied the nature of resin derived from 2,6-Diaminopyridine and terphthalic acid[4].Kapse et al have studied semiconducting behavior of the terpolyligand derived from p-hydroxyacetophenone,quinhydrone and melamine[5].Masram et al studied the electrical conductivity of resin derived from salicylic acid,butylenesdiamines and formaldehyde[6].Gurnule et.al have reported semiconducting studies of 8-hydroxyquinoline-melamine/biuret-formaldehyde terpolymer resin[7,8]. Borkar et al. studied electrical and optical properties of conducting polymer[9.10]

The present study deals with the synthesis and characterization of like 2,4-dihydroxybenzaldehyde, ethylene diamine and formaldehyde [2,4-DHBEDF] terpolymer resin by spectral methods for the first time. The synthesized terpolymer was characterized by elemental analysis, UV-VIS, FT-IR,1H-NMR, intrinsic viscosity and number average molecular weight. The electrical conductivities of four 2,4-DHBEDFcopolymer resins are studied over wide range of temperature.

II. EXPERIMENTAL

The important chemicals like 2,4-dihydroxybenzaldehyde, adipamide and formaldehyde used in the preparation of various new 2,4-DHBAF terpolymer resins were procured from the market and were of chemically pure grade.

A. Synthesis of 2,4-DHBEDF Copolymer resin

The 2,4-DHBEDF-Iterpolymer resin was prepared by condensing 2,4-dihydroxybenzaldehyde(1.3812gm, 0.1mol), ethylene diamine(0.601gm, 0.1mol), formaldehyde(7.5ml, 0.2mol) in the mole ratio of 1:1:2 in the presence of 2MHCl as a catalyst at 122+2oC for 6h in an oil bath with occasional shaking to ensure through mixing. The separated cream colourterpolymer resin was washed with hot water to remove unreacted starting

materials and acid monomers. The properly washed resin was dried, powered and then extracted with diethyl ether to remove 2,4-dihydroxybenzaldehyde - formaldehyde copolymer which might be presentalong with 2,4-DHBEDF terpolymer. The terpolymer resin was purified further by dissolving in 8% aqueous sodium hydroxide solution, filtered and reprecipited by gradual drop wise addition of ice cold 1:1 (v/v) concentrated hydrochloric acid/distilled water with constant and rapid stirring to avoid lump formation. The process of reprecipitation was repeated twice. theterpolymer sample 2,4-DHBEDF-I thus obtained was filtered, washed several times with hot water, dried in air, powered and kept in vacuumdesicator. The reaction and suggested structure of 2,4-DHBEDF-I is given in Fig. 1.
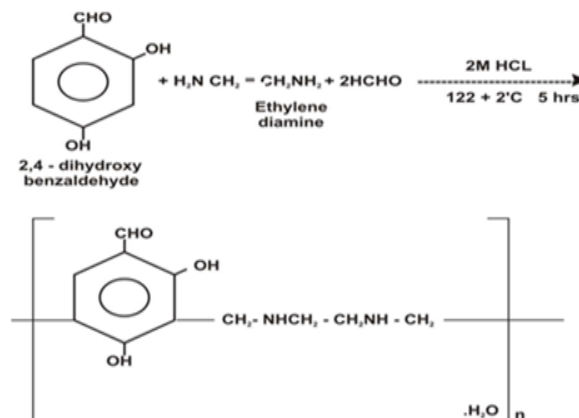
Fig.1: Preparation of2, 4-DHBEDF-1 Copolymer Resin

In the same way the other terpolymer resin viz.2,4-DHBEDF-II, 2,4-DHBEDF -III, 2,4-DHBEDF -IV were prepared with the molar ratios 2:1:3, 3:1:4, 4:1:5.

III. CHARACTERIZATION OF2,4-DHBEDFTERPOLYMER RESIN
A. Physicochemical and Elemental Analysis
The terpolymer resin was subjected to micro analysis for C, H and N on an ElementalVario EL III Carlo Erba-1108 elemental analyzer. The number average molecular weight was determined by conductometric titration in DMSO medium using ethanoic KOH as the titrant by using 25 mg of sample. A plot between specific conductance vs the miliequivalents of KOH required for neutralization of 100 gm of copolymer resin was made. Inspection of such plot revealed that there were many breaks in the plot. From this plot first break and last break were noted. On the basis of average degree of polymerization the average molecular weight has to be determined by following eq

= x Repeat unit weight

The intrinsic viscosity was determined using a Tuan-Fuoss viscometer at six different concentrations ranging from 0.3% to 0.05% wt % of resin in DMSO at 30oc. Intrinsic viscosity was calculated by the Huggins eq. and Kramer's eq.

B. Spectral and surface analysis
Electronic (UV-Visible) spectra of terpolymer resin in DMSO was recorded with a double beam spectrophotometer in the range of 200-850 nm at Kamla Nehru Mahavidyalaya, Nagpur.FT-IR spectra of 2,4-DHBEDFterpolymer resin was recorded in najol mull with Perkin –Elmer Spectrum RX-I,FT-IR spectrophotometer in KBr pallets in the range of 4000-500 cm-I at SAIF , Punjab University, Chandigarh.1H NMR spectra was recored with Bruker Advance-II 400 NMR spectrophotometer using DMSO as solvent at SAIF , Punjab University, Chandigarh.The surface analysis was performed using scanning electon microscope at different magnification at VNIT Nagpur.

C. Electrical Conductivity Measurements
The electrical conductivity of 2,4-DHBEDF copolymer resin was measured over a wide range of temperature (303-423K) in their pellets form using Auto LCR-Q meter 4910. To prepare the pellet the copolymer resin was thoroughly ground in pestle and mortar. The well powered copolymer was palatalized isostatically in a steel die at 10 tones/inch with the help of hydraulic press. The pellet was hard and crack free. On both sides of pellet, a thin layer of colloidal graphite in acetone was applied to ensure a good contact with the electrode.

IV. RESULTS AND DISCUSSION
A. Spectral and surface studies

The UV-Visible spectrum of all four 2,4-DHBEDF terpolymer resin has been shown in Fig. 2. All the four 2,4-DHBEDFterpolymer resin displayed two broad bands at 280-290 nm and 240-250 nm. The observed position of the absorption bands indicates the presence of a carbonyl group and hydroxyl group which is in conjugation with the aromatic nucleus. Theband at 240-250 nm is more intense which is accounted for a π-π* transition while the less intense band at 280-290 may be due to n-π*transition[11,12]
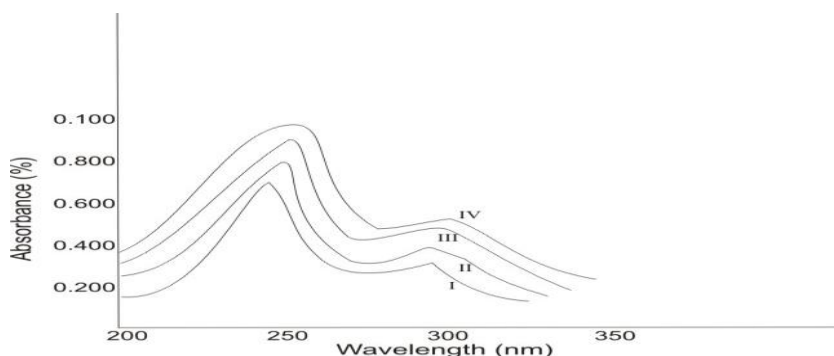
Fig. 2 UV-visible Spectra of 2,4-DHBEDF Terpolymer Resins

B. Infrared Spectra

The IR spectra of all four 2, 4-DHBEDF terpolymer resins are presented in fig 3. IR spectrarevealed that all four 2,4-DHBEDF terpolymer resin give rise to nearly same pattern of spectra. A broad band appeared at the region 3750-3749 cm-1 may be assigned to stretching vibration of phenolic –OH group exhibiting intramolecular hydrogen bonding [13]. A peak at 1465-146 cm-1 may be ascribed to aromaticskeletal ring. The band at 1556-1557 cm-1 is due to –NHstretching. . A band at 856-857cm-1indicates the presence of tetrasubstituted aromatic ring.1, 2,3,5 substitution in aromatic ring was confirmed.
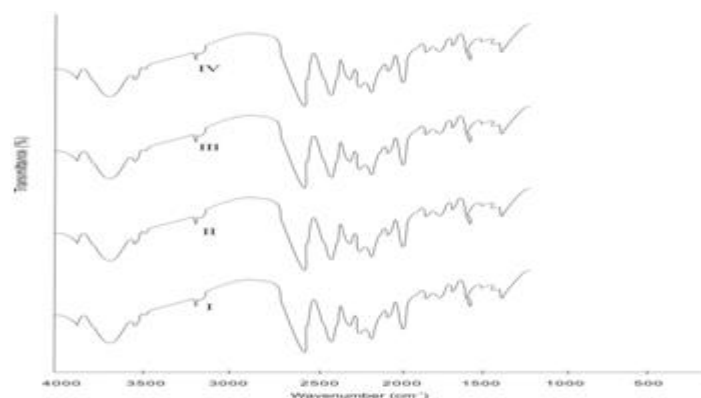
Fig. 3.Infra Red Spectra of 2,4-DHBEDF Terpolymer Resins

C. Nuclear Magnetic Resonance spectroscopy

1H NMR spectra of all 2,4-DHBEDF terpolymer resin are shown in fig 4. The signal in the region of 4.65-4.68 ppm may be due to methylene proton of Ar-CH2-N. The signal in the region 5.37-5.38 ppm may be due to proton of –NH bridge. The weak multiplate signal in the region signal in the range of 7.30-7.38 ppm may be due to aromatic proton(Ar-H). The signal in therange of 9.5-9.56 may bedue to phenolic hydroxyl group [14].
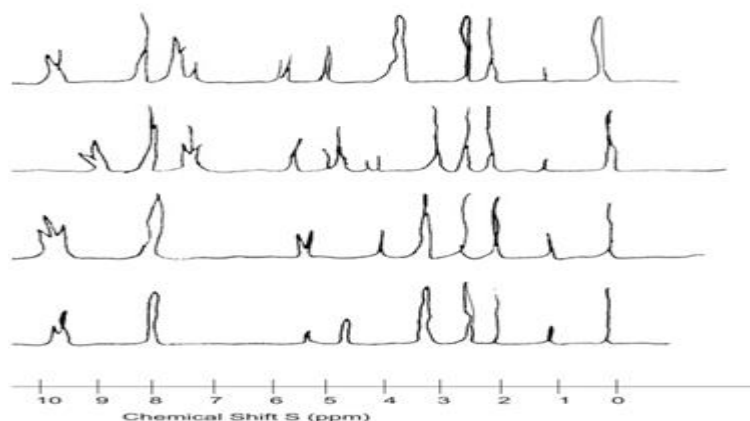
Fig. 4 1H NMR Spectra of 2,4-DHBEDF Terpolymer Resin

D. Scanning electron microscopy (SEM)

Surface analysis is generally used in understanding the surface features of the materials. The morphology of the reported sample was investigated by scanning electron micrograph at different magnification which is shown in fig 5.for 2,4-DHBEDF. It gives the information of surface topography and defects in the structure. The morphology of polymer resin shows spherulites and fringed and scattered model. The spherulites are complex polycrystalline formation having as good as smooth surface and having deep pits in the photograph. This indicates the crystalline nature of 2, 4-DHBEDF terpolymer resin sample. Thus by SEM micrograph morphology of the resin shows the transition between crystalline and amorphous nature, when compared to other resin, the 2,4-DHBEDFterpolymer resin is more amorphous in nature, hence shows higher metal ion exchange capacity.
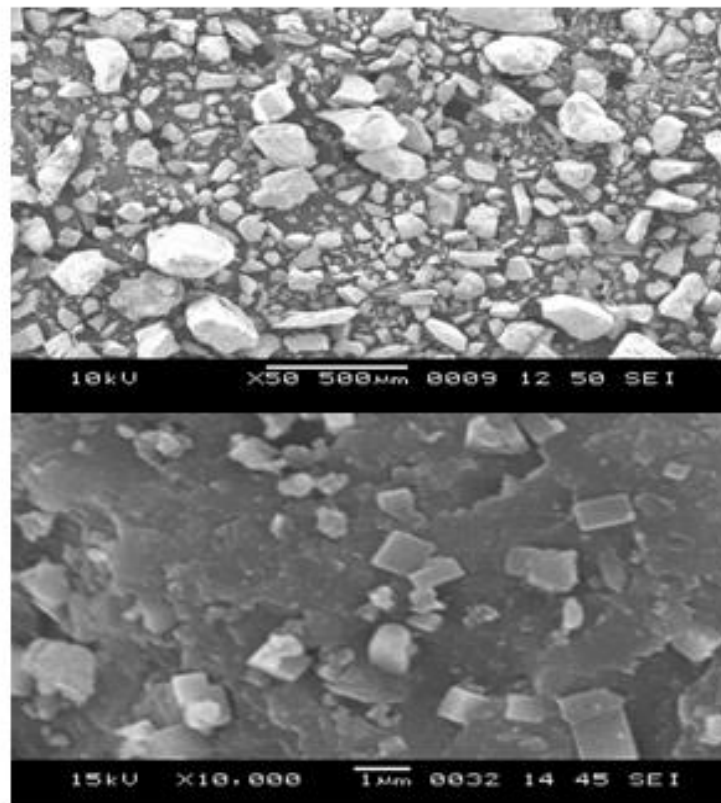
Fig. 5. SEM Micrograph of 2,4-DHBEDF-I Terpolymer resin

E. Electrical Conductivity for 2,4-DHBEDF copolymer

The electrical conductance of polymeric material depends on porosity, pressure, method of synthesis and atmosphere. Activation energy is not affected by these parameters and therefore it is fairly reproducible. The magnitude of activation energy depends on the number of loosely bound electrons present in semiconducting materials. Resins are well known for their behavior as semiconductors. The electrical conductivity varies exponentially with the absolute temperature according to well-known relationship ……………….(1)

Where, σ =Electrical conductivity at temperature T

σ o=Electrical conductivity at temperature T∞ i.e.

constant (Pre-exponential conductivity)

E_a = Activation energy of electrical conductance

K = Boltzmann constant = 1.38 x 10-23 J/K/molecule

T = Absolute temperature

The logarithmic form of equation (1) is written as

A plot of log σ vs1/T is plotted which is shown in fig. The plots are linear with negativeslope.

This indicates the semiconducting nature of resin. The values of activation energy and electrical conductivity for 2,4-DHBEDF copolymer resin are given in Table1.
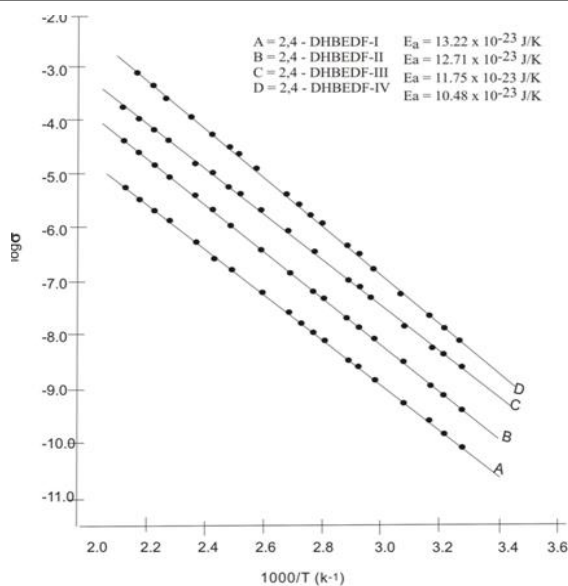
Fig- 6 Electrical conductivity plots of 2,4-DHBEDF copolymers

The sequence of electrical conductivity is found to be 2,4-DHBEDF-I < 2,4-DHBEDF-II < 2,4-DHBEDF-III < 2,4-DHBEDF-IV, As the number of rings increases in the structure of repeat unit of copolymer, increase the π electrons, conjugation and delocalization which may increase the electrical conductivity due to increase in forbidden energy gap between valence and conduction band. The order of thermal activation energy is just reverse of electrical conductivity 2,4-DHBEDF-I > 2,4-DHBEDF-II > 2,4-DHBEDF-III > 2,4-DHBEDF-IV.[15,16], The temperature dependence of the electrical conductivity (Fig 6) is found to be linear in the

Terpolymers	Electrical Conductivity		DT	DE
	313 K	423 K	(K)	(J/K)
2,4-DHBEDF -I	3.06×10^{-10}	1.02×10^{-7}	313 – 423	13.22×10^{-23}
2,4-DHBEDF -II	2.63×10^{-9}	6.37×10^{-6}	313 – 423	12.71×10^{-23}
2,4-DHBEDF -III	3.01×10^{-8}	6.85×10^{-5}	313 – 423	11.75×10^{-23}
2,4-DHBEDF -IV---	3.12×10^{-7}	1.13×10^{-3}	313 – 423	10.48×10^{-23}

temperature range under study showing thereby that Wilson's exponential law is obeyed.

V. CONCLUSIONS

1. A copolymer 2,4-DHBEDF, based on the condensation reaction of2,4-Dihydroxybenzaldehyde and ethylene diaminewithformaldehyde in the presence of acid catalyst was prepared.

2. Electrical conductivity of all the four 2,4- DHBEDF copolymer resinSincreaseS with the increase in temperature. Hence these copolymers may be ranked as semiconductors.

3. The energy of activation is found to be in the order 2,4-DHBEDF-I > 2,4-DHBEDF-II >2,4-DHBEDF-III > 2,4-DHBEDF-IV and electrical conductivity 2,4-DHBEDF-I < 2,4-DHBEDF-II < 2,4-DHBEDF-III < 2,4-DHBEDF-IV

TABLE 1-ELECTRICAL CONDUCTIVITY DATA OF 2,4-DHBEDF TERPOLYMER RESINS

REFERENCES
1. Genies E.M., Syed A.A., tsintavis.,Mol.Cryst.Liq. Cryst.,121.181(1985)

2. Bakr,N.A., Abdel-hamidM.I.,Designed monomers and polymers, 10,2653-2658(1995).

3. Gupta A.N.,Hiwase V.V.,Kalambe A.B., Der Pharma Chemica.,4(3),2012,1153-1159.

4. Urade D.N., Hiwase V.V., Kalambe A.B., Archives of Applied Science Reasearch,4(5),2012 ,1991-1995.

5. Kapse S.K., Hiwase V.V., Kalambe A.B.,J Chemical and Pharmaceutical Research, 4(3),2012,1734-1739.

6. PancholiH,B.,Patel M.,J.Indian Chem.Soc.75,86(1998).

7. Gurnule W.B., Juneja H.D., and Paliwal L.J., Asian J Chem.,2000,12,753.

8. Gurnule W.B., Juneja H.D., and Paliwal L.J., UltraSci.,2001,13,222.

9. Borkar A.D.,Umre S.S., and Gupta M.C.,ProgCryst Grow Charact Mat.,2002,44,88.

10. Borkar A.D.,Umre S.S., and Gupta M.C.,PolymPlast Tech Eng.,2001,40(2),225.

11. Singru, R.N.Zade, A. B. Gurnule, W.B.2010,Iranian Polymer Journal., 19(3), 169-183.

12. Burkanudeen, R.Azarudeen, M. RiswanAhamed, P. Ramesh, N. Vijayan, 2010, Int. J. of Chem. And Env.Engg., 1(1), 29-34.

13. Joshi, J. D. Patel, N. B. Patel, S. D, 2006, Iran.Polym. J., 15, 219-226.

14. Silverstein, R. M. Webster, F. X. Spectrometric identification of organic compounds, John Wiley and Sons, New York, 1998.

15. Nandekar K.A., Dontulwar J.R., and Gurnule W.B., Der Pharma Chemica,2012,4(4),1644-1652.

16. Ahamed M.A.R., Azarudeen R.S., Mylyswamy K and BurkanudeenA.R.,IranPolym J., 2010,19(8), 635-646.

USE OF IONIC LIQUID PERSPECTIVES IN THE SYNTHESIS OF 3-ARYL-4-SUBSTITUTED COUMARINS FROM O-HYDROXY CARBONYL COMPOUNDS

Ali Abdulraheem Abdul Karem[1*], Mrs. Sangita Sanjay Makone[3] and Dr. Sandeep Nivruttirao Niwadange[2]

[1,3]Chemical Sciences Research Laboratory, School of Chemical Sciences, Swami Ramanand Teerth Marathwada University, Vishnupuri, Nanded-431606, Maharashtra, India
[2]Shri Govindrao Munghate Art's & Science College, Kurkheda, Gadchiroli-441209.Maharashtra, India

ABSTRACT

The given method introduces the ionic liquid perspectives in synthesis of 3-aryl-4-substituted coumarins from o-hydroxy carbonyl compounds. Method includes the intramolecular cyclization of the esters of substituted aldehyde and 2-hydroxyaromatic ketones which used to the synthesis of 3-aryl-4-substituted coumarins by using ionic liquid in PEG-400 as a green solvent at room temperature. The advantages of this method are short reaction time, avoiding harsh reaction conditions, high yield and ease of easy work up and reuse of ionic liquid.

Key-words- 3-aryl-4-substituted coumarins, o-hydroxy carbonyl compounds, ionic liquid, PEG-400, room temperature.

INTRODUCTION:

Coumarins represent a class of organic compounds, which occurs naturally in a number of plants. It is heterocyclic compound possessing phenolic and heterocyclic ring with oxygen heteroatom. Coumarins are simple or having substituents in the phenolic nucleus and in the heterocyclic ring. Coumarins are also well known for their considerable biological and medical activities as they form a family of active compounds. Coumarin (2H-1-benzopyran-2-one) (1a) moiety has following structure and is a widely occurring secondary plant metabolite. Coumarin is isomer of chromone (1b)
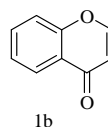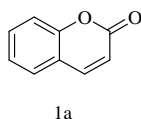
Coumarin derivatives exists widely in nature especially in plants and many of them show a wide range of biological activities, coumarins play an important role in the reaction natural and synthetic organic chemistry. Coumarins and their derivatives are used in the fields of biology, medicine and polymer science. They are also present or used in perfumes, cosmetics, cigarettes, [1-5], alcoholic beverages [6] and laser dyes [7]. Coumarins have been found to be connected with a number of cases of homicide and suicide in Korea [8]. Coumarins were first synthesized using Perkin reaction in 1868, and many simple coumarins are still prepared through this method. In the early 1900s, the Knoevenagel reaction emerged as an important synthetic method to synthesize coumarin derivatives with carboxylic acid at the 3-position [9,10]. To date, many other synthetic methods for coumarins have been reported, including the Pechmann [11], Reformatsky [12] and Wittig reactions [13, 14]. Coumarin derivatives are readily synthesized by the above mentioned reactions; however, they usually require harsh reaction conditions and non-environmentally friendly solvents. Recently some good methods for synthesis of coumarin have developed[15-17]. For instance, ionic liquids have attracted extensive interest as environmentally benign reagent to their favorable properties, and a variety of catalytic reactions have been successfully conducted using ionic liquids as solvent [18-20].

Many reported methods [21-28] suffer from strong acidic conditions, prolonged reaction times, low yields and high cost of the reagents. This obviously warranted further investigation into finding an alternative method to afford mild reaction conditions, short reaction times, and better yields. Our experiments using ionic liquids (ILs) as green catalyst provided the answer. In recent times, the use of ionic liquids (ILs) as green solvents in organic synthesis process has gained considerable significance because of their negligible vapor pressure, solvating ability and easy recyclability, Additionally, some ILs possesses inherent Lewis/Bronsted acidity which promotes and catalyzes organic transformations in excellent yields. On the basis of the findings of advantageous, herein we report a mild and efficient protocol promoted by ionic liquid, 1-hexyl-3-methyl-imidazolium chloride ([hmim]Cl) in excellent yield and short reaction times. The literature survey for synthesis of coumarins and perspective of ionic liquid promote to develop this method. Thus, the non-volatile ionic liquids were effectively recovered and reused. The process does not require any additional catalyst (**Scheme 01**).

Present work:

1] **Materials and Method:** All the chemicals were purchased from Aldrich, Spectro-chem, sd fine chemicals and were used without further purification, unless otherwise stated. All melting points were measured on Veego digital melting point apparatus and are uncorrected. IR spectra were measured as KBr pellets on a Perkin Elmer Spectrum RX FTIR spectrophotometer. The NMR spectra were recorded on a Brucker Avance II spectrometer with TMS as internal standard ^{1}H NMR were run in deuteratd chloroform (CDCl$_3$). Chemical shifts ($\square$) are referred in terms of ppm.

2] **General Procedure for synthesis of ester precursor:** In 100 ml round bottom flask substituted 2-hydroxyaromatic ketones (1 mmol) and substituted phenylacetic acid (1.5mmol) dissolved in sufficient amount of pyridine. To this mixture phosphorus oxychloride (POCl$_3$, 1.5mmol) was added drop wise under cooling with continuous stirring at room temperature for 5-10 minutes. Progress of reaction is monitored. After completion of the reaction water is poured and washed well with 10% HCl and then 10% NaHCO$_3$ organic layer is separated and dichloromethane is evaporated. The product obtained as ester.

3] **General procedure for synthesis of 3-aryl-4-substituted coumarins derivatives:** An ester 1mmol dissolved in 5ml of PEG-400and 1mmol [Hmim]Clwas added reaction mixture was stirred at room temperature for two hours. After the reaction was completed, it was carefully poured into crushed ice and neutralized with dilute HCl. The precipitate was filtered, washed with water, and dried. The crude product was recrystallized from methanol and the product thus isolated were subjected to further purification by column chromatography of silica 20% ethyl acetate in petroleum ether as eluent and fully characterized. On the other hand, concentrated mixture of ionic liquid is collected from filtrate along with PEG-400. Results are recorded in the
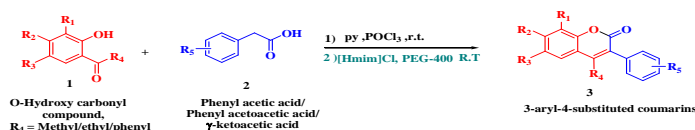
Scheme 01: Synthesis of of 3-aryl-4-substituted coumarins from o-hydroxy   carbonyl compounds by using ionic liquid at room temperature.

Table 01:Synthesis of 3-Aryl-4-Substituted Coumarins.

Sr. no.	R$_1$	R$_2$	R$_3$	R$_4$	R$_5$	Yield (%)	Mp. ^{o}C)
1	H	H	CH$_3$	CH$_2$CH$_3$	4-Cl	87	185
2	H	H	CH$_3$	CH$_2$CH$_3$	H	88	150
3	H	H	Cl	CH$_2$CH$_3$	H	91	172
4	H	H	Cl	CH$_2$CH$_3$	4-Cl	91	189-191
5	Cl	H	Cl	CH$_2$CH$_3$	4-Cl	92	180
6	Cl	H	Cl	CH$_2$CH$_3$	H	72	140
7	Cl	H	Cl	CH$_3$	3-OCH$_3$	75	158-160
8	Cl	H	Cl	CH$_3$	H	92	176-178
9	Cl	H	Cl	CH$_3$	4-OCH$_3$	92	170-172
10	Cl	H	Cl	CH$_3$	4-Cl	94	190-191
11	H	H	Cl	CH$_3$	H	94	193
12	H	H	CH$_3$	CH$_3$	H	92	172
13	H	H	H	CH$_3$	H	92	156-157
14	H	OH	H	CH$_3$	H	93	225-228
15	H	H	Br	H	H	90	170-171
16	H	H	H	H	H	92	125-126
17	H	H	H	H	4- OCH$_3$	94	140-141
18	H	H	H	H	4-Cl	94	185-186
19	H	H	Cl	CH$_2$CH$_3$	4-OCH$_3$	93	158-160

RESULT AND DISCUSSION:

In recent times, the use of ionic liquids (ILs) as green solvents in organic synthesis process has gained considerable significance because of their negligible vapor pressure, solvating ability and easy recyclability, Additionally, some ILs possesses inherent Lewis/Bronsted acidity which promotes and catalyzes organic transformations in excellent yields. On the basis of the findings of advantageous, herein we report a mild and efficient protocol promoted by ionic liquid, 1-hexyl-3-methyl-imidazolium chloride ([hmim]Cl) in excellent yield and short reaction times. The literature survey for synthesis of coumarins and perspective of ionic liquid promote to develop this method. Thus, the non-volatile ionic liquids were effectively recovered and reused. The process does not require any additional catalyst (**Scheme 01**).

To check the efficiency and scope of given process, phenyl acetic acid were treated with various substituted o-hydroxy carbonyl compounds. The resultant synthesized coumarine derivatives are summerized in **Table-1**, which shows that all reactions runs very smoothly and the desired substituted coumarine derivatives were produced at excellent yields in short reaction times. As shown in Table-1, electron withdrawing group had major effect on the reaction time and yields of the products. However, electron donating groups slightly increased reaction time and decreased the yields of corresponding products. The reusability of ionic liquid was tested in the synthesis for coumarine derivatives. The given reaction smoothly carried with phenyl acetoacetic acid and □-ketoacetic acid (**Scheme 02 & 03**).
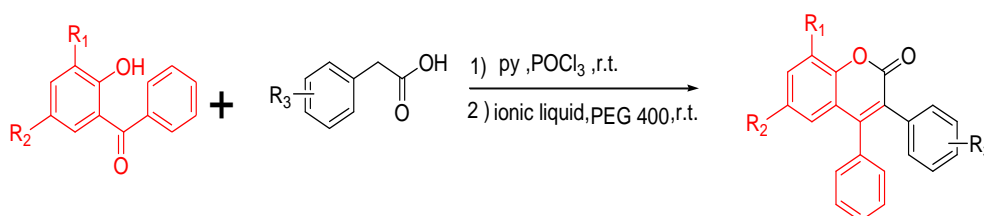
IL=[hmim]Cl

Scheme 02

The resultant synthesized coumarine derivatives are summerized in **Table-02.**

Table 2: Synthesis of 3-Aryl-4-Phenyl Coumarins.

Product	R₁	R₂	R₃	Yield (%)	Mp. °C
1	H	Cl	H	93	152-153
2	H	CH₃	H	89	208-209
3	H	CH₃	4-OCH₃	93	200-202
4	Cl	Cl	H	75	220-222
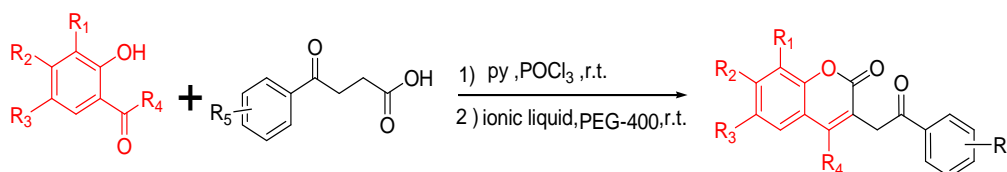
IL=[hmim]Cl

Scheme 03

The resultant synthesized coumarine derivatives are summerized in **Table-03.**

Table 03: Synthesis of Coumarins from gamma ketoacid.

Product	R₁	R₂	R₃	R₄	R₅	Yield (%)	Mp. °C
1	H	H	CH₃	CH₂CH₃	4-OCH₃	91	139
2	Cl	H	Cl	CH₃	4-OCH₃	93	218-219

CONCLUSION:

The protocol offers advantages in terms of simple and easy procedure, fast reaction rate, mild reaction conditions and excellent yields of the product, the used ionic liquid was recovered and reused for three times gives satisfactory yield of the products. Reuse and simplicity for the ease of products are effective perspectives of the ionic liquid used for synthesis of 3-aryl 4-substituted coumarin compounds.

Spectral Data of Some selected compounds:
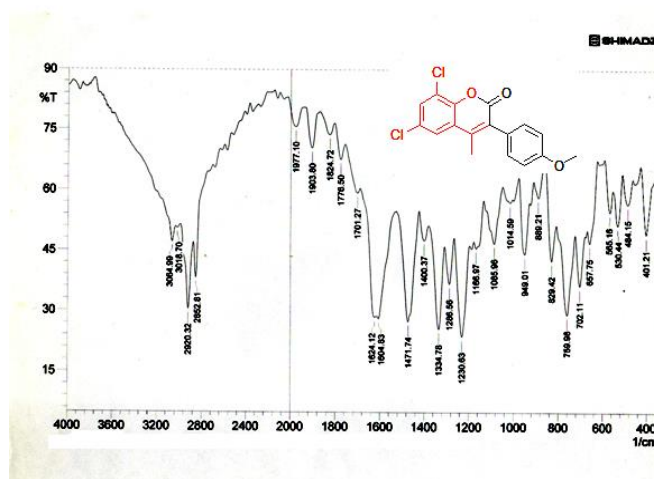
Fig. 1: IR spectra 6,8-dichloro-3-(4-methoxyphenyl)-4- methyl-2*H*-chromen-2-one
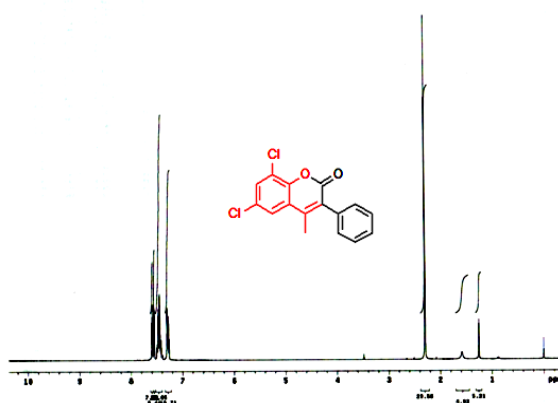
Fig. 2: ¹H NMR spectra of 6,8-dichloro-4-methyl-3-phenyl-2*H*- chromen-2-one

REFERENCES:-

[1] J. J. Yourick, R.L. Bronaugh, *J. Appl. Toxicol.*, 17(1997) 153.

[2] R. O' Kennedy, R. D. Thornes, Coumarins: Biology Applications, and Mode of Action, John Wiley & Sons, New York, 1997.

[3] B.E. Nielson, V.E. Heywood in the Biology and Chemistry of the Umbelliferae, Academic Press,London, 1971.

[4] R.D.H. Murray, J. Mendez, S.A. Brown, The Natural Coumarins, Occurrence, Chemistry and Biochemistry, John Wiely & Sons, New York, 1982.

[5] H. Yamazaki, M. Tanaka, T. Shimada, *J. Chromatogr.* B 721 (1999) 13

[6] M.E.F. Izquierdo, J.Q. Granados, V.M. Mir, M.C.L. Martinez, *Food Chem.* 70 (2000) 251.

[7] S.R. Trenor, A.R. Shultz, B.J. Love, T.E. Long, *Chem. Rev.* 104 (2004) 3059.

[8] S.W. Park, B.S. Seo, E.H. Kim, D.H. Kim, K.J. Paeng, *J. Forensic Sci.,* 41 (1996) 685.

[9] E. Knoevenagel, Ber. Dtsch. Chem. GesBrelin, 37(1904) 4461.

[10] A.M. Song, X.B. Wang, K.S. Lam, *Tetrahedron Lett.*,41 (2003) 1775.

[11] H. von Pechmann, C. Duisberg, *Chem. Ber.*, 37 (1884) 929.

[12] R.L. Shriner, *Org. React.*, 1 (1942) 1.

[13] N.S. Narasimahan, R.S. Mali, M.V. Barve, *Synthesis*, (1979) 906.

[14] Yavari, R. Hekmat-Shoar, A. Zonouzi, *Tetrahedron Lett.,* 39 (1998) 2391.

[15] F.F. Ye, J.R. Gao, W.J. Sheng, J.H. Jia, *Dyes Pigments*, 77 (2008) 556.

[16] J. Oyamada, T. Kitamura, *Tetrahedron*, 62 (2006) 6918.

[17] M. Maheswara, V. Siddaiah, G.L.V. Damu, Y.K. Rao, C.V. Rao, *J. Mol.   Catal.*, A 255 (2006) 49.

[18] T. Welton, *Chem. Rev.*, 99 (1999) 2071.

[19] P. Wasserscheid, W. Keim, Angew. *Chem. Int. Ed.*, 39 (2000) 3772.

[20] R. Sheldon, *Chem. Commun.*, (2001) 2399.

[21] S.K. Gadakh, S. Dey, A. Sudalai, *J.Org.Chem.,***2015**, *80*, 11544-11550.

[22] L. S. da Silveira Pinto, M.V.N. deSouza, *Synthesis*, **2017**, *49*, 2555-2561.

[23] Souad Bouasla, Juan Amaro-Gahete, Dolores Esquivel, M. Isabel Lopez,   Mabrouk Teguiche 3 and Francisco J. Romero-Salguero, *Molecules***, ***2017, 22*, 2072

[24] W. Xuefeng, L. Tong, Z. Danqing, Z. Qian, W. Jie., *Org. Chem. Front.***,** 2017, **4**, 2455-2458

[25] L. Dinparast, S. Hemmati, G. Zengin, A. Akbar Alizadeh,   M. B.   Bahadori, H. S. Kafil, S. Dastmalchi, *Chemistry Select, 2019, 4*, 9211–9215

[26] K. Taksande, D. S. Borse & Pradeep Lokhande, *An International   Journal for Rapid Communication of Synthetic Organic Chemistry,   2010, 40:15*, 2284-2290.

[27] Y. Yamaguchi, Naozumi Nishizono, Daisuke Kobayashi, Teruki   Yoshimura, Keiji Wada, Kazuaki Oda**,***Bioorganic & Medicinal   Chemistry Letters,***2017,** *27, 12,*2645-2649**.**

[28] V. K. Srivastav, M. Tiwari, X. Zhangand X-J. Yao, *Indian J. Pharm.   Sci.*, **2018**, 8(1), 18-117.

SYNTHESIS AND CHARACTERIZATION OF NANOPARTICLES OF B-D-LACTOSYL THIOCARBAMATES

Shankesh C Zyate and Poonam T Agrawal[*]
Department of Chemistry, Shri. R.L.T. College of Science, Akola

ABSTRACT

Antimicrobial activity address the crucial problem of increasing microbial resistance against antibiotics. The study includes the comparison of synthesized nanoparticles of Lactosyl thiocarbamates & Lactosyl thiocarbamides with its bulk. It appeared interesting to carry out the antimicrobial activity, which shows the improvement in Lactosyl nanoparticles than bulk one. The characterization of new thiocarbamates and biologically made nanoparticles has been carried out by usual chemical transformation, NMR, IR and Mass spectral studies and the characterization of prepared nanoparticles were done by antimicrobial activity, melting point difference, X-ray diffraction and U. V. spectroscopy.

Keywords— Thiocarbamates, thiocarbamides, nanoparticles, lactose

I. INTRODUCTION

In recent years, there has been a considerable interest in the field of Nanotechnology. As defined by size is naturally very broad, including field of science as diverse as surface science, organic chemistry, molecular biology, semiconductor physics, energy storage, micro fabrication, molecular engineering etc. Highly reactive nature of N-linked sugar isothiocyanate and isocyanate appears to promise its great applicability in the synthesis of thiocarbamates and carbamates which find the wide spread use in pharmaceutical industries. Has the potential to make a great impact on human health, ranging from prevention to diagnosis and treatment of disease. Antimicrobial activity tests confirms how effective a drug is. The application of nanotechnology in medicine Isothiocyanates and isocyanates are a group of very reactive chemical compounds. Once they have reacted, the resulting product is usually less harmful than the chemical itself. This chemical is used in the manufacture of carbamates and thiocarbamates. Due to high reactivity towards compounds containing active hydrogen atom isocyanates and isothiocyanates are one of the most versatile classes of functional groups. The high yields and lack of byproducts with this type of reaction have led to their commercial exploitation in the polymer field, agrochemicals and pharmaceuticals. Reactions with carbon nucleophiles provide a useful synthetic access to substituted amides and other derivatives.

Sugar isothiocyanates rank among the most versatile synthetic intermediates in carbohydrates chemistry1-3. They plays a vital role in the preparation of a broad series of functional groups such as thioamides4, isonitrile, carbodiimide and N-thiocarbonyl derivatives5-7 allowing, simultaneously, the covalent coupling of a quite unrestricted variety of structures to the saccharide part. More ever, isothiocyanates are important reagents in heterocyclic chemistry8-9 which may be exploited in the synthesis of nucleosides10 and other N-glycosyl11-12 structures. Dialdehyde starch nanoparticles are useful carrier for anticancer drug because of their small size, good thermal stability, low biological toxicity and slowly anticancer drug releasing to strengthen drug effect13.

II. EXPERIMENTAL

Determining the difference between melting point of compounds and their nanoparticles is one way to test if the nanoparticle is prepared or not. So the M.P. of compounds and their nanoparticles has been taken using melting point apparatus. The prepared Compounds and their nanoparticles have been screened for antimicrobial activity using Cup plate agar diffusion method. By measuring zone of inhibition in mm antimicrobial activity has been studied. By using DMSO as a solvent the concentration of compound were 1 mg/ ml. Amikacin (100 µg/ml) was used as a standard. Compounds were screened for antimicrobial activity against microbes (listed in table 2) in nutrient agar medium. H1 NMR data of the compounds were measured using CDCl3 solvent on 300 MHz frequency. And their chemical shift values are in (ppm) units using TMS as a reference. IR spectral data of the compounds were recorded on FTIR-RXI spectrophotometer. Confirmation of products and reaction progress carried out by TLC using Hexane : Ethyl acetate solvent system and identification of spots carried out by using iodine chamber, UV chamber and KMnO4 spray.

III. METHOD OF PREPERATION

Step 1 : preparation of Lactose Octabenzoate: 55 ml dry Pyridine and 55 ml dry Chloroform were taken in a 1 lit. tight cork glass bottle and cooled in an ice-salt bath. To this solution previously prepared cooled solution of 55 ml Benzoyl Chloride in 55 ml dry Chloroform was added with constant stirring. To this mixture 20 gm. of dry powder of Lactose was added in small instalments with constant stirring by maintaining the temperature

below 5 oC. After 24 hrs. mixture was washed several times with dil. Aq. Sulphuric acid, followed by aq. Sodium Bicarbonate and lastly with water. By using separating funnel Chloroform layer was separated which contains desired product. Product was triturated several times with petroleum ether until white powder obtained with M.P. 112 o C.

Step 2 : Synthesis of hepta-O-benzoyl-α-D Lactosyl Bromide

The fine powdered of lactose octabenzoate (10gm) was added to the brominating agent (4g Red Phosphorus + 40 ml Glacial Acetic acid + 15 ml molecular Bromine). Then flask was kept for 2 hrs at room temperature. Then 70 ml Chloroform was added to the reaction mixture followed by vigorous shaking. The resultant mixture was poured in an ice cold water to separate Chloroform layer. It was washed several times with aq. Sodium bicarbonate to remove excess of acetic acid followed by aq. Sodium metabisulphite to remove excess of bromine and finally 2-3 times with water. By using separating funnel the solution was removed and addition of petroleum ether results a solid mass (20 gm).

Step 3: Synthesis of hepta-O-benzoyl-β-D-lactosyl isothiocyanate: To a suspension of hepta-O-benzoyl-α-D Lactosyl bromide (15gm) in sodium, 60 ml dried xylene and 5g lead thiocyanate was added. The reaction mixture was refluxed for 3 hrs, gentle shaking. Solution was then cooled and liberated lead bromide was removed by filtration. The xylene filtrate was treated with petroleum ether with stirring, a white solid mass obtained. This solid was expected hepta-O-benzoyl-β-D-lactosyl isothiocyanate. M. P. 116-120 o C.

Step 4: Synthesis of N-lactosylated Thiocarbamates and : Reaction mixture of hepta-O-benzoyl-β-D-lactosyl isothiocyanate with various alcohols has been refluxed for 5 hrs. On cooling and mixing with water most of the alcohols gave a white granular solid was purified by Chloroform-Petroleum ether.

Step 5: Synthesis of N-lactosylated Thiocarbamides: Reaction of hepta-O-benzoyl-β-D-lactosyl isothiocyanate and various aryl amines has been carried out in boiling benzene for 3 hrs. The solvent benzene was distilled off and sticky mass was isolated as residue. Then triturated several times with petroleum ether was converted to granular solid. Crystallized from chloroform-ether.

Step 6 : Preparation of Nanoparticles (Biologically) : Small pieces of potato was boiled in little amount of water in a beaker for about 10 min. Filtered the semi hot solution through filter paper, remaining filtrate obtained called potato extract. 1 gm. of compound was dissolved in 2 ml of DMSO, clear solution was obtained. Then 2-3 drops of potato extract was added to the clear solution, suddenly white precipitate of nanoparticles was obtained.

IV. SCHEME
R1= a) ethyl b) methyl c) n-propyl d) isopropyl e) n-butyl f) t-butyl

R2= a) Phenyl b) o-tolyl c) m-tolyl d) p-tolyl e) o-Cl-phenyl f) m-Cl-phenyl g) p-Cl-phenyl

V. RESULT AND DISCUSSION

(Table 1)

Sr. No.	Alcohols	1-hepta-O-benzoyl-β-D-lactosyl-3-aryl thiocarbamates	Yield %	Melting point of Bulk °C	Melting point of Nanoparticles °C
1.	Ethyl	O-ethyl thiocarbamate	76	125-130	152-155
2.	Methyl	O-methyl thiocarbamate	74	143	144-149
3.	n-propyl	O-n-propyl thiocarbamate	75	158-160	1142-144
4.	Isopropyl	O-isopropyl thiocarbamate	78	132-137	143-145
5.	n-butyl	O-n-butyl thiocarbamate	63	128	159-161
6.	t-butyl	O-t-butyl thiocarbamate	67	145	167-170

(Table 2)

Sr. No.	Aryl amines	1-hepta-O-benzoyl-β-D-lactosyl-3-aryl thiocarbamides	Yield %	Melting point of Bulk °C	Melting point of Nanoparticles °C
1.	Aniline	-3-phenyl thiocarbamide	72	125-130	97-99
2.	o-toluidine	-3-o-tolyl thiocarbamide	76	143	122
3.	m-toluidine	-3-m-tolyl thiocarbamide	88	158-160	131-135

4.	p-toluidine	-3-p-tolyl thiocarbamide	78	132-137	107-110
5.	o-Cl-Aniline	-3-o-Cl-phenyl thiocarbamide	88	128	102-105
6.	m-Cl-Aniline	-3-m-Cl-phenyl thiocarbamide	84	145	128-131
7.	p-Cl-Aniline	-3-p-Cl-phenyl thiocarbamide	87	148-152	130-133

The characterization of compounds have been confirmed by IR spectroscopy which shows C=S, N-H, C-N, C=O, C-O stretching frequencies at different absorption bands. H1 NMR shows signal due to N-H proton at 8.06 ppm and Lactosyl protons at 5.58 – 3.79 ppm. and benzoyl protons at 6.8 – 3.9 ppm. The Characterization of nanoparticles has been carried out by UV visible spectroscopy. The band gap difference increases as the size of nanoparticles decreases. The decrease in melting point confirms the nanoparticles were prepared.

Antimicrobial activity (Thiocarbamates) (Table 3)

Antimicrobials	Bulk	Nanoparticles
E. coli	11 mm	15 mm
S. aureus	11 mm	14 mm
S. typhi	10 mm	14 mm
P. vulgaris	12 mm	15 mm
Amikacin	10 mm	17 mm
Clandamycine	12 mm	18 mm
DMSO	31 mm	24 mm

Antimicrobial activity (Thiocarbamides) (Table 4)

Antimicrobials	Bulk	Nanoparticles
E. coli	10 mm	14 mm
S. aureus	11 mm	16 mm
S. typhi	11mm	15 mm
P. vulgaris	11 mm	16 mm
Amikacin	10 mm	17 mm
Clandamycine	12 mm	16 mm
DMSO	32 mm	23 mm

*Including the well diameter of 8 mm. **Zone of inhibition in mm (15 or less) resistance, (16-20 mm) moderate and (> 20 mm) sensitive.

The prepared Compounds and their nanoparticles have been screened for antimicrobial activity using Cup plate agar diffusion method. By measuring zone of inhibition in mm antimicrobial activity has been studied. By using DMSO as a solvent the concentration of compound were 1 mg/ ml. Amikacin (100 µg/ml) was used as a standard. Compounds were screened for antimicrobial activity against microbes (listed in table 2) in nutrient agar medium. Zone of inhibition of nanoparticles were more than bulk, which confirms better antimicrobial activity of nanoparticles in comparison to bulk one.

VI. CONCLUSION
Nanoparticles shows better antimicrobial activity than bulk. The study includes the comparison of synthesized nanoparticles of Lactosyl thiocarbamates & Lactosyl thiocarbamides with its bulk. Data observed in the observation table shows that nanoparticles of both thiocarbamates and thiocarbamides have improved antimicrobial activity than the bulk one. Carbohydrate nanoparticles are beneficial for the medicinal purposes like anti-cancer, drug delivery system, recognition of antigens and many other pharmacological applications.

REFRENCES :
1. Ogura, H., Takahashi, H., Takeda, K., Sakaguchi, M., Nimura, N., & Sakai, M. (1975). Heterocycles., 3, 1129

2. Witczak, Z. J. (1986). Adv. Carbohyd. Chem. Biochem., 44, 91

3. De ,K. K., Shaiu, G. T. & Harmon, R. E. (1975). J. Carbohy. Nucleos Nucleot., 2, 171-176

4. Fernandez-bolanos, J. G., Zafra, E., Robina, I., & Fuentes, J. (1999). Carbohydr. Lett., 3, 239-246

5. Linkletter , B.A., & Bruice, T. C. (1998). Bioorg. Med. Chem. Lett., 8, 1285-1290

6. Avalos, M., Babiano, R. P.,Cintas, J. L., & Jimenez, J. C. (1993) Tetrahedron,49, 2676-2690

7. Arya , D.P., & T.C. Bruice. (1993). J. Am. Chem. Soc., 120, 6619-6620

8. Gasch, C., Pradera, M. A., Salameh, B. A. B., Molina, J. L., & J. Fuentes. (2000).Tetrahedron: Assymmetry,11, 2435

9. Pradera,M. A., Molina, J. L., & Fuentes, J. (1995). Tetrahedron, 51, 923

10. Fruentes, J., Molina, J. L., & Pradera, M. A. (1993). Tetrahedron: Assymmetry, 9, 2517-2532

11. Saleh, M. A. (2000). Sulfur Litt., 23(6), 265

12. Abdel-Megeed, M. F., Saleh, M. A., Aly ,Y. A., & Abdo, I. M. (1995). Nucleos. Nucleot. and Nucleic acids, 14, 1985

13. YU DanMi, XIAO SuYao, TONG ChunYi, CHEN Lin & LIU XuanMing. (2007). Chinese Science Bulletin, 52(21), 2913-2918.

14. Chopade, R. S., Bahekar, R. H., Khodekar, P. B., & Bhusari, K. P. (2002). Arch. Pharma. (Weinheim), 335 (8), 381.

15. Lalatsa, A., Barbu, E. (2016). Int. Rev. of Neurobiology., (130), 115-152.

16. El-Boubbou, K., Zhu , D. C., Vasileiou, C., Borhan , B., Prosperi, D., Li, W., Huang, X. (2010). J. Am. Chem. Soc., (132), 4490-4499.

17. Parry, A. L., Clemson, N.A., Ellis, J., Bernhard, S.S.R., Davis, B. G., Cameron, N. R. (2013). J. Am. Chem. Soc., (135), 9362-9365.

18. Lai, C. H., Lin, C. Y., Wu, H. T., Chan, H. S., Chuang, Y. J., Chen, C. T., Lin, C. C. (2010). Adv. Funct. Mater., (20), 3948-3958.

19. Biswas, S., Medina, S. H., Joseph, J., Barchi, Jr. (2015). Carbohydrate research., (405), 93-101.

20. Moskvin, M., Horak, D. (2016). Physiol., Res., 65(2), 43-51.

21. Angellier, H., Choisnard, L., Molina, B. S., Ozil, P., Dufresne, A. (2004). Biomacromolecules., (5), 1545-1551.

22. Aldao, D. C., Sarka, E., Ulbrich, P., Mensikova, E. (2018). Czech J. Food Sci., 36.

23. Li ,Yu Xin., Zhao, Wei Guang., Li, Zheng Ming., Wang, Su Hua., & Dong, Wei Li. (2006). Syn. Comm., 34(11), 1471-1477

24. Mote , S. P., & Deshmukh, S. P. (2011). Rasayan J. Chem., (4), 29-35.

SYNTHESIS AND CHARACTERIZATIONS OF SCHIFF BASES OF 4-N,N DIMETHYL AMINOBENZALDEHYDE WITH SUBSTITUTED 2-AMINOBENZOTHIAZOLE& THEIR ANTIBACTERIAL SCREENING

Shruti P. Ingole

Shri Shivaji Science College, Amravati, Maharashtra, India

ABSTRACT

A series of substituted 2-aminobenzothiazole were incorporated with 4-N,N dimethyl amino benzaldehydeunder acidic condition. The novel synthesized imine products have been elucidated by H1 NMR, IR and mass spectral data. The prepared compounds were screened for Antibacterial activity. In particular, chloro and Nitro substituted compounds showed the best activities in the series.

Key-words: Substituted 2-aminobenzothiazole, 4-N,N dimethyl aminobenzaldehyde, Schiff bases, Antibacterial Screening.

INTRODUCTION

Synthesis and antimicrobial activity of 2-aminobenzothiazole and its derivatives is reported [1]. Further, their other pharmacological activities such as anticancer, antiulcer, antihistaminic, anti-inflammatory activity and analgesic activities also reported [2-6]. It was envisaged that the compounds containing these moieties in their molecular frame work might show enhanced biological activity. Increasing physiological importance of oxygen donor organic compounds [7] and active role played by coordination certain metal ions to them [8] is of interest towards use in synthesizing and studying structural aspects of metal complexes with some oxygen, sulphur and nitrogen donor ligands [9]. The aromatic benzothiazole nucleus is associated with a variety of antihistamine activity [10], pharmacological actions [11] such as fungicidal [12] and leishmanicides activities [13]. The complexes of the ligand 2- amino acetate, 6-chloro benzothiazole with some transition metal ions have been studied [14]. In the present study we now report the synthesis of complexes of 4, 6-dinitrobenzothiazole-2-amine acetateand their study of magnetic properties for the wide range of applications.

MATERIALS AND METHODS

Synthesis of Schiffbase of Substituted 2-Aminobenzothiazole: A mixture of substituted 2-aminobenzothiazole (0.1 mol) and 4 - N,N Dimethyl aminobenzaldehyde (0.1 mol) and 2 to 3 drops of H_2SO_4 has been refluxed for 3 hrs. The resultant yellow precipitate is filtered and crystallized from ethanol. The steps in the synthesis of schiff base of substituted 2-aminoacetic benzothiazole are shown in

figure 1.

Substituted 2-Amoinobenzothiazole   4- N,NDimethyl aminobenzaldehyde

Reflux 3 - 4 Hrs| Conc. H₂SO₄

4-(N,N-(dimethylamino)benzylidene)-substituted 2-amino benzothiazole

R= -Cl, -Br, -CH₃, -NO₂, -F.
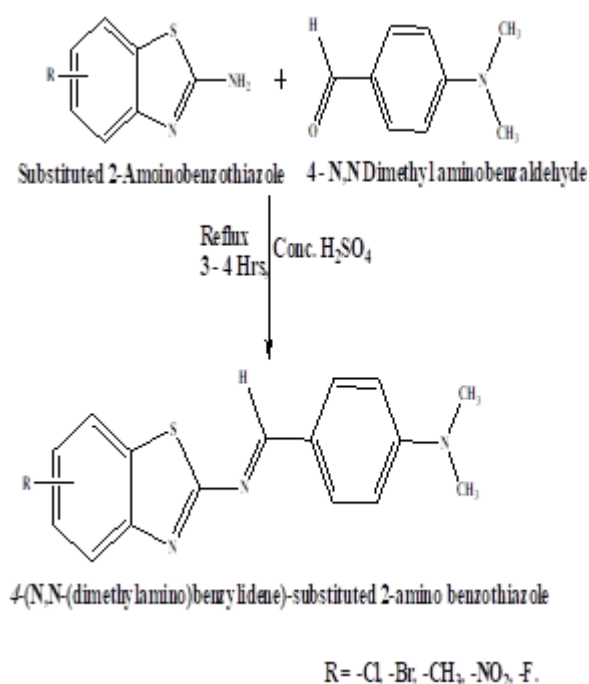
Instrumentation: FT-IR spectra in the range, 4000-200 cm^{-1}, were recorded on 8300 Shimadzu Spectrophotometer, UV-visible spectra were measured by using Shimadzu 160 spectrophotometer in the range 200-1000 nm. The magnetic susceptibility values of the prepared complexes were obtained at room temperature using Magnetic Susceptibility on Bruker Magnet B.M.6, The ^{1}H nuclear magnetic resonance spectra were recorded on a BRUKER ADVANCED II 400 MHz spectrometer in DMSO as a solvent, relative to the internal standard Tetramethylsilane (TMS). Melting points were recorded on a Tanco Laboratory melting point apparatus.

4-(N,N-(dimethylamino)benzylidene)-4,6-dinitro-2-amino benzothiazole (SB-1):

Solid, mp 195°C, **UV (λmax) in ethanol:** 258 nm, **(IR) υmax (KBr/cm-1):** 3375.66 (NH), 3181.24(Ar=C-H), 1538(C=N), 1244.85(CN), 1265.12 (C-S), 1387.75 and 1517.84 (NO$_2$). ^{1}**H-NMR (δ-ppm):** 3.46 (s, 2H, NH$_2$), 7.77 (d, aryl H, adjacent to sulphur), 8.88 (d, aryl H, adjacent to NO$_2$).

4-(N,N-(dimethylamino)benzylidene)-4,6-dichloro-2-aminobenzothiazole (SB-2):

Solid, mp 186°C, **UV (λmax) in ethanol:** 255 nm, **(IR) υmax (KBr/cm-1):** 3300.20 (NH), 3100.24(Ar=C-H), 1538(C=N), 1244.85(CN), 1256.12 (C-S),

^{1}**H-NMR (δ-ppm):** 3.46 (s, 2H, NH$_2$), 7.77 (d, aryl H, adjacent to sulphur), 8.88 (d, aryl H, adjacent to Cl).

4-(N,N-(dimethylamino)benzylidene)-4,6-dibromo-2-aminobenzothiazole(SB-3):

Solid, mp 200°C, **UV (λmax) in ethanol:** 258 nm, **(IR) υmax (KBr/cm-1):** 3375.66 (NH), 3181.24(Ar=C-H), 1538(C=N), 1244.85(CN), 1265.12 (C-S),

^{1}**H-NMR (δ-ppm):** 3.46 (s, 2H, NH$_2$), 7.77 (d, aryl H, adjacent to sulphur), 8.88 (d, aryl H, adjacent to Br).

4-(N,N-(dimethylamino)benzylidene)-4,6-dimethyl-2-aminobenzothiazole(SB-4):

Solid, mp 189°C, **UV (λmax) in ethanol:** 258 nm, **(IR) υmax (KBr/cm-1):** 3375.66 (NH), 3181.24(Ar=C-H), 1538(C=N), 1244.85(CN), 1265.12 (C-S),

^{1}**H-NMR (δ-ppm):** 3.46 (s, 2H, NH$_2$), 7.77 (d, aryl H, adjacent to sulphur), 8.88 (d, aryl H, adjacent to CH$_3$).

4-(N,N-(dimethylamino)benzylidene)-4,6-difluoro-2-aminobenzothiazole(SB-5):

Solid, mp 189°C, **UV (λmax) in ethanol:** 258 nm, **(IR) υmax (KBr/cm-1):** 3375.66 (NH), 3181.24(Ar=C-H), 1538(C=N), 1244.85(CN), 1265.12 (C-S).

^{1}**H-NMR (δ-ppm):** 3.46 (s, 2H, NH$_2$), 7.77 (d, aryl H, adjacent to sulphur), 8.88 (d, aryl H, adjacent to CH$_3$).

RESULTS AND DISCUSSION

Infra-red spectroscopy: The above given data of FT-IR spectrum of the ligand, shows a characteristic stretching absorption bands at 3375.66 cm^{-1} (NH), 3181.24 Cm^{-1} (Ar=C-H), 1538 Cm^{-1} (C=N), 1244.85 Cm^{-1} (C-N), 1265.12 cm^{-1} (C-S). The reaction between this ligand with Ni (II), Cu (II), Zn (II) and Cd (II) gave different types of complexes. In the free ligand, the bands at 1730 and 1057 cm^{-1} were assigned to the stretching of C=O and C-O of the hydroxyl in the carboxyl ate group. On complexation these bands were shifted to a lower frequency region. This shift is probably due to the complexation of the metal to the ligand through oxygen of the carbonyl group, the disappearance of the hydrogen from hydroxyl group on complexation indicate the complexation is through the oxygen atom. Stretching of metal-oxygen bands of the complexes appeared in low frequency region (400-600) cm^{-1}.

NMR spectroscopy: The 1H NMR data of the 4, 6-dinitrobenzothiazole-2-amine; 4, 6-dinitrobenzothiazole-2-amine-acetic acid (LH) and its complexes were soluble in DMSO. The spectral data gave support for the interpretation of composition of the complexes, as explain above. The changes observed are the evidences of complexation had happened because the chemical shift of a compound is heavily depended on the environment of proton. The 1HNMR spectrum of the complexes confirmed the disappearance of OH signal at 11.69 ppm in

the free ligand. The δ 7.24-8.92 ppm resonance signal protons of the aromatic ring shifted to the higher field upon complexation, while the proton of the -CH2 aliphatic group shifted to higher field also. It is most likely that shift is due to the decrease of electron density at carbon atoms when oxygen is bonded to metal ion.

Antibacterial activity: The titled compounds were screened for their antibacterial activity using disc diffusion method. The bacterial organisms used included both gram positive and gram negative strains like Staphylococcus aureus, Escherichia coli, Salmonella enteric Serparatyphi, Klebsiella Pneumonia and Pseudomonsaeruginosa.

For antibacterial susceptibility testing of title compounds, the sterile disc of 6 mm diameter (SD067, Hi-Media, Mumbai) was loaded with 20µl of title compound solution (1000 µg/ml) in DMF. The discs were then placed at centre on the Mueller-Hinton agar seeded with bacterial inoculums approximately 106 CFU/ ml, incubated at 37° C for 24 hrs and growth inhibition zone formed around disc was measured. Test was done in triplicate and mean value was considered as inhibition zone. Solvents were used as controls and showed no inhibitions in preliminary studies. All the synthesized complexes exhibited moderate to good activity against the test organisms.

Table: Antimicrobial Activity

Compound	Gram positive bacteria	Gram negative bacteria			
	Staphylococcus aureus	Salmonella entericaSerparaTyphi	Escherichia Coli	Klebsiella Pneumonia	Pseudomons aeruginosa
(SB-1)	++	+++	++	+	++
(SB-2)	++	++	+	++	+
(SB-3)	+	-	++	+	+
(SB-4)	+	+	+	+	-
(SB-5)	++	+	++	+	++

+++ = Zone size 16-22 mm; ++ = Zone size 9-15 mm; + = Zone size 6-8 mm;

— = No inhibition.

CONCLUSION:

The compounds4-(N,N-(dimethylamino)benzylidene)-4,6-substituted-2-amino benzothiazolewere successfully synthesized by condensation method and confirmation of formation of compounds were done by 1H NMR, IR, UV-Vis & Mass. All the compounds showed good yield. The compoundswere further proceeds for Antibacterial activity in which all the compounds showed good results against gram positive and gram negative bacteria especially nitro and chloro substituted schiffbases showed a remarkable activities.

REFERENCES:

1. G. M. Sreenivas, E. Jayachandran and B. Shivkumar, *IndianJ.Heterocyclic Chem.*, 14 **, 2004**, 89.

2. F. Russo, G. Romeo, N.A Santagati, A. Caruso, V. Cutuli, D.Amore, *European Journal of Medicinal Chemistry*, 29**, 1994**,564.

3. Katsura, Y. Inove,Y. Nishino,S. Tomoi,M. and Takashgi,H. *Chem.pharm. Bull   (Tokyo),*4,   **1993**, 1818.

4. Kuhler, T. C, Swanson,M, Scherbuchin,V, Larsson,H, Mellgard,B, and   Sjostrom, J.E, *Journal of Medicinal Chemistry*, 41, **1998** ,1777.

5. S.N. Sawney, S.P. Singh, and O.P. Bansel, ,*Indian J.Chemistry,* 44B , **2001**, 125.

6. Remers, Gibs G.J, and . M.J Weiss, „*J Heterocycl. Chem.,* 6**, 1969**, 835.

HYDROGEN PRODUCTION USING WATER SPLITTING METHOD WITH MOLYBDENUM DIOXIDE: SHORT REVIEW

Suchitra N. Sapaka and Anamika V. Kadam[*]

Department of Physics, The Institute of science, Dr. Homi Bhabha State University, Fort, Mumbai India

ABSTRACT

In the last few years, hydrogen fuel has gained more importance due to its environmentally friendly nature. Hydrogen production from renewable sources is more focused by researchers for a carbon dioxide-free environment. To produce hydrogen, water splitting is an effective method and it can be done by Solar based methods like Electrolysis, Photo electrochemical method, some Biological methods, etc. An effective photo catalyst is needed for all these solar-based water-splitting methods. This short review combined some recent water splitting experiments. The main focus of this article is to split water using Molybdenum Dioxide with some other additives as a catalyst.

Keywords— Molybdenum Dioxide, Solar based water splitting methods, Hydrogen evolution, Oxygen evolution.

INTRODUCTION

Energy is one of the most important aspects of modern life for sustained development. Energy sources are divided into two types: renewable and non-renewable sources. For some centuries we are using non-renewable sources and became highly dependent on them. This high dependency leads them to depletion. Also, Climate change is a serious issue of concern and for the long-term existence of life on earth, we need to think more about clean and renewable energy sources for the future. For some decade's world is using renewable energy sources and in past few years, it gained more significance due to global warming. The population of the world is assumed to be tripled by the year 2030[1]. The report issued by the international energy agency states that the energy demands of the world will be twofold by the year 2030[2].

Hydrogen fuel is a clean source of energy and it is one of the best alternatives to fossil fuels to fulfill the high demand for energy in the future. Previously, several studies focused on hydrogen fuel as the most significant solution for a better environment and sustainability [3, 4]. Hydrogen fuel has many advantages some of them can be listed as high energy conversion efficiencies, abundance, production from water with no emissions, different forms of storage (e.g. gaseous, liquid, or in together with metal hydrides), long-distance transportation, ease of conversion to other forms of energy, etc. But the main disadvantage is, most of the hydrogen production methods are with high production costs [4, 5]. Several methods are available to produce hydrogen, some of them are Natural Gas Reforming, Bio-Derived Liquids Reforming, Coal and Biomass Gasification, Thermochemical, Water Electrolysis, Biological, Photo-electrochemical, etc. Among them, Natural gas steam reforming is the most commonly used process for hydrogen production that results in heavy greenhouse gas emissions. Around 50% of the global hydrogen demand is met by natural gas steam reforming, 30% comes from oil reforming, 18% from coal gasification, 3.9% from water electrolysis, and 0.1% from other sources [7]

Fig. 1 Distribution of global Hydrogen Energy demand from various methods.

Hydrogen production from clean and abundant sources with environmentally benign methods is called "green hydrogen production" and is very important to avoid the harmful impacts of fossil fuel utilization on human health, climate, and on the environment [4, 8, 9]. Water splitting is one of the best renewable ways to produce hydrogen because water is abundantly available on our Earth. Solar energy has been considered promising since it is independent of location in comparison to hydropower and wind power. The combination of abundant sunlight and water resources provides a reasonable scope for hydrogen generation by solar water splitting [10].

Photobiological water splitting, photocatalytic water splitting, and thermochemical water splitting are the simplest Solar based hydrogen production approaches but, require large solar concentrators making this method highly expensive and less preferred [11]. Biophotolysis is depending on the method of microorganism and it is divided into water biophotolysis and organic biophotolysis [12]. Water biophotolysis is superior to organic biophotolysis regarding CO2 emission [13], toxic effects of enzymes along with yield of hydrogen, and limitations of scaling up the process [14].

Overall water splitting can be achieved by electrochemical, photochemical, photo electrochemical as well as thermochemical water splitting by using catalysts [15]. Electrochemical hydrogen evolution is efficient and can produce hydrogen or oxygen in high purity ($\approx$ 100%). Water splitting by electrolysis needs considerable effort in developing electrodes and electrolytes with low-cost catalysts and long-term durability. The electrodes include cathodes for the hydrogen evolution reaction (HER) and anodes for the oxygen evolution reaction (OER) [15, 16]. Traditional water electrolysis is usually carried out under either acidic conditions with a proton exchange membrane (PEM) or in alkaline media with a diaphragm. Under standard conditions, a thermodynamic potential of 1.23V is required to drive electrochemical water splitting, which corresponds to an energy input of $\Delta G = 237.1$ kJ mol^{-1} .[36].

In Acidic solution:

Two half reactions are-

$2H_2O \rightarrow O_2 + 4H^+ + 4e^-$ $\qquad$ $E^0 = 1.23$ V

$4H^+ + 4e^- \rightarrow H_2$ $\qquad$ $E^0 = 0$ V

As a result: $2H_2O \rightarrow 2O_2 + 2H_2$ $\qquad$ $E^0 = 1.23$ V

And In Alkline solution:

Two half reactions are-

$4OH^- \rightarrow O_2 + 2H_2O + 4e^-$ $\qquad$ $E^0 = 0.40$V

$2H_2O + 4e^- \rightarrow 2H_2O + 4OH^-$ $\qquad$ $E^0 = 0.83$V

As a result: $2H_2O \rightarrow 2O_2 + 2H_2$ $E^0 = 1.23$ V
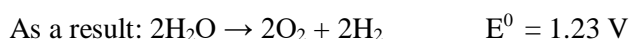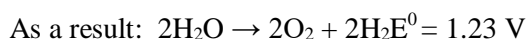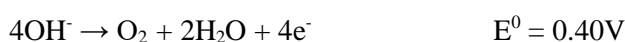
Where, E^0 is Thermodynamic Potential vs. Normal $\quad$ Hydrogen Electrode.
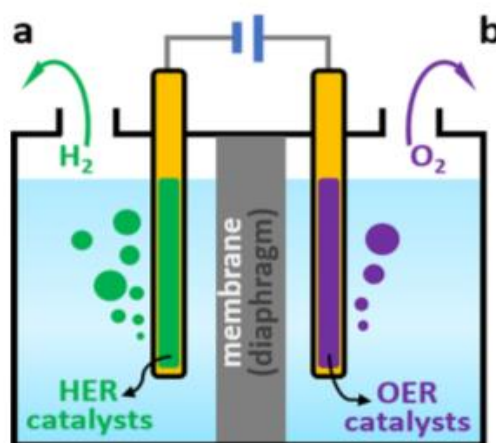
. Fig. 2 Scheme of traditional water electrolyzers for Hydrogen and Oxygen evolution [36].

ROLE OF NANOMATERIALS IN WATER SPLITTING
An active catalyst is required to achieve the efficient hydrogen evolution reaction (HER) and high conversion efficiency. Different nanomaterials have been studied as a photocatalyst for Electrolysis and Photoelectrochemical water splitting methods. Nanoparticles are the building block for photocatalyst as their mass and charge transfer is fast and they exhibit increased light absorption and reduced light scattering [17, 18]. The bandgap of nanomaterials can be tuned to absorb in a particular wavelength by varying size and, in principle, cover the whole solar spectrum. The electronic band structure can be controlled by doping. Bottom-up growth approaches, which use smaller components to produce larger and more complex structures which allow

scalable synthesis of single-crystal nanostructures on flexible substrates under mild conditions, leading to lightweight and low cost. The electrode coated with nanoparticles suspended/dispersed in the reaction medium (water) shows improved photocatalytic activities [19].

.NANOMATERIALS FOR WATER SPLITTING

TiO2 has potentially been used in water separation as a photocatalyst since the 1970s due to its low cost, abundance, and stability on Earth. But the bulk TiO2 has a large bandgap (3.03-3.18 eV) so it shows weak performance in solar light absorption [20, 21]. ZnO nanomaterials have been extensively discovered in the water segment with a bandgap of ~ 3.3 eV. But the photocatalytic efficiency of ZnO is low because its band structure is similar to that of TiO2, showing poor visible light absorption and low photocatalytic quantum efficiency [22, 23]. Semiconductor quantum dots such as CdS [21], CdSe, CdTe [26], Ag2S, have some unique properties for water splitting such as tunable absorption properties, high stability, suitable for solar spectrum and, multiple bandgap sensitizations [24]. Hematite (a-Fe2O3) has a bandgap of ~2.1 eV, which facilitates it to absorb about 40% of solar light [16].WO3 nanomaterials also show good performance in PEC water splitting with a bandgap ~2.5-2.7eV [26, 27]. Bismuth vanadate (BiVO4) has bandgap 2.4-2.6 eV [22]. Earth-abundant transition-metal dichalcogenides (TMDs) with general formula MX2 (M = transition metal; X = chalcogen) including two-dimensional (2D) layered materials, such as MoS2 , WS2 , MoSe2 , WSe2 , TaS2 and TiS2 etc., and pyrite phase structured TMDs (CoSe2 , CoS2 , NiS2 , NiSe2 , FeS2 and so on) are being developed at rapid pace for water splitting [19]. Platinum is one of the most efficient electrocatalysts for hydrogen evolution, but it is not suitable at a large scale, due to its high cost and scarcity [28-30].

MOLYBDENUM DIOXIDE WITH ADDITIVES FOR WATER SPLITTING

Molybdenum dioxide (MoO2) has recently been tested as a good material for water splitting. Nanometric MoO2 has attracted technical interest due to its interesting physicochemical properties [32]. It also has important properties such as energy storage, soft magnetic and optical materials [31]. The MoO2 film is highly absorbent and shows a direct band-to-band transition where the bandgap energy (e.g.) depends on the thickness of the film and is in the range of 2.38-2.53 eV. Both its amorphous appearance and direct bandgap with high absorption coefficient make MoO2 film an ideal candidate as an electrode for photovoltaic and photoelectrochemical solar cells [31].

Vivek Ramakrishnan et al. in 2018, presented, in situ growth of metallic MoO2 films on fluorine-doped tin oxide (FTO) and MoO2 powder in a solution that was achieved simultaneously by a simple hydrothermal process employing citric acid as the surfactant. H-MoO2 film/FTO displays a low on-set overpotential of 72 mV with a Tafel slope of 84.1 mV dec^{-1}, and the powder form exhibits an onset overpotential of 46 mV with a Tafel slope of 71.6 mV dec^{-1}. They observed the film on FTO was disc-shaped nanostructures, whereas the powder form contained microspheres formed by disc-shaped NSs. Interestingly, both FTO and solution-phase MoO 2 NSs were devoid of any other polymorphic forms [33]. Weijun Ye et.al prepared sub-5 nm MoO2 /graphene composites by the one-step hydrothermal method in 2019. They uses the combined action of ascorbic acid and graphene to achieve an ultra-small scale through a simple, efficient and environmentally friendly one-step hydrothermal method. For phase structure characterization they used X-ray diffraction, transmission electron microscopy, and energy dispersive spectrometer. The report concluded that ascorbic acid could reduce molybdate ions to MoO2, while graphene could prevent the agglomeration of nanocrystals. Galvanostatic charge-discharge cycling, cyclic voltammetry, and electrochemical impedance spectroscopy were used. The initial reversible specific capacity was 1072.8 mAh·g^{-1} with coulombic efficiency of 65.4% and remained 579.6 mAh·g $^{-1}$ after 100 cycles. The combination of sub-5 nm MoO2 particles and graphene effectively improved the electron/ion transport and buffered the volume expansion of electrodes [34]. In 2020, Osama Rabi et.al published a review on the synthesis of molybdenum carbide and its hybrids as catalysts for electrochemical water splitting. He reported recent research progress on the Mo2C for HER mechanism. Transition metals carbides are formed by inserting carbon atoms in the lattice of the transition atoms. They discussed the application of Mo2C related to its activity, durability, activation, and deactivation mechanism of the catalyst. They concluded the physicochemical properties of Mo2C and its hybrids can be enhanced by optimizing the synthesis route and carbon precursor that affects the size, shape, surface area, crystal structure, and surface state, higher surface area Mo2C with good crystal structure can be obtained through the solid-state reaction method. The comparison of pure Mo2C with metal loaded Mo2C, showed that the lower temperature activity and stability were increased by loading another transition metal on molybdenum carbide, (i.e carbon-based materials like graphene and materials like nitrogen-doped Mo2C have shown significant results for HER mechanism [35].

Ideal band gap of semiconducting material for water splitting is 1.23eV. Molybdenum Dioxide has band gap in the range of 2.38-2.53 eV and it depends on the thickness of the film. For electrochemical water activation the

hydrogen-annealed MoO2 is good hydrogen evolution reaction (HER) catalyst with good stability. HER catalytic activity also the onset potential, current density and Tafel slope of MoO2 nanostructures are improved by hydrogen annealing. In the experiment of MoO2 with graphene, the combination of substitute of 5 nm Molybdenum Dioxide particles and graphene effectively improved the electron/ion transport and bufferd the volume expansion of electrodes. It is reported by many researchers that the Mo2Cexhibits higher durability and high active sites also producing hydrogen at 20mA cm^{-2} for almost 20 to 30 h. Molybdenum Dioxide with additives shows good electrocatalytic performance to split the water.

Water splitting is one of the best way to store renewable enrgy. Presently, we have some inexpensive semicoconducting materials as a good catalysts to split water but they have stability and durability limitations. This study presented review of some recent water splitting experiments for hydrogen and oxygen evolution. In future, for more stability and durability, more combinations of these additives with MoO2 will be investigated.

CONCLUSIONS
Solar based water splitting methods are the best ways to split water into hydrogen and oxygen. For that we need semiconducting materials with some fascinating characteristics. Ideally, we need catalyst that can show a good accomplishment of absorption of light, separation of the photo-generated charge carriers, it must be highly stable. Molybdenum is earth abundant transition metal and its oxide, Molybdenum Dioxide is recently investigated as a good catalyst for solar based water splitting application. It is inexpensive as compared to Platinum. By adding some additives with Molybdenum Dioxide we can improve it's electrocatalytic performance.

REFERENCES
[1] Sarah Farrukh, Xianfeng Fan, Kiran Mustafa, Arshad Hussain, Muhammad Ayoub, Mohammad Younas. Nanotechnology and the Generation of Sustainable Hydrogen. ISBN 978-3-030-60402-8 (eBook), Springer Nature Switzerland AG 2021.

[2] Eia US, Monthly energy review, 2017.

[3] Dincer Ibrahim ; Environmental and sustainability aspects of hydrogen and fuel cell systems ; International Journal of Energy Research ,Vol 31,2007, Pg. 29-55.

[4] Ibrahim Dincer, Canan Acar; Review and evaluation of hydrogen production methods for better sustainability; International Journal of Hydrogen Energy; Vol 40, 2015, Pg. 11094-11111, ISSN 0360-3199.

[5] Acar C, Dincer I.; Comparative assessment of hydrogen production methods from renewable and non-renewable sources; International Journal of Hydrogen Energy; Vol 39, 2014 , Pg1-12.

[6] FreedomCAR and Fuel Partnership. Report: hydrogen production overview of technology options.2009.

Website:http://www.energetics.com/resourcecenter/products/ communication/Documents/hydrogen-productionbrochure. pdf.

[7] Muradov NZ, Veziroglu TN. From hydrocarbon to hydrogen- carbon to hydrogen economy.International Journal of Hydrogen Energy; Vol 30, 2005, Pg 225-237, ISSN 0360-3199.

[8] Levin DB, Chahine R.; Challenges for renewable hydrogen production from biomass. International Journal of Hydrogen Energy; Vol 35, 2010, Pg 4962-9.

[9] Awad AH, Veziroglu TN.; Hydrogen vs. synthetic fossil fuels; International Journal of Hydrogen Energy, Vol 9, 1984, Pg 355-66.

[10] N.-L. Wu, M.-S. Lee; Enhanced TiO2 photocatalysis by Cu in hydrogen production from aqueous methanol solution; Int. J. Hydrog. Energy , Vol 29, 2004, Pg 1601–1605.

[11] A. Steinfeld, Int. J. Hydrog; Int. J. of Hydrogen Energy , Vol 27, 2002, Pg 611–619.

[12] I. Akkerman, M. Janssen, J. Rocha, R.H. Wijffels, Int. J. Hydrog. Energy 27 (2002) 1195–1208.

[13] D. Das, T.N. Veziroglu, Int. J. Hydrog. Energy 33 (2008) 6046–6057.

[14] Y. Guan, M. Deng, X. Yu, W. Zhang, Biochem. Eng. J. 19 (2004) 69–73.

[15] S. Licht; Thermochemical solar hydrogen generation; Chemical communication, 2005, Pg 4635–4646.

[16] Uttam Gupta, C.N.R. Rao; Hydrogen generation by water splitting using MoS2 and other transition metal dichalcogenide; Nano Energy, Vol 41, 2017, Pg 49-65.

[17] Josny Joy, Jinu Mathew, Soney C. George. Nanomaterials for Photoelectrochemical Water Splitting-Review;International Journal of Hydrogen Energy, Vol 43,2018, Pg 4804 -4817.

[18] Zhong Y, Ueno K, Mori Y, Shi X, Oshikiri T, Murakoshi K. ; Plasmon-assisted water splitting using two sides of the same SrTiO 3 single-crystal substrate: conversion of visible light to chemical energy. Angew Chemie Int Ed , Vol 53, 2014, 10350-4.

[19] Zhang JZ; Metal oxide nanomaterials for solar hydrogen generation from photoelectrochemical water splitting; MRS Bull, Vol 36, 2011, Pg 48-55.

[20] Hakon Eidsvåg, Said Bentouba, Ponniah Vajeeston, Shivatharsiny Yohi and Dhayalan Velauthapillai. TiO2 as a Photocatalyst forWater Splitting—An Experimental and Theoretical Review. Molecules, MDPI,Vol 26, 2021, Pg 1687.

[21] Isimjan TT, Rohani S, Ray AK; Photoelectrochemical Water Splitting for Hydrogen Generation on Highly Ordered TiO_2 Nanotubes Fabricated by Using Ti As Cathode. International Journal of Hydrogen Energy, Vol.37, 2012, Pg 1.

[22] Zhang J, Zhu W, Liu X.; Stable Hydrogen Generation from Vermiculite Sensitized By Cds Quantum Dot Photocatalytic Splitting of Water under Visible-Light Irradiation; Dalton Trans, Vol 43, 2014, Pg 9296-302.

[23] Dong Y, Wu R, Jiang P, Wang G, Chen Y, Wu X.; Efficient Photoelectrochemical Hydrogen Generation from Water using a Robust Photocathode formed By Cdte QDs and Nickel Ion; ACS Sustain Chem Eng, Vol 3, Pg 2429e34.

[24] Xu L, Ya L, Jinzhan S, Mingtao L, Liejin G. Facile Preparation of Bivo4 Nanoparticle Film by Electrostatic Spray Pyrolysis for Photoelectrochemical Water Splitting. Hydrogen Energy, Vol 40(38), 2015; Pg 12964-72.

[25] Olivier M, Dimitrios R, Leonid S, Tom. a R, Gustav P, Panagiotis L.; Production of Hydrogen by Water Splitting in a Photoelectrochemical Cell Using a Bivo4/Tio2 Layered Photoanode. Electrochem Acta, Vol 251, 2017, 244-249.

[26] Wolcott A, Smith WA, Kuykendall TR, Zhao Y, Zhang. Photoelectrochemical Study of Nanostructured ZnO ThinFilms for Hydrogen Generation from Water Splitting. AdvanceFunction Mater 2009;19:1849e56.

[27] Zhang X, Liu Y, Kang Z. 3D Branched ZnO Nanowire Arrays Decorated with Plasmonic Au Nanoparticles for High Performance Photoelectrochemical Water Splitting. ACS Appl Mater Interfaces 2014;6:4480e9.

[28] Fengmei Wang, Tofik Ahmed Shifa, Xueying Zhan, Yun Huang, Kaili Liu, Zhongzhou Cheng, Chao Jiang and Jun He; Recent advances in transition-metal dichalcogenide based nanomaterials for water splitting; Nanoscale , November 2015, DOI: 10.1039/c5nr06718a.

[29] J. Li, et al.; In situ synthesis of molybdenum carbide/N-doped carbon hybrids as an efficient hydrogen-evolution electrocatalyst, RSC Adv. 8 (31) (2018) 17202–17208.

[30] M.J. Torres, et al., Electrocatalytic hydrogenation of cinnamaldehyde in a PEM cell: the role of sodium hydroxide and platinum loading, Mol. Catal. 492 (2020) 110936.

[31] Nijolė Dukstiene & Dovile Sinkeviciute. Photoelectrochemical Properties of MoO_2 Thin Films. Journal of Solid State Electrochemistry. 2013. DOI: 10.1007/s10008-012-1985-z.

[32] Oscar Marin-Flores, Su Ha. Activity and Stability Studies Of MoO2 Catalyst for the Partial Oxidation of Gasoline. Applied Catalysis a General. 2009. 352(1-2):124-132 DOI:10.1016/j.apcata.2008.09.036.

[33] Vivek Ramakrishnan, C. Alex, Aruna N. Nair, and Neena S. John; Designing Metallic MoO 2 Nanostructures on Rigid Substrates for Electrochemical Water Activation; Chemistry A European Journal, Vol 24 2018, Pg 1 – 10.

[34] Weijun Ye, Pinjie Zhang, Liwei Su 1, Lianbang Wang; One-Step Synthesis and Lithium Storage Performance of Sub-5-nm MoO 2 -Graphene Nanocomposites; Advances in Material Chemistry, Vol 7(4), 2019, Pg 53-60.

[35] Osama Rabi, Erum Pervaiz, Rubab Zahra, Maryum Ali, M. Bilal Khan Niazi; An inclusive review on the synthesis of molybdenum carbide and its hybrids as catalyst for electrochemical water splitting; Molecular Catalysis, Vol 494, 2020, Pg 111116.

[36] Bo You, Yujie Sun; Innovative Strategies for Electrocatalytic Water Splitting; Account of Chemical Research, Vol 51,7, 2018, Pg 1571–1580.

PREPARATION AND STRCUTURAL STUDIES OF SOME BIS POLYMERIC COMPLEXES

Vaishali P. Meshram

Department of Chemistry, Dharampth M. P. Deo Memorial Science College, RTM Nagpur University, Nagpur, Maharashtra, India

ABSTRACT

Synthesis of inorganic polymer is an emerging field that covers a wide range of disciplines including the frontiers of chemistry, materials, medicine, electronics, optics sensors, information storage, energy conversion, environmental protection aerospace and many more. Chelate polymers have important applications in medical sciences like controlled drug delivery, artificial organs and protein synthesis. Some polymers can be made to be electrically conductive and offer potential for the semiconductor industry and as lightweight electrodes and electrolytes for batteries for automotive and aerospace applications. Newly developed polymers exhibit unusual optical properties that have attracted significant interest from the defense industries. Besides the synthesis of chelate polymers and examination of their thermal stability, present work describes structural characterization of these chelate polymers on the basis of elemental analyses infrared and reflectance spectra, magnetic and thermal studies. Since polymeric chelates are thermally resistant and have a large number of practical applications. Recently some chelate polymers have been synthesized, characterized and their thermal stability has been studied. Ligands of hydroxamic acid with adipic acid, azelaic acid, succinic acid, sebasic acid and subaric acid have been prepared in benzene medium by condensation process Now a day's proton NMR technique can be used for determination of stereochemical structure and conformational analysis of polymer compounds. The chemical shift in NMR spectrum, indicates that what type of hydrogen atoms are present e.g., methylene, methyl groups, olefins, ethers, esters and aromatic compounds. 2D-NMR methods have been used as a powerful and reliable techniques for determination of compositional and configurationally structure of co-ordination polymer. Polyvinyl pyridine and its copolymers have important applications as polyelectrolyte, polymer regents and in electrical applications. These ligands have been synthesized and characterized by various instrumental techniques.
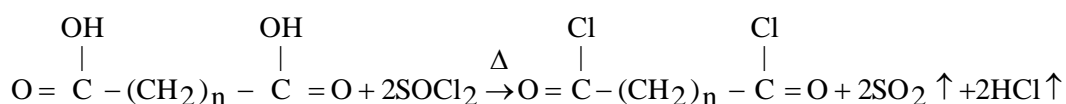
Keywords –complexes, polymeric ligands, IR studies, spectral studies.

EXPERIMENTAL

Chemicals: All the chemicals used were AR grade (Merck). The solvents used were doubled distilled before used.

Instrumentions: ^{1}H-NMR (CDCl$_3$, DMSO-d$_6$) spectra were recorded on Bruker model DRX-30 NMR Spectrophotometer using TMS as internal reference (δ ppm)Carbon, Hydrogen and Nitrogen contents were analyzed on an EA 1108 Carlo Erba Elemental analyzer instrument at CDRI Lucknow. FTIR spectra were recorded on a Bruker IFS 66V Germany, spectrometer using the KBr technique at Regional Sophisticated Instrumentation Center, IIT Chennai. Reflectance spectra of the chelate polymers in solid state were recorded on a single beam Karl-Zeiss Jena, specord M-400 spectrophotometer, finely powdered barium sulphate was used as a reference material in the studies of reflectance spectra. Magnetic susceptibility of chelate polymers was determined by the Gouy's method at room temperature using mercury tetrathiocyanatocobaltate (II) as standard. The non-isothermal measurement of Mn (II), Co (II), Ni (II) and Zn (II) were carried out using a TGS-2 thermogravimetric analyzer along with a TADS computer system at the Regional Sophisticated Instrumental Center, Nagpur University, Nagpur. The thermocouple used was Pt-Pt-Rh with a temperature range of 20-1000^{0}C, 12mg sample was taken and the heating rate 15^{0}C/min was employed. The thermal analyses were carried out in air atmosphere and mass loss was recorded continuously on the recorder.

Preparation of dichloride of adipic, azelaic, succinic, sebasic and subaric acid: A quantity of (0.1m mol) dry acid and (0.25m mol) double distilled thionyl chloride was taken in 100ml dry round-bottomed flask fitted with water condenser provided with guard tube containing unhydrous calcium chloride. Flask was heated on a water bath for about 2-3 hours, till clear solution was obtained. The reaction mixture was then refluxed under reduced pressure for 30 min. to remove sulphur dioxide, hydrogen chloride and unreacted thionyl chloride.

$$O=\overset{\overset{\displaystyle OH}{|}}{C}-(CH_2)_n-\overset{\overset{\displaystyle OH}{|}}{C}=O+2SOCl_2 \xrightarrow{\Delta} O=\overset{\overset{\displaystyle Cl}{|}}{C}-(CH_2)_n-\overset{\overset{\displaystyle Cl}{|}}{C}=O+2SO_2\uparrow+2HCl\uparrow$$

(1) *n=4* for adipic acid (2) *n=7* for azelaic acid (3) *n=2* for succinic acid (4) *n=8* for sebasic acid (5) *n=6* for subaric acid.

Preparation of ligand: In present investigation, a modified method Priyadarshini and Tandon[6] based on Schotten Baumann reaction, was used for the preparation of hydroxamic acid. In this procedure hydroxylamine hydrochloride and vacuum distilled acid chloride in stoichiometric ratio were reacted at low temperature 0^0C or lower in diethylether medium containing aqueous suspension of sodium bicarbonate. Hydroxamic acid was prepared by the reaction of acid dichloride with excess of hydroxylamine hydrochloride in aqueous ethanol medium containing suspension of sodium bicarbonate, (0.25M) hydroxylamine hydrochloride A.R. grade, ethanol (50 ml) and sodium bicarbonate (0.5 M) and distilled water (25 ml) were placed in 500 ml beaker and acid dichloride was added (0.1 M) dissolved in 100 ml diethyl ether by dropping funnel during a period of 45 minutes with constant stirring. Mechanical stirrer was used for this. The stirring was further continued for 15 minutes. A granular solid mass was separated which was filtered and triturated with saturated solution of sodium bicarbonate in a porcelain mortar to remove any acidic impurities present and was then filtered and re-crystallized out in ethanol: DMF mixture. This ligand is reported first time in the present work and hence characterized by elemental and infrared spectral analyses[1-4]. The reaction of ligand formation has shown in Fig.1
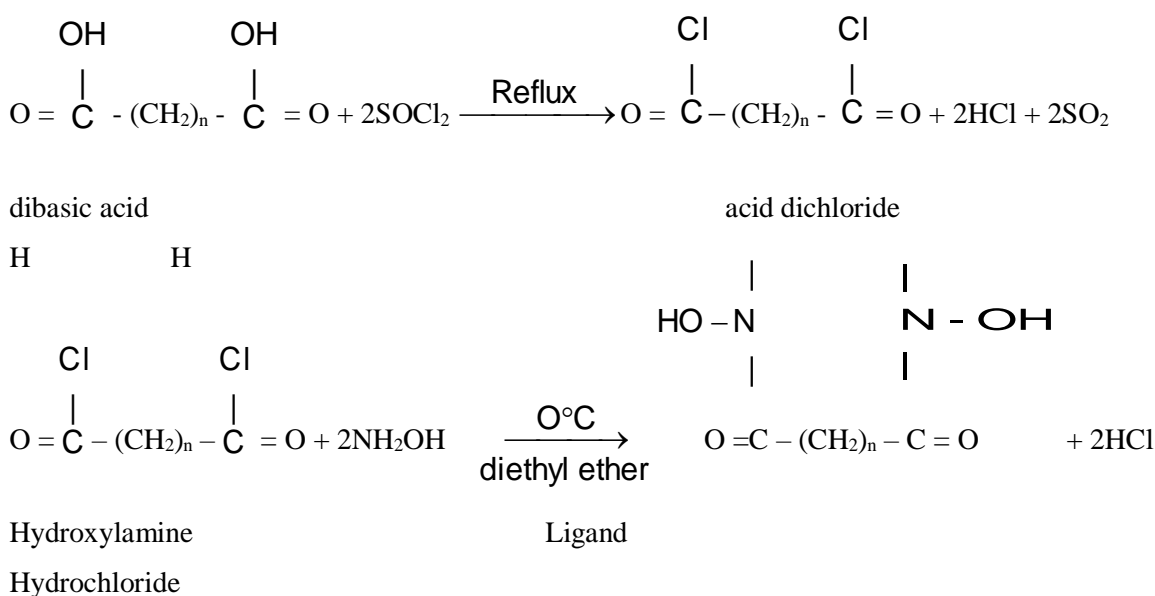

dibasic acid

acid dichloride

Hydroxylamine
Hydrochloride

Ligand

Fig. 1 - Synthesis of hydroxamic acid (ABHA)

Synthesis of chelate polymers of ligand

Chelate Polymers of with Mn (II), Co (II), Ni (II) and Zn (II) have been prepared by dissolving metal acetate (0.01M) separately in minimum amount of DMF and was added to a solution of hydroxamic acid (0.01 M) in (25 ml) DMF. The reaction mixtures were heated on an oil bath with constant stirring at 120 ^{0}C temperature. The chelate polymers generally appeared after 24-hrs heating on an oil bath. These chelate polymers obtained were filtered, washed thoroughly first with hot DMF and then with absolute alcohol and dried.

RESULTS AND DISCUSSION:

The ^{1}H-NMR Spectrum of hydroxamic acid ligands with adipic acid, azelaic acid, succinic acid, sebasic acid and subaric acid in acetone solvent along with complete assignments of resonances signals for aliphatic and aromatic protons are shown[5-6]. The NMR signal around δ(chemical shift) 2.05-2.40 ppm is assigned to the over laps of –CH2-protons of Ligands [7] . The aromatic protons of two phenyl groups are appeared at δ 7.48-7.63 ppm due to the presence of(-NHC=O) amide groups attached directly to benzene ring [8] and other resonance signal around δ 7.35-7.47 ppm is assigned due to two protons of benzene ring at which bromine attached[9-10] .

The resonance weak signal around δ 4.54-5.64 ppm is assigned to –NH-region of ligands and other weak signal around δ 8.24-8.27 ppm is assigned two protons of amide group (-NHC=O) [11] . In the infrared spectrum of the ligands a weak bands appeared from 3427-3480 cm^{-1} due to the presence of stretching vibration of the NH group [12]. Another sharp bands observed from 1606-1700 cm^{-1} may be assigned due to the C=0 stretching vibration[13] . A weak band appeared from 2882-2940 cm^{-1} may be assigned due to stretching vibrations of –CH2– groups.

Composition of the polymeric unit: the composition of the polymeric unit was assigned on the basis of detailed study of elemental analyses. The presence of water of crystallization was ascertained on the basis of thermal studies. The composition of polymeric unit is $[M(II)L]_n$, $\{[M'(II) (L) 2H_2O]H_2O\}_n$ whereas (M= Zn(II), (M'= Mn(II), Ni (II) and Co(II)) (L = ABHA ligand).On the basis of elemental analyses, infrared spectra, reflectance spectra, magnetic measurements and thermal studies, the proposed structure of these chelate polymers .

Infrared spectral studies: In infrared spectra, a broad band appears at 3257 cm^{-1} in ABHA ligand may be assigned to the O-H stretching vibration [14]. A band appears at 1664 cm^{-1} in ABHA may be due to the resonating structure of the N-N-(C=O)-OH moiety. A band appears at 968 cm^{-1} may be assigned to the N-O stretching vibration.

The hydroxamic acids generally form five membered chelate ring with a metal ion and coordination takes place through >N-O and >C=O oxygen. As is anticipated, a band due to the O-H group disappears in polymers. Whereas a band due to the carbonyl group is shifted towards lower frequency side indicates that there is the formation of C=O $\rightarrow$ M coordinated bond. The N-O band in polymers found to have been shifted slightly to higher frequency side with increase in its intensity. A medium band appears in the region of lower frequency may be assigned to the M-O bonding in chelate polymers. Thus, from the above discussion and from the consideration of potential donor atoms of the polyligands, it can be concluded that the substituted-bis-hydroxamic acids act as bidentate ligands and participated in bonding through the phenolic oxygen and the oxygen of the C=O group to give neutral linear chain chelate polymers.

REFERENCES:

1. L.M.Jackman and S.Sternhell, Application of Nuclear Magnetic Resonance Spectroscopy in organic chemistry, 2nd Ed.(Oxford;Pergaman Press,1969).

2. J.S.Waugh, Analytical Chemistry, 65, no.17 (1993)725A-9A.

3. A.S.Brar and R.J.Kumar, Polym.Sci.Part A; Poly.chem. 84(2002)50.

4. A.S.Brar, Hooda S.and Kumar R., J.Polym.Sci. Part A; 84(2002)50.

5. Sunita Hooda, Rajeev Kumar and Manpreet Kumar, Indian J.of chemistry, 43 A (2004)527-531.

6. Vogels, Text book of Practical Organic Chemistry, Fifth Edition, Revised by Briam S. Furniss, Antoy J. Hannaford, Peter W. Smith and Austin R. Tatchell, 965.

7. R. J. Abraham, J.Fisher and P.Loftus, Introduction to NMR Spectroscopy (New York, Wiley, 1998).

8. Michael Mcgregor, NMR Spectroscopy, Hand book of instrumental Techniques for Analytical Chemistry, 316.

9. A. E. Tonelli, NMR Spectroscopy and Polymer Microstructure, The conformational connection (New York; VCH, 1989).

10. Laurent F.Groux,Thomas Weiss,Dastigin N.Reddy,Preston A.Chase,Warren E.Piers,Tom Ziegler,Masood Parvez and Jordi Benet-Buchhotz,J.AM.Chem.Soc.Vol.127,No.6(2005)1865.

11. Robert M.Silverstein, Francis X.Webster, Spectrometric Identification of Organic Compounds, John Wiley and Sons Inc.New York, 1998.

12. W. B. Gurnule, P.K.Rahangdale, L.J.Paliwal and K.B.Kharat, Reactive and Functional Polymers 55(2003)255-265.

13. Ashaq Hussain, Sheikh H. N.and Kalsotra B.L., J.Indian Chem. Soc., 83,531-535, (2006).

14. Azza A. A. Abu-Hussen, Journal of Coordination Chemistry, Vol. 59, No. 2, 157-176, (2006).

INCORPORATING MACHINE LEARNING WITH BLOCKCHAIN TO ENLIVENING EDUCATIONAL SYSTEM

Mustufa Nullwala
Assistant Professor, Department of Information Technology, JVM's Degree College, Airoli, Navi Mumbai, Maharashtra, India University of Mumbai

ABSTRACT
Technology has advanced tremendously and this advancement in technology is being incorporated in the education sector as well. Blooming technologies like Artificial Intelligence, Cloud Computing Machine Learning, Blockchain, etcetera will change conventional education to make it a better platform. Data on the blockchain is immutable. It has a wide range of applications in various fields where security is of prime importance. Degree certificates of the students can be stored on the blockchain which can be accessed or shared by students to their employers. This is a very secure method and there is no worry of loss of data. There are various learning algorithms in machine learning which can predict the future based on experience. The incorporation of machine learning in the educational sector will be of great help as better outcomes can be got with the present conditions. When Blockchain Technology is incorporated with Machine Learning then certain predictions can be made beforehand through Machine Learning and they can be stored in the blockchain in a secured manner. In this study, the use of blockchain technology and machine learning in the education sector is discussed.

Keywords— Artificial intelligence, Blockchain, Machine learning, security, education sector, Smart Contracts

I. INTRODUCTION
Blockchain is a system of recording information in such a way that it is impossible to change, hack or delete from a blockchain system. Blockchain is a type of database in which data is stored in chronological order in form of blocks. Data stored in blockchain systems are immutable. Data cannot be deleted or altered. [3]

Machine learning is a major branch of Artificial Intelligence that is based on the notion that systems can learn from data, experience, and patterns. It is the study of various computer algorithms that improve with experience and data. [2]

A) Blockchain in Education System
Blockchain is decentralized distributed database system.[11] Blockchain technology can be used in the education system. Blockchain technology can change the way in which records of degrees, certificates, diplomas, academic papers and students' credentials are kept in the educational institution. Blockchain eliminates the need of intermediary verification of the documents. Using blockchain technology, accreditation process of the institution can also be made hassle free. It will be an easy process to verify the quality of education institution has to offer. Use of Blockchain technology in education system can also reduce the cases of fraud. Documents entered on blockchain system are verified, hence there is no chance any forged documents will be entered in blockchain. Proper use of blockchain can ensure honesty in education qualification of the students. Blockchain technology can also be used to create and maintain the Curriculum Vitae of students. These Curriculum Vitae will be digital documents and they can be shared by the Universities to the employers. Blockchain technology can also be used to keep records of students' identity which will be uniform across all the institutions. This will ease the process wherein student wants to enroll in multiple courses in different institutions or universities. [8] It will also reduce paper-based processes in the campus or university. Blockchain also can be used within the institution for the attendance purposes of the students. It can also be used to keep records of assignment completion by the students. Blockchains can also be made smart contract capable. Programming of courses can be made on blockchain and these courses will be activated when certain conditions will be met. For example, students can be assigned tasks related to their courses. These tasks will be automatically verified on blockchain by smart contracts on completion. Students will be awarded credits based on their tasks. [5]

B) Machine Learning in Education System
Machine Learning is an important branch of Artificial Intelligence. The use of Machine Learning in the education system can positively influence education. A huge amount of data is generated through existing Learning Management Systems and various other E-Learning platforms. Analysis of this data is done using various analytical tools. Current analytical tools can be replaced with machine learning algorithms. [2] These algorithms will not only analyze the current data but will also predict future data. It sometimes becomes difficult for teachers to understand and address the educational needs of the students. One approach of teaching may not fit

all students. Artificial Intelligence can collect, compile and analyze data of every student from all the platforms and sources. This analysis can be used by teachers to create personalized content for every student. Machine learning can examine students' educational data and develop a pattern of the way of his learning. For example, Artificial Intelligence can analyze and tell the method of learning which a student particular student understands better. Artificial Intelligence can examine student's educational data and tell whether a student's understanding and performance are better when he reads or solves assignments or listen to lectures or watch a video. Artificial Intelligence can also identify if a student is struggling with any particular or particular type of concept. This will help the teachers to design course material according to the student. Artificial Intelligence can also be used to predict future jobs for students. Based on the analysis of data collected of their courses, curricular and extra-curricular activities, prediction can be done about the interest of the student by using various artificial intelligence algorithms. Also, the type of jobs in which the student can excel can be predicted.

II. INTEGRATION OF BLOCKCHAIN AND ARTIFICIAL INTELLIGENCE

Integration of Blockchain Technology and Artificial Intelligence can be done in three phases. The first phase will be the implementation of Artificial Intelligence especially machine learning. This phase will analyze the data of the students. It will predict the pattern of studying of the individual students. It will also predict future jobs which are suitable for the student based on his capability and interest. The Implementation of Blockchain technology will be the second phase. It will act as a database. It will store students' identity, certificates, degrees, diplomas, etc. in a very secure manner. Courses of the curriculum can also be developed and evaluation can also be done on the blockchain. Smart Contracts can be used for the purpose of evaluation of students based on completion of assignments. In the third phase, machine learning and blockchain integration take place and they work in harmony. Machine learning will predict suitable jobs for the students; their education records are available in the blockchain which can be shared with employers. In this way, machine learning and blockchain can work together in the educational system.

III. CHALLENGES

A major challenge in using Artificial Intelligence and Blockchain technology is the immaturity of the technologies. Artificial Intelligence especially Machine learning offered by Microsoft, IBM, Amazon has not yet reached large masses. They have certainly not reached the education sector. The cost of implementation of Blockchain is more. Incorporation of Blockchain and Artificial Intelligence in the existing systems will be a tedious task initially. Once it is done it can have great positive changes in the education system.

IV. CONCLUSION

The future of the education system depends on the smart use of blooming technologies like Blockchain technology and Artificial Intelligence, especially Machine Learning. Using these technologies will bring about a positive change in the existing conventional method of teaching by integrating smart technologies. Blockchain and Artificial Intelligence will play a major role in bringing a revolution to the education sector. It has an intensive implementation in cryptocurrency. Now, blockchain is proving to be an important asset in other sectors as well. Blockchain offers security, transparency, the immutability of data, integrity due to which it can be used in the educational sector to enhance educational standards. On the other hand, artificial intelligence has proved its efficiency in many fields. As built-in algorithms can be easily included in applications, the use of artificial intelligence has also increased in various fields including the education sector. Online education will benefit a lot from the integration of blockchain technology and artificial intelligence in the education sector.

REFERENCES

[1] Ateniese, G., Faonio, A., Magri, B., & De Medeiros, B. (2104). Certified bitcoins. In: International Conference on Applied Cryptography and Network Security. pp. 80–96. Springer.

[2] Boden, M. (1998). Creativity and artificial intelligence. In Artificial Intelligence. 103 (1-2), p. 347- 356. Elsevier. DOI: https://doi.org/10.1016/S0004- 3702(98)00055-1

[3] Brandão, A., São Mamede, H., & Gonçalves, R. (2018). Systematic review of the literature, research on Blockchain technology as support to the trust model proposed applied to smart places. In World Conference on Information Systems and Technologies (pp. 1163-1174). Springer,

[4] Cham. Burbules, N. C. (2014). Meanings of "ubiquitous learning". Education Policy Analysis Archives, 22, 104. doi:10.14507/epaa.v22.1880

[5] Chakrabarti, A., & Chaudhuri, A. K. (2017). Blockchain and its Scope in Retail. International Research Journal of Engineering and Technology. 4(7), July.

[6] Cope, B., & Kalantzis, M. (Eds.). (2010). Ubiquitous learning. Chicago: University of Illinois Press.

Retrieved fromhttp://manchesterileap.pbworks. com/f/Ubiquitous+Learning+Boo k+Review.docx

[7] Decker, C., & Wattenhofer, R. (2104). Bitcoin transaction malleability and MtGox. In European Symposium on Research in Computer Security. pp. 313–326. Springer.

[8] Grech, A., & Camilleri, A. F. (2017). Blockchain ineducation. Publications Office of the European Union 2017, 132 S. - (JRC Science for Policy Report). Luxembourg.

[9] Hwang, G. J., & Tsai, C. C. (2011). Research trends in mobile and ubiquitous learning: A review of publications in selected journals from 2001 to 2010. British Journal of Educational Technology

[10] McKnight, L. W., Etwaru, R., & Yu, Y. (2017). Commodifying Trust: Trusted Commerce Policy Intersecting Blockchain and Internet of Things.

[11] Nakamoto, S. (2008). Bitcoin: A peer-to-peer electronic cash system. Retrieved from the web on 21/Feb/2019 in http://bitcoin.org/bitcoin.pdf

INTERNATIONAL MARKETING ASPECTS OF INFLUENCING END USER SATISFACTION WITH MONOCULTURALIZATION TO DISEMBEDDING AS PER NATIONAL BORDERS

Onkar Prakash Mone

Assistant Professor, Department of BMS, JVM's Degree College, Airoli, Navi Mumbai, Maharashtra, India, University of Mumbai

ABSTRACT

Monoculturalism is the policy of allowing the expression of the culture of a single social group in a specific area. certain multi-ethnic societies, dominant groups believe that their cultural practices are superior to those of minority groups, similar to the concept of ethnocentrism which involves judging another culture, based on the values and standards of one's own culture. Instead a suppression of different ethnic groups within a given society, sometimes monoculturalism acts as the active preservation of a country's national culture via the exclusion of external influences. Market economy is a disembedded economy in fact comprises two main statements: (1) disembeddedness means the predominance of transactions and social interactions that are not submerged in social relationships but are based on economic self-interest and (2) disembeddedness also means the absence of social control over the economic process of production and distribution. This paper attempts a reality check on the challenges and opportunity that International marketing presents for the current and future and identifies the key points for a country strategy that will take full advantage of the potential offered by parent company to create and forge more 'personal' and ' immediate' relationships with their customers.

Keywords – Monoculturalism, Disembedded, International marketing, Mumbai

I. INTRODUCTION

International marketing means marketing activities in between different countries. All countries participate in international marketing and secure certain benefits such as availability of goods urgently needed, earning of foreign exchange and acceleration in the process of economic growth. Large scale exporting acts as an engine of economic growth. Expansion of business is a natural need and expansion is necessary for survival and growth. There are various factors that encourage companies to expand business beyond national boundaries. Such factors are also called motivators of international marketing.

II. FACTORS

This paper adopted five essential factors for end user satisfaction which are categorized into 1)convenience 2)functionality 3)price 4)reliability and

5)visibility. Convinces refers to the degree to which customers considers navigating through m- commerce transaction free of efforts. Functionality represents the simplicity and frequency of using mobile technologies regardless time and place. Price factor refers to the degree of perceived level of possible expenses to m-commerce adoption. Reliability represents the degree to which customers perceives the quality of goods and channels, while visibility shows the perceived customers satisfaction to visual information and site design.

III. OBJECTIVE

- To study aspects of influencing end user satisfaction.
- To study international marketing.
- To Study monoculture & disembedding

IV. MONOCULTURALIZATION TO DISEMBEDDING

1. *Finding a niche in an established market*

Carving out a niche market is an effective way of gaining and retaining popularity, since advertisments and products can be targeted at a specific group of consumers.

2. *Give the customers a voice*

A huge social media presence and worldwide sensation on social media platform is important key. Regular use of social media to share about happening, sharing and commenting on how they embrace the daily grind.

3. *Organising consumer focused events*

To bring different communities together and introduce them to the product or brand at the event then connect with them digitally and socially to keep the bond continued.

4. Cultural difference

In order to remain competitive in a globalized world, it is critical to develop product that are able to satisfy a very diverse customer base. Culture is one of the most effective yet complicated elements that organisation need to understand in order to provide great product in accordance with the customers' needs.

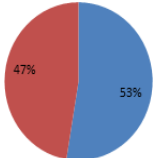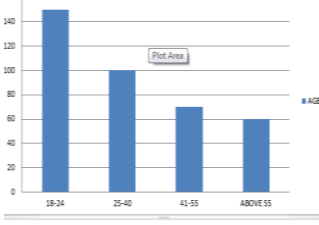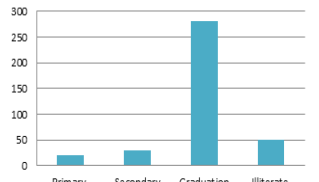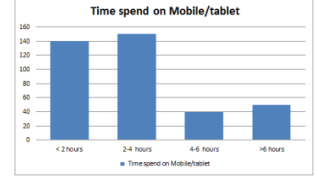**TABLE 1: DISTRIBUTION OF RESPONDENTS BY GENDER, AGE AND USAGE.**

Questions asked to 380 people		Frequency	%	Diagrammatic representation
1. Gender Female Male	Male	200	52.63	
	Female	180	47.36	
2.Age	18-24	150	41.66	
	25-40	100	26.31	
	41-55	70	18.42	
	Above 55	60	15.79	
3.Education	Primary	20	52.63	
	Secondary	30	78.94	
	Graduation	280	73.68	
	Illiterate	50	13.18	
4.Time spend on Mobile/tablet	< 2 hours	140	36.84	
	2-4 hours	150	39.47	
	4-6 hours	40	10.53	
	>6 hours	50	13.16	

TABLE 2: CHANGES IN USAGE

Questions	Before 2019		In 2020	
	YES	NO	YES	NO
1.M-commerce usage for purchase	71.02%	28.98%	80%	20%
2.Payments via apps	56%	44%	60%	40%
3.Online Shopping	58%	42%	64%	36%
4.Banking services	61.35%	38.65%	65.75%	34.25%
5.Receiving pre-discount coupons from physical stores	32.02%	67.98%	45.45%	54.55%
6.Receiving pre-discount coupons from M-commerce	35.52%	64.48%	40.53%	59.47%
7.Improvement in Quality Product/Service	40%	65%	52%	48%
8.Satisfaction as a user	49%	51%	58%	42%
9.Satisfaction as a consumer	43%	57%	51%	49%
10. Is product/service user friendly?	46%	54%	53%	47%
11. Is product/service consumer focus	60%	40%	71%	29%
12. International product is trustworthy.	38%	62%	49%	51%

V. ANALYSIS

As the survey has been done among 400 people from whom only 380 responded. Among them approx. 52% were male and 47% were female. The larger section was between 18-24 years.

The relevant changes can be seen in the table 2. As the usage of international product has increased by 8.98% . The user of online shopping has been increased by 6%. The daily activity of banking handling online has increased by 4.4% .The relatively big changes can be seen in the pre-discount coupons provided by the physical store i.e. 16.98%. As from the competition fear or so the physical stores are giving discount coupons to the customers as to attract more. Which in turn is beneficial for the consumers. On the other hand the pre coupons provided by the physical stores has increased by 5.01%. There is a relatively slight change in the improvement of product quality also which is margined by 12%. Moreover, the satisfaction of users has increased by 9% and of consumer has been increased 8%. Products/Services has became more user friendly as compared to previous year with that it has also increased quality, goodwill, performance by 11%. It can also be analysed that it became more trustworthy 9%. From the overall we can see that, there is a visible influence of international products on the habits, preference and taste of consumer.

Because of improving technology and access now people are more prone to the foreign products/brands.

VI. CONCULSION

There are various factors considered for study and it was found that there is need to focus on the customer's satisfaction. Firstly the quality of service plays an important factor for meeting customer satisfaction. Almost 50% of the respondent is satisfied with the quality which is positive sign and there is rise in consumer satisfaction as compared to previous year. Secondly the factor of trust is important people are not much in favour of international products for monetary transaction for which the quality, safety and security needs to be taken care of. The area requires attention which will help to gain customer satisfaction. All said and done, with the growth in E-Commerce & Physical stores the future is bright, provided the product/service providers convince the users that it is a safe, handy and cost-effective for end user.

REFERENCES

1. https://www.referralcandy.com/blog/reebok-marketing-strategy/

2. https://www.statista.com/statisti cs/273057/value-of-the-most-valuable-fast- food-brands-worldwide/

3. https://digitalscholarship.unlv.edu/thesesdissertations/1370/

4. http://web.mit.edu/kken/Public/papers1/Cultural%20Diversity.htm

5. https://medium.com/@bobbyahv/embedding-product-culture-c158e0212c36

6. https://hbr.org/2012/07/cultural-change-that-sticks

AN INTRODUCTION TO BLOCKCHAIN TECHNOLOGY

Shakuntala Kulkarni

Assistant Professor, Department of Computer Science, JVM's Degree College, Airoli, Navi Mumbai, Maharashtra, India,University of Mumbai

ABSTRACT

Blockchain Technology is a very secure system of recording information. Information stored on a Blockchain system aims to ensure high transparency, data security, and integrity as it is very difficult to hack or cheat a blockchain system. A blockchain is basically a decentralized digital ledger of transactions that is duplicated and distributed across the entire network of computer systems that are on the blockchain system. Blockchain technology can bring about significant changes in the business environment as well as other sectors. This technology can change the way the business is perceived and it can transform the economy. The main application of Blockchain Technology is for cryptocurrencies such as Bitcoin. There are several other applications of Blockchain Technology such as in Government sectors, banking and finance industry, accounting and business process management, HeathCare sector, Education sector, etc. This study attempts to explore applications of blockchain, its opportunities and challenges, and also future applications of blockchain.

Keywords:- Blockchain Technology, Ledger, Transactions, SmartContracts, Database, cryptography

I INTRODUCTION

Blockchain technology is a computer protocol. It is used for recording and storing digital information on multiple computers in a secure way. An important element in Blockchain technology is Ledger which is similar to a relational database. A block in a blockchain is a list of digital records. These digital records are stored in an encrypted manner. Using a cryptographic signature, each block is chained to the next block in a linear order. A copy of the last transaction since the last block was added is also stored in the blocks [4]. The share block which is also called a ledger is linked to all the participants on

the Blockchain system. Any update in the transactions is validated and confirmed by these participants, hence there is no need for third-party validation [4]. Blockchain stores and distributes data in a very secure manner. Blockchain can solely be updated by an accord between participants and a transaction cannot be changed or deleted [2].

Blockchain is a system which is decentralized and distributed. It cannot be hacked, altered, or disrupted as a traditional database with a user access control system. Data in the blockchain system is immutable. Even the system administrator cannot alter or delete the data on the blockchain ledger since the data stored in the blockchain is time-stamped and is stored in a chronological order using a cryptographic signature.

A. *Characteristics of Blockchain Technology*
Following are the characteristics of Blockchain:-

1. Blockchain is distributed ledger.

2. It is decentralized data management system.

3. Blockchain aims at data security, transparency, and data integrity.

4. Data on the Blockchain system cannot be tempered.

5. Data on Blockchain cannot be forged.

6. There is no risk of centralized data failure.

7. Blockchain has high efficiency and low cost.

B. *Types of Blockchain*
There are many types of Blockchains, out of which three important types are:-

1. Public Blockchain

2. Private Blockchain

3. Consortium Blockchain which is also called HybridBlockchain

1) *Public Blockchain*

In a public blockchain, anyone can do transactions on the system. These transactions are transparent and anonymous. Bitcoin is the best example of a public blockchain. Public Blockchain is decentralized. Since the transactions are anonymous, this type of blockchain is vulnerable to attacks.[4] [8]

2) *Private Blockchain*

In Private Blockchain, all the members in the system are known. Participants cannot read or write in the blockchain system unless they have permission or an invitation from the other participants to join the network. Transactions in private blockchain are secret. Private blockchains are used by large companies. For example, there can be a private blockchain for a bank wherein there can be restricted access to its various stakeholders.[4] [8]

3) *Consortium Blockchain*

Consortium Blockchain is a hybrid of both Private and Public Blockchain. If consortium blockchain is chosen by an enterprise then it can have its own private blockchain network to share among the participants.[4] [8]

II APPLICATIONS OF BLOCKCHAIN

A. *Smart Contracts*

Smart Contract is a computerized protocol that acts like any ordinary contract. It is written in computer code and it is executed in Blockchain environment. [3] The most important implementation of Blockchain technology is creating fully automated smart contracts. These types of contracts do not have any human involvement. Smart Contracts are used in Entertainment industries to ensure that royalties of music or film are transferred to everyone involved in a transparent way. Smart Contracts are used in Healthcare sector to maintain synchronization between payers, providers and drug manufacturers. Smart contracts are also used in Insurance sectors. Insurance products can be automated by use of Smart contracts. Error or fraud in insurance sector can be minimized using Smart Contract.

B) *Implementing e-Government*

Blockchain is a very secure system. It records all the transactions on a distributed ledger which increases transparency, it also prevents fraud, has data integrity. Hence, blockchain has an important application in Government. The use of blockchain in government operations will increase efficiency which will lead to an increase in trust in the public sector. Thus, using a distributed ledger in the government sector is a way to improve the transparency of the budget process, and also it reduces corruption factors.

C) *Financial industry*

Blockchain technology has great potential to reduce the cost of transactions. It can reshape the economy. Blockchain was developed for Bitcoin. Bitcoin is the most popular decentralized digital currency.[5] Blockchain when used in the banking sector can solve lots of problems related to exchanging of data and money. [8] Blockchain provides services in a secured manner and in a low cost. Hence, if blockchain is used in financial settlements then it will also increase the reliability of financial statements.

III ADVANTAGES OF BLOCKCHAIN TECHNOLOGY

Data integrity: - Data in the Blockchain system is immutable. Once the data is stored, it cannot be altered or deleted by individual participants. It can only be done with consensus from all the participants. [7]

Reliability: - There is no single point of failure in blockchain due to which it is highly reliable.[8]

Security: - All the transactions on the blockchain system are time-stamped with a cryptographic digital signature. This signature is a unique 64-digit alphanumeric hash code. [7]

High Availability: - Since blockchain technology is a decentralized system, the data is highly available and accessible. Decentralization: - Blockchain is a decentralized system. It eliminated the involvement of any third party which reduces the overhead cost. [6]

Transparency: - All the transactions done on the blockchain systems are transparent.

IV CHALLENGES IN BLOCKCHAIN TECHNOLOGY

Cost:- Blockchain has an initial setup cost. The users have to pay for tall transactions taking place on Blockchain.

Latency issue:- Blockchain has a complex verification process. It is not appropriate for massive transactions, as these transactions will take a lot of time to complete.

Integration issues:- Blockchain is a completely new technology. It requires a lot of changes in the existing system to incorporateblockchain.

V CONCLUSION

Blockchain technology has high potential in solving problems related to data integrity, data security, transparency. The use of blockchain in various fields can enhance security and prevent fraud. Blockchain has a wide range of applications in the health sector, entertainment industry, insurance sector, financial sector, education sector. If properly used, blockchain can bring about arevolution in these sectors. Blockchain can give innovative solutions to the problems faced in these fields. However, the implementation of blockchain can be costly as well as time- consuming. Integration of blockchain with the existing system can also be challenging. Blockchain won't replace the existing system anytime soon but it can be a complementary application to the existing system.

REFERENCES

[1] Ahram, T. et al., (2017). Blockchain technology innovations. 2017 IEEE Technology & Engineering Management Conference (TEMSCON) (Jun. 2017), 137–141.

[2] Fanning, K. & D.P., Centers, (2016). Blockchain and Its Coming Impact on Financial Services", Journal of Corporate Accounting & Finance, 27(5), pp. 53–57.

[3] Gates M., (2017). Blockchain: Ultimate guide to understanding blockchain, bitcoin, cryptocurrencies, smartcontracts and the future of money. Create Space Independent Publishing Platform, 2017.

[4] Glaser, F. & Bezzenberger, L., (2015). Beyond Cryptocurrencies—A Taxonomy of Decentralized Consensus Systems. 23rd European Conference on Information Systems, Munster, 1-18

[5] Nakamoto S., (2008). Bitcoin: A peer-to-peer electronic cashsystem.

[6] Porru, S., Pinna, A., Marchesi, M., & Tonelli, R., (2017). BlockchainOriented Software Engineering: Challenges and New Directions", 39th International Conference on Software Engineering Companion, pp. 169–171.

[7] Swan M., (2015). Blockchain: Blueprint for a new economy.O'Reilly Media, Inc, Sebastopol, CA, U.S.A.

[8] Tapscott, D., & Tapscott, A., (2016). Blockchain Revolution: How the Technology Behind Bitcoin Is Changing Money, Business and the World. New York, NY: Penguin Random House

[9] Walport M., (2016). Distributed Ledger Technology: Beyond Blockchain. UK Government Office for Science, Tech.Rep, pp. 19

NEED OF DIGITALIZATION IN EDUCATION

Dr. Sunitha Joshi

Department of Information Technology, JVM'S Mehta Degree College, Airoli, Navi Mumbai

ABSTRACT

The learners of today are different and digital learning is the key to students' long-term success. Variety of reasons might be the cause. When we understand below and get your classroom in order for this new wave of education, Digital learning is appearing as the panacea for all sorts of problems that ail the education sector. By embracing digital devices and connected learning, colleges can not only connect to one another to boost learning or share insights, experience, and communications skills, but it also lets teachers enjoy a level playing field, where all types of colleges have access to the same learning and opportunities. Digital mode of assessments provides students fast feedback on their understanding, permitting both students and instructors focus their efforts on where further understanding is most required.

Keywords— Digital learning, education, digital Devices

INTRODUCTION

Digital curriculum is not one time investment. The syllabus content also must be regularly upgraded when technologies change. Technology change will have an important impact on existing content. This situation is similar to what corporate had to deal with when device manufacturers stopped supporting their flash-based e-Learning content, and HTMLS came to the foray. Digital learning in colleges is going to rise in future as more and more colleges adopt it, but it has its fair share of challenges. Colleges that adopt digital learning and new technology need thorough information on challenges they can face.

EMERGING TRENDS OF DIGITAL EDUCATION

2.1 DIGITALIZED CLASSROOM/FLIPPED CLASS ROOMS A GROWING TREND

A complete revolution is needed to see the new change. Teachers teaching in the classroom can capture the students and the fall strength in the class by digital screens. Thus, facilitating each child to get the same has come and input from the teachers. This digital technology has increased the student involvement as it involves the various instructional styles. Each madent gets it ca to world-class education, which is not easy to impart by the traditional white chalk and black board teaching. This new way of learning environment is compiled more personalized interest of student and giving more joy in the learning. With this technological inclusion in the college teaching the students study as enjoyable, easy, competent and above all interesting. The aim of a teacher however should be to create such an atmosphere which makes every student wants to study.

2.2 Video based learning.

Video-based learning has compounding with digital marketing has setup in Indian Education Sector and has made education engaging, entertaining and exploring. This system provides students learning leisure period with flexible timings as per the suitable timing enabling his creativity, fun using very interesting Apps, podcasts, videos, interactive software, e books and online interactive electronic boards. Children are excited and operative with interest to manage the showcase via their intelligence, exploring the weak teacher skills of teachers and assist them in public with pride and honour and recognition

2.3 Massive open online course (MOOCS) & other distance learning programs.

A huge amount of open online course (MOOC) is a web-based system enabled huge participation and open access via the online. India is taken into account to be the most important mark for MOOCs within the world after the USA. If we consider the population of India which is massive and availability of large open online course (MOOC) have opened the gateways for tons of Indians in terms of bringing an academic revolution. Online distant learning programs provides a great opportunity to avail top quality learning with the assistance of internet connectivity

III - ADVANTAGES OF DIGITAL LEARNING

Digital Learning has become very popular with time. The following are the advantages of Digital Learning: Physical Boundaries Digital Learning has to locational and time restrictions. In case of face-to-face learning, the location limits the group of learners to those who have the ability to participate in the area. But this is at the case in digital learning. In digital learning, there is no physical restriction and the learner can attend the sessions anytime, anywhere according to his/her comfort. Digital learning enabling the involvement of students more as compared to traditional learning method. Through digital learning, a course is often designed during

a way that creates it interactive and fun through the utilization of multimedia. Even, the more recently developed methods of gamification are often wont to enhance the engagement factor.

3.1 Cost Effective Digital learning is cost effective way of education as compared to traditional learning. In digital learning, here is a god chance that you don't have to pay exorbitant amounts of money to acquire textbooks for college or college. As textbooks often become obsolete after a certain period the time, e-learning is definitely a cost-effective way of learning because of the reduced cost. It can be established in digital learning as you can study at the time that suits you. In digital education, the student can study at the time of own comfort.

CONCLUSION:

Using Digital Learning based technology has never that easy to improve learning in all levels and all for all people of different areas. By use of technology, new changes in licensed educational resources has improved, and by using tools it removed difficulties in all time learning process Improved class room teaching and learning standards thus allowing all learners to access resources with sufficient expertise in planning tools to execute them thoroughly. Teachers who are well familiar with teaching learning system can play a lot bigger role in development of such tools. These tools will add the knowledge, skills, and competencies of educators. With aid of such tools like learning dashboards and collaboration and communication helps to connect teachers and families with more ease. All this is possible only by a strong dedication and inclination to learning for change. It also helps every stack holder in the teaching and learning system to improve learning for students. Overall, the use of technology gives the good outcome to support in teaching and learning process.

REFERENCES

1. Biswas, Preeti (2015, September 29), Only 28.84% schools in Telangana have Internet, times View, The Times of India. p.5.

2. Dahiya. S. Surender (2009) Educational Technology –Towards Better Teacher Performance. Delhi: Shipra Publications.

3. Simmons Carl and Hawkins Claire (2009) Teaching ICT. New Delhi : SAGE Publications India Pvt. Ltd.

4. Ms Vidushi Daga, Clone Futura Education. A Report on the Future of MIT Education, July 2014,Scholarship Positions An article of Dr. Ali Al Nuaimi, Director of the Abu Dhabi Education Council.

5. An article of Jahir Kameel, SaaS Marketer. An article of P.Krishnkumar, Senior Vice President, Consumer & Small Business Dell, India

6. McCaffrey, D. F., Lockwood, J. R., Koretz, D. M., & Hamilton. L. S. (2003). Evaluating value-added models for teacher accountability. Santa Monica, CA: RAND.Retrieved from http://www.rand.org/pubs/monographs/2004/RAND MG158.pdf.

7. Rivkin, S. G., Hanushek, E. & Kain, J. F. (2005). Teachers schools,and ademicachievement.Econometrica,73(2),417- 458.

CORPORATE SOCIAL   RESPONSIBILITY ACCOUNTINGWITH REGARDS TO PUBLIC LTD. COMPANIES IN INDIA

Mrs. Riyu Rahul Haldankar

Assistant Professor, JVM Mehta College Airoli, Navi Mumbai, University of Mumbai, Maharashtra, India

ABSTRACT

In Indian economy a new plant took root i.e., Corporate Social Responsibility. From last Century Indian Companies engaged in such activities. Private organizations & Government also try to collaborate for social benefits. Social Responsibility activities are initiated to earn trust & goodwill in Society. Still social Responsibility is just a welfare scheme launched by firms. Many Public ltd. companies are profoundly engaged in such activities & try to fulfil their responsibility towards society. There Applicability in accounting system is rare.

As per Companies Act 2013 section 135, Companies fulfilling eligibility criteria must spend at least 2% of their net profit of three preceding financial years towards corporate social responsibility activities. It is found that their applicability in financial statements is still confusing. This research paper tries to clear the idea about accounting applicability of social responsibility perform by Indian companies & also Challenges faced by firm in accounting applications.

Keywords: Corporate Social Responsibility, Responsibility Accounting Philanthropy, Company Act 2013

I.   INTRODUCTION

Every business is an important part of the society, Business depends on society for the resources requiredto them hence they must understand the responsibilities towards the society. From last century,many organizations try to initiate in social responsibility of their firm by handling some of the social issues of Indian society.

Corporate social responsibility of the companies is philanthropic in nature but with the changing scenario the nature of CSR is also changing. It has many folds like Economic, social cultural& charitable. The meaning of social responsibility is also changing day by day. Now we can say that it is continue commitmentof business firm to behave ethically & contribute toward economic development keeping social responsibility in mind.

Social responsibility accounting is a framework created to analyze the companies' social performance. It is mandatory for every company to contribute towards social responsibility through various activities. India is one of the countries in the world who make it compulsory. Still, some of the companiesare unaware about it.

A per company Act 2013, section 135 it is mandatory for Indian companies as well as foreign companies who have branch or project in India spend at least 2% of their average Net profit in every financial year preceding to three financial years towards CSR & also disclose it in their accounting reports like Profit & loss account, cash flow statementetc.

II.   DEFINATIONCorporate social responsibility

CSR means companies sense of responsibility towards the community & environment (both social & ecological) in which it operates. It is also called as corporate conscience, corporate citizenship or responsibility business. It is a form of corporate self- regulation integrated into a business model. It is basedon four-fold economic, social cultural & philanthropy.

Responsibility accounting

It is a practice of integrating non-financial measures into financial reporting. It is also called as sustainability accounting. It consists various enclose terms like social accounting & auditing, environmental accounting, social responsibility reporting, non-financial reporting. It can be disclosingas per prescribed manner in accounts too.

Philanthropy

It means the love & humanity in the sense of caring, nourishing, developing, enhancing, what it means to be human. In business terms it is a initiative for material gain for society in terms of charity. But not allcharity is philanthropy because charities aim to relieve pain but philanthropy address the root cause of problem.

Company Act 2013 Section 135 Schedule vii

The company act 2013 lay down a framework for all companies meeting the prescribed criteria tocontribute 2% of their average net profit made during three immediately preceding financial year for CSR

CSR Activities	In cash	Yet to bepaid	total
1.construction/acquisition of any asset			
2.on purpose other than above			

CSR in India

Among other countries, India has one of the oldest purpose. This CSR rule will be for companies including foreign companies having branch or project in India meeting criteria like turnover exceeding to 1000 crore, their net worth more than 500 crore & annual net profit exceeding 5 crores. This will start effecting from 1st April 2014.

Disclosure in accounts

CSR can be disclosing in Profit & loss account debit side as CSR expenditure. Break up should be shown innote as follow:

Disclosure to be made in notes to the cash flow statement (where applicable)

Details of related partly transactions

e.g., Contribution to trust controlled by company in relating to CSR expenditure as per section 18 related partly disclosure.

III. SIGNIFICANCE

It is found that social responsibility cannot be properly elaborated by companies. Many companies perform corporate governance or business ethics in business & think that they fulfill their responsibilities towards society. Many companies still in confuse state about applicability in their accounting system. They also unaware about the disclosure of CSR in accounting reports. This paper may help them to overcome their confusion. It will help to measure the performance at different parameters.

CSR in World

World aware about the CSR from last century. In early 50's many European countries try to promote green consciousness in society. They also develop green movements for the people. Whereas in western in countries CSR is restrict up to business ethics, they look after their workforce care about them. Many US & European companies dismissed CSR as imperialist construct as much as luxury. Asian & Latin American countries awake thereafter.

In recent decade, India & Brazil have taken lead in making business which adopts policies based on social responsibility & environmental consciousness. United Nations play a significant role in CSR. They create universal acceptance of idea of CSR.

Traditions of CSR. Indian companies aware about social responsibility from late 18th centuries in India have five phases. The **FIRST PHASE** diverges by charity & philanthropy. The **SECOND PHASE** will be influenced by Mahatma Gandhi's Trusteeship theory. The **THIRD PHASE** of CSR is from 1960-80 where mixed economy found. Various law relating to labour & environmental standards came into existence. The **FOURTH PHASE** starts from 1980 till 2013. Indian companies started CSR as integrated business strategy. The term like Globalization, economic liberalization was undertaken whereas close attention towards CSR activities growing. In **Current Phase** industries like TATA, Mahindra & Mahindra, Infosys, Coca cola contribute in society through various activities like Trust, NGO's, Maternal & child health, Diseases like AIDS, sports & academic like arts & cultural education to children in society.

IV. OBJECTIVES

1. To understand the term social responsibility accounting briefly.

2. To study various changes in regulatory framework lay down by Company Act 2013.

3. To aware Indian companies towards applicability as social responsibility accounting & their disclosure in accounting system.

4. To provide information about framework of SRA.

5. To examine whether the selected companies disclosing CSR expenditure under report.

6. To examine the funding mobilization for responsibilities by companies.

7. To compare the CSR practices of selected companies in India.

V. METHODOLOGY

The research is a descriptive in nature based on secondary data. The annual reports of selected companies used for the data required for research. Financial year 2015-16 have been considered for it. A sample of 5 companies has been chosen for the study. Random sampling method has been used.

VI. HYPOTHESES

1. All selected companies are not disclosing environment expenditure under CSR report.

2. CSR expenditure has been varied depending on Net Profit/loss of the company.

VII. ANALYSIS AND INTREPRETATION OF DATA:

CSR and Environment Expenditure for 2019-20
(₹ In Crore)

Name of the Company	Net Profit	CSR Exp to be incurred	CSR exp actually spent
Bharat Heavy Electricals Ltd.	1649.80	Nil	15.27
Bharat Petroleum Corporation Ltd (BPCL)	11940	238.8	925.9
Coal India Ltd.	11280.88	225.62	194
Hindustan Petroleum Corporation Ltd.	2637.26	52.75	182.84
Indian Oil Corporation Ltd.	21762	435.24	5433.78

(Source-Compiled through Annual Report)

Table shows that Bharat Heavy Electricals Ltd. had spent more on CSR expenditure than budgeted

CSR expenditure whereas Net Profit was be negative still they spent on CSR expenditure i.e., Rs.15.27 crore. In case of Bharat Petroleum Corporation Ltd (BPCL) the budgeted CSR expenditure is Rs.238.8 crore still company has spent Rs. 925.9 crore. The budgeted CSR expenditure of Coal India Ltd is Rs.225.62 crore & in actual they spent Rs. 194 crore. and Hindustan Petroleum Corporation Ltd. spent Rs. 182 crore which is more than budgeted. Indian Oil Corporation Ltd. spend Rs. 5433.78 crore which is way more than budgeted.

VII. RESULT OF HYPOTHESES

1. All selected companies disclosing CSR expenditure in their annual report.

2. Annual report of the all-selected companies and analyses and on that basis, hypothesis is accepted.

3. After comparing CSR report of selected companies, it shows that companies had spent more on CSR as compare to budgeted CSR.

VIII. CONCLUSIONS AND FINDINGS

CSR is a developing process in country like India. Companies is aware about The CSR & their spending. Still companies try to disclose in their accounting system properly. Government & private firms' collaboration is the necessity of the current scenario of CSR initiatives. It found difficult for the single firm to bring changes in society. It is collaborative work where all take initiatives in it.

The selected companies are disclosed their CSR activities to the activities referred to in Schedule VII of Companies Act. 2013. All eligible companies included CSR expenditure in the specified format in their annual reports. All companies spend more for the CSR against their budgeted CSR whereas they have Net profit or net loss.

Corporate social responsibility accounting is an effective tool to communicate company's social responsibility practices to interested and connected parties. The findings of the study show that more than 70% companies out of selected companies have initiated some good social projects and disclosed CSR expenditure under annual report.

IX. REFERENCES

1. CSR in Indian efforts to bridge welfare gap. Jayantisarkar & subroto sarkar. Aug 2015

2. Corporate social responsibility: An analysis of impact & challenges in India. May 2014 3.Participation of Private sector companies in India Sumona ghosh. Feb 2014

4. Master thesis in financial accounting. Kristine joinjail 2012

5. Corporate social responsibility in india. Dr.Moon. Moon Urmila.

6. Corporate social responsibility: review of literature.

7. http://www.cuts-international/.org/pdf/draft-CSR/rules-2013.pdf

8. www.academia.edu.

9. Annual Reports of sample companies.

ELEMENTARY COMPLEX VALUED FUNCTIONS

Pintoo Jaiswar

Assistant Professor, Department of Mathematics and Statistics, University of Mumbai
JVM's Degree College, Airoli, Navi Mumbai, Maharashtra, India

ABSTRACT

All very much familiar with using complex valued functions during process of expansion in day to day life. In this research paper ,we will see the importance of elementary complex valued functions like trigonometry function, exponential function and logarithmicfunction. However, we will see how one can make multiple trigonometry formulae using least number of formulae. Also, we will try to understand relationship between trigonometry functions and hyperbolic functions. Trigonometry function and hyperbolic function play a very energetic role while establishing their relationship.

Keywords: *"i", Complex variable, Trigonometric function.*

I INTRODUCTION

In this paper, we try to understand how the relation between different complex valued functions which are used for analyticity. Here, we are going to establish relation between trigonometry function, hyperbolic function and also we will try to understand hyperbolic function and logarithmic function. Trigonometry functions are most beautiful complex valued and essential functions for understanding any concepts of complex analysis.

Also one can construct all factorisation and De-factorisation formulae of a trigonometric functions .

II PROBLEM/STRUCTURE

A. A. Trigonometric function:

We've very fruitful Euler's formula as

$e^{i\theta} = (cos\theta + i\, sin\theta)$ and $e^{-i\theta} = (cos\theta - i\, sin\theta)$ $\qquad$ (1)

Therefore we 've $e^{iz} = (cosz + i\, sinz)$ $\quad$ and $\quad e^{-iz} = (cosz - i\, sinz)$ $\qquad$ (2)

After adding equations of (2) we get $cosz = \frac{(e^{iz}+e^{-iz})}{2}$ and subtracting equations of (2) we get $sinz = \frac{(e^{iz}-e^{-iz})}{2i}$.

$sinz = \frac{(e^{iz}-e^{-iz})}{2i}$ $\quad$ is called as complex sine function and $cosz = \frac{(e^{iz}+e^{-iz})}{2}$ $\quad$ is called as complex cosine function.Complex sine and cosine functions yield following identities:

$sin^2(z) + cos^2(z) = 1$, for all z$\in$ $\mathbb{C}$.(3)

$1+tan^2 (z) = sec^2(z)$, for all z$\in$ $\mathbb{C}$. $\qquad$ (4)

$1+cot^2(z) = cosec^2(z)$, for all z$\in$ $\mathbb{C}$. $\qquad$ (5)

B. Hyperbolic function:

Complex sine hyperbolic function given by

$sinh(z) = \frac{(e^z - e^{-z})}{2}$ $\quad$ (6)

And Complex cosine hyperbolic function given by $cosh(z) = \frac{(e^z + e^{-z})}{2}$ $\qquad$ (7)

By replacing "z" of equation (6) by "iz" we get relationship $sin(iz) = i.sinh(z)$ and also replacing "z" of equation (7) by "iz" we get relationship $cos(iz) = cosh(z)$.

C.Exponential function:

Let $z = a + bi$ be any complex variable where "a" is real part of z and "b" is an imaginary part of z .

e^z is called as complex exponential function,where "z" is a complex variable.

$e^z = e^{(a+bi)} = e^a.e^{bi} = e^a(cosb + isinb)$ from equation (1).

We have following properties of exponential functions:

Let $z_1 = a_1 + b_1 i$ and $z_2 = a_2 + b_2 i$ be complex variables.

(a) $e^{z_1 . z_2} = e^{(z_1 + z_2)}$, for all $z_1, z_2 \in \mathbb{C}$.

(b) $\frac{e^{z_1}}{e^{z_2}} = e^{(z_1 - z_2)}$, for all $z_1, z_2 \in \mathbb{C}$.

(c)   The modulus of complex exponential function e^z is equals to e^a .

(d)   An argument of complex exponential function e^z is equals to $(b + 2k\pi), for\ k = 0, \pm1, \pm2, \dots\dots$.

i.e $\arg(e^z) = (b + 2k\pi), for\ k = 0, \pm1, \pm2, \dots\dots$.

D. Logarithmic function:

A logarithmic function of non-zero complex variable $z = re^{i\theta}$,where $(-\pi < \theta \leq \pi)$ is given by

$log(z) = ln(r) + i(\vartheta + 2k\pi)$, for $k = 0, \pm1, \pm2, \dots\dots$.

We've following properties related to logarithmic function as follows:

Let $z_1 = a_1 + b_1 i$ and $z_2 = a_2 + b_2 i$ be complex variables.

(a) $log(z_1 . z_2) = log(z_1) + log(z_2)$

(b) $log(\frac{z_1}{z_2}) = log(z_1) - log(z_2)$

(c)   The modulus of non-zero complex variable $z = re^{i\theta}$ is equals to r.

(d) $arg(z_1 . z_2) = \arg(z_1) + \arg(z_2)$.

RESULTS

For trigonometric function we are having following results as follows:

Let $z_1 = a_1 + b_1 i$ and $z_2 = a_2 + b_2 i$ be complex variables in $\mathbb{C}$.

a) $sin(z_1 + z_2) = sin(z_1) cos(z_2) + cos(z_1) sin(z_2)$

b) $sin(z_1 - z_2) = sin(z_1) cos(z_2) - cos(z_1) sin(z_2)$

c) $cos(z_1 + z_2) = cos(z_1) cos(z_2) - sin(z_1) sin(z_2)$

d) $cos(z_1 - z_2) = cos(z_1) cos(z_2) + sin(z_1) sin(z_2)$

e) $tan(z_1 + z_2) = \frac{tan(z_1) + tan(z_2)}{1 - tan(z_1) tan(z_2)}$

f) $tan(z_1 - z_2) = \frac{tan(z_1) - tan(z_2)}{1 + tan(z_1) tan(z_2)}$

g) $sin(2z) = 2\ sin(z)\ cos(z)$, for all $z \in \mathbb{C}$.

h) $cos(2z) = cos^2(z) - sin^2(z)$, for all $z \in \mathbb{C}$ and many more formulae can be formulated using these formulae.

For hyperbolic function we are having following results as follows:

Let $z_1 = a_1 + b_1 i$ and $z_2 = a_2 + b_2 i$ be complex variables in $\mathbb{C}$.

a) $sinh(z_1 + z_2) = sin\,h(z_1) cos\,h(z_2) + cos\,h(z_1) sinh(z_2)$

b) $sinh(z_1 - z_2) = sin\,h(z_1) cos\,h(z_2) - cos\,h(z_1) sinh(z_2)$

c) $cosh(z_1 + z_2) = cos\,h(z_1) cos\,h(z_2) - sin\,h(z_1) sinh(z_2)$

d) $cosh(z_1 - z_2) = cos\,h(z_1) cos\,h(z_2) + sin\,h(z_1) sinh(z_2)$

e) $tanh(z_1 + z_2) = \frac{tan\,h(z_1) + tanh(z_2)}{1 - tanh(z_1) tanh(z_2)}$

f) $tanh(z_1 - z_2) = \frac{tanh(z_1) - tanh(z_2)}{1 + tanh(z_1) tanh(z_2)}$

g) $cosh^2(z) - sinh^2(z) = 1$, for all $z \in \mathbb{C}$.

h) $sech^2(z) + tanh^2(z) = 1$, for all z∈ ℂ.

i) $coth^2(z) - cosech^2(z) = 1$, for all z∈ ℂ.

Moreover, the complex exponential function e^z is a periodic function with a period of $2\pi i$ that is

$e^{(z+2\pi i)} = e^z$, as $e^{2\pi i}$ = cos2π + isin2π = 1 + i× 0 = 1 + 0 = 0.

REFERENCES

- Conway, J.B.(1978),”*Function of one complex variable*”, New York.,2nd edition Springer-Verlag.

- Howie,J.M.(2003) , “*Complex Analysis*”, Springer undergraduate text in mathematics.

- Lars, V. A.(1979),”*Complex Analysis An introduction to the theory of analytic functions of one variable* “, NewYork, 3rd edition McGraw Hill Inc.

- Nair,M. T. (2008),”*Complex Analysis-A short course*”, New Delhi,2nd edition, Hindustan Book Agencies(‘trim’ series).

- Remmert, R. (1989),”*Theoryof Complex Functions*”, Germany, 2nd edition Graduates Texts in Mathematics, Springer.

- Shirali, S.,&Vasudeva,H. (2011),”*MultivariableAnalysis*”, London, Springer-Verlag.

- Kaur , S. (2018),“*Complex Variable and Applications*”, University of Delhi.

- SCHAUM’s Outines (2009),”*Complex Variables*”, 2nd edition, New York, McGraw Hill Companies.

- Fisher, S. D.(1999) ,”*Complex Variables* “,New York, 2nd edition, Dover Publication.

- Ponnusamy, S., & Silverman, H. (2006),” *Complex Variables with Applications*”.Birkhauser Boston.

- Gamelin, T. W. (2001),”*Complex Analysis*”, New York , Undergraduate Text in Mathematics, Springer.

- Adreescu,T.,&Andrica, D. (2006) ,”*Complex Numbers from A to ..Z*”, U.S.A., Library of Congress Cataloguing.

- Rudin, W.(1987),“*Real and complex analysis*”, New York,3rd edition McGraw Hill Series in Higher Mathematics

- Shashtri, A.R.(2010),”*Basic Complex Analysis of One Variable*”,2nd edition, Springer .

- Alpay , D.(2015),”*An Advanced Complex Analysis Problem Book*”, Switzerland, Springer International Publishing.

- Sarason ,D. (2007), “*Complex Function Theory*”, 2nd edition, Barkeley, California.

- American Mathematical Society.

- Stein,E.M.,&Shakarchi, R. (2002),”*Complex Analysis*”, Princeton, New Jersey.

- Kasana, H.S.(2005) ,”*ComplexVariables: Theory and Applications*”2nd edition ,New Delhi.

- Brawn, J.W.,&Churchill, R. V. (2009), “*Complex analysis and Applications*”, New York, 8th edition McGraw Hill Series in Higher Mathematics.

PROTECTING DATABASES AGAINST AN ATTACKS

Dr. Sanjivani Nalkar

Computer Science Department, JVM's Degree College, Mumbai University

ABSTRACT

Day by day, preparation of the data becomes very fast and is kept at place called database. This data is processed easily and efficiently. In Database management system different operations like manipulation and maintenance are performed. It is important to secure the data for organization. If data has been protected from any database attack then it will be a secure data. Some security models have been developed for securing database and these databases are dealing with different issues. It is very difficult for securing database for selecting an appropriate model. In this paper I have made discussion on some of the attack and methods for avoiding it. To protect a database and maintain the security is very complicated task for companies.

Keywords— Threats, Attacks, Security, Database, DBMS, Security

INTRODUCTION

We can define database as a collected work of processed data which is gathered on the system. Legitimate users are allowed to use saved data and analyze fast. It is may have a set of views, tables and queries. Within database, the stored data are organized which support the process that requires information storing and retrieval. To interact with database by using user interface we have database management system. As per many IT experts, many peoples from industries doesn't know which tables and columns has sensitive data as they might have handling any other application. Though we have complete knowledge of the database, it will be very hard to protect our data. Hence we can say that database security means securing data against any internal or external attack. It involves different types of controls regarding to administrative, technical and physical control. Protecting confidential data stored in database comes under database security. There are many layers of security in database as system administrator, database administrator, security officer, developers and employee and security can be broken at any of these levels only

II. DATABASES THREATS

Now a days technologies are being developed so different kind of attacks are existing for the databases. Firstly we will discuss about the existing attacks on databases and then will focus on techniques to secure our databases.

Excessive privileges-

In this technique the authorized user may misuse the privilege for unauthorized task. Misuse of privileges may comes as Excessive privilege abuse, unused privilege abuse and legitimate privilege abuse. This type is more dangerous as authorized user are making misuse of data and creates more risk. These authorized peoples may be company employee or ex-company employee

Countermeasures-

1. It can be stop by providing proper audit trail.

2. By using access control policy do not grant unnecessary privileges to all users

SQL Injection-

In most of the cases the data supplied by user as an input is used to dynamically build sql statements and it directly affects the databases. In SQL injection the original intent of any application is manipulated by the attacker and supplied to database directly. We can divide SQL Injection in two ways as-

SQL Injection and NOSQL Injection

Countermeasures-

i. Try for implementing MVC architecture

ii. Instead of direct queries make use of stored procedure.

Malware-

Different types of malwares, spear phishing emails can be used to penetrate organization and steal data. Without knowing of malware attack the legitimate user becomes a medium for these groups to access network and data of organization.

Countermeasures-

To avoid malware we have to enable firewall protection and install antivirus.

Weak audit trail-

Organization having weak database audit mechanism will increase risk in all levels. Most of this audit mechanism are unaware of the end user as all activities are associated with the users account name. Visibility, reporting and forensic analysis are vulnerable as there is no proper link to specific user. And finally with knowing or unknowingly the legitimate user with administrative access to database can turn off native database auditing to hide his fraudulent activities.

Countermeasures–

Always offer granular data collection and use network based audit appliances.

Weak Authentication-

In this attackers can assume the identity of legitimate database users. In this a specific attack includes brute force attack, social engineering attack etc.

Unmanaged Sensitive Data-

Many times the company employees may forget the passwords for old backup databases. This may contain any sensitive information. In such case this will exposed to threats if specific controls and privileges are not implemented properly

Countermeasures of unmanaged Sensitive Data

i.   The sensitive data in the database must be encrypted.

ii. Controls and permissions to the databases must be required to implement.

G. Denial Of Service-

It is a general type of attack which contains denial of access to network application or data to intend user.

Countermeasures-

Apply a network Intrusion Detection System (IDS) as it can automatically detect and respond to SYN attacks.

III.CONTROL METHODS FOR DATABASE THREATS

To protect and remove the threats every organization should have certain security policy which must be implemented. In this policy the authentication is important because if it is proper then the threats will be minimum. Following are some methods by which we can secure our database.

A. Access control- It is basic fundamental services which any database should have. It is used to protect the data from unauthorized read and write operations. This policy ensure that all communication to the database and other system objects must follow this policy. Controlling includes file permission, program permission and data rights.

B. User Identification /Authentication- in this technique it is required that you should identify your users and this identification must be done prior to their privileges and access rights determination by you. It is very basic method since it ensures the security of identification process of definite set of peoples who access the data. This identification helps to secure the sensitive data and protect it from being modified by unauthorized user. Attacker can take different approaches like bypass privilege escalation, Default Password, authentication, Password Guessing by brute force and rainbow attack .

C. Accountability and auditing- it is used to monitor and record actions related to configured database. It is also used to maintain an audit trail for user action performed in system. It is used to ensure the physical integrity of the data so that database is handled through auditing and for keeping the records.

D. Encryption- in this the information is converted into a cipher text so that nobody can read it except those people who has it's key for cipher text. This cipher or encoded text is called as encrypted data.

IV. CONCLUSION

Finally summarizing all this, access protection starts with user who can access data and what type of data attackers want to access. The topics discussed here gives the information of different threats and it's security

issues of databases. This paper focused on threats and its possible counter measures that can be possible to secure data in databases.

REFERENCES

[1] Sohail IMRAN, Dr Irfan Hyder, Security Issues in Database, Second International Conference on Future Information Technology and Management Engineering, 2009.

[2] Mr. Saurabh Kulkarni, Dr. Siddhaling Urolagin, Review of Attacks on Databases and Database Security Techniques, Facility International Journal of Engineering Technology and Database Security Techniques Research, Volume 2, Issue 11, November-2012.

[3] Shelly Rohilla, Pradeep Kumar Mittal, Database Security: Threats and Challenges, International Journal of Advanced Research in Computer Science and Software Engineering, Volume 3, Issue 5, May 2013.

ROLE OF DATABASE IN BLOCK CHAIN TECHNOLOGY

Sarita Sarang
Assistant Professor, Department of Computer Science, JVM's Degree College, Airoli, Navi Mumbai, Maharashtra, India, University of Mumbai

ABSTRACT
As of late, Bitcoin has acquired exceptional attention both from industry and the scholarly community. The fundamental technology that empowers Bitcoin (or all the more for the most part cryptographic money) is called blockchain. At the center of the blockchain innovation is a datastructure that keeps record of the exchanges in the network.The uncommon component that recognizes it from existing technology is its permanence of the put away records. To accomplish immutability,it utilizes agreement and cryptographic systems.

Keywords:- Blockchain, Distributed Database, Implementations of Database

I INTRODUCTION

A blockchain is really a data set since it is a computerized record that stores data in information structures called blocks. A data set in like manner stores data in information structures called tables. Be that as it may, while a blockchain is a data set, an information base isn't a blockchain. They are not compatible it might be said that however the two of them store data, they contrast in plan. There is additionally a distinction in reason between the two, which is maybe what isn't obvious to the individuals who need to comprehend why blockchains are required and why data sets are more qualified for putting away certain information.

Database
A conventional data set is an information structure utilized for putting away data. This incorporates information that can be questioned to assemble bits of knowledge for organized revealing utilized by substances to help business, monetary and the executives choices. Government additionally utilize information bases to store huge arrangements of information which scale to a great many records.

Blockchain
A blockchain stores data in uniform estimated blocks. Each square contains the hashed data from the past square to give cryptographic security. The hashing utilizes SHA256 which is a single direction hash work. This hashed data is the information and advanced mark from the past block, and the hashes of past blocks that goes right back to the absolute first square delivered in the blockchain called a "beginning square". That data is gone through a hash work that then, at that point focuses to the location of the past block. A blockchain information structure is an illustration of a Merkle Tree, which is utilized as a proficient method to confirm information.

Blockchain Database :
A blockchain information base uses blockchain innovation to make an unchanging record of exchanges. Blockchain innovation depends on shared decentralized exchanges implying that it is a dispersed record. This offers more noteworthy security and eliminates the requirement for any single controlling element that holds organization rights over the data set. [4]

The information structure includes information being recorded in blocks. As each new square or exchange is recorded, it is added to the past one to shape a chain of information records or a blockchain. Subsequently, a blockchain contains each exchange recorded since the record was begun.A blockchain as a data set can contain any data, be that as it may, blockchains are not actually acceptable at putting away immense measures of information because of organization constraints and cost, and so forth On account of the open-source digital currency Bitcoin, just data like proprietorship, a timestamp, and other little subtleties are recorded in the record.[5]

II HOW TO IMPLEMENT A BLOCKCHAIN DATABASE
A) Operational Blockchain Data Store With Enterprise
An operational data store (ODS) is utilized for functional announcing and in deciding.In our joined circulated/blockchain stack data set, the functional information will address all the data being gotten from business measures that are not associated with the blockchain data set. To consolidate the blockchain highlight of decentralization, the information base should be constrained by at least two directors, every one of whom is working from an alternate area. On account of an organization situated in a solitary country, these heads could

be situated in two separate workplaces, while on account of a worldwide, they could be situated in various nations.[1]

B) Non-Operational Blockchain Data With Enterprise
To work with customer admittance to the information base, a non-functional methodology is required. This methodology includes setting up mediators who can get to the data hung on the blockchain data set and send it to clients.While customers would not have the option to get to the data set itself, they would in any case have the option to get the data contained in the information base. A vital advantage of this methodology is the short-idleness time frames when contrasted with a standard blockchain information base.]2]

C) Operational Blockchain Data With Consortium
The consortium approach is more in accordance with customary blockchain philosophy. A consortium could be comprised of however many people or organizations as is required. This would guarantee that the information base was totally decentralized and that nobody individual or organization kept up with control. Every one of the organizations would go about as individual hubs and subsequently be needed to keep up with the data set. Such a methodology is ideal for store network the board and so forth.[3]

d) Non-Operational Blockchain Data With Consortium
Indeed, delegates would be set up to permit customers to get to the information held in the data set. Organizations that hold individual information or deals data that may be needed by outside gatherings and subsidiary associations, who are not approved to get to the data set straightforwardly, would profit with such a data set execution model.

IV CONCLUSION
We are seeing the growth of blockchain applications reaching far beyond the initial craze of Bitcoin. A consequence of the fast adoption of the technology is that, in many cases,a blockchain is often used as an architectural component in a large-scale distributed software system to store data, which not only vary widely in both format and content, but also express a range of complex application domain requirements.Therefore, carefully examining blockchains to understand and assess its capabilities and issues as a data store is a timely and relevant topic to the academic and industry communities who are looking to use the technology.

REFERENCES
[1] Blockchain technology: principles and applications.Research handbook on digital transformations. 2016 Sep 30

[2] Riple, https://ripple.com/files/ripple consensus whitepaper.pdf(accessed 15 th Feburary, 2018)

[3]   Dennis, R., and Owen, G. (2015). Rep on the block: A next generationreputation system based on the blockchain. 2015 10th InternationalConference for Internet Technology and Secured Transactions (Icitst),131138.

[4] https://hackernoon.com/databases-and-blockchains-the-difference-is-in-their-purpose-and-design-56ba6335778b

[5] https://www.devteam.space/blog/how-to-use-blockchain-to-build-a-scalable-database

COVID-DASHBOARD: A REAL-TIME DASHBOARD FOR COVID WITH ALERTS

Mrs. Janhavi Kshirsagar

Department of Computer Science, JVM's Mehta Degree College, Airoli, Navi Mumbai, INDIA

ABSTRACT

The entire world is going through COVID pandemic situation. There is a need to have understandable and accurate display of related information. The conception can be implemented using interactive maps. Working on existing stages and planning easy to use and intelligent are among the significant undertakings to play out a precise representation of the data. Existing APIs are used to implement important resources of individuals. Equipment has been created which cautions the client at whatever point new cases, passing and recuperation happen. The deceivability of the information will be made available around the world. It would help individuals to analyze data, take action, recognize errors in data and understand the trends. It would assist the authorities to drive their emergency reaction like imposing restrictions. This would help the public authority specialists to force a time limit or force explicit limitations on the concerned locale. Through this paper it is intended to decrease the spread of rumors.

Keywords— Internet of Things, Conception, Real-time systems, styling, Data visualization, User interfaces, Application programming interfaces

INTRODUCTION

A new virus named Novel Corona virus which was first found in China. This virus has a family of extensive family of viruses. Common symptoms found in patients are cold, fever, cough and respiration problem. This virus gets transmitted from human to human through sneezing or coughing. Governments have set up emergency helpline numbers and spread awareness about it through social media. Officials are continuously updating Corona virus related information like affected population, deaths, hospital bed availability etc. through websites.[1] No cure, vaccine or synthesized drug is ready to fight this virus completely. A specific treatment approved by the World Health Organization (WHO) is not available to cure the novel coronavirus. Infected individuals should ensure that they take supportive care and improve their immune power to obtain symptom relief. If a person comes in contact with an infected person with positive symptoms of Corona virus, then health must be monitored for 4 weeks from the day of occurrence of the symptoms[2]. WHO has recommended quarantine period of 2 to 4 weeks, maintain minimum 1 meter distance between each other, avoid using common facilities, prefer well ventilated and sanitized room [3]. A picture means thousands of words, hence visuals captured by human brain lasts for a longer time. If a picture is created with relevant information then it can seek upto 65% of human attention. Hence pictures, videos, infographics plays a vital role in spreading awareness through webpages, social media handles etc.[4]

Corona virus is continuing to spread globally with now more than 6000000 plus cases worldwide. The global death toll has surpassed 400000 plus. Hence, a dashboard was developed that would display real-time data. Hardware will send alerts as per updated activity.

Block Diagram
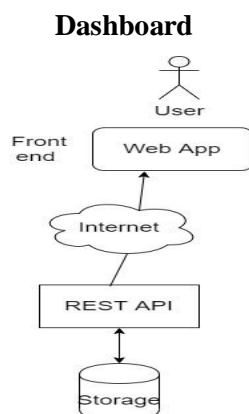
Fig. 1 Web based dashboard

A web based APP demands data via internet from the API and receives information at real time against the demand.
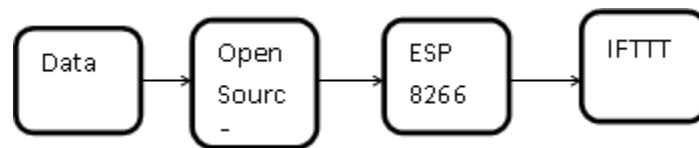
Hardware Scheme for alerts

Fig. 2 Hardware Scheme

The API is designed to post data on open source cloud like Thing Speak service. ESP 8266 (Node MCU) captures data from the API. An alert via E-mail is generated when new cases are reported.

Case studies

Some dashboards which exists and widely used are

o *World Health Organization Dashboard*

It represents WHO data in a user-friendly way to help keep communities safe, alert, and informed. The dashboard, which is interactive, is available in a desktop and mobile-friendly version. The dashboard's beautiful and clean interface maps confirmed cases and deaths and highlights how the corona virus is spreading over time to provide an update on a community's risks and to empower people to make knowledgeable decisions [5].

o *COVID 19 India*

They are using state bulletins and official handles like Twitter and government websites to upgrade their numbers. Volunteers verify the data and push a Google sheet and an API [6].

Technology used

For the development of real time dashboard, group of technologies and frameworks are used. It helps in developing WebApps, Apps and other related products.

Dashboard

ReactJS (JavaScript): React is a virtual Document Object Model that is properly structured and quite a user interactivity is handled by it. It has the final say on performance[7]. It helps in loading the web pages fast.

REST API: Representational state transfer, called REST API (application program interface), is a set of rules for implementing Web services with a proper architectural style defined. It works as an interface between HTTP protocol systems to manage data handling.

The system deployment requires few other APIs and libraries.

Hardware

A microcontroller board with WiFi feature suits best for this application like Node MCU. It is a 32 bit microcontroller board which can be easily connected to open source cloud and IFTTT. Arduino IDE is preferred to be used for programming it[8][9].

System Working

The useEffect hook is used to retrieve the data from an API with Axios. Then it is stored in the local state variable with the state hook's update functionality. Since state variables are updated after every change, the component automatically upgrades itself and the effect is called once more in action. It retrieves the data again and again. Thus, it automatically upgrades on the change of values in the API.

- The data from the state variables are then passed to the region allocated by the map. Hence, vital information such as active death and recovery are accurately displayed onto the map. By clicking on the state, the district level view is visible along with the zone colour. As soon as the API is updated, it is automatically reflected. API used are

- Total cases info API - corona.lmao.ninja/v2/all

- Country-wise info API -

- corona.lmao.ninja/v2/countries/

- India state wise info API covid19india.org/data.json

- Indian district wise info API covid19india.org/state/ district wise.json

- Indian district zone wise info API covid19india.org/zones.json

- Indian resources district wise info API covid19india.org/resources/resources.json

Algorithm1:

a. Initialize the Node MCU module.

b. Establish internet connection via WiFi.

c. Check the connection established

i   If NO, go back to a

ii If yes, then

d. Retrieve data from cloud (worldometer.info) cases, deaths, recovery etc.

e. Repeat after fixed interval

Algorithm2:

a. Initialize hardware setup (Node MCU).

b. Establish internet connection via WiFi.

c. Check the connection established

i. If NO, go back to a

ii. If Yes, then

d. Trigger IFTTT WebHooks

e. Push email to registered Email ID with cases, deaths and recovery.

f. If values updated, go back to e else wait.

IFTTT employs a simple trigger-event logic and works with a variety of services for triggers and events. Webhooks support GET and POST requests, with POST requests allowing for the sending of JSON data for more complicated events. The GET request is used in this scenario. The data that has been fetched onto node mcu is now available. IFTTT webhooks are triggered and notifications are sent when new cases, deaths, or recoveries occur. These notifications are sent via IFTTT's Webhooks service, which involves sending an email to the user with updates on cases, deaths, and recoveries.

Advantages

- Improved analysis

• Areas can be labelled as COVID-19 hot spots or containment zones based on the number of cases and their frequency in a certain area. Longer lockdowns and more aggressive testing would be preferable in these regions. As a result, these studies can be carried out using the current configuration.

- Immediate action

• Given the current situation, government officials could order a complete lockdown or lift or relax some restrictions in some areas.

- Recognizing patterns

• Mathematical and data modelling tools may be able to provide genuine evidence and insights on the disease's transmission, severity, and intensity, which could aid in disease-fighting decision-making.

• The patterns will aid in modelling disease transmission projections as well as assessing and designing control tactics.

- Error detection

• Errors can be identified by comparing the numbers to other sources and references.

• Transparency would be improved, and the storey would be more accessible to the general public.

- Recognizing Current Trends

• The trend, similar to working from home, will continue in the next months, and adopting will enable the company achieve exponential growth.

- Receive notifications

• Emails would be sent out in response to notifications, keeping users informed.

Results

Fig. 3 Statistical Data
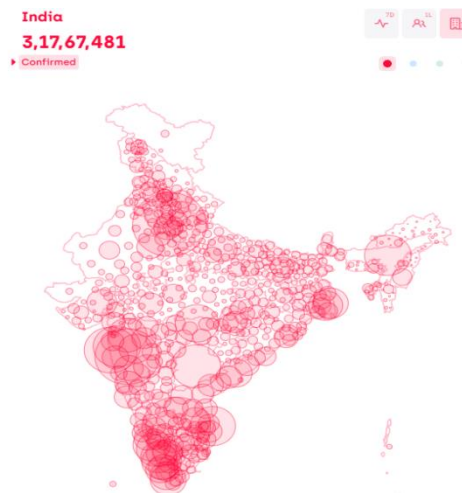
Fig 4. Demographic Page

Fig. 5. Cases reported (Statewise data can be captured)

Figure Fig.3 indicates the recent statistical data collected from website through API shows number of cases reported, active cases, recovered and deceased numbers. Figure Fig. 4 shows demographic representation of a country. The circles indicate the affected areas. Figure Fig.5 shows number of cases per state or union territory within India.

In the similar way, information about the entire world or specific country and its states can be obtained. This retrieved information can be used to do analysis towards number of cases registered, recovered and deceased from a particular state/country per hour/day/week/month. The statistical data obtained can further be used for many other relevant disease analyses.

CONCLUSION

In the present scenario, we need a dashboard which assists or directs us by sending emails, visualising through the dashboard, and receiving information about nearby important resources to keep the user informed and transparent. As a result, the user-friendly dashboard would assist users of various backgrounds in learning more about the places most affected by the pandemic's expansion. Customize your views and gain granular insights by filtering by location. During the COVID-19 situation, making a good impact. The worldwide health crisis would eventually lead to the proliferation of disease-related rumours. It urges governments and scientists to take decisive action to fully inform global citizens about the corona virus. As a result, hardware would be used to initiate updates. The resources would assist those who are ignorant, uninformed, or stranded in obtaining accurate information.

REFERENCES

[1] Coronavirus disease (COVID-19): Frequently Asked Questions Arfa Javaid - MAR 26, 2020 19:14 IST [Online]. Available: https://www.jagranjosh.com/general-knowledge/faqs-on-coronavirus-1584967984-1

[2] Myth busters [Online]. Available: https://www.who.int/emergencies/diseases/novel-coronavirus-2019/advice-for-public/myth-busters

[3] World Health Organization. Considerations for quarantine of individuals in the context of containment for coronavirus disease (COVID-19) Interim guidance. 2020, [cited 2020 Mar 2]. Available from: https://www.who.int/internal-publications-detail/considerationsfor-quarantine-of-individuals-in-the-context-of-containment-forcoronavirus-disease-(covid-19).

[4] Scientific reasons people are wired to respond to visual marketing Priyanka Desai [Online]. Available: https://yourstory.com/2018/04/scientific-reasons-visual-marketing

[5] WHO Coronavirus Disease (COVID-19) Dashboard [Online]. Available:- https://covid19.who.int/

[6] COVID19-India API ,A volunteer-driven API for COVID-19 stats & patient tracing in India [Online]. Available:- https://api.covid19india.org/

[7] React Virtual DOM Explained in Simple English Adhithi Ravichandran-Adhithi Ravichandran [Online]. Available: - https://programmingwithmosh.com/react/react-virtual-dom-explained/

[8] Software [Online]. Available: - https://www.arduino.cc/en/main/software

[9] NodeMCU Documentation [Online]. Available: https://nodemcu.readthedocs.io/en/master/

MANUSCRIPT SUBMISSION

GUIDELINES FOR CONTRIBUTORS

1. Manuscripts should be submitted preferably through email and the research article / paper should preferably not exceed 8 – 10 pages in all.

2. Book review must contain the name of the author and the book reviewed, the place of publication and publisher, date of publication, number of pages and price.

3. Manuscripts should be typed in 12 font-size, Times New Roman, single spaced with 1" margin on a standard A4 size paper. Manuscripts should be organized in the following order: title, name(s) of author(s) and his/her (their) complete affiliation(s) including zip code(s), Abstract (not exceeding 350 words), Introduction, Main body of paper, Conclusion and References.

4. The title of the paper should be in capital letters, bold, size 16" and centered at the top of the first page. The author(s) and affiliations(s) should be centered, bold, size 14" and single-spaced, beginning from the second line below the title.

<div align="center">

First Author Name1, Second Author Name2, Third Author Name3

1Author Designation, Department, Organization, City, email id

2Author Designation, Department, Organization, City, email id

3Author Designation, Department, Organization, City, email id

</div>

5. The abstract should summarize the context, content and conclusions of the paper in less than 350 words in 12 points italic Times New Roman. The abstract should have about five key words in alphabetical order separated by comma of 12 points italic Times New Roman.

6. Figures and tables should be centered, separately numbered, self explained. Please note that table titles must be above the table and sources of data should be mentioned below the table. The authors should ensure that tables and figures are referred to from the main text.

EXAMPLES OF REFERENCES

All references must be arranged first alphabetically and then it may be further sorted chronologically also.

- **Single author journal article:**

Fox, S. (1984). Empowerment as a catalyst for change: an example for the food industry. *Supply Chain Management*, *2*(3), 29–33.

Bateson, C. D.,(2006), 'Doing Business after the Fall: The Virtue of Moral Hypocrisy', Journal of Business Ethics, 66: 321 – 335

- **Multiple author journal article:**

Khan, M. R., Islam, A. F. M. M., & Das, D. (1886). A Factor Analytic Study on the Validity of a Union Commitment Scale. *Journal of Applied Psychology*, *12*(1), 129-136.

Liu, W.B, Wongcha A, & Peng, K.C. (2012), "Adopting Super-Efficiency And Tobit Model On Analyzing the Efficiency of Teacher's Colleges In Thailand", International Journal on New Trends In Education and Their Implications, Vol.3.3, 108 – 114.

- **Text Book:**

Simchi-Levi, D., Kaminsky, P., & Simchi-Levi, E. (2007). *Designing and Managing the Supply Chain: Concepts, Strategies and Case Studies* (3rd ed.). New York: McGraw-Hill.

S. Neelamegham," Marketing in India, Cases and Reading, Vikas Publishing House Pvt. Ltd, III Edition, 2000.

- **Edited book having one editor:**

Raine, A. (Ed.). (2006). *Crime and schizophrenia: Causes and cures.* New York: Nova Science.

- **Edited book having more than one editor:**

Greenspan, E. L., & Rosenberg, M. (Eds.). (2009). *Martin's annual criminal code:Student edition 2010.* Aurora, ON: Canada Law Book.

- **Chapter in edited book having one editor:**

Bessley, M., & Wilson, P. (1984). Public policy and small firms in Britain. In Levicki, C. (Ed.), *Small Business Theory and Policy* (pp. 111–126). London: Croom Helm.

- **Chapter in edited book having more than one editor:**

Young, M. E., & Wasserman, E. A. (2005). Theories of learning. In K. Lamberts, & R. L. Goldstone (Eds.), *Handbook of cognition* (pp. 161-182). Thousand Oaks, CA: Sage.

- **Electronic sources should include the URL of the website at which they may be found, as shown:**

Sillick, T. J., & Schutte, N. S. (2006). Emotional intelligence and self-esteem mediate between perceived early parental love and adult happiness. *E-Journal of Applied Psychology*, 2(2), 38-48. Retrieved from http://ojs.lib.swin.edu.au/index.php/ejap

- **Unpublished dissertation/ paper:**

Uddin, K. (2000). A Study of Corporate Governance in a Developing Country: A Case of Bangladesh (Unpublished Dissertation). Lingnan University, Hong Kong.

- **Article in newspaper:**

Yunus, M. (2005, March 23). Micro Credit and Poverty Alleviation in Bangladesh. *The Bangladesh Observer*, p. 9.

- **Article in magazine:**

Holloway, M. (2005, August 6). When extinct isn't. *Scientific American, 293*, 22-23.

- **Website of any institution:**

Central Bank of India (2005). *Income Recognition Norms Definition of NPA*. Retrieved August 10, 2005, from http://www.centralbankofindia.co.in/ home/index1.htm, viewed on

7. The submission implies that the work has not been published earlier elsewhere and is not under consideration to be published anywhere else if selected for publication in the journal of Indian Academicians and Researchers Association.

8. Decision of the Editorial Board regarding selection/rejection of the articles will be final.

INTERNATIONAL JOURNAL OF RESEARCH

IN MANAGEMENT & SOCIAL SCIENCE

INDIAN ACADEMICIANS AND RESEARCHERS ASSOCIATION

Membership No: M / M – 1365

Certificate of Membership

This is to certify that

XXXXXXXX

is admitted as a

Fellow Member

of

Indian Academicians and Researchers Association

in recognition of commitment to Educational Research

and the objectives of the Association

Date: 27.01.2020

Director

President

INDIAN ACADEMICIANS AND RESEARCHERS ASSOCIATION

Membership No: M / M – 1365

Certificate of Membership

This is to certify that

XXXXXXXXXX

is admitted as a

Life Member

of

Indian Academicians and Researchers Association

in recognition of commitment to Educational Research

and the objectives of the Association

Date: 27.01.2020

Director

President

INDIAN ACADEMICIANS AND RESEARCHERS ASSOCIATION

Membership No: M / M – 1365

Certificate of Membership

This is to certify that

XXXXXXXX

is admitted as a

Member

of

Indian Academicians and Researchers Association

in recognition of commitment to Educational Research

and the objectives of the Association

Date: 27.01.2020

Director

President

IARA Organized its 1ˢᵗ International Dissertation & Doctoral Thesis Award in September'2019

1ˢᵗ International
Dissertation & Doctoral Thesis Award
(2019)

Organized By

Indian Academicians and Researchers Association (IARA)

EPH EMPYREAL PUBLISHING HOUSE

www.editedbook.in

Publish Your Book, Your Thesis into Book or Become an Editor of an Edited Book with ISBN

BOOKS PUBLISHED

JUSTICE SHAFIQUL HAQUE
Reflections and Juridical Thoughts
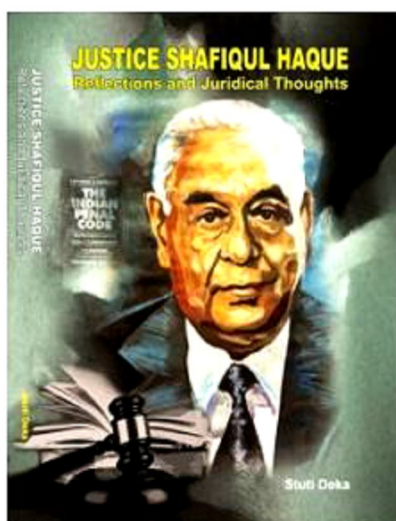
Stuti Deka

Dr. Stuti Deka
ISBN : 978-81-930928-1-1

Digital India
A road ahead

Edited by
Dr. Tazyn Rahman
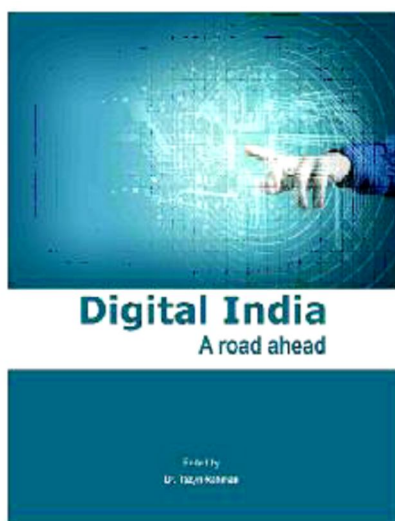
Dr. Tazyn Rahman
ISBN : 978-81-930928-0-4

A Guide to INJECTION MOULDING TECHNIQUE

Dinbandhu Singh

Mr. Dinbandhu Singh
ISBN : 978-81-930928-3-5

EDUCATIONAL RESEARCH ON Jammu and Kashmir

Edited by
Dr. Ismail Thamarasseri
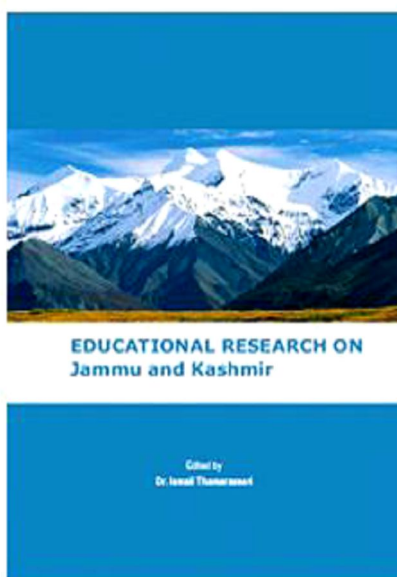
Dr. Ismail Thamarasseri
ISBN : 978-81-930928-2-8

6 SEASONS OF SUCCESS
Solutions To Paint Your Tomorrow

Ram Jaladurgam   Dr. S. Anand Reddy
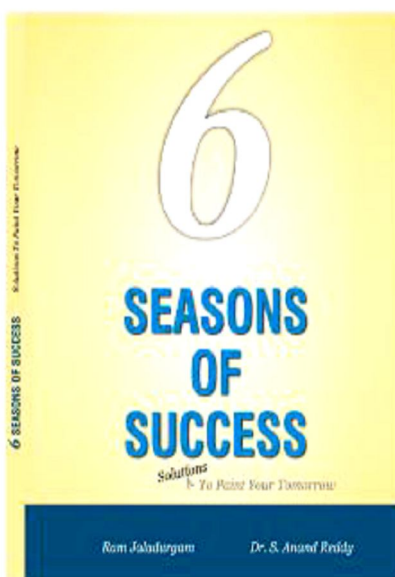
Ram Jaladurgam
Dr. S. Anand Reddy
ISBN : 978-81-930928-5-9

BUSINESS SUSTAINABILITY AND CONTEMPORARY PRACTICES
Business Management Cases

Edited By:
Dr. Sanjeev Bansal
Dr. Vijit Chaturvedi
Dr. Tazyn Rahman
Dr. Parikshit Joshi
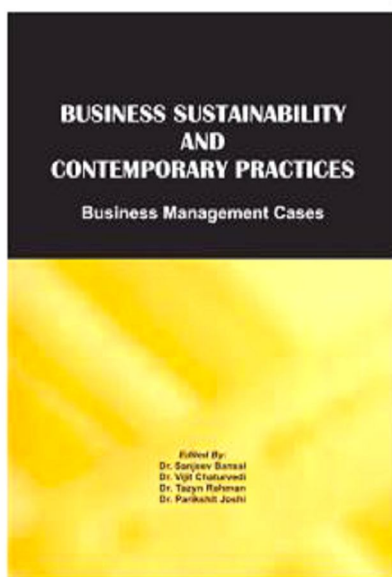
Dr. Sanjeev Bansal, Dr. Vijit Chaturvedi
Dr. Tazyn Rahman, Dr. Parikshit Joshi
ISBN : 978-81-930928-6-6

ALGORITHMIC COMPOSITION
In
Hindustani Music

Ashish Kumar Sinha, Dr. Soubhik Chakraborty
Dr. Amritanjali
ISBN : 978-81-930928-8-0

Business Perspectives in Emerging Markets
Business Management Cases
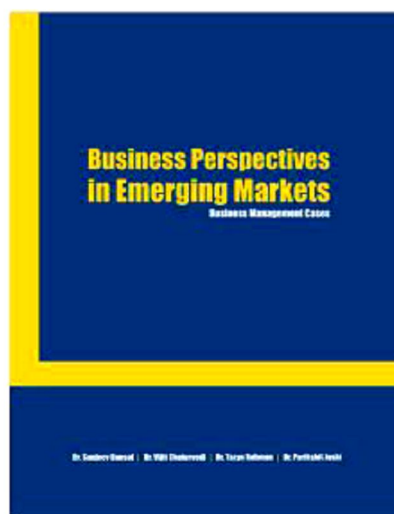
Dr Sanjeev Bansal, Dr. Vijit Chaturvedi
Dr. Tazyn Rahman, Dr. Parikshit Joshi
ISBN : 978-81-936264-0-5

Performance Management Practices FOR IT COMPANIES

Dr. Jyotsna Golhar
Dr. Sujit Metre
ISBN : 978-81-936264-6-7

FINANCIAL PERFORMANCE EVALUATION OF
Product Innovation

Dr. Aarushi Kataria

Dr. Aarushi Kataria
ISBN : 978-81-936264-3-6

COMPUTER BASED MASTERY LEARNING VS TRADITIONAL LEARNING
AN EMPIRICAL STUDY
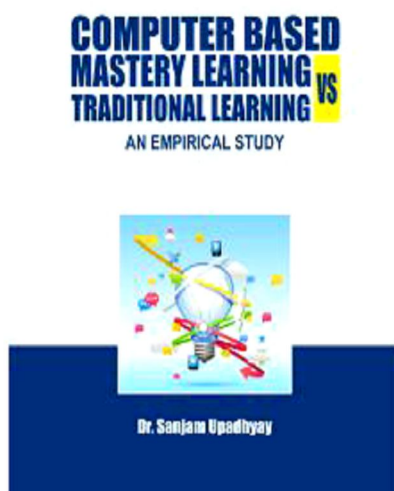
Dr. Sanjam Upadhyay

Dr. Sanjam Upadhyay
ISBN : 978-81-936264-5-0

HRD Practices in LIC
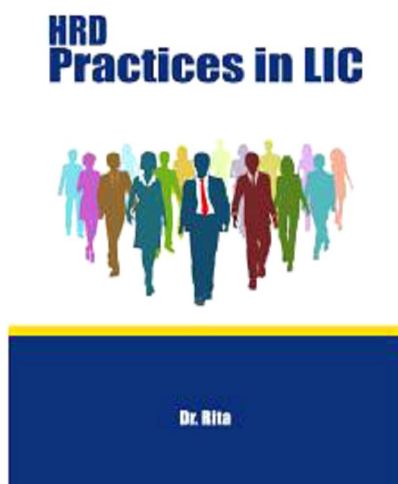
Dr. Rita

Dr. Rita
ISBN : 978-81-930928-7-3

Price Competitiveness of Indian Banking Sector in Post Liberalisation Era : An Empirical Analysis

Dr. Manas Ranjan Panda
Dr. Prabodha Kumar Hota

Dr. Manas Ranjan Panda, Dr. Prabodha Kr. Hota
ISBN : 978-81-930928-4-2

NATIONAL CONFERENCE ON INNOVATIVE TRENDS IN CIVIL ENGINEERING
April 13 - 14, 2018

DEPARTMENT OF CIVIL ENGINEERING
POORNIMA UNIVERSITY
PROCEEDINGS
ISBN: 978-81-936264-7-4
www.poornima.edu.in

Poornima University
ISBN : 978-8193-6264-74

MIDITOC 2K18
PROCEEDINGS OF THE CONFERENCE ON MARKETING IN DIGITAL INDIA:
TRENDS, OPPORTUNITIES & CHALLENGES
THEME: INDIA INTERNET MARKETING
19th - 20th FEBRUARY, 2018

Institute of Public Enterprise
ISBN : 978-8193-6264-4-3

**Vitamin D Supplementation
in SGA Babies**

Dr. Jyothi Naik, Prof. Dr. Syed Manazir Ali
Dr. Uzma Firdaus, Prof. Dr. Jamal Ahmed
ISBN : 978-81-936264-9-8
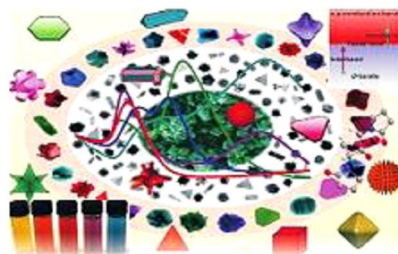
**Gold Nanoparticles:
Plasmonic Aspects And Applications**

Dr. Abhitosh Kedia
Dr. Pandian Senthil Kumar

Dr. Abhitosh Kedia
Dr. Pandian Senthil Kumar
ISBN : 978-81-939070-0-9

**Social Media Marketing and
Consumer Behavior**

Dr. Vinod S. Chandwani

Dr. Vinod
S. Chandwani
ISBN : 978-81-939070-2-3

**Select
Research Papers of**
Prof. Dr. Dhananjay Awasarikar

Prof. Dr. Dhananjay Awasarikar

Prof. Dr. Dhananjay
Awasarikar
ISBN : 978-81-939070-1-6

Recent ReseaRch
Trends in ManageMenT

Dr. C. Samudhra Rajakumar
Dr. M. Ramesh
Dr. C. Kathiravan
Dr. Rincy V. Mathew

Dr. C. Samudhra Rajakumar, Dr. M. Ramesh
Dr. C. Kathiravan, Dr. Rincy V. Mathew
ISBN : 978-81-939070-4-7

Recent ReseaRch
Trends in Social Science

Dr. C. Samudhra Rajakumar
Dr. M. Ramesh
Dr. C. Kathiravan
Dr. Rincy V. Mathew

Dr. C. Samudhra Rajakumar, Dr. M. Ramesh
Dr. C. Kathiravan, Dr. Rincy V. Mathew
ISBN : 978-81-939070-6-1

**Recent Research
Trend in
Business Administration**

Dr. C. Samudhra Rajakumar
Dr. M. Ramesh
Dr. C. Kathiravan
Dr. Rincy V. Mathew

Dr. C. Samudhra Rajakumar, Dr. M. Ramesh
Dr. C. Kathiravan, Dr. Rincy V. Mathew
ISBN : 978-81-939070-7-8

**Recent Innovations in
Biosustainability and Environmental
Research II**

Dr. V. I. PAUL
Dr. M. Muthulingam
Dr. A. Elangovan
Dr. J. Nelson Samuel Jebastin

Dr. V. I. Paul, Dr. M. Muthulingam
Dr. A. Elangovan, Dr. J. Nelson Samuel Jebastin
ISBN : 978-81-939070-9-2

**Teacher
Education:**
Challenges Ahead

Sajid Jamal
Mohd Shakir

Sajid Jamal
Mohd Shakir
ISBN : 978-81-939070-8-5

Project ManageMent

Dr. R. Emmaniel
ISBN : 978-81-939070-3-0

The *théâtre engagé*
American Drama from the '29 Crash to World War II
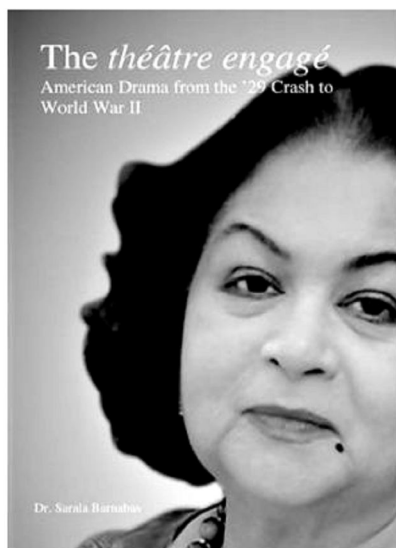
Dr. Sarala Barnabas

Dr. Sarala Barnabas
ISBN : 978-81-941253-3-4

Corporate Entrepreneurship

AUTHORS
Dr. M. Banumathi
Dr. C. Samudhra Rajakumar

Dr. M. Banumathi
Dr. C. Samudhra Rajakumar
ISBN : 978-81-939070-5-4

VIJANAN
COMMERCE AND MANAGEMENT
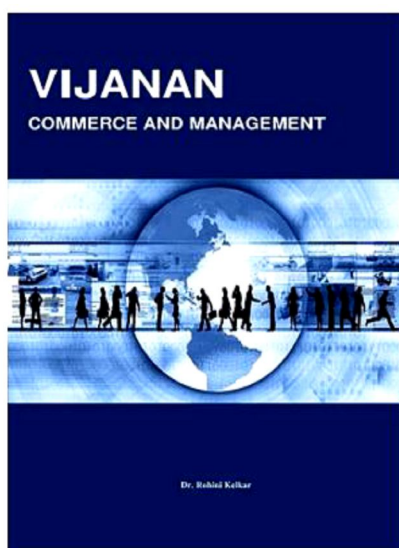
Dr. Rohini Kelkar

Dr. (Mrs.) Rohini Kelkar
ISBN : 978-81-941253-0-3

Recent Research Trends in
Management and Social Science

Dr. Tazyn Rahman

Dr. Tazyn Rahman
ISBN : 978-81-941253-2-7

VIJANAN
INFORMATION TECHNOLOGY

N. Lakshmi Kavitha
Mithila Satam
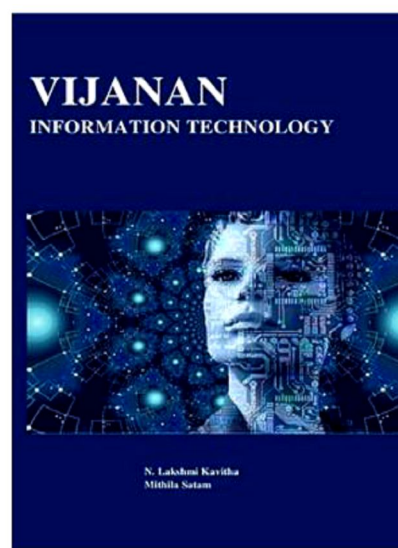
Dr. N. Lakshmi Kavitha
Mithila Satam
ISBN : 978-81-941253-1-0

Emerging Research
Trends in Management and Social Science

Dr. Hiresh Luhar
Prof. Arti Sharma
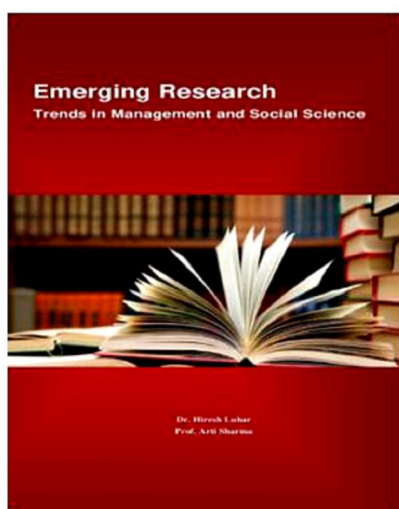
Dr. Hiresh Luhar
Prof. Arti Sharma
ISBN : 978-81-941253-4-1

Life of Slum Occupants
& **Saving Pattern**

Dr. Hiresh S. Luhar
Dr. Ashok S. Luhar
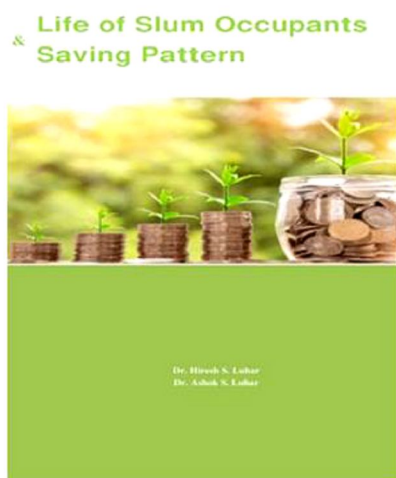
Dr. Hiresh S. Luhar
Dr. Ashok S. Luhar
ISBN : 978-81-941253-5-8

Computerised Information System:
Concepts & Applications

Babita Kanojia
Dr. Arvind S. Luhar

Dr. Babita Kanojia
Dr. Arvind S. Luhar
ISBN : 978-81-941253-7-2

SKILLS FOR SUCCESS

SK Nathan
SW Rajamonaharane

Dr. Sw Rajamonaharane
SK Nathan
ISBN : 978-81-942475-0-0

Witness Protection Regime
An Indian Perspective

Aditi Sharma

Aditi Sharma
ISBN : 978-81-941253-8-9

Self-Finance Courses:
Popularity & Financial Viability

Dr. Ashok S. Luhar
Dr. Hiresh S. Luhar

Dr. Ashok S. Luhar
Dr. Hiresh S. Luhar
ISBN : 978-81-941253-6-5

SMALL SCALE INDUSTRIES MANAGEMENT
Issues, Challenges and Opportunities

Dr. B. Augustine Arockiaraj

Dr. B. Augustine Arockiaraj
ISBN : 978-81-941253-9-6

SPOILAGE OF VALUABLE SPICES BY MICROBES

Dr. Kuljinder Kaur

Dr. Kuljinder Kaur
ISBN : 978-81-942475-4-8

Financial Capability of Students: An Increasing Challenge in Indian Economy

Dr. Priyanka Malik

Dr. Priyanka Malik
ISBN : 978-81-942475-1-7

THE RELATIONSHIP BETWEEN ORGANIZATION CULTURE AND EMPLOYEE PERFORMANCE: HOSPITALITY SECTOR

Dr. Rekha P. Khosla

Dr. Rekha P. Khosla
ISBN : 978-81-942475-2-4

A GUIDE TO
TWIN LOBE BLOWER AND ROOT BLOWER TECHNIQUE

Dilip Pandurang Deshmukh

Dilip Pandurang Deshmukh
ISBN : 978-81-942475-3-1

SILVER JUBLIEE
COMMEMORATIVE LECTURE SERIES
2019-SNGC

Dr. D. Kalpana
Dr. M. Thangavel

Dr. D. Kalpana, Dr. M. Thangavel
ISBN : 978-81-942475-5-5

Indian Commodity
Futures and Spot Markets

Dr. Aloysius Edward J

Dr. Aloysius Edward J.
ISBN : 978-81-942475-7-9

Correlates of Burnout Syndrome Among Servicemen

Dr. Rosemary Obiagaeri Ekechukwu

Dr. R. O. Ekechukwu
ISBN : 978-81-942475-8-6

Advances in
Mathematical Sciences
(A Collection of Survey Research Articles)

Edited By
Dr. Zakir Ahmed

Dr. Zakir Ahmed
ISBN : 978-81-942475-9-3
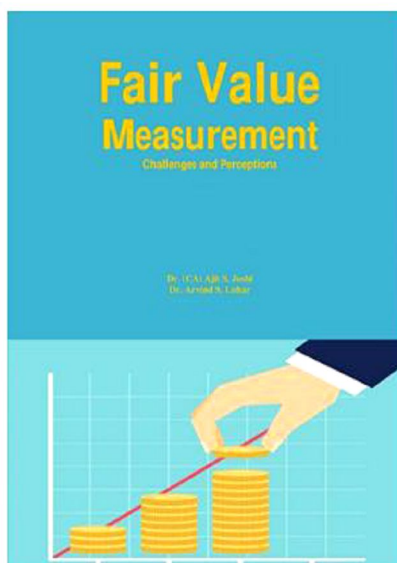
Fair Value
Measurement
Challenges and Perceptions

Dr. (CA) Ajit S. Joshi
Dr. Arvind S. Luhar

Dr. (CA) Ajit S. Joshi
Dr. Arvind S. Luhar
ISBN : 978-81-942475-6-2
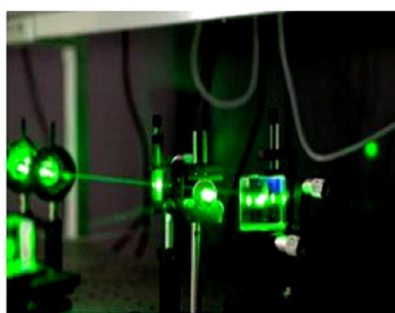
NONLINEAR OPTICAL CRYSTALS FOR LASER
Growth and Analysis Techniques

Madhav N Rode
Dilipkumar V Mehsram

Madhav N Rode
Dilip Kumar V Mehsram
ISBN : 978-81-943209-6-8
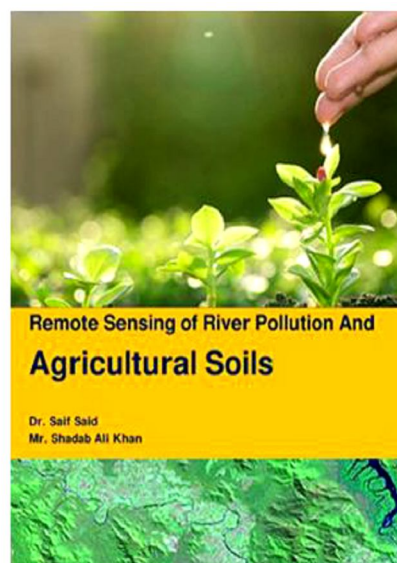
Remote Sensing of River Pollution And
Agricultural Soils

Dr. Saif Said
Mr. Shadab Ali Khan

Dr. Saif Said
Shadab Ali Khan
ISBN : 978-81-943209-1-3
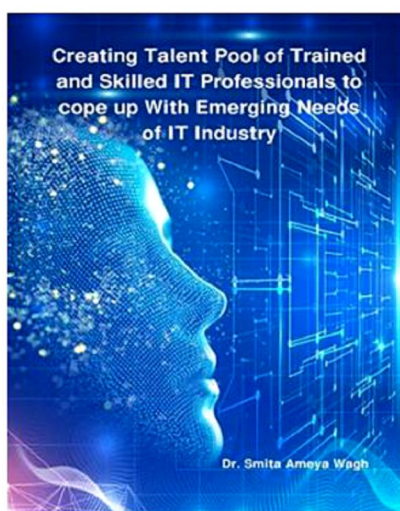
Creating Talent Pool of Trained and Skilled IT Professionals to cope up With Emerging Needs of IT Industry

Dr. Smita Ameya Wagh

Dr. Smita Ameya Wagh
ISBN : 978-81-943209-9-9
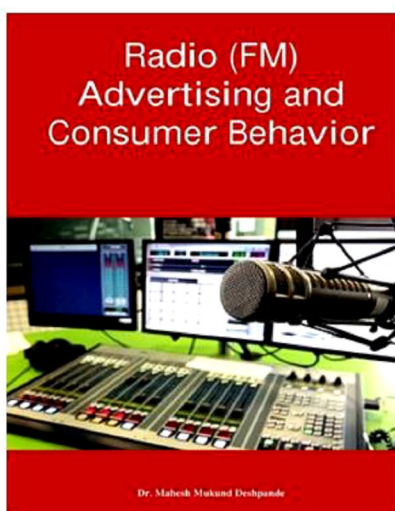
Radio (FM) Advertising and Consumer Behavior

Dr. Mahesh Mukund Deshpande

Dr. Mahesh Mukund Deshpande
ISBN : 978-81-943209-7-5
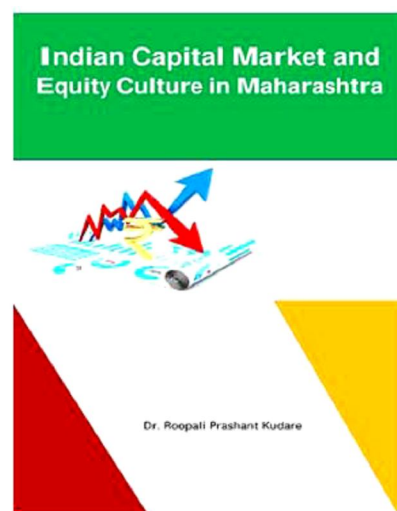
Indian Capital Market and Equity Culture in Maharashtra

Dr. Roopali Prashant Kudare

Dr. Roopali Prashant Kudare
ISBN : 978-81-943209-3-7

A Text book of
unified syllabus of
Practical Botany
(B.Sc. 1st year)

S. Saad, S. Bushra, A.A. Khan

S. Saad, S. Bushra, A. A. Khan
ISBN: 978-81-944069-9-0

Radiology: A Bridge in
Biophysics
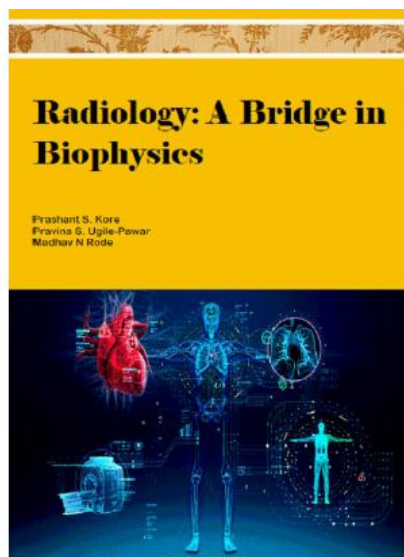
Prashant S. Kore
Pravina S. Ugile-Pawar
Madhav N Rode

Prashant S. Kore
Pravina S. Ugile-Pawar
Madhav N Rode
ISSN: 978-81-944069-7-6

Mixed Magnetic
Oxides

Dilipkumar V Meshram
Madhav N Rode

Dilipkumar V Meshram and
Madhav N Rode
ISSN: 978-81-944069-6-9

QUALITY OF
WORK LIFE – A SERVICE PERSPECTIVE

Dr. Vijaya Lakshmi Pothuraju

Dr. Vijaya Lakshmi Pothuraju
ISBN : 978-81-943209-2-0

National Level Seminar
On
'E-Business: A Paradigm Shift in the 21ˢᵗ Century'
January 30ᵗʰ & 31ˢᵗ 2020

Organized by
Department of Commerce & Management

Sponsored by
Savitribai Phule Pune University, Pune
(under Quality Improvement Programme)

Kamala Education Society's
Pratibha College of Commerce and Computer Studies,
Accredited by NAAC with "B" Grade (CGPA 2.68)

PROCEEDINGS

Pratibha College
ISBN : 978-81-944813-2-4

STATE LEVEL SEMINAR
on

'Emerging Environmental Challenges
&
Its Sustainable Approaches'

7ᵗʰ & 8ᵗʰ, February 2020

Sponsored by
Savitribai Phule Pune University, Pune
(under Quality Improvement Program)

PROCEEDINGS

Organized by
Department of Environmental Science
Kamala Education Society's
Pratibha College of Commerce and Computer Studies,
(Accredited with NAAC "B" Grade)
Tel. (Off.) : 8600100942/45, 020-65111411
www.pcccs.org.in

Pratibha College
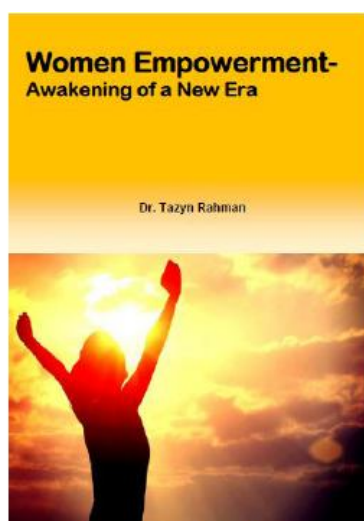ISBN : 978-81-944813-3-1

Women
Empowerment

Dr. Tazyn Rahman
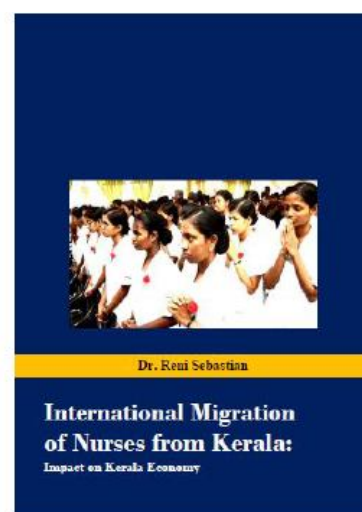
Dr. Tazyn Rahman
ISBN : 978-81-936264-1-2

Women Empowerment-
Awakening of a New Era

Dr. Tazyn Rahman

Dr. Tazyn Rahman
ISBN : 978-81-944813-5-5

Dr. Reni Sebastian

International Migration
of Nurses from Kerala:
Impact on Kerala Economy
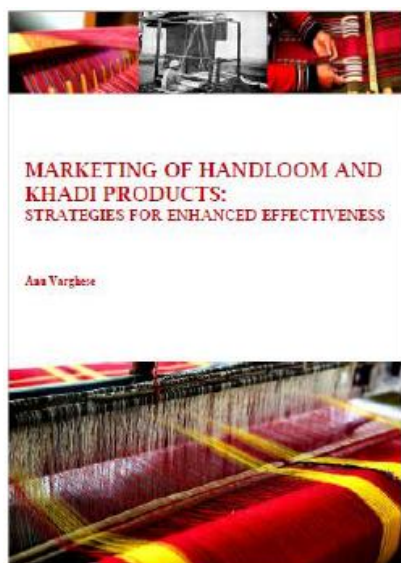
Dr. Reni Sebastian
ISBN : 978-81-944069-2-1

Dr. Vijay Prakash Gupta
ISBN : 978-81-944813-1-7

Dr. Deepa Vijay Abhonkar
ISBN : 978-81-944813-6-2

Arasu Engineering College
ISSN: 978-81-944813-4-8

Dr. Anu Varghese
ISBN : 978-81-944069-4-5

Dr. Renuka Vanarse
ISBN : 978-81-944069-1-4

INDIAN ACADEMICIANS & RESEARCHERS ASSOCIATION

Major Objectives

- To encourage scholarly work in research

- To provide a forum for discussion of problems related to educational research

- To conduct workshops, seminars, conferences etc. on educational research

- To provide financial assistance to the research scholars

- To encourage Researcher to become involved in systematic research activities

- To foster the exchange of ideas and knowledge across the globe

Services Offered

- Free Membership with certificate
- Publication of Conference Proceeding
- Organize Joint Conference / FDP

- Outsource Survey for Research Project
- Outsource Journal Publication for Institute
- Information on job vacancies

Indian Academicians and Researchers Association

Shanti Path ,Opp. Darwin Campus II, Zoo Road Tiniali, Guwahati, Assam
Mobile : +919999817591, email : info@iaraedu.com www.iaraedu.com

EPH EMPYREAL PUBLISHING HOUSE

- Assistant in Synopsis & Thesis writing

- Assistant in Research paper writing

- Publish Thesis into Book with ISBN

- Publish Edited Book with ISBN

- Outsource Journal Publication with ISSN for Institute and private universities.

- Publish Conference Proceeding with ISBN

- Booking of ISBN

- Outsource Survey for Research Project

Publish Your Thesis into Book with ISBN "Become An Author"

EMPYREAL PUBLISHING HOUSE
Zoo Road Tiniali, Guwahati, Assam
Mobile : +919999817591, email : info@editedbook.in, www.editedbook.in